Spring 2014

Interactions of Endoxifen and other major metabolites of Tamoxifen with human sulfotransferases SULT2A1, SULT1E1, and SULT1A1*1 : implications for the therapeutic action and toxicity of Tamoxifen

Edwin Jermaine Squirewell
University of Iowa

INTERACTIONS OF ENDOXIFEN AND OTHER MAJOR METABOLITES OF TAMOXIFEN WITH HUMAN SULFOTRANSFERASES SULT2A1, SULT1E1, AND SULT1A1*1: IMPLICATIONS FOR THE THERAPEUTIC ACTION AND TOXICITY OF TAMOXIFEN

by

Edwin Jermaine Squirewell

A thesis submitted in partial fulfillment of the
requirements for the Doctor of Philosophy degree in
Pharmacy (Medicinal and Natural Products Chemistry)
in the Graduate College of The University of Iowa

May 2014

Thesis Supervisor: Professor Michael W. Duffel

Graduate College
The University of Iowa
Iowa City, Iowa

CERTIFICATE OF APPROVAL

_____

PH.D. THESIS

_____

This is to certify that the Ph.D. thesis of

Edwin Jermaine Squirewell

has been approved by the Examining Committee
for the thesis requirement for the Doctor of Philosophy
degree in Pharmacy (Medicinal and Natural Products Chemistry) at the May
2014 graduation.

Thesis Committee: _____
Michael W. Duffel, Thesis Supervisor

_____
Jonathan A. Doorn

_____
Robert J. Kerns

_____
David L. Roman

_____
Daniel M. Quinn

To Him who is able to do immeasurably more than all we ask or imagine, according to His power that is at work within us, to Him be glory in the Church and in Christ Jesus throughout all generations, forever and ever! Amen.

ACKNOWLEDGMENTS

There are not enough words to fully express my gratitude and thanks to those who have contributed to my personal development as a scientist and as well as my personal life outside of research. To my mentor, Professor Michael Duffel, thank you so much for your unconditional help, guidance, and support throughout my graduate career. You are a teacher and friend. We rejoiced together with each new discovery in my research, and you helped me through each hurdle in graduate school with a positive attitude. Thank you for understanding my medical needs and health concerns. You are approachable, and you counseled me through numerous times of frustration and anger. You made me feel appreciated and gave me confidence in times where I questioned my own abilities. I'm proud to be a product of your laboratory and a carrier of your name throughout the remainder of my career.

To my doctoral committee members (Drs. Michael Duffel, Jonathan Doorn, Robert Kerns, David Roman, and Daniel Quinn), I want to show my great appreciation for your efforts in helping me to obtain this PhD degree. Whether in the classroom or in the hallways, you each greeted me with a warm, friendly welcome and enhanced my understanding of medicinal chemistry through coursework and discussion. Thank you for the letters of recommendation and the cooking tips (i.e. Dr. Quinn). Thank you, Drs. Roman and Kerns, for allowing me to use your lab-space at times during my thesis research. Also, thank you, Dr. Doorn, for granting me access to your "diabetes in a drawer" and informing me that the lab decorations were paper snakes, not giant colons. In addition, thank your for providing a quiet desk for concentration while in the midst of writing my dissertation.

I would like to thank Dr. Lynn Teesch, Dr. Santhana Vellupillai, and Vic Parcel for providing the assistance and training for my analytical work in the high resolution mass spectrometry and NMR facilities. You were each gracious in allowing me the use of your

personal time in order to interpret and comprehend the data of my research. In addition, thank you, Fabian Grimm, Eric Rodriguez, Louis Mullins, and Victoria Parker for providing a friendly and comfortable working environment in Dr Duffel's lab. Each of you was always there when I desperately needed a laugh. I truly value the time we shared together as colleagues and wish the best for each of you in pursuit of your careers.

To my parents – Eddie and Sherry Squirewell, and grandmothers – Emma Burgess and Sally Farrow, thank your for nurturing me into the man that I am today. Your unconditional love and support gave me the confidence to pursue this advanced degree. At the same time, your love kept me grounded in my faith as a Christian and Follower of Christ. Thank you for your thoughts and prayers. Thank you for serving as a soundboard when I need to express my frustrations and rants, as well as my success and accomplishments. We always envisaged the day when I would complete my PhD, and that day has now come. Thank you, Mom and Dad, for your endless love and care for me. You were generous in allowing me the use of a vehicle while in graduate school and significantly alleviated my financial burdens as a student. You both carried me through emotional strife up until adulthood, and I'm proud to be your son. Grandma, you did amazing things for me. You and Granny are incredible women and I thank you both for your emotional, spiritual, and financial support, for helping with unexpected bills, and for helping to ensure that I maintained a comfortable quality of life while pursuing my graduate studies. To my uncle and God-father, Bryant Burgess, thank you for your mentorship, advice, support (financially, emotionally, and spiritually) throughout my life. To my brother, Eddie Bernard Squirewell, I love you and thank you for your wonderful words of encouragement through the years. I wish you the best in your professional studies and look forward to the day when you'll be both my brother and colleague.

ABSTRACT

Although tamoxifen has been successfully utilized in the treatment and prevention of estrogen-dependent breast cancer for decades, its use is limited by its low incidence of endometrial cancer. The carcinogenic effects of tamoxifen are complex and may involve a combination of estrogen receptor-mediated hormonal effects as well as the metabolic activation of tamoxifen to reactive electrophiles that are genotoxic. Moreover, a significant population of patients develop clinical resistance to tamoxifen, which leads to breast cancer recurrence and a decrease in patient survival. Therefore, the goal of the current study was to examine the interactions of major metabolites of tamoxifen with the human cytosolic sulfotransferases hSULT2A1, hSULT1E1, and hSULT1A1*1.

Changes in the catalytic activity of hSULT2A1 by tamoxifen metabolites may inhibit the formation of the genotoxic α-sulfooxy tamoxifen intermediate catalyzed by this enzyme. Moreover, tamoxifen metabolites might interfere in the inactivation of hydroxysteroids catalyzed by hSULT2A1 as a part of the variable responses to tamoxifen therapy. Endoxifen was the most potent inhibitor of the hSULT2A1, which suggests that this metabolite may inhibit the role of hSULT2A1 in the metabolic pathway for genotoxicity that is seen with tamoxifen. *N*-desmethyltamoxifen (N-desTAM) was a substrate for the hSULT2A1, and the product of this reaction, *N*-desmethyltamoxifen sulfamate (N-desTAM-S), displayed greater inhibition of the enzyme than its unconjugated precursor. Thus, endoxifen, N-desTAM, and N-desTAM-S might serve protective roles in some tissues as they may inhibit the role of hSULT2A1 in the genotoxicity of tamoxifen.

Metabolites of tamoxifen were then examined as inhibitors of hSULT1E1 and hSULT1A1*1 due to the roles of these enzymes in the inactivation of estrogens. Each of the metabolites studied were weak inhibitors of hSULT1E1; thus, endoxifen is not likely to promote increased estrogen signaling in breast tissue when administered as an independent breast cancer therapeutic agent in ongoing clinical trials. However, 4-

hydroxytamoxifen (4-OHTAM) was a very potent inhibitor of hSULT1A1*1 when examined with estradiol as substrate. This suggests the potential for 4-OHTAM to interfere in estrogen metabolism in tissues where hSULT1A1*1 is expressed and hSULT1E1 is not. This information will be useful when interpreting the clinical trials of endoxifen and will aid in the design of related molecules

TABLE OF CONTENTS

LIST OF TABLES

LIST OF FIGURES

LIST OF ABBREVIATIONS

3β-HSD	3β-hydroxysteroid dehydrogenase
4-OHTAM	4-Hydroxytamoxifen
4-OHTAM-S	4-Hydoxytamoxifen sulfate
17β-HSD	17β-hydroxysteroid dehydrogenase
α-OHTAM	α-Hydroxytamoxifen
AI	Aromatase Inhibitor
AICc	Corrected Akaike Information Criterion
BCPT	Breast cancer prevention trial
BSA	Bovine Serum Albumin
cDNA	Complimentary deoxyribonucleic acid
CH_2Cl_2	Dichloromethane (methylene chloride)
CYP	Cytochrome P450
DCNP	2,6-Dichloro-4-nitrophenol
DE-52	Diethylaminoethyl cellulose
DHEA	Dehydroepiandrosterone
DHEA-S	Dehydroepiandrosterone sulfate
^{3}H-DHEA	Tritiated Dehydroepiandrosterone
DiMeIm	1,2-Dimethylimidazole
DMSO-d*6*	Deuterated dimethylsulfoxide
DTT	Dithiothreitol
E1	Estrone
E2	Estradiol
E3	Estriol
E-64	Trans-epoxysuccinyl-*L*-leucylamido-(4-guanidino)-butane
E. coli	Escherichia coli

ER	Estrogen Receptor
ESI-MS	Electrospray ionization mass spectrometry
Endoxifen	4-Hydroxy-*N*-desmethyltamoxifen
FDA	U.S. Food and Drug Administration
FMOs	Flavin-containing monooxygenases
HA	Hydroxyapatite
HER2	Human epidermal growth factor receptor 2
HPLC	High perfomance liquid chromatography
hSULT1A1*1	Human phenol sulfotransferase variant 1
hSULT1E1	Human estrogen sulfotransferase
hSULT2A1	Human hydroxysteroid sulfotransferase
IARC	International agency for research on cancer
IC50	Half-maximal inhibitory concentration
IPTG	Isopropyl-1-thio-D-galactopyranoside
Kd	Dissociation constant
kDa	Kilodalton
Ki	Inhibition constant
kcat	Catalytic turnover (turnover number of an enzyme)
kcat/Km	Catalytic efficiency
Km	Michaelis-Menten constant
KOH	Potassium hydroxide
LB	Luria broth
LC-MS	Liquid chromatography mass spectrometry
MeOH	Methanol
MeOD	Deuterated methanol
N-desTAM	*N*-desmethyltamoxifen
N-desTAM-S	*N*-desmethyltamoxifen sulfamate

NH_4CO_2H	Ammonium formate
NMR	Nuclear magnetic resonance
NSABP	National surgical adjuvant breast and bowel project
PAP	Adenosine 3'-5'-diphosphate
PAPS	3'-Phosphoadenosine-5'-phosphosulfate
[^{35}S]-PAPS	Radiolabeled [^{35}S]-3'-Phosphoadenosine-5'-phosphosulfate
PCB	Polychlorinated biphenyl
PCR	Polymerase chain reaction
PMSF	Phenylmethyl sulfonyl fluoride
pNP	Para-nitrophenol
pNPS	Para-nitrophenyl sulfate
PREG	Pregnenolone
PREG-S	Pregnenolone sulfate
^{3}H-PREG	Tritiated pregnenolone
r^2	Conventional correlation coefficient
rHSTa	Rat liver hydroxysteroid sulfotransferase
SDS-PAGE	Sodium docecyl sulfate-polyacrylamide gel electrophoresis
SERM	Selective estrogen receptor modulator
STAR	Study of tamoxifen and raloxifene
STS	Steroid sulfatases
SULT	Sulfotransferase
TAM-NO	Tamoxifen-*N*-oxide
TB	Terrific Broth
TLC	Thin layer chromatography
Tris-HCl	Tris (hydroxymethyl)aminomethane hydrochloride
Vmax	Maximum enzyme velocity
Zn	Zinc

CHAPTER 1

INTRODUCTION

Breast Cancer Prevalence and Disease Stages

Breast cancer is a disease characterized by abnormal and rapid cellular proliferation of luminal mammary epithelial cells in breast tissue and is currently the most common form of cancer among women in the U.S. (1). In 2013, an estimated 232,340 new cases of breast cancer and 39,620 deaths were expected for diagnosed women according to the American Cancer Society (2), and about 1 in 8 American women (just under 12%) will develop the disease in their lifetime (3). Breast cancer has been documented in men (4, 5), however, the lifetime risk of a man developing the disease is only 1 in 1000 (3) with 2,240 new cases of breast cancer and 410 deaths expected in diagnosed men as of 2013 (2).

Breast cancer progresses in 5 stages, as described by the National Cancer Institute (6), and usually begins with the formation of a lump or tumor underneath the breast, which can spread into nearby tissues, lymph vessels, or through the blood. In stage 0 breast cancer the abnormal cells have not spread beyond the lining of the breast. This stage is classified as "noninvasive" and is usually detected accidently during a biopsy of an unrelated breast lump. Stage 1 breast cancer is subdivided into two categories, 1A and 1B: in stage 1A the tumor size is 2 cm or less and has not spread to other parts of the body whereas the tumor size in stage 1B measures 2 cm or less and is sometimes accompanied by small clusters of breast cancer cells that have spread to the lymph nodes. Patients with stage 1 breast cancer generally have a good prognosis and are treated with adjuvant hormone therapy, and in some cases, radiation therapy. Stage 2 breast cancer is divided into two categories, 2A and 2B: in stage 2A either the tumor is 2 – 5 cm in size and has not spread to the lymph nodes or there is cancer in the lymph nodes that is not accompanied by a tumor in the breast; in stage 2B, the breast tumor is 2 - 5 cm in size and is accompanied with small clusters of breast cancer cells in the lymph nodes, axillary lymph nodes, or lymph nodes near the

sternum. As seen in those with stage 1 breast cancer, patients diagnosed with stage 2 of the disease generally have a good prognosis and are treated with adjuvant systemic therapy such as hormone therapy and radiation therapy; however, local therapy such as surgery is also a treatment option for stage 2 breast cancer. The third stage of breast cancer is divided into three categories, 3A, 3B, and 3C: in stage 3A, either a tumor of any size is found in the breast and the cancer has spread up to 9 axillary nodes, or the tumor is larger than 5 cm and is accompanied by small clusters of breast cancer cells in lymph nodes near the sternum; in stage 3B, a tumor of any size has spread to the chest wall (causing swelling and ulcers) or the cancer has spread to the skin (inflammatory breast cancer); in stage 3C, a tumor of any size has spread to the chest wall and to 10 or more axillary lymph nodes. Stage 3 breast cancer is usually treated with chemo- and radiation-therapy prior to surgery; and when the cancer has spread beyond the breast into other areas of the body such as the bones, brain, lungs, or liver it is classified as stage 4. This stage is treated with hormonal, chemo, targeted, and radiation therapy. Women with stage 4 breast cancer have a much lower 5-year survival rate (22%) than women diagnosed with breast cancer at earlier stages (7).

Breast Cancer Types and Current Therapies

Breast cancer is characterized according to the cancer cell genotype and requirements for proliferation. These cells are classified as hormone-receptor-positive (estrogen or progesterone receptor), HER2 positive (human epidermal growth factor receptor 2), which promotes cancer cell proliferation (8), and triple positive (all of the above), or triple negative (none of the above). Estrogen-receptor-(ER)-positive breast cancer accounts for nearly 75% of all breast cancer cases (9, 10) and is commonly treated with endocrine agents such as aromatase inhibitors (AIs) and selective estrogen receptor modulators (SERMs)

Aromatase inhibitors effectively inhibit the synthesis of estrogen in postmenopausal women by selectively binding to the active site of estrogen synthase (aromatase) (11). This function inhibits the catalytic activity of the aromatase in the conversion of testosterone into estradiol and deprives the cancerous cells of an estrogen source. The chemical structures of aromatase inhibitors are illustrated in Figure 1. Non-steroidal aromatase inhibitors such as Letrozole and Anastrozole bind reversibly to aromatase through competitive inhibition, whereas steroidal inhibitors such as exemesthane (Aromasin) bind irreversibly to the enzyme as a suicide inhibitor (12). While systemic studies have shown that aromatase inhibitors significantly prolong disease-free survival and reduce the recurrence of breast cancer in ER-positive patients (13, 14), AIs are limited in their use as endocrine agents due to musculoskeletal side effects such as arthralgia (15, 16) and bone fractures (17) that often result in AI discontinuation (18).

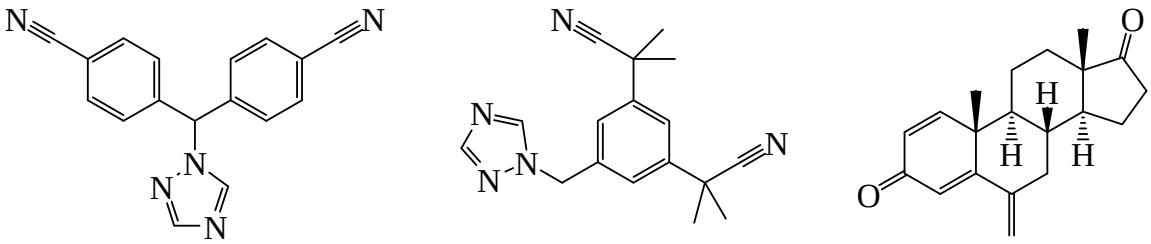

Figure 1. Chemical structures of aromatase inhibitors utilized in breast cancer treatment.

SERMS are a class of endocrine agents that act directly on the estrogen receptor. The mechanism(s) of SERMs are complex and may involve a combination of actions such as inhibition of estrogen-induced DNA transcription (19), growth factor secretion (20), regulation of apoptosis (21), as well as non-genomic mechanisms such as reducing membrane fluidity (22, 23), inhibition of calcium channels (24, 25), and inhibition of P-glycoprotein-mediated drug transport as a mechanism to reverse multidrug resistance (26).

First generation SERMSs consist of triphenylethylene derivatives such as tamoxifen (Nolvadex) and torimefene (Fareston), whereas second generation SERMs are made up of benzothiophene derivatives such as raloxifene (Evista). Third generation SERMs includes bazedoxifene, lasofoxifene, and ospemifene; however, these therapies are not approved for the treatment of breast cancer.

Tamoxifen Therapy and Pharmacology

Tamoxifen has been successfully utilized for decades in the treatment and prevention of estrogen-dependent breast cancer in women at high risk of developing the disease as well as a palliation for those with metastatic cancer (27-32). Tamoxifen was originally approved in 1977 by the U.S. Food and Drug Administration (FDA) for the treatment of advanced breast cancer, and was later approved as an adjuvant therapy in combination with chemotherapy (1985) or alone (1986) for the treatment of node-positive breast cancer in postmenopausal women (33). In 1990, approval was obtained from the FDA for the use of tamoxifen in pre- and postmenopausal women with node-positive-ER-positive breast cancer, and in 1993, the FDA approved the indication for the use of tamoxifen to treat advanced breast cancer in men (33). In a landmark Breast Cancer Prevention Trial (BCPT) conducted by researchers from the National Surgical Adjuvant Breast and Bowel Project (NSABP), tamoxifen was shown to reduce the incidence of invasive and non-invasive breast cancer by 49% and 45%, respectively, in women at high risk for developing the disease (30). However, results from this study also demonstrated that the net benefit of tamoxifen therapy was limited by age, race, and the level of breast cancer risk.

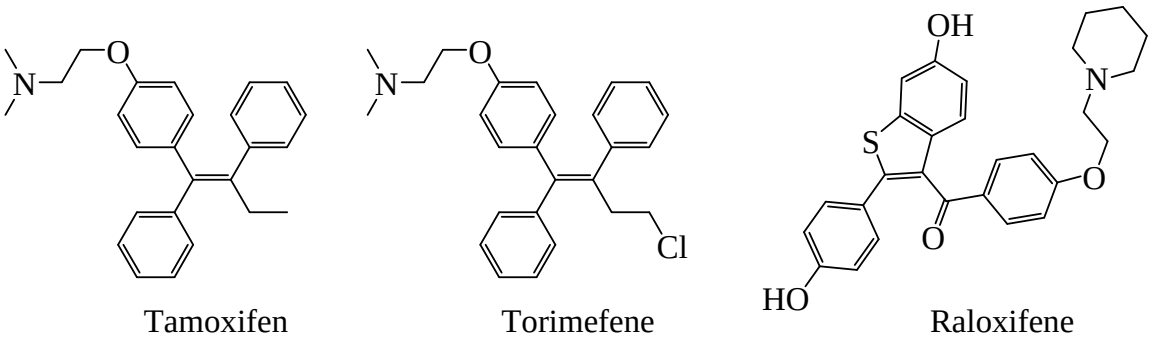

Figure 2**.** Chemical structures of SERMs utilized in breast cancer treatment.

Tamoxifen is generally well tolerated in most women, but some adverse events do occur with tamoxifen. For example, tamoxifen therapy is associated with an increased risk for the development of deep venous thrombosis and pulmonary embolism (34-36). Hot flashes are also reported in tamoxifen users (28, 31) and are sometimes treated by the co-administration of selective serotonin re-uptake inhibitors (SSRIs); however, these agents may affect the efficacy of tamoxifen by inhibiting the activity of CYP2D6, an enzyme that is important in final-step conversion of tamoxifen into one of its active metabolites (37). Of serious concern for a subpopulation of patients is an increased risk for the development of endometrial cancer as a side effect of tamoxifen therapy (38, 39). The carcinogenic effects of tamoxifen are complex and may include a combination of ER-mediated hormonal effects and metabolic activation of tamoxifen metabolites to electrophiles that are genotoxic (40-42). Toremifene, a chlorinated analogue of tamoxifen **(**Figure 2), was FDA-approved in 1997 as an anticancer therapeutic agent and was observed to be similar to tamoxifen in the treatment of pre- and postmenopausal early-stage ER-positive breast cancer (43-46); however, toremifene has lower genotoxicity than tamoxifen (47, 48) and may be considered as a safer alternative by avoiding the development of endometrial cancer. Moreover, raloxifene (Figure 2) was shown to significantly reduce the risk of ER-positive breast cancer in randomized clinical trials (49, 50) and was later approved in 2007

for the treatment and prevention of invasive breast cancer in postmenopausal women at high risk of developing the disease. While raloxifene therapy is associated with an increased risk of venous thromboembolic disease (50), it does not increase the risk of endometrial cancer that is seen in tamoxifen-treated women. Raloxifen was previously evaluated relative to tamoxifen for the treatment of post-menopausal breast cancer in the Study of Raloxifene and Tamoxifen (STAR) conducted by the NSABP (51). Results from this study determined raloxifene to be as effective as tamoxifen in reducing the risk of invasive breast cancer, with fewer cases of uterine cancer in raloxifen-treated women compared to those who received tamoxifen.

Tamoxifen inhibits estrogen-induced DNA transcription as its primary function in breast tissue (Figure 3). Tamoxifen also induces apoptosis (52), possibly through the down-regulation of anti-apoptotic proteins (53), and invokes transition delays in the G1-phase of the cell-cycle (54) to prevent cancer cell proliferation. In addition to its anti-estrogenic effects in the breast, tamoxifen has estrogenic activity in the bone and uterus (33) and thus can be classified as either an agonist or antagonist, depending on the tissue. The mechanism of uterine stimulation by tamoxifen is not completely understood, but studies have shown that a pure steroidal anti-estrogen (ICI 164,384) reversed the growth stimulation by 4-hydoxytamoxifen (a clinically active tamoxifen metabolite) in cultured endometrial and breast cells, which suggests that the agonist effects of tamoxifen are mediated through the estrogen receptor (55, 56). Watanabe *et al*. demonstrated that the agonist effects of tamoxifen vary with cell type, estrogen responsive element (ERE) context, and estrogen receptor subtypes, which might explain part of the tissue-specific effects of tamoxifen observed *in vivo* (57). As a SERM the agonist actions of tamoxifen have a favorable effect on lipids (58, 59) and may promote cardiovascular health. Moreover, these actions may preserve bone mineral density (60), which is important considering the use of tamoxifen in postmenopausal women who may be at high risk for osteoporosis. Unfortunately, the agonist activity of tamoxifen in the uterine tissue remains

a hurdle for tamoxifen therapy due to the potential for the development of endometrial cancer (61). This highlights the need for a SERM that provides neutral and anti-estrogenic activity in the endometrium and breast, respectively, but retains favorable tissue-selective estrogenic activity in bone and cardiovascular system (62). As summarized by Pinkerton *et al.* (63), it is unlikely that a single molecule will provide the beneficial effects of classical estrogens without increasing the risk of breast and uterine cancers, blood clots or stroke based on the pharmacology of current SERMS.

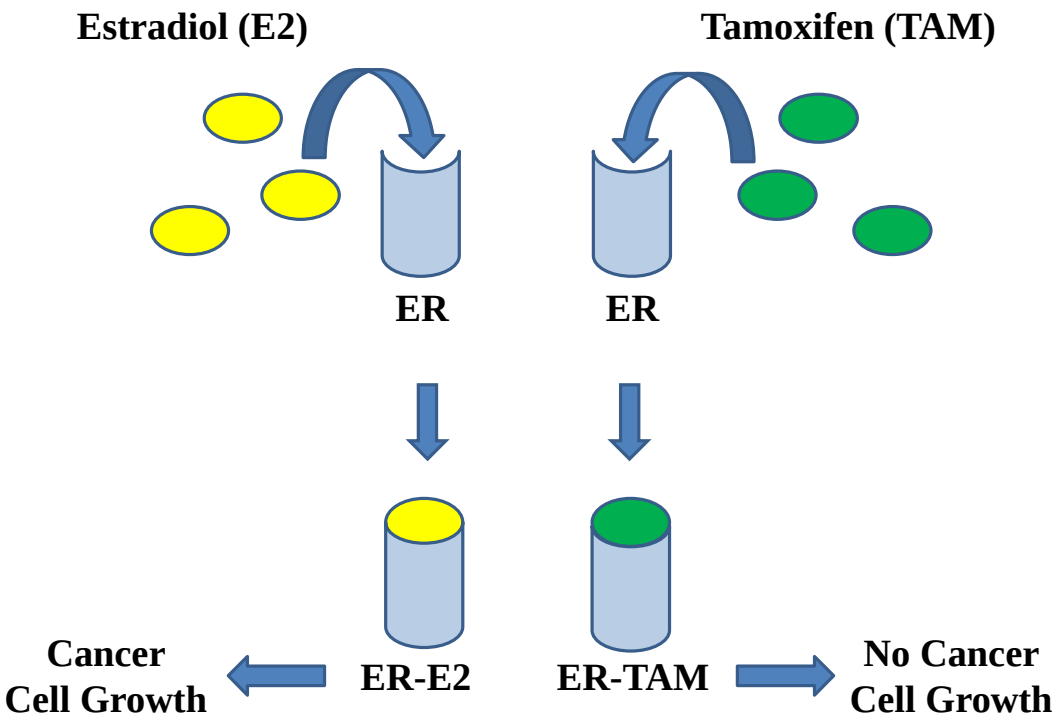

Note: Tamoxifen competitively binds to the estrogen receptor (ER) to inhibit cancer cell growth stimulation due to the binding of estradiol.

Figure 3. Illustration of the mechanism of action for tamoxifen in breast cancer cells.

Roles of Metabolism in the Therapeutic Action and Toxicity of Tamoxifen

Tamoxifen is classified as a pro-drug and must be converted into its active form(s) to elicit maximum efficacy. Tamoxifen is initially metabolized through oxidative reactions catalyzed by several forms of cytochrome p450 (CYP), and the chemical structures of these metabolites are shown in Figure 4. The most abundant of these initial metabolites in humans is *N*-desmethyltamoxifen (N-desTAM), which is formed via an oxidative demethylation reaction catalyzed by CYPs 2D6, 3A4, 1A1, and/or 1A2 (64, 65). N-desTAM is further oxidized at the para position in a reaction catalyzed by CYP2D6 to form 4-hydroxy-*N*-desmethyltamoxifen (endoxifen) (65). Endoxifen is a major, clinically active metabolite that is 100 times more potent as an anti-estrogen than tamoxifen itself, and is equipotent with another CYP-mediated oxidative metabolite, 4-hydroxytamoxifen (4-OHTAM) (66, 67). Although 4-OHTAM was the first metabolite of tamoxifen identified with high affinity for the ER (68), endoxifen was found to be present at higher serum concentrations than 4-OHTAM (69, 70) and is now considered to be the major metabolite responsible for the therapeutic action of tamoxifen. Moreover, endoxifen has been shown to target the ER for degradation, block ER transcriptional activity, and inhibit estrogen-induced breast cancer cell proliferation even in the presence of tamoxifen, N-desTAM, and 4-OHTAM (71). The microsomal flavin-containing monooxygenases (FMOs) catalyze oxidation of the tertiary amine of tamoxifen to form tamoxifen-*N*-oxide (TAM-NO) (72), a metabolite that is also of recent interest due to its potential role(s) in the activity of tamoxifen (69). Additional metabolic products of tamoxifen include the CYP3A4-mediated oxidative metabolite, α-hydroxytamoxifen (α-OHTAM) (73), as well as sulfate conjugates, glucuronide conjugates, and various minor metabolites (74).

Despite the beneficial effects of tamoxifen treatment in breast cancer, tamoxifen is toxic in the human endometrium and is currently listed as a human carcinogen by the International Agency for Research on Cancer (IARC) (75). One of the major potential

genotoxic species derived from tamoxifen is its α-sulfooxy metabolite (Figure 4) (40, 76). This metabolite is derived from the CYP3A4-catalyzed oxidation of tamoxifen to an allylic α-hydroxy derivative (α-OHTAM) that is then a substrate for the human hydroxysteroid sulfotransferase 2A1 (hSULT2A1) (76). The resulting sulfuric acid ester is a good leaving group and forms an electrophilic, resonance-stabilized carbocation intermediate that reacts with nucleophilic sites on DNA, thereby forming covalent tamoxifen-DNA adducts (76). The endometrial effect due to the metabolic activation of tamoxifen is plausible given the expression of CYP3A4 protein and hSULT2A1 mRNA in this tissue (77). Other proposed metabolic activation pathways involve the oxidation of 4-OHTAM and metabolite E (an *O*-dealkylated derivative of 4-OHTAM) to electrophilic quinone methides (78-80), as well as the conversion of 4-OHTAM to 3,4-dihydroxytamoxifen, which is then oxidized to a highly reactive *o*-quinone that binds to proteins and DNA (81, 82). The formation of tamoxifen-DNA adducts in the endometrium has been proposed to be a key step that leads to the formation of endometrial cancer in a small, but significant number of patients.

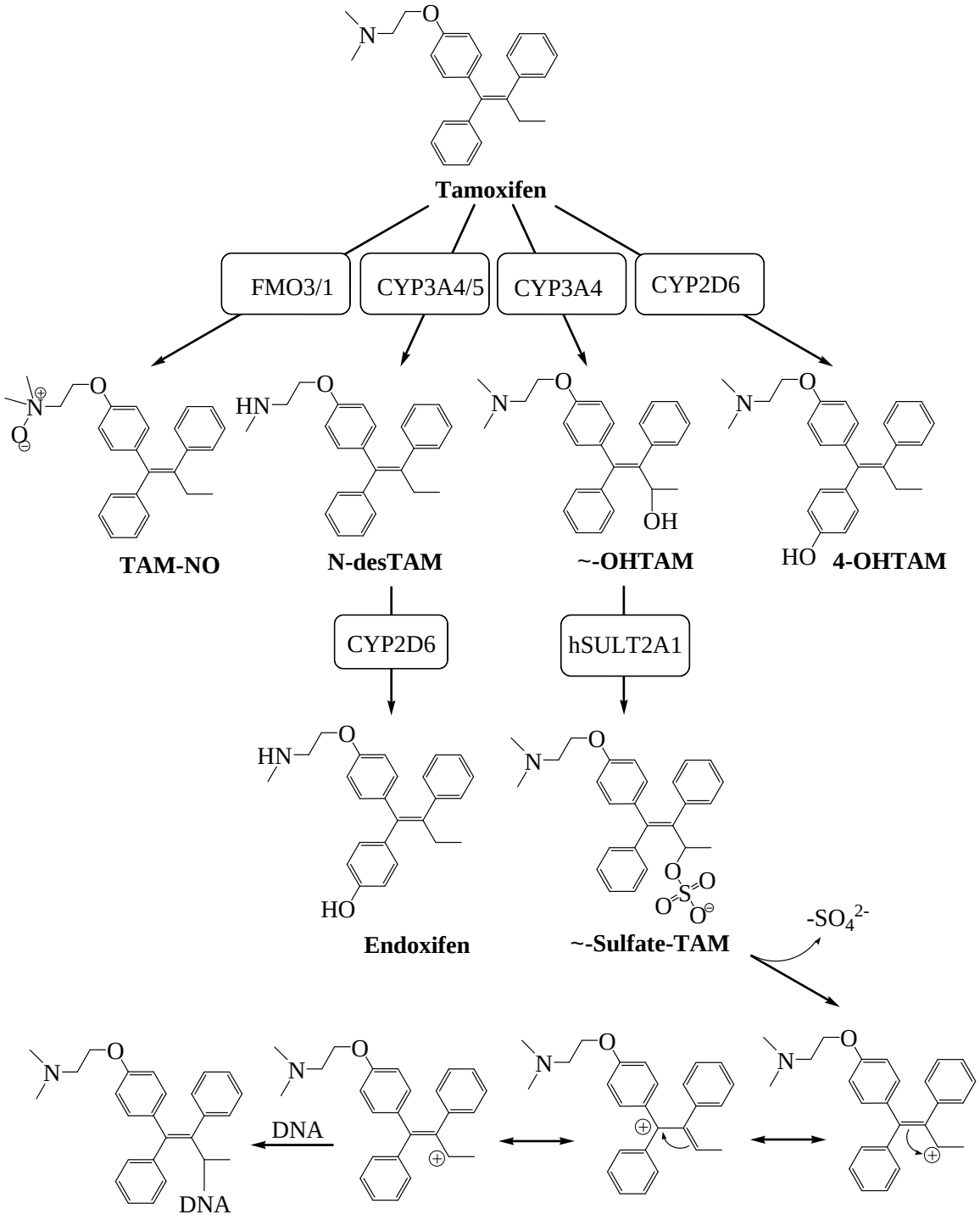

Figure 4. Tamoxifen metabolism and route of metabolic activation.

In addition to its endometrial effects in humans, tamoxifen causes DNA adducts in rat liver and is listed as a potent hepatocarcinogen in rodents (83, 84). Some studies suggest α-OHTAM is hepatotoxic in the absence drug-metabolizing enzymes (85), while others propose that the sulfation of α-OHTAM by rat liver hydroxysteroid sulfotransferase (rHSTa) is the major pathway of metabolic activation for DNA-alkylation in rat liver tissue (86). Randerath *et al*. demonstrated that the level of tamoxifen-DNA adducts in rodents decreased when co-administered with pentachlorophenol, a potent inhibitor of acetyltransferase, which suggests that acetylation could also be involved in the bioactivation of tamoxifen (87). However, Kim *et al*. did not detect DNA adducts in human or rat liver cytosols treated with α-OHTAM and acetyl CoA (coenzyme for acetyltransferase), but adducts were observed in cytosolic fractions incubated with PAPS (co-substrate for sulfotransferase), which suggest that tamoxifen-DNA adducts are derived from sulfation, not acetylation, of α-OHTAM. (88). It should also be noted, however, that pentachlorophenol may also inhibit hSULT2A1 in these studies, since it would also serve as a competing substrate for the enzyme (89). The exact cause for the species differences in the carcinogenic response to tamoxifen is unknown, although studies in human, rat, and mouse hepatocytes indicate a lower metabolic conversion of tamoxifen to α-OHTAM and lower sulfation of α-OHTAM in human hepatocytes (90) could be part of the reason why tamoxifen is not hepatotoxic in humans.

Tissue Distributions and Physiological Concentrations of Tamoxifen Metabolites

Metabolites of tamoxifen are distributed to a variety of tissues such as the lung, liver, brain, breast, pancreas, muscle, bone, and ovaries (91), and the tissue concentrations of the metabolites are reported to be up to 100-fold higher than those in serum (66, 91, 92). The average plasma concentrations of tamoxifen metabolites reported from several

investigators are summarized by Brauch *et al* (74), and these values are represented in the following table.

Compounds	**Mean Plasma Conc. (nM)**	**Effect on the ER**
Tamoxifen	190 – 420	Weak antagonist
N-desTAM	280 – 800	Weak antagonist
Endoxifen	14 – 130	Strong Antagonist
TAM-NO	15 – 24	Weak Antagonist
4-OHTAM	3 – 17	Strong Antagonist
α-OHTAM	1	None

Note: Adapted from (74) with modifications.

Table 1. Ranges of the average plasma concentrations of tamoxifen and its major metabolites.

Clinical Trials of Endoxifen

Nearly half of patients who are treated with tamoxifen for ER-positive cancer fail to respond to the therapy, and those that do respond generally acquire resistance to tamoxifen during treatment. As summarized by Dorssers *et al.* (93), resistance to tamoxifen could be related to changes in the tumor cell environment, alteration in the structure and function of the ER, or changes in the pharmacology of tamoxifen itself. Pharmacogenetic differences may also contribute to the variability in responses to tamoxifen and its clinical effectiveness (74, 94-104). While such differences may be of use in individualizing dosages of tamoxifen, another strategy has been to investigate the administration of endoxifen as an antitumor drug through clinical trials (NCT01327781 and NCT01273168; ClinicalTrials.gov). These studies anticipate that endoxifen therapy will be more effective than tamoxifen in the treatment of breast cancer by eliminating the

need for metabolic activation by CYP2D6, which is polymorphic (74, 105). Moreover, there is no literature evidence that supports the role of endoxifen in tamoxifen-induced toxicity or its involvement in the endometrial side effects of tamoxifen. Thus, endoxifen may be a promising candidate as a safer and more effective anticancer therapeutic agent.

Introduction to Sulfotransferases

Sulfation represents a major route of metabolism for many endogenous and exogenous molecules, hormones, drugs, toxins, peptides, and lipids. This reaction was first observed in 1876 by Bauman who detected phenyl sulfate in urine samples of patients treated with phenol (106). In later years, the name "sulfotransferase" was used for those enzymes responsible for catalyzing the sulfation of molecules in biological systems, which currently includes bacteria, insects, plants, and mammals (107-109). These enzymes are localized in the cell cytosol or the within the membranes of the golgi apparatus, and they function by catalyzing the transfer of a sulfuryl moiety from the natural donor substrate PAPS (3'- phosphoadenosine-5'-phosphosulfate) to an acceptor molecule to form a sulfuric acid (sulfate) ester and PAP (adenosine-3', 5'-diphosphate) (Figure 5). Sulfotransferases that are bound in the membrane of the Golgi apparatus are responsible for the sulfation of macromolecules such as peptides, proteins, lipids, and carbohydrates to regulate their structural characteristics and physiological function (110, 111), whereas the mammalian cytosolic sulfotransferases (SULTs) are responsible for the sulfation of xenobiotics (i.e. drugs) and small endogenous molecules such as steroids, bile acids, and neurotransmitters to regulate steroid hormone homeostasis as well as other physiological processes (112). Sulfation often serves as a mechanism of inactivation for elimination by forming water-soluble products that are excreted in the urine, although minoxidil-sulfate is one example of an exception to this (113). Additionally, some SULT-catalyzed reactions can lead to the metabolic activation of xenobiotics through the formation of electrophilic sulfuric acid esters (110, 114).

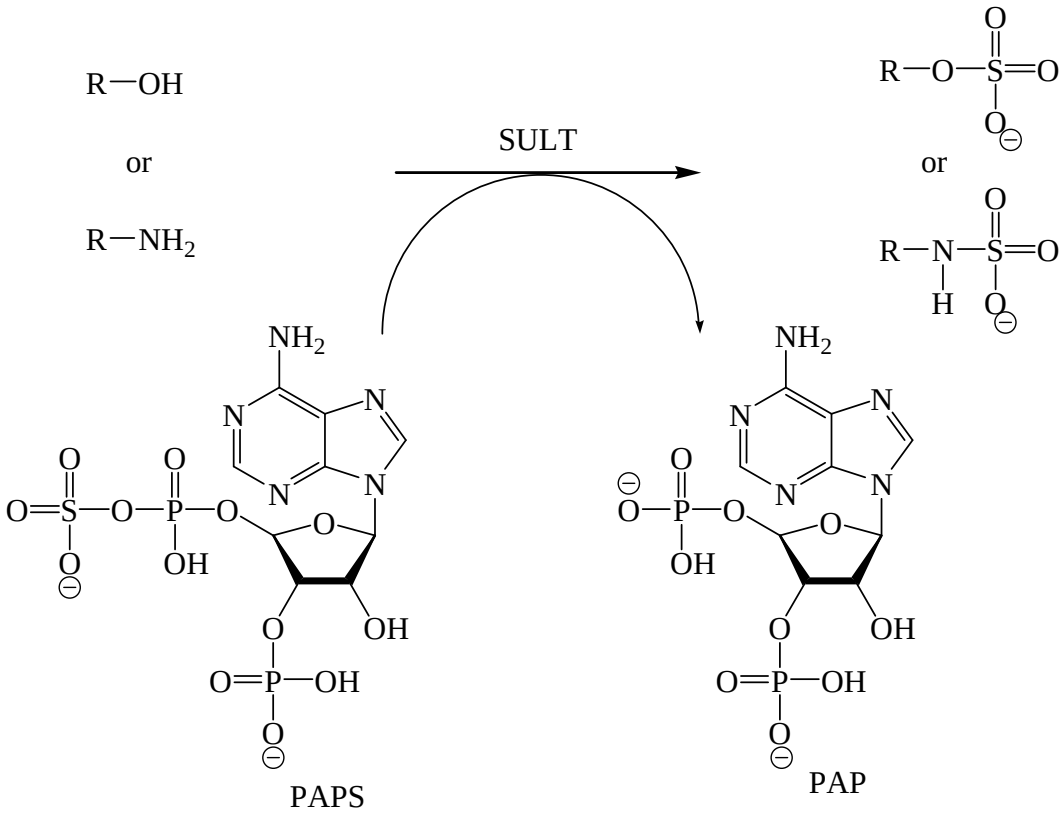

Note: The sulfuryl acceptor is represented by R-OH (phenols and alcohols) or R-NH2 (amines). PAPS is the obligatory donor substrate and the products formed are PAP and either a sulfuric acid ester (sulfate) or sulfamate.

Figure 5. The general sulfation reaction catalyzed by sulfotransferases

Nomenclature of Sulfotransferases

Until the recent decade the nomenclature for sulfotransferases was arbitrary at best, confusing at worst. The previous naming system for SULTs was based of the most-preferred substrate for an individual SULT, such as the dehydroepiandrosterone (DHEA) SULT or the estrogen (EST) SULT. However, most of these enzymes have overlapping substrate specificities that made it difficult to correctly identify a particular SULT member among other SULTs, and this was further complicated because individual research groups adapted their own abbreviations for SULTs. For example, the DHEA sulfotransferase is synonymous to both the bile acid sulfotransferase and hydroxysteroid sulfotransferase,

which are abbreviated in literature as DHEA-ST, HST or ST2A1. Nagata et al (109) created a nomenclature system whereby the prefix "ST" preceded cytosolic SULT families. Their system divided gene families into subfamilies based on sequence similarity and substrate specificity, but conflicted with the nomenclature system adopted for the human genome and was poorly utilized in the research field of SULTs. In 2004, Blanchard *et al*. published a nomenclature system for the cytosolic SULT superfamily that is now widely accepted by the scientific community (108). This system was applied to 65 SULT cDNAs and 18 SULT genes from eukaryotic organisms and states that SULTs sharing at least 45% amino acid sequence identity are members of the same family, whereas those sharing at least 60% identity are members of the same subfamily. SULT families and SULT subfamilies are designated by an Arabic numerical and alphabetical character, respectively, and unique isoforms are identified by an additional Arabic numerical following the subfamily designation. For example, hSULT1E1 is a human cytosolic sulfotransferase of family 1, subfamily E, and isoform 1.

Sulfotransferase Families

The human cytosolic SULT gene superfamily is comprised of 4 different families: SULT1, SULT2, SULT4, and SULT6. Family 1 SULTs exhibit the widest tissue distribution of any cytosolic SULT family (112) and utilize a broad range of substrates such as phenols, catechols, oximes, benzylic alcohols, iodothyronines, N-hydroxyarylamines, as well as steroid hormones such as estrone and estradiol (115-123). This family of SULTs contains the human estrogen sulfotransferase (hSULT1E1) which has been extensively studied due to its involvement in the regulation of estrogen metabolism in ER-positive breast cancer (124-127). Family 2 SULTs catalyze the sulfation of hydroxysteroid hormones such as pregnenolone (PREG) and DHEA, alcohols, bile acids, and some aliphatic amines (128-132). The human hydroxysteroid sulfotransferase 2A1 (hSULT2A1) belongs to this family of SULTS and is one of the most highly expressed

isoforms in human liver in addition to SULTs 1A1 and 1E1. Family 4 SULT members were cloned from both human and rat brain cDNA libraries by Falany *et al*. (133) and have unknown substrate specificity and a selective expression in brain tissue (133, 134). There is evidence for only one member of the family 6 SULT (SULT6B1). Although the substrate specificity for SULT6B1 has not been fully characterized, expression-profiling studies show an expression of the enzyme in the human testis (135).

Structural Properties of Sulfotransferases

SULTS are globular proteins with a characteristic α/β fold and a central 4-5 stranded parallel β-sheet that is bordered by α helices. The β-sheet forms the catalytic site and the binding region of PAPS, which consists of an N-terminal 5'-phosphosulfate binding (5'-PSB) motif, a central 3'-phosphate-binding (3'-PB) sequence, and a β-strand-loop-helix (P-loop). This binding region of PAPS is highly conserved in all SULTs at the amino acid level (111) and is utilized in the identification of newly cloned SULTS from cDNAs (111, 136). The substrate binding region of each SULT has structural differences that convey the substrate specificity of the enzyme. For example, the L-shaped substrate binding pocket of hSULT1A1 is quite flexible and can undergo significant deformations to accommodate a variety of structurally different substrates (137, 138). Other enzymes such as the rat hydroxysteroid sulfotransferase STa have a stereoselective substrate specificity (139), likely due to steric effects at the substrate binding region of this protein. Most cytosolic SULTs are dimers in their catalytically active form due to the hydrophobic interactions of a conserved, zipper-like peptide sequence (KXXXTVXXXE) that mediates homo- as well as hetero-dimerization between monomers (140). Dimerization has been shown to play a role in the kinetic mechanism and stability of some human cytosolic SULTs (141, 142).

Substrate Inhibition in SULT-Catalyzed Reactions

Substrate inhibition is a characteristic phenomenon of many SULT-catalyzed reactions, wherein the catalytic rate of the enzyme decreases at high substrate concentrations (Figure 6). This is often explained by the formation of non-productive dead-end complexes, allosteric regulation, and non-productive substrate binding. Ternary dead-end complexes form when a substrate binds to a product-bound enzyme before the product has left the active site of the enzyme; increasing the substrate concentration increases the frequency of dead-end complexes and slow the catalytic activity of the enzyme. These

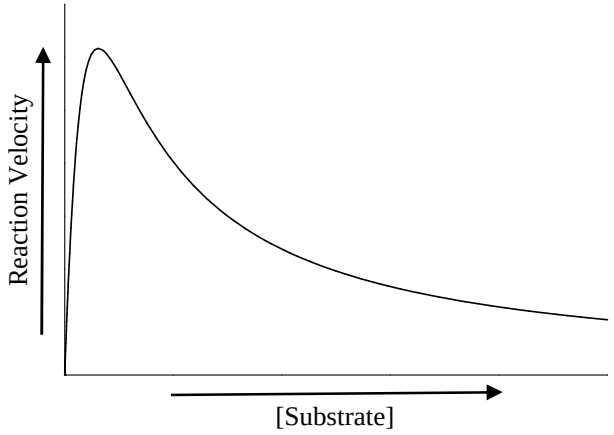

Figure 6. A representation of substrate inhibition in an enzyme-catalyzed reaction

complexes have been observed in kinetic studies with hSULT2A1 (129) and hSULT1E1 (143). For hSULT1E1, it has been postulated that two molecules of substrate and one molecule of PAPS bind to one subunit of hSULT1E1 to form an [E-PAPS-S-S] complex, which assumes that substrate inhibition occurs through binding at an allosteric site since no crystallographic evidence exists for two molecules of estradiol simultaneously occupying the substrate-binding site of the enzyme. Other studies have utilized crystallography to show that DHEA binds in a non-productive orientation to the active site

of hSULT2A1 (144), and the same has been observed for the binding of estradiol to hSULT1A1 (117).

Human Hydroxysteroid Sulfotransferase 2A1 (hSULT2A1)

Human SULT2A1 catalyzes the sulfation of various endogenous and exogenous molecules (112, 145-147) and is involved in the detoxication of xenobiotics (i.e. drugs) that contain alcohol and phenol functional groups. Moreover, it catalyzes the sulfation of DHEA and PREG (110, 148), two of the most abundant circulating steroid hormones in humans. DHEA, PREG, and their corresponding sulfates are important in fetal development (149), brain development (150), cognition (151), age (152), cardiovascular function (153), and other processes that are involved in normal physiological function. For example, changes in the endogenous concentrations of DHEA and DHEA-S are associated with disease states such as rheumatoid arthritis, schizophrenia, liver disease, lupus, and renal disease (154). Steroid sulfoconjugates have a greater half-life and bioavailability in blood circulation through interactions with serum binding proteins (154). Thus, hSULT2A1 is important in the distribution and maintenance of steroid hormone homeostasis.

Cloning and Biochemical Characterization of hSULT2A1

In 1989, Falany and co-workers were the first to purify and characterize hSULT2A1 from human liver cytosol (148). Their studies indicated an enzyme with a subunit molecular mass of 35 kDa that was catalytically active as a homodimer in solution. The interface between subunits of the dimer was elucidated in later studies as the KTVE dimerization sequence motif (140). Human SULT2A1 was successfully cloned from human liver cDNA by PCR amplification, and subsequently expressed and purified from COS-1 cells by Otterness *et al*. (155). The resulting protein displayed sulfating activity towards DHEA and was determined to be 285 amino acids in length and encoded by 855

nucleotides from human liver cDNA. DHEA is the natural endogenous substrate for hSULT2A1, and it is the preferred substrate for use in purification and kinetic studies with the enzyme (129, 156, 157). Chang *et al*. also determined the pH optimum for hSULT2A1 (pH 7 to 8) as well as the optimum temperature for the enzyme (40ºC) when examined with DHEA as substrate (156). The enzyme is sensitive to 2,6-dichloro-4-ninitrophenol (DCNP) inhibition (158) and displays substantial substrate inhibition during DHEA sulfation with maximal enzyme activity at DHEA concentrations from 2 – 4 µM (129).

Tissue Distribution of hSULT2A1

DHEA-sulfate (DHEA-S) is abundant in both the human fetal and adult adrenal gland due to the high expression of hSULT2A1 in these tissues (148, 159-161). The enzyme is also highly expressed in the liver (162), intestines (163), and the stomach lining (164). Expression of hSULT2A1 in the human liver is associated with the sulfation and detoxication of bile acids (162), whereas the expression in the gastrointestinal tract is associated with the detoxication of xenobiotics due to the broad substrate specificity of hSULT2A1 (165). Other tissues such as the ovary and prostate express hSULT2A1 at lower levels (166), and recent studies show an expression of the enzyme in endometrial glandular and surface epithelium (77, 167).

Substrate Specificity of hSULT2A1 and its Role in Drug Metabolism and Detoxication

Human SULT2A1 is the only family 2 SULT isoform identified in human liver (148) and utilizes a broad range of substrates. Common substrates for this enzyme include bile acids such as cholic acid, lithocholic acid, and deoxycholic acid (128). Bile acids are the toxic byproducts of steroid biosynthesis, and these molecules have been implicated in the pathogenesis of diseases such as liver cirrhosis (168), cholestasis (169), and colorectal cancer (170, 171). The sulfation of bile acids by hSULT2A1 serves as a mechanism to

prevent their toxic action and accumulation in tissue. Other substrates for hSULT2A1 include therapeutic agents such as acetaminophen (172), tibolone (173), 4-OHTAM (174), as well as environmental toxicants such as hydroxylated polychlorinated biphenyls (OHPCBs) (175), and pentachlorophenol (89). Moreoever, hSULT2A1 is responsible for the N-sulfoconjugation of desipramine and quinolone drugs such as ciprofloxacin, moxifloxacin, and garenoxacin (132), owing to its role in the sulfation of amines. The chemical structures of some representative substrates for hSULT2A1 are shown in Figure 7.

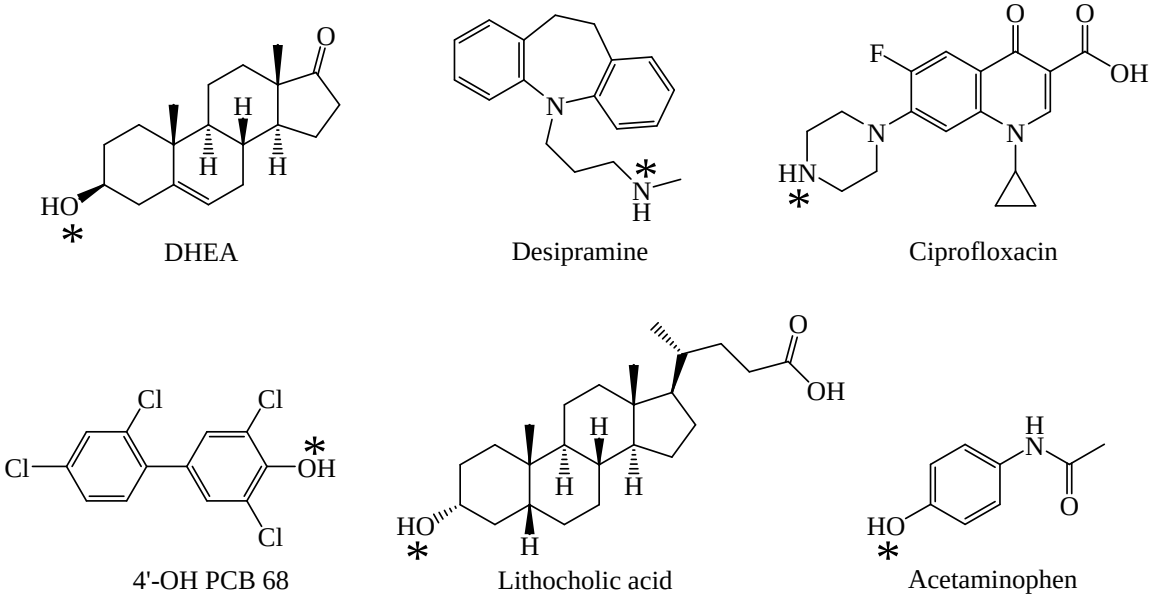

Note: The asterisk (*) marks the position of sulfoconjugation by hSULT2A1

Figure 7. Chemical structures of several representative substrates for hSULT2A1.

Roles of hSULT2A1 in Steroid Metabolism and Carcinogenesis

DHEA and PREG are two of the best known substrates for hSULT2A1 and their sulfation *in vivo* is important for the bio-synthesis of other steroid hormones such as androgens and estrogens. PREG is derived from the CYP-catalyzed cleavage of cholesterol and undergoes a two-step enzymatic conversion to form DHEA, which is then converted to DHEA-S by hSULT2A1 (154) (Figure 8). DHEA-S circulates in the blood where it is taken up by peripheral and adrenal tissues and hydrolyzed back to DHEA by sulfatase enzymes (154). DHEA and DHEA-S serve as the precursors to approximately 50% of androgens in adult men, 75% of active estrogens in premenopausal women, and nearly 100% of active estrogens in postmenopausal women (176). Moreover, DHEA-S and PREG-S are important in fetal maturation and serve as precursors for the placental production of estrogen and progesterone during pregnancy (177).

Despite the function of hSULT2A1 in steroid metabolism, the sulfation of some benzylic and allylic alcohols catalyzed by this enzyme can sometimes generate electrophilic products that are reactive towards DNA and proteins (85, 145, 178-182). As seen in Figure 4 with the sulfation of α-OHTAM, the sulfate moiety becomes a good leaving group when facilitated by induction and resonance-stabilization (114). As a result, a strongly electrophilic carbocation is formed that can then react with nucleophilic sites on DNA and proteins, and the accumulation of adducts in genomic DNA is proposed to be a key step in the development of malignancy and cancer (183-185).

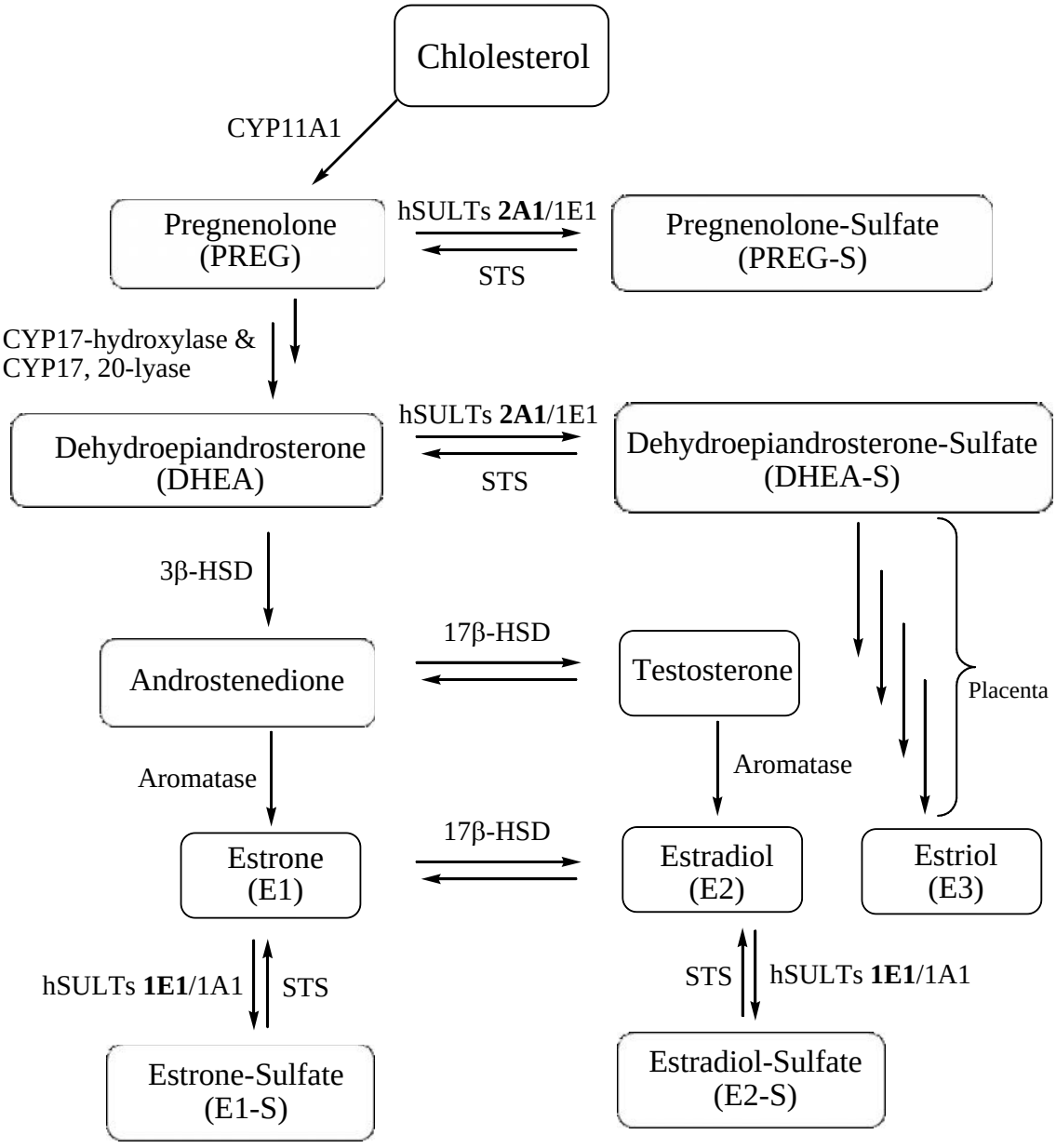

Note: 3β-HSD = 3β hydroxysteroid dehydrogenase, 17β-HSD = 17β hydroxysteroid dehydrogenase, STS = steroid sulfatase. The major hSULT involved in each step of the metabolic pathway is highlighted in bold font.

Figure 8. A general metabolic pathway for the biosynthesis of selected hydroxysteroids (DHEA and PREG) and estrogens (estrone, estradiol, estriol).

Human Estrogen Sulfotransferase 1E1 (hSULT1E1)

Human SULT1E1 catalyzes the sulfation of estrogens and various endogenous and exogenous molecules that contain phenol functional groups. Although known to catalyze the sulfation of DHEA and PREG, hSULT1E1 functions primarily in the sulfation of estrone, estradiol, and estriol. Estradiol exerts its effects to promote cell growth and proliferation when bound to the ER (186). Estradiol is conjugated by hSULT1E1 to form estradiol-sulfate, which prevents the parent hormone from binding to, and thereby activating, the ER. This mechanism protects the peripheral tissues from excessive estrogenic effects and is associated with tumor regression in ER-dependent carcinomas (187). Estrogen is important in regulating biological responses in normal and cancerous endocrine tissues, such as the breast and endometrium (188). Moreover, estrogen is important in fetal maturation, but excessive exposure has been linked to abnormal development and mammary morphology after birth (189, 190). Therefore, hSULT1E1 plays an important role in the regulation of estrogen metabolism and homeostasis in adults and the human fetus.

Estrogen Biosynthesis and Mechanism of Action

Estrogens are synthesized in the ovaries and peripheral tissues in premenopausal women, but are only synthesized in peripheral sites in postmenopausal women after the ovaries lose their physiological function. As reviewed by Rizner *et al.*, peripheral tissues such as adipose tissue, bone, brain, and cancerous endometrium produce estradiol from DHEA-S, DHEA, and androstenedione, which are relatively high in postmenopausal women with plasma concentrations of approximately 1.8 µM, 6.6 nM, and 1.9 nM, resepectively (191). DHEA is converted into estrone by a two-step enzymatic reaction catalyzed by 3β-hydroxysteroid dehydrogenase and aromatase; estrone is then converted into estradiol by hydroxysteroid (17β) dehydrogenase (192). Peripheral tissues release estrogens into circulation as their corresponding sulfoconjugates, which are then

hydrolyzed back into the parent estrogens by sulfatases. The mean plasma concentrations of estrone and estradiol are 70 pM and 30 pM respectively (191), with estradiol being the more potent of the two. Estriol is known as the fetal estrogen and is synthesized from placental 16α-hydroxydehydroepiandrosterone sulfate (16α-OHDHEA-S) (193). An illustration of this biosynthetic pathway is shown in Figure 8.

Tissue Distribution of hSULT1E1

Human SULT1E1 is the only SULT expressed in normal breast epithelial cells (194) and is distributed to a variety of other human adult and fetal tissues. As summarized by Miki *et al.* (195), hSULT1E1 is highly expressed in adult adrenal gland, mammary glands, and placenta. Other adult tissues such as the brain, aorta, liver, lung, intestines, and uterus express hSULT1E1 at considerable levels, however, no expression of hSULT1E1 is observed in the spleen and pancreas. This enzyme is highly expressed in fetal lung, liver, intestine, thyroid, and kidney, which emphasizes the important role of hSULT1E1 in regulating estrogen metabolism in the developing fetus. Other studies have shown that hSULT1E1 is expressed in the skin and prostate (196) as well as the endometrium (197, 198), but is rarely expressed in breast cancer cells (199). This is important because changes in the activity or expression of hSULT1E1 may increase estrogen exposure and estrogen-receptor-mediated effects that promote cellular proliferation and tumor progression (1).

Cloning and Biochemical Characterization of hSULT1E1

In 1994, Aksoy *et al*. were the first to identify hSULT1E1 by cDNA cloning and expression in COS-1 cells (200). This was performed by amplifying a 512 nucleotide portion of human liver template cDNA using PCR (polymerase chain reaction) primers that were designed based on the highly conserved SULT1E1 sequences in non-human cDNA; the resulting transcript was a 35.1 kDa protein with detectable activity towards estrone.

Her *et al*. determined the structure and chromosomal localization of the *hSULT1E1* gene one year later in 1995 (201). In the same year, Falany *et al.* published the bacterial expression and characterization of hSULT1E1 from human liver cDNA (202), which they determined was a 294 amino acid protein (35.1 kDa) encoded by 994 nucleotides. Human SULT1E1 is sensitive to DCNP inhibition (203), is catalytically active as a dimer, and displays potent substrate inhibition during estradiol sulfation with maximal enzyme activity at estradiol concentrations from 15 – 20 nM (143). Kinetic studies with hSULT1E1 are usually performed at physiological pH (202, 204), although Zhang *et al.* determined the catalytic mechanism of the enzyme at pH 6.3 (143). It should be noted that high concentrations of PAPS inhibit hSULT1E1 under these conditions (i.e., pH 6.3) but shows no substrate inhibition at pH 7.4 (202).

Substrate Specificity of hSULT1E1

Estradiol is one of the best known substrates for hSULT1E1, and it has the highest affinity for the enzyme compared to other steroid substrates such as estrone and estriol. Human SULT1E1 also catalyzes the sulfation 17β-ethinyl estradiol (203), an orally available therapeutic steroidal estrogen, and resveratrol, which is a polyphenolic derivative found in grapes, red wine, and peanuts (205, 206). Resveratrol is an alternate substrate and inhibitor of the hSULT1E1-catalyzed sulfation of estradiol (194, 207), which suggests the potential for this molecule to interfere in estrogen metabolism. Genotoxic catecholestrogens such as 2-hydroxyestrone, 2-hydroxyestradiol, 4-hydroxyestrone, and 4-hydroxyestradiol are substrates for hSULT1E1 and their sulfation serves as a mechanism of inactivation to prevent the formation of reactive quinones (208). As seen in Figure 9, other substrates for hSULT1E1 include phytoestrogens such as diadzein and genistein (204, 209), SERMS such as raloxifene and 4-OHTAM (174), and β-naphthol (210).

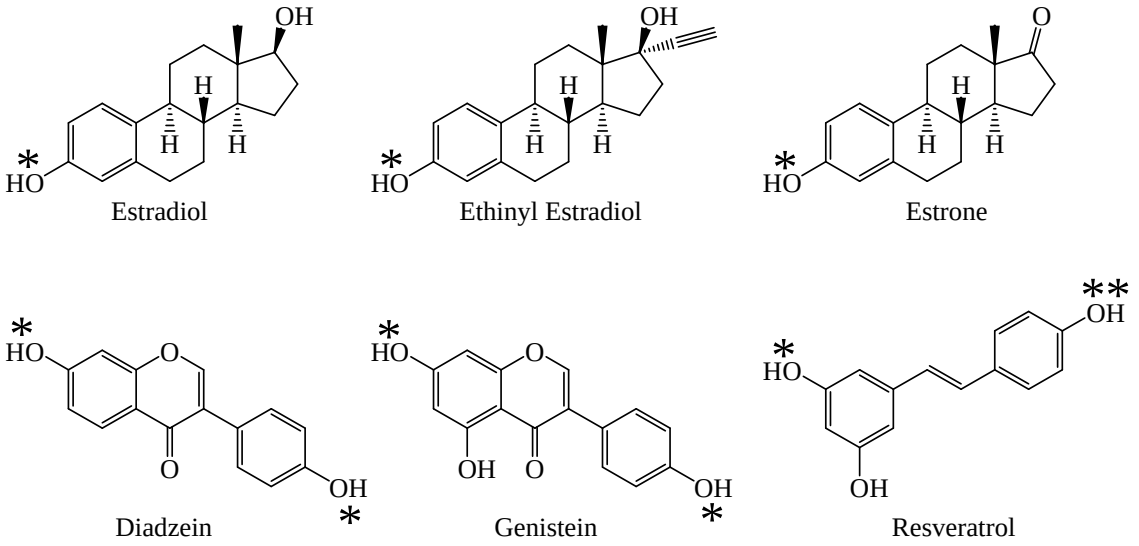

Note: The asterisk (*) marks the position(s) of sulfoconjugation by hSULT1E1. The double asterisk (**) marks the most preferred site of sulfation (205).

Figure 9. Chemical structures of several representative substrates for hSULT1E1.

Human Phenol Sulfotransferase 1A1*1 (hSULT1A1*1)

Human SULT1A1 was previously known as the phenol-sulfating sulfotransfersase, and it catalyzes the sulfation of various endogenous and exogenous molecules, steroid hormones, monoamines, and small, planar substrates. This enzyme is heavily involved in drug metabolism and has thirteen alleles encoding four alloenzymes that alter the catalytic activity and thermal stability of hSULT1A1, and these polymorphisms may have clinical consequences in individual responses to some therapeutic agents that require metabolism by this enzyme (211, 212). The most common SULT1A1 alloenzyme is the *1 variant (211, 213), and it has been extensively studied in relation to the therapeutic outcome and pharmacogenetics of tamoxifen (100, 102, 214-216). Other SULT1A1 polymorphisms include the thermally labile *2 alloenzyme, which has lower enzymatic activity and is defined by an Arg213His amino acid change from the conversion of guanine to adenosine at nucleotide 638. The *3 alloenzyme is defined by a Met223Val change from the

conversion of adenosine to guanine at nucleotide 667, however, the functional significance of hSULT1A1*3 remains unknown (118). Also of unknown phenotype is the *4 alloenzyme, which is defined by an Arg37Gln amino acid change from the transition of guanine to adenosine at nucleotide 110. Relative frequencies of the*1, *2, *3, and *4 alloenzymes of hSULT1A1 are 0.674, 0.313, 0.10, and 0.003, respectively (211).

*Cloning and Biochemical Characterization of hSULT1A1*1*

In 1989, Falany and his group were the first to purify hSULT1A1 from human liver cytosol to reveal hSULT1A1 as an active enzyme with an apparent molecular mass of 68 kDa and a subunit molecular mass of 32 kDa, which suggested that the enzyme was catalytically active as a dimer (217). Human hSULT1A1 was then successfully cloned from human liver cDNA library, and subsequently expressed in COS-7 cells (218). The resulting protein displayed detectable sulfation activity towards minoxidil and p-nitrophenol (pNP), and it was determined to be 295 amino acids in length with a predicted molecular mass of 34 kDa and encoded by 1206 base pairs from full-length cDNA. Raftogianis *et al*. later reported nucleotide polymorphisms associated with phenotypic variations in the activity and thermal stability of hSULT1A1 from the platelets of patient blood, and through their sequencing studies was revealed the discovery of 4 alleles of the parent enzyme: hSULT1A1*1, hSULT1A1*2, hSULT1A1*3, and hSULT1A1*4 (211). The hSULT1A1*1 alloenzyme is relatively resistant to heat inactivation (219, 220), is sensitive to DCNP inhibition (221), and is structurally stable as a homodimer with a pH optimum of 6.5 when examined with β-naphthol as substrate and p-nitrophenyl sulfate (pNPS) as the sulfuryl donor (142). However, the enzyme does not display substrate inhibition under these pH conditions during estradiol sulfation (118).

*Tissue Distribution and Substrate Specificity of hSULT1A1*1*

Human SULT1A1 is the most highly expressed SULT in human liver (222) and mediates the sulfation of phenolic substrates such as minoxidil (223), p-nitrophenol (224), and β-naphthol (225). The enzyme also functions in the sulfation of steroidal estrogens such as estradiol (110) and 17β-ethinyl estradiol (226), as well as proximate carcinogens such as dietary heterocyclic amines (227) and 2-methoxyestradiol (228). Other substrates for hSULT1A1 include raloxifene (174), 4-OHTAM (118, 174), and the circadian rhythm indole hormone, 6-hydroxymelatonin (229). Figure 10 illustrates several representative substrates for hSULT1A1*1. The enzyme is expressed in fetal liver (230), the growing placenta (231), blood platelets (219), as well as the intestines, kidney, and lungs (222). Epigenetic studies show a silencing of the hSULT1A1 gene in early breast carcinogenesis (232), which suggests a potential for expression of the enzyme in breast cancer tissue.

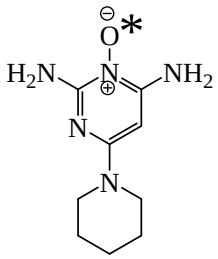

Minoxidil

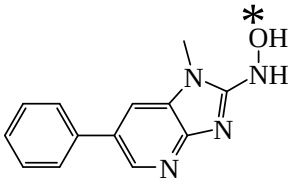

N-hydroxy-PhIP

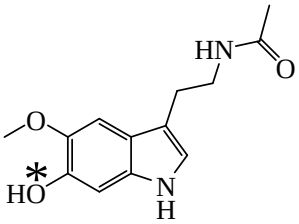

6-hydroxymelatonin

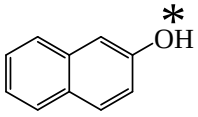

2-naphthol

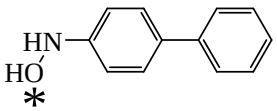

N-hydroxy-4-aminobiphenyl

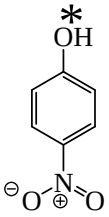

4-nitrophenol

Note: The asterisk (*) marks the position of sulfoconjugation by hSULT1A1*1.

Figure 10. Chemical structures of several representative substrates for hSULT1A1*1.

*Human SULT1A1*1 and Its Role in the Therapeutic Action of Tamoxifen*

While hSULT1E1 is the principal enzyme responsible for the sulfation of estrogens at physiological concentrations, hSULT1A1*1 is also capable of sulfating estrogen, albeit at micromolar concentrations (110, 233). The catalytic function of hSULT1A1*1 is important in tissues where hSULT1E1 is absent or poorly expressed, as appears be the case in breast tumor tissues (187, 199). Shatalova *et al*. demonstrated that estradiol-treated cells expressing high-activity hSULT1A1*1 proliferated at a significantly lower rate when compared to control cells (233), which suggests a role for the enzyme in tumor depression through the inactivation and excretion of estrogens. However, Seth *et al*. showed that SULT1A1 mRNA is up-regulated 10-fold in breast cancer cells treated by 4-OHTAM (234), which is a known substrate for hSULT1A1*1 (118, 235). Even though up-regulation of the expression of SULT1A1 might decrease estrogen levels, the sulfation of 4-OHTAM catalyzed by hSULT1A1*1 might be a disadvantage to tamoxifen therapy by reducing the bioavailability and effective concentrations 4-OHTAM. Interestingly, later studies have found a strong association between patient survival and the high activity hSULT1A1*1 allele (100, 214), which suggests that the sulfation product, 4-OHTAM-S, has therapeutic benefit and an activity different from inactivation and excretion. This was later confirmed by Mercer *et al*., who demonstrated an 80% increase in apoptosis in MCF7-hSULT1A1*1 expressing cells treated with 4-OHTAM. They concluded that breast cancer cells expressing the high activity hSULT1A1*1 alloenzyme enhanced the anti-proliferative and apoptotic properties of 4-OHTAM, which suggests a unique role for the enzyme and 4-OHTAM-S in tamoxifen efficacy and therapy (216). Therefore, hSULT1A1*1 plays an important role in the metabolism and therapeutic action of tamoxifen, as well as the metabolism of estrogen in cancerous endocrine tissues.

*Roles of hSULT1A1*1 in Carcinogenesis*

Despite the role of hSULT1A1*1 in the inactivation of many hormones and drugs, some reactions catalyzed by this enzyme can lead to the metabolic activation of xenobiotics to reactive electrophiles. For example, the hSULT1A1*1 is associated with arylamine and heterocyclic amine-induced carcinogenesis via the sulfation of N-hydroxy heterocyclic amines such as, N-hydroxy-2-amino-l-methyl-6-phenylimidazo[4,5-b]pyridine (N-OH-PHip) and N-hydroxy-4-aminobiphenyl (a compound present in tobacco smoke) (236, 237). Moreover, this enzyme functions in the sulfation of benzylic alcohols derived from alkyl-substituted polycyclic aromatic hydrocarbons (PAHs) (119, 180, 238). PAHs are environmental carcinogens that have been shown to be mutagenic in human breast tissue (239). The sulfoconjugates of PAHs are converted into ultimate carcinogens when the sulfate moiety becomes a good leaving group due to induction and resonance stabilization. Refer to figure 11 for the resonance stabilization of the carbocations formed from the SULT-catalyzed sulfation of benzylic alcohols and N-hydroxy aromatic amines.

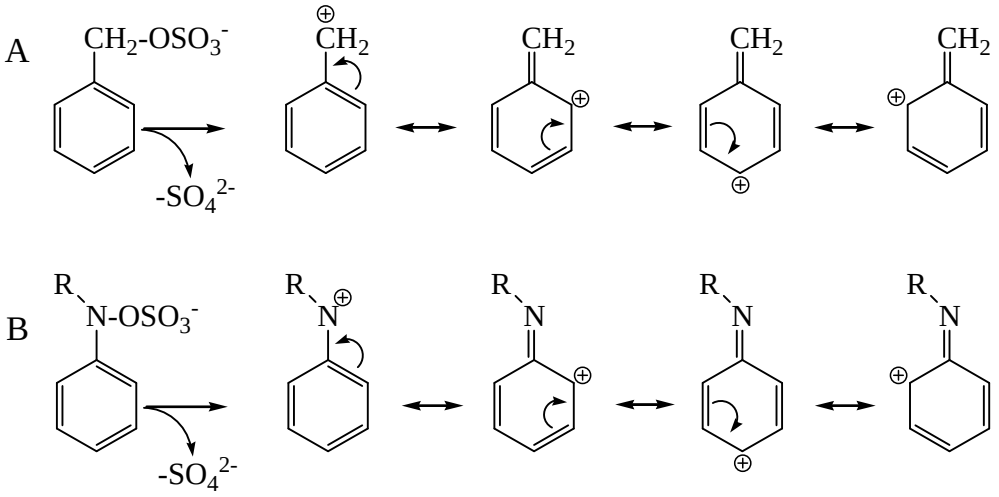

Figure 11. Resonance stabilization of carbocations formed from the sulfate cleavage of (A) benzylic alcohols and (B) aromatic hydroxylamines. Adapted from (119) with slight modifications.

Roles of hSULTs 2A1, 1E1, and 1A1*1 in Steroid and Tamoxifen Metabolism

As is clear from the discussion above, human cytosolic SULTs 2A1, 1E1, and 1A1*1 regulate steroid hormone homeostasis via the sulfation of endogenous steroid substrates for the enzymes. Human SULT2A1 catalyzes the sulfation of DHEA and PREG to their corresponding sulfuric acid esters, which inactivates these molecules as precursors for the biosynthesis of testosterone and estrogen in adults and the developing fetus. Estradiol is the most potent estrogen hormone in humans, and it regulates normal physiological growth and maturation in endocrine-responsive tissues such as the breast and endometrium. Estradiol is efficiently conjugated to its inactive sulfuric acid ester in a reaction catalyzed by hSULT1E1 at physiological substrate concentrations, but it is also sulfated, to a lesser extent, in reactions catalyzed by hSULT1A1*1 in those tissues where hSULT1E1 is unavailable or poorly expressed. Estrogen inactivation due to the action of hSULT1E1 and hSULT1A1*1 is required to prevent excessive estrogenic activity in the surrounding tissues, and this is an importance component in maintaining normal endocrine function. Moreover, the catalytic activity of these enzymes is vital in drug metabolism and can either enhance or diminish the pharmacological or toxicological effects of therapeutics. For example, hSULT1A1*1 is involved in the inactivation of phenolic metabolites of tamoxifen (i.e. 4-OHTAM and endoxifen), while hSULT2A1 is involved in the metabolic activation of the α-OHTAM metabolite to initiate adduct formation. The efficacy of tamoxifen therapy is also dependent upon the regulation of active and inactive estrogens *in vivo*. Since tamoxifen inhibits estrogen-induced DNA transcription at the estrogen receptor, changes in the catalytic activity of hSULT1E1 or hSULT1A1*1 could increase the physiological concentrations of active estrogen and decrease the efficacy of tamoxifen. Therefore, hSULTs 2A1, 1E1, and 1A1*1 are important in the therapeutic action and toxicity of tamoxifen.

CHAPTER 2

STATEMENT OF HYPOTHESIS

Although tamoxifen is a successful agent for the treatment and prevention of breast cancer, its use is limited by a low incidence of endometrial cancer in some patient populations. (27-29, 38, 39). Furthermore, nearly half of patients who are treated with tamoxifen fail to respond to the therapy and some see a recurrence of breast cancer after initial therapy. The therapeutic action of tamoxifen is dependent on the *in vivo* formation of its active metabolites, 4-OHTAM and endoxifen, which bind to the estrogen receptors in breast cancer tissue to inhibit estrogen-induced DNA transcription. Estrogens are derived from steroid substrates catalyzed by hSULT2A1 and are tightly regulated in tissues due to the activity of hSULT1E1 and hSULT1A1*1.

The human hydroxysteroid sulfotransferase 2A1, hSULT2A1, catalyzes the sulfation of various endogenous and exogenous molecules (112, 145-147). Although the detoxication of many hydrophobic xenobiotics that contain alcohol functional groups is one of the important roles of hSULT2A1, the sulfation of some benzylic and allylic alcochols catalyzed by this enzyme can sometimes generate bioactive electrophilic products that are reactive towards DNA and proteins, (85, 145, 178-181). For example, hSULT2A1 catalyzes the formation of an α-sulfooxy metabolite of tamoxifen that is reactive towards DNA, (40, 76) which is proposed to be a key step in the metabolic activation of tamoxifen that leads to the development of endometrial cancer is some tamoxifen-treated women.

The human estrogen sulfotransferase 1E1, hSULT1E1, catalyzes the sulfation of estradiol at low (nanomolar) concentrations, which constitutes a major physiological function of this enzyme. The sulfation of estradiol protects peripheral tissues from excessive estrogenic effects and is associated with tumor regression in estrogen-dependent cancer (187). Estrogen homeostasis is also regulated by hSULT1A1*1 in certain tissues

where the hSULT1E1 is not available or is poorly expressed, which appears to be the case in breast tumor tissue (187, 199). An additional advantage of hSULT1A1*1 is the ability for this enzyme to enhance the apoptotic properties of 4-OHTAM in breast cancer cells (216) This highlights the need to maintain the catalytic activity and functional integrity of human cytosolic SULTs *in vivo*.

The hypothesis for the current investigation is that endoxifen, 4-OHTAM, and other major tamoxifen metabolites regulate the catalytic activity of hSULTs 2A1, 1E1, and 1A1*1 and thereby have a potential to modulate the therapeutic action and toxicity of tamoxifen. Due to the involvement of hSULT2A1 in the metabolism and transport of steroid hormones and in the genotoxicity of the α-hydroxy metabolite of tamoxifen, the current study will evaluate the potential for metabolites of tamoxifen to inhibit the catalytic activity of the enzyme. Such inhibition could prevent the formation of the genotoxic α-sulfooxy metabolite in tissue such as the endometrium or it might alter steroid hormone homeostasis by interfering with the inactivation of steroid substrates for the hSULT2A1. This study will also evaluate the potential for the metabolites to interfere in the inactivation of estrogens catalyzed by hSULT1E1 and hSULT1A1*1. Alterations in the catalytic activity of either enzyme may increase the physiological concentrations of unconjugated (active) estrogen, which will likely cause excessive estrogenic hormonal effects in endocrine tissues such as the endometrium and breast. These events will compromise the efficacy of tamoxifen as a SERM and may explain the resistance to therapy. Moreover, increases in the physiological concentrations of estrogen may augment the risk for the endometrial carcinogenesis when combined with the reactive α-sulfooxy derivative catalyzed by hSULT2A1. Lastly, changes in the catalytic activity of hSULT1A1*1 may affect the therapeutic action of tamoxifen by altering the bioavailability of the active metabolites. For example, the expression of hSULT1A1*1 in breast cancer is associated with an increased patient survival (100, 214), which is likely due to the hSULT1A1*1-catalyzed sulfation of 4-OHTAM in breast cancer cells (216). However, the sulfation of

the tamoxifen metabolites in non-cancerous tissue will likely serve as a mechanism of elimination to promote excretion of the active form(s) of the drug. Therefore, depending on the tissue, the activity of hSULT1A1*1 can either enhance or diminish the effects of tamoxifen.

The hypothesis will be tested by expressing and purifying recombinant hSULT2A1, hSULT1E1, and hSULT1A1*1 from a bacterial system to obtain the proteins in sufficient quantities for kinetic studies without the use of His-tags or fusion proteins. This method is intended to preserve the structural and functional integrity of the proteins for kinetic studies. Tamoxifen metabolites will then be purchased or synthesized, as appropriate, and investigated as inhibitors of the hSULT2A1-catalyzed sulfation of DHEA and PREG. Afterwards, the metabolites will be investigated as inhibitors of the hSULT1E1- and hSULT1A1*1-catalyzed sulfation of estradiol. Since inhibitors of an enzyme could be exerting their effect through serving as alternate substrates, this possibility will also be investigated. LC-MS will then be utilized to characterize the product(s) of sulfation catalyzed by hSULT2A1, hSULT1E1, or hSULT1A1*1 from enzyme reaction mixtures.

CHAPTER 3

INTERACTIONS OF TAMOXIFEN METABOLITES WITH HUMAN HYDROXYSTEROID SULFOTRANSFERASE SULT2A1

Introduction

Given the complexity of the carcinogenic response to tamoxifen and the potential role(s) of hSULT2A1, the first goal of the current study was to determine the interactions of tamoxifen and its major metabolites with hSULT2A1. It was hypothesized that the major metabolites of tamoxifen could inhibit the catalytic activity of hSULT2A1 and modulate the toxicity due to the action of the enzyme. It was also hypothesized that the metabolites could compete with the genotoxic metabolite, α-OHTAM, or physiological hydroxysteroids for sulfation by catalyzed hSULT2A1. Since radiolabelled α-OHTAM was not available, [^{3}H]-DHEA and [^{3}H]-pregnenolone were used as substrates in order to study inhibition of the hSULT2A1-catalyzed reaction.

Expression and Purification of Recombinant hSULT2A1

Human SULT2A1 was expressed and extracted from BL21 (DE3) *Escherichia coli* (*E. coli*) using a previously described procedure (89, 175). The enzyme was purified using DE-52 anion exchange chromatography followed by two hydroxyapatite columns to homogeneity as determined by sodium dodecyl sulfate polyacrylamide gel electrophoresis (SDS-PAGE). A single band with an approximate molecular mass of 34 kDa was observed, and this was consistent with the previously reported mass of the hSULT2A1 (148). Protein concentration was determined at each step of the purification process with a modified Lowry method using bovine serum albumin as a standard (240). Chromatography fractions were analyzed for enzyme activity using DHEA as substrate in a previously reported methylene blue assay (241, 242).

The Inhibition of hSULT2A1 by Major Tamoxifen Metabolites

Endoxifen, 4-OHTAM, TAM-NO, and N-desTAM were investigated as inhibitors of hSULT2A1 using DHEA and pregnenolone as substrates at pH 7.4. The sulfation of either DHEA or pregnenolone was initially examined using a concentration range between 0.2 – 20.0 μM for DHEA and 0.5 – 22.0 μM for pregnenolone in order to determine the concentrations of each substrate where minimal substrate inhibition occurred (Figure 12). Kinetic constants derived from the sulfation of DHEA and PREG are listed in Table 2. Endoxifen, 4-OHTAM, N-desTAM, and TAM-NO were all inhibitors of DHEA sulfation (Figure 13), however, tamoxifen did not exhibit significant inhibition of hSULT2A1 up to the limits of its solubility in the assay (data not shown). Endoxifen, 4-OHTAM, and TAM-NO displayed greater than 95% inhibition of the enzyme within their solubility limits, whereas N-desTAM reached only approximately 30% inhibition at its limit of solubility. As seen in Table 3, the calculated IC_{50} (half-maximal inhibitory concentration) values ranged from 1.7 μM to 11 μM for the inhibition of the sulfation 1.0 μM DHEA, with endoxifen being the most potent inhibitor. The inhibitor dissociation constant (Ki), catalytic efficiency constant (kcat/Km), Michaelis-Menten constant (Km), and maximal velocity (Vmax) for inhibitors of the hSULT2A1-catalyzed sulfation of DHEA are shown in Table 3, with the mechanism of inhibition and initial velocity data in Figures 14 and 15. Endoxifen, 4-OHTAM, and TAM-NO were noncompetitive inhibitors with Ki values of 2.8 μM, 19 μM, and 9.6 μM, respectively, whereas N-desTAM was a competitive inhibitor of DHEA sulfation with a Ki value of 17 μM.

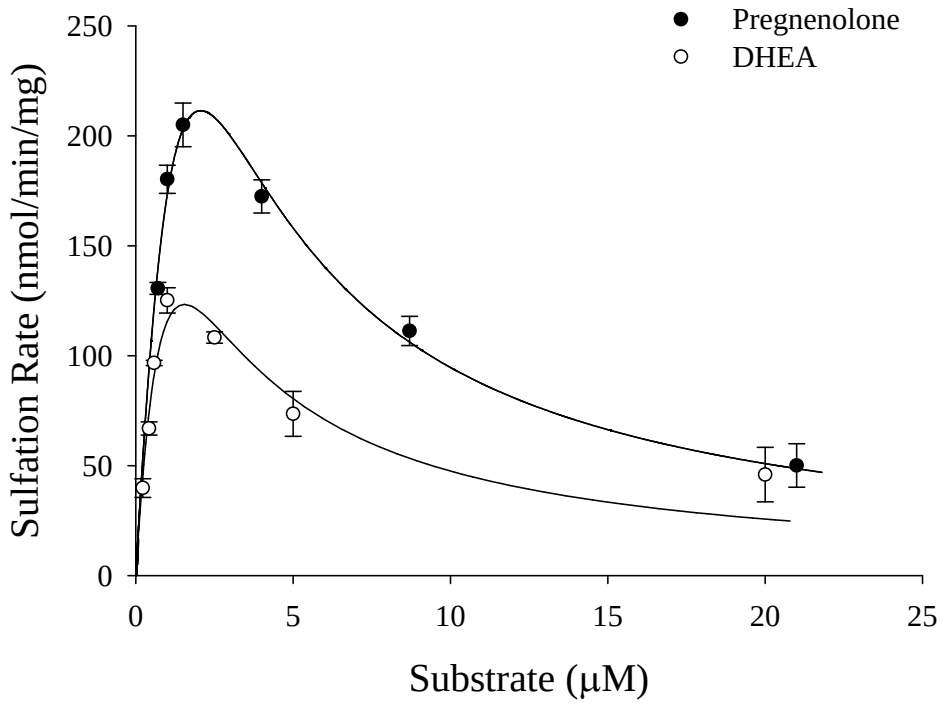

Figure 12. Initial velocities of hSULT2A1-catalzed sulfation of DHEA and PREG in the presence of 200 μM PAPS. Data are the means ± standard error from triplicate determinations and were fit to a standard uncompetitive substrate inhibition equation. Refer to Table 18 (Chapter 7) for rate equations.

Substrate	**Km**	**Vmax**	**kcat/Km**	**Ki**
	μM	*nmol/min/mg*	$min^{-1}\mu M^{-1}$	*μM*
DHEA	1.7 ± 0.8	498 ± 141	15.8	1.4 ± 0.7
PREG	4.4 ± 2.3	1112 ± 480	17.0	1.0 ± 0.5

Note: Data are the means ± standard error from triplicate determinations. Calculation of kcat values was based on 67,356 as the dimeric molecular mass of hSULT2A1.

Table 2. Kinetic constants derived from the hSULT2A1-catalyzed sulfation of DHEA and PREG.

Metabolite	IC_{50}	Ki	Km (DHEA)	Vmax (DHEA)	kcat/Km (DHEA)
	μM	*μM*	*μM*	*nmol/min/mg*	*$min^{-1}μM^{-1}$*
Endoxifen	1.7 ± 0.4	2.8 ± 0.2	0.7 ± 0.1	243 ± 17	21.8
N-desTAM	8.3 ± 2.6	17 ± 2	0.8 ± 0.1	260 ± 24	22.0
4-OHTAM	10 ± 1	19 ± 2	0.5 ± 0.1	178 ± 7	23.6
TAM-NO	11 ± 1	9.6 ± 0.2	3.5 ± 0.5	592 ± 75	11.4

Note: Data are the mean ± standard error from triplicate determinations. Calculation of kcat values was based on 67,356 as the dimeric molecular mass of hSULT2A1.

Table 3. The sulfation of DHEA was determined using varied concentrations of inhibitor and either 1.0 μM DHEA (for IC_{50} values) for 0.2 μM – 1.0 μM DHEA for determination of the mechanism of inhibition and related kinetic constants.

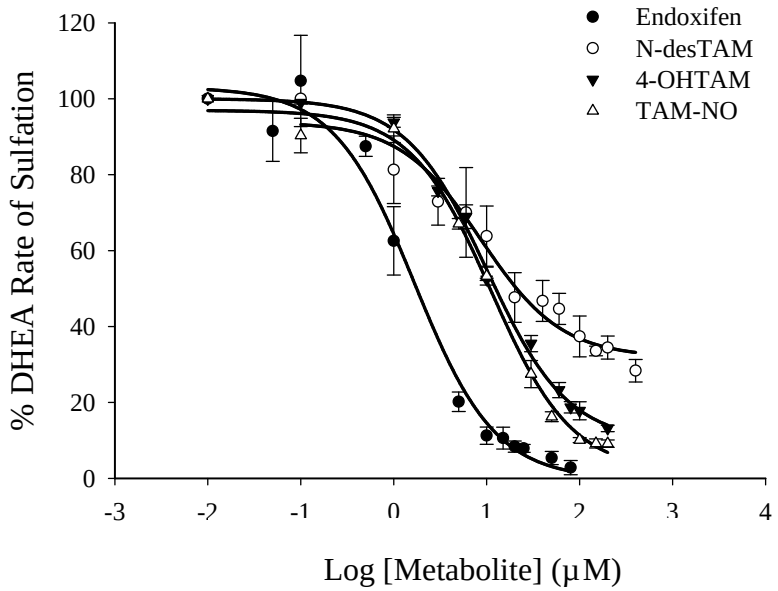

Figure 13. Inhibition of the hSULT2A1-catalyzed sulfation of 1.0 μM DHEA by major metabolites of tamoxifen. Sulfation rates of uninhibited controls for endoxifen, N-desTAM, 4-OHTAM, and TAM-NO were approximately 87, 98, 97, and 111 nmol/min/mg, respectively. Data are the mean ± standard error from triplicate determinations and were fit to a sigmoidal dose-response equation (Table 18, Chapter 7).

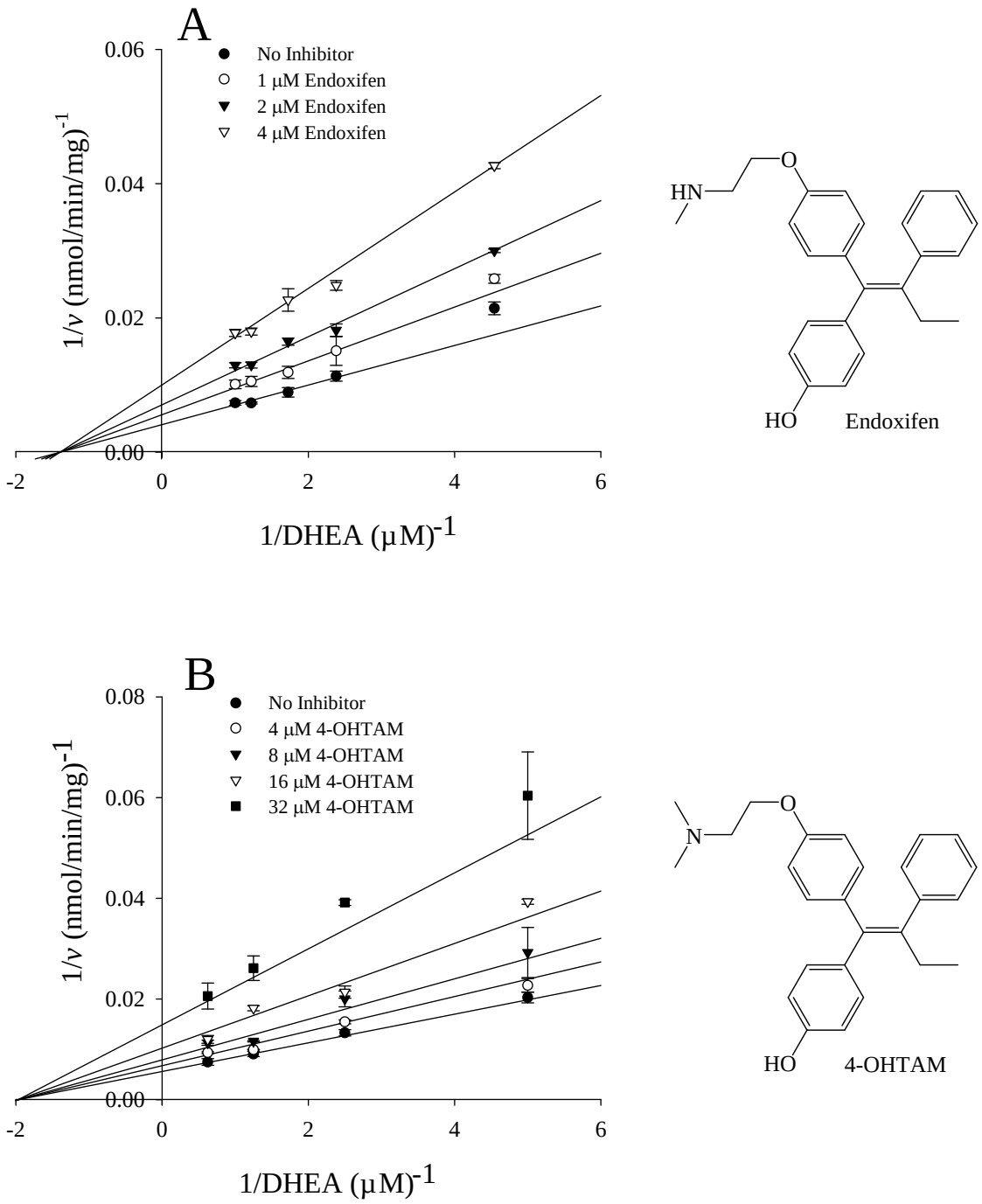

Figure 14. Noncompetitive inhibition of the hSULT2A1-catalyzed sulfation of DHEA by endoxifen (A) and 4-OHTAM (B). Data are the mean ± standard error from triplicate determinations. Refer to Table 18 (Chapter 7) for rate equations.

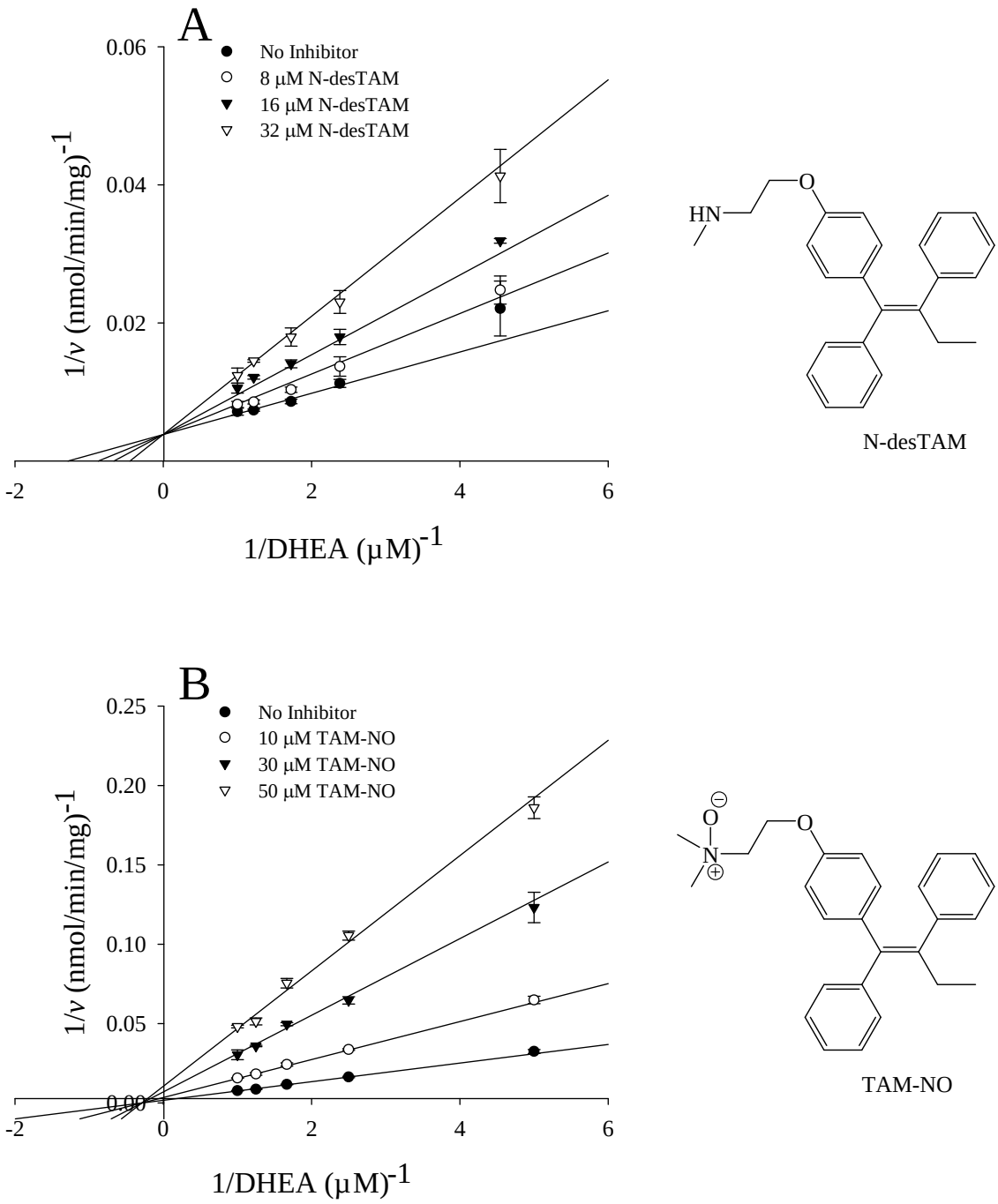

Figure 15. Competitive inhibition of the hSULT2A1-catalyzed sulfation of DHEA by N-desTAM (A), and noncompetitive inhibition of DHEA sulfation by TAM-NO (B). Data are the mean ± standard error from triplicate determinations. Refer to Table 18 (Chapter 7) for rate equations.

Following the inhibition studies with DHEA, metabolites of tamoxifen were then investigated as inhibitors of PREG to determine if the inhibition observed was affected by the substrate utilized. Endoxifen, 4-OHTAM, N-desTAM, TAM-NO were inhibitors of pregnenolone sulfation (Figure 16), and the percent inhibition by each metabolite was similar to the studies with DHEA The calculated IC_{50} values ranged from 2.7 μM to 16 μM for the inhibition of 0.4 μM PREG, with endoxifen being the most potent inhibitor. The kinetic parameters Vmax, Km, Ki, and kcat/Km for inhibitors of the hSULT2A1-catalyzed sulfation of PREG are reported in Table 4, with the kinetic mechanism of inhibition and initial velocity data in Figures 17 and 18. Endoxifen, 4-OHTAM, and TAM-NO were either mixed or noncompetitive inhibitors with Ki values of 3.5 μM, 12.7 μM, and 16.9 μM, respectively, whereas N-desTAM was best described as a competitive inhibitor of PREG sulfation with a Ki value of 9.8 μM.

Metabolite	**IC_{50}**	**Ki**	**Km (PREG)**	**Vmax (PREG)**	**kcat/Km (PREG)**
	μM	*μM*	*μM*	*nmol/min/mg*	*$min^{-1}μM^{-1}$*
Endoxifen	2.7 ± 1.1	3.5 ± 0.7	1.2 ± 0.3	330 ± 54	18.6
N-desTAM	15 ± 1	9.8 ± 1.2	2.1 ± 0.5	630 ± 130	20.0
4-OHTAM	17 ± 1	13 ± 2	2.0 ± 0.5	520 ± 100	17.0
TAM-NO	16 ± 1	17 ± 1	2.3 ± 0.5	650 ± 120	19.0

Note: Data are the mean ± standard error from triplicate determinations. Calculation of kcat values was based on 67,356 as the dimeric molecular mass of hSULT2A1.

Table 4. The sulfation of PREG was determined using varied concentrations of inhibitor and either 0.4 μM PREG (for IC_{50} values) for 0.20 μM – 1.0 μM PREG for determination of the mechanism of inhibition and related kinetic constants.

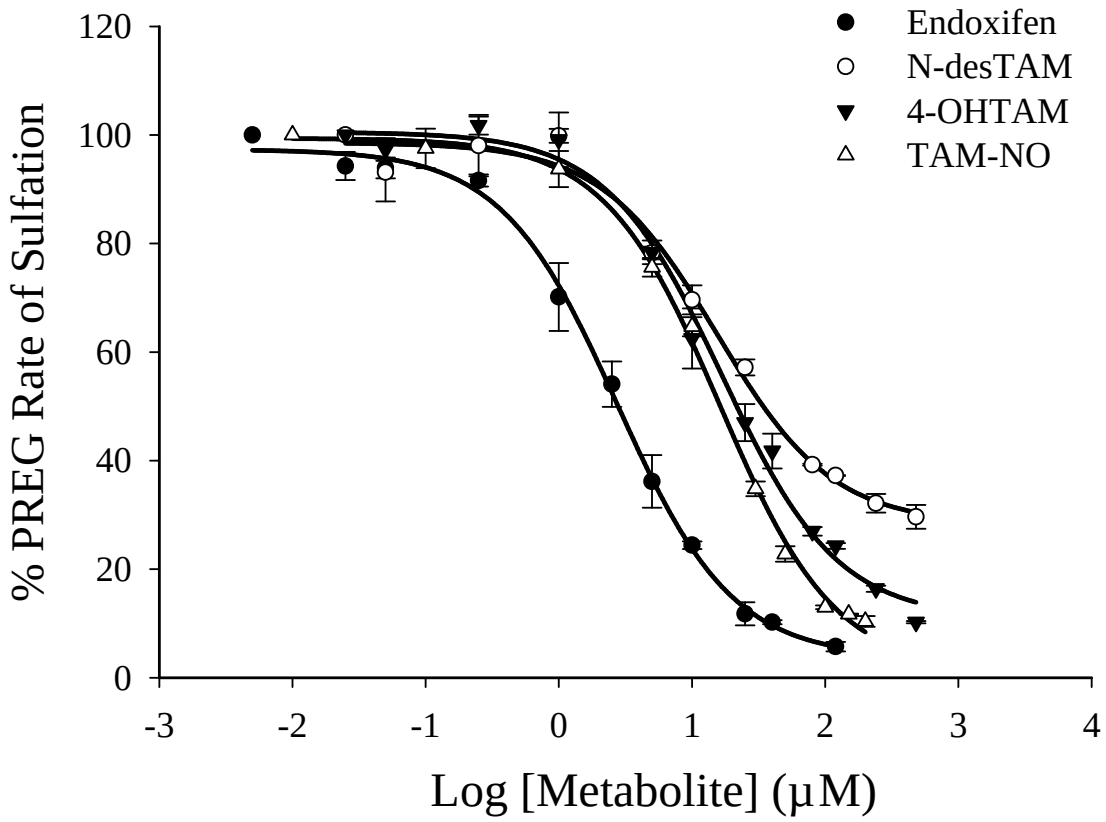

Figure 16. Inhibition of the hSULT2A1-catalyzed sulfation of 0.4 µM PREG by major metabolites of tamoxifen. Sulfation rates of uninhibited controls for endoxifen, N-desTAM, 4-OHTAM, and TAM-NO were approximately 63, 92, 68, and 90 nmol/min/mg, respectively. Data are the mean ± standard error from triplicate determinations and were fit to a sigmoidal dose-response equation (Table 18, Chapter 7)

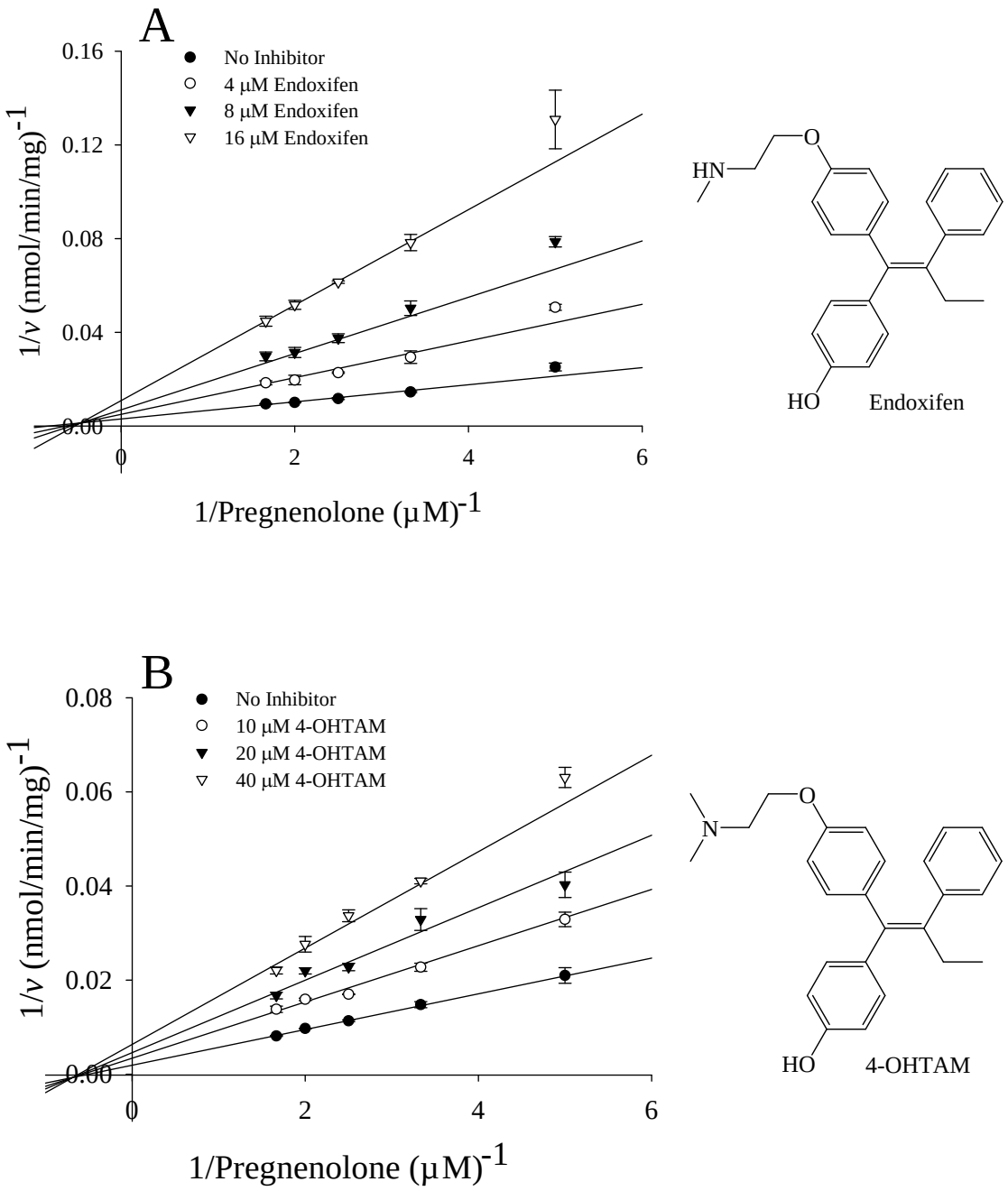

Figure 17. Mixed inhibition of the hSULT2A1-catalyzed sulfation of PREG by endoxifen (A) and 4-OHTAM (B). Data are the means ± standard error from triplicate determinations. Refer to Table 18 (Chapter 7) for rate equations.

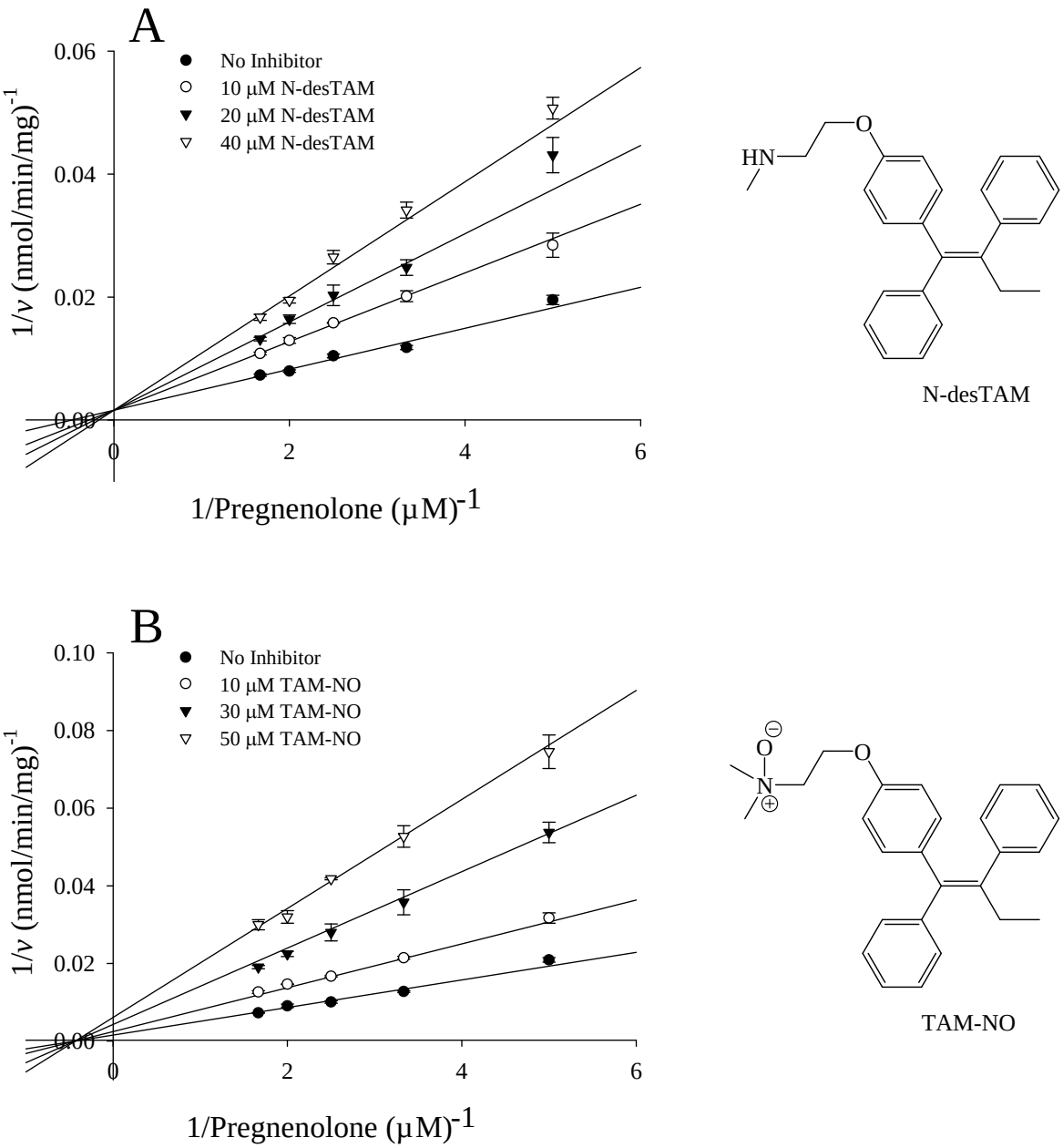

Figure 18. Competitive inhibition of the hSULT2A1-catalyzed sulfation of PREG by N-desTAM (A), and noncompetitive inhibition of PREG sulfation by TAM-NO (B). Data are the means ± standard error from triplicate determinations. Refer to Table 18 (Chapter 7) for rate equations.

Characterization of 4-OHTAM, N-desTAM, and Endoxifen as Substrates for hSULT2A1

Previous studies have shown that hSULT2A1 is capable of catalyzing the sulfation of 4-OHTAM at low concentrations (174), however, the kinetics of the hSULT2A1-catalyzed sulfation of 4-OHTAM has not been characterized. Since the *N*-sulfoconjugation of aliphatic secondary amines is catalyzed by this enzyme (132), hSULT2A1 was examined for its ability to catalyze the sulfation of N-desTAM and endoxifen. 4-OHTAM, N-desTAM, and endoxifen were determined to be substrates for the enzyme, although the low rates of sulfation of endoxifen prohibited the ability to obtain reliable kinetic constants with endoxifen (Figure 19). The kinetics of 4-OHTAM sulfation was best described using a Michaelis-Menten equation (i.e., no substrate inhibition was evident) whereas the data for the sulfation of N-desTAM was best described using a substrate inhibition model (Figure 20). The kinetic constants for the sulfation of 4-OHTAM and N-desTAM catalyzed by hSULT2A1 are summarized in Table 5. The enzyme displayed higher catalytic activity with 4-OHTAM than with N-desTAM as seen by the 6.3-fold higher kcat/Km.

Since the sulfamate of N-desTAM (i.e., N-desTAM-S) has not been previously reported as a metabolite, it was synthesized as a standard to confirm the mass of N-desTAM-S formed in enzymatic reactions (Figure 21). The sulfate of 4-OHTAM (4-OHTAM-S) was also synthesized as a standard for LC-MS studies (Figure 22); however, earlier studies report the synthesis of 4-OHTAM-S using an alternative strategy (243). In the current study, 4-OHTAM-S was synthesized from (*Z*)-4-OHTAM using sulfuryl imidazolium triflate as the sulfation reagent, however, the proton NMR spectrum of 4-OHTAM-S shows evidence of (*Z*) and (*E*) isomers of 4-OHTAM-S (See Appendix, Figure A-12). It is predicted that the inter-conversion of (*Z*)-4-OHTAM to its corresponding (*E*) isomer occurs in the initial stage of synthesis when the sample is first dissolved in methylene chloride, where chlorine radicals may abstract the phenolic proton of 4-OHTAM to form a quinone radical that can be delocalized through the ring system to

disrupt the alkene bond of 4-OHTAM. Nevertheless, the pattern of isomerization observed with 4-OHTAM-S is also observed in the reference proton NMR spectrum of ≥ 70% (Z)-4-OHTAM (remainder is primarily the (*E*) isomer of 4-OHTAM) as shown in the Appendix, Figures A-13, A-14, and A-15. It should be noted that the isomeric purity of (*Z*)-4-OHTAM was confirmed by proton NMR (See Appendix, Figure A-16) prior to its use in the synthesis of 4-OHTAM-S. Synthetic standards for endoxifen were not prepared due to the complexity involved in synthesizing site-selective sulfoconjugates of this metabolite.

The enzymatic reactions were analyzed by LC-MS, and the negative ion ESI-MS of the product formed by the hSULT2A1-catalyzed sulfation of N-desTAM is seen in Figure 23. Endoxifen-sulfate was also identified as a product of sulfation catalyzed by hSULT2A1. Analysis of the enzyme-catalyzed reaction revealed a product m/z of 452.1930 by negative ion ESI-MS (Figure 24). Endoxifen has two potential sites for sulfation, but it was determined that sulfation had occurred at the phenolic hydroxyl group due to the single charge of the parent mass when analyzed in negative ion mode. Sulfation of the aliphatic amino group of endoxifen would result in a doubly charged species with an approximate m/z of 226, and no evidence of this species was observed in the samples. The product of 4-OHTAM sulfation (4-OHTAM-S) is shown in Figure 25 with a m/z of 466.2050, as determined by negative ion ESI-MS. The retention times of 4-OHTAM-S, N-desTAM-S, and endoxifen-sulfate from LC chromatographs (See Appendix, Figures A-1, A-2, and A-3) were 16.30 min, 21.99 min, and 16.07 min, respectively.

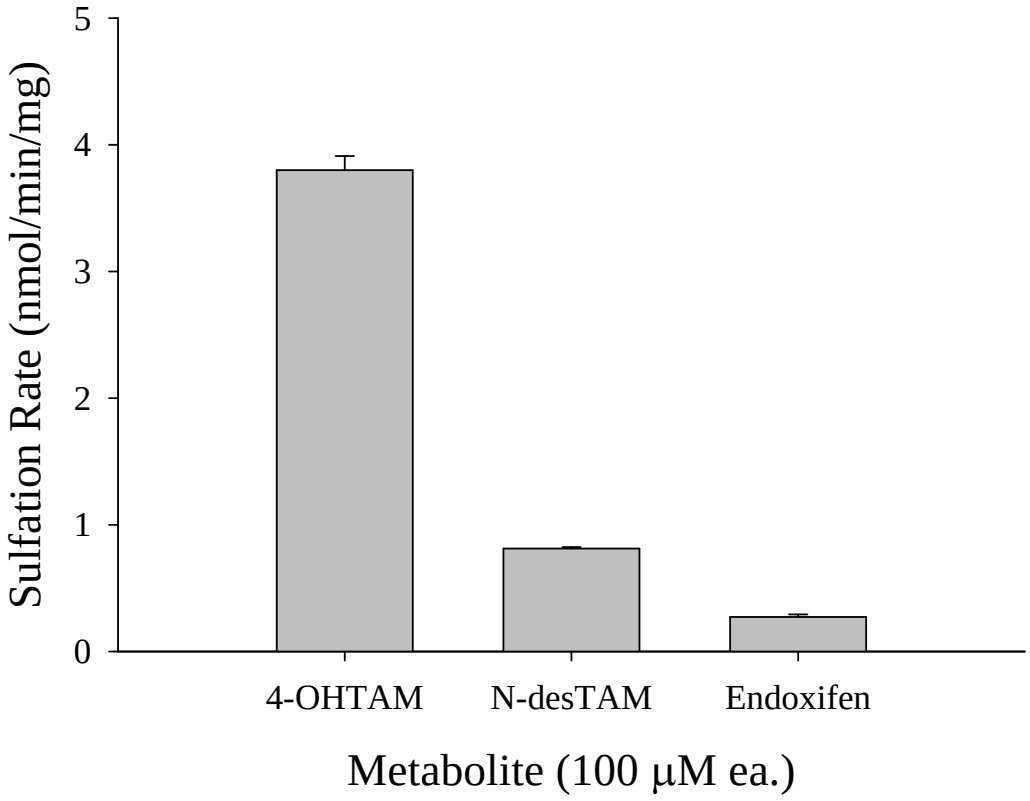

Figure 19: Substrate determination studies for the hSULT2A1-catalyzed sulfation of 4-OHTAM, N-desTAM, and endoxifen. Data are the means ± standard error from triplicate determinations

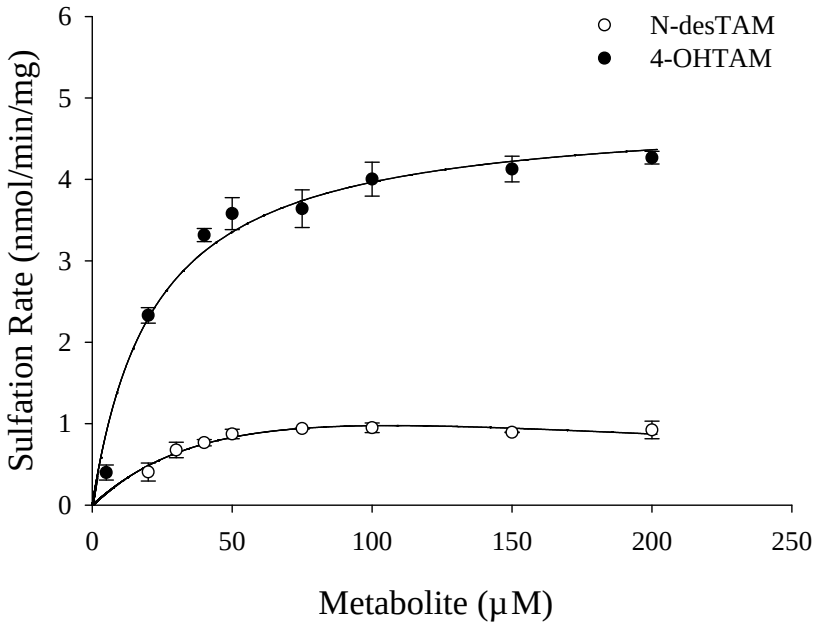

Figure 20. Initial velocities of the hSULT2A1-catalyzed sulfation of 4-OHTAM and N-desTAM. Data are the means ± standard error from triplicate determinations and were fit to either a standard Michaelis-Menten equation (for 4-OHTAM) or an uncompetitive substrate inhibition equation (for N-desTAM). Refer to Table 18 (Chapter 7) for rate equations.

Metabolite	**Km**	**Vmax**	**kcat/Km**	**Ki**
	µM	*nmol/min/mg*	$min^{-1}\mu M^{-1}$	*µM*
4-OHTAM	22 ± 3	4.9 ± 0.1	0.015	
N-desTAM	73 ± 50	2.3 ± 4.4	0.0024	156 ± 135

Note: Data are the means ± standard error from triplicate determinations. Calculation of kcat values was based on 67,356 as the dimeric molecular mass of hSULT2A1

Table 5. Kinetic constants for the hSULT2A1-catalyzed sulfation of 4-OHTAM and N-desTAM.

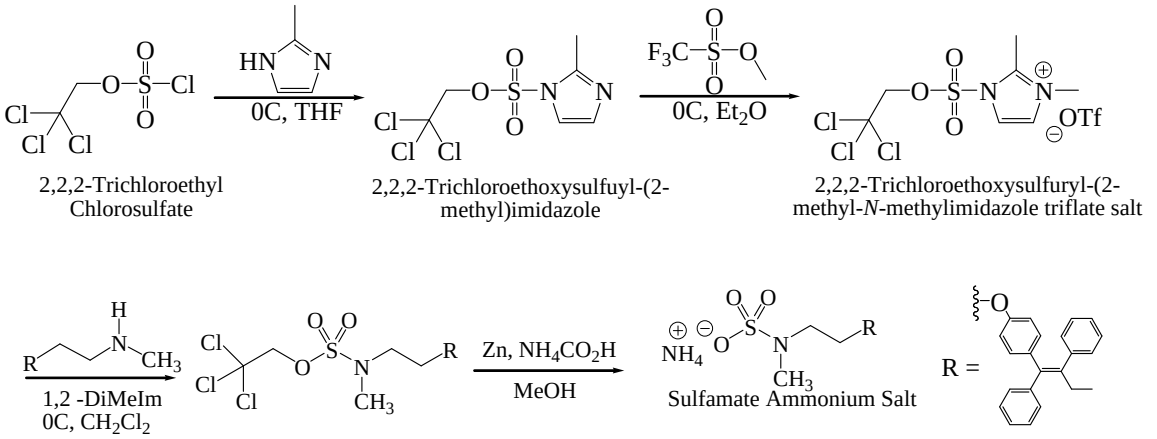

Figure 21. Synthesis of N-desTAM-S. The percent molar conversion of N-desTAM to its corresponding sulfamate was 90%

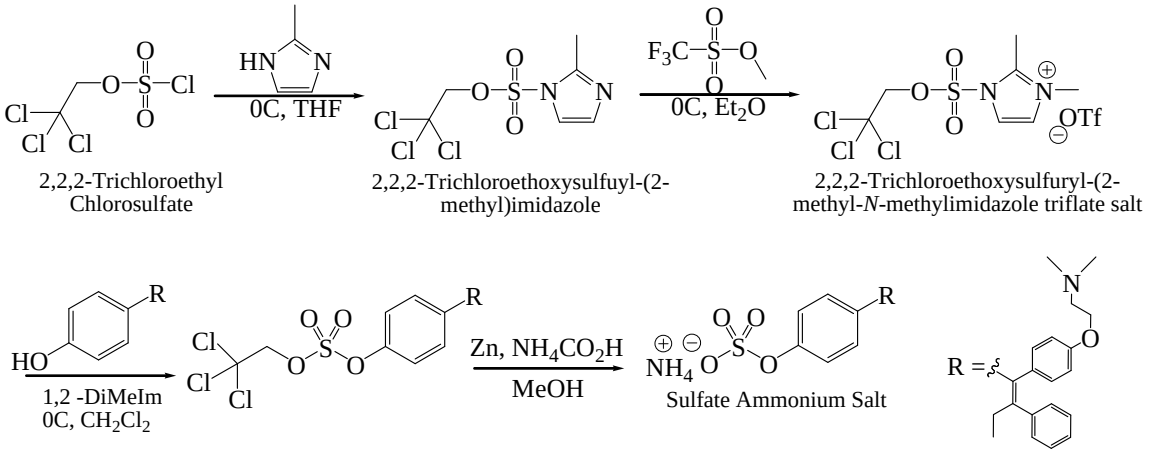

Figure 22. Synthesis of 4-OHTAM-S. The percent molar conversion of 4-OHTAM to its corresponding sulfate was 36%.

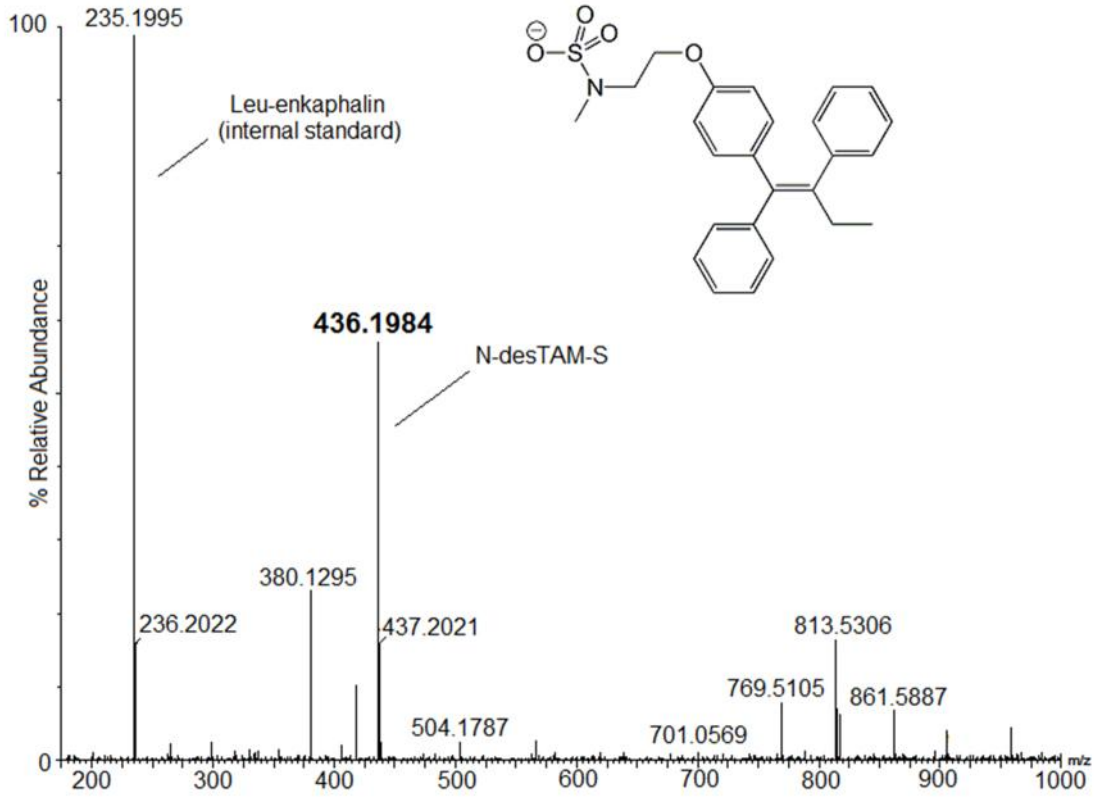

Figure 23. LC-MS analysis of N-desTAM-S as a product of sulfation catalyzed by hSULT2A1. The theoretical calculated m/z of N-desTAM-S is 436.1588 $[M - H]^-$.

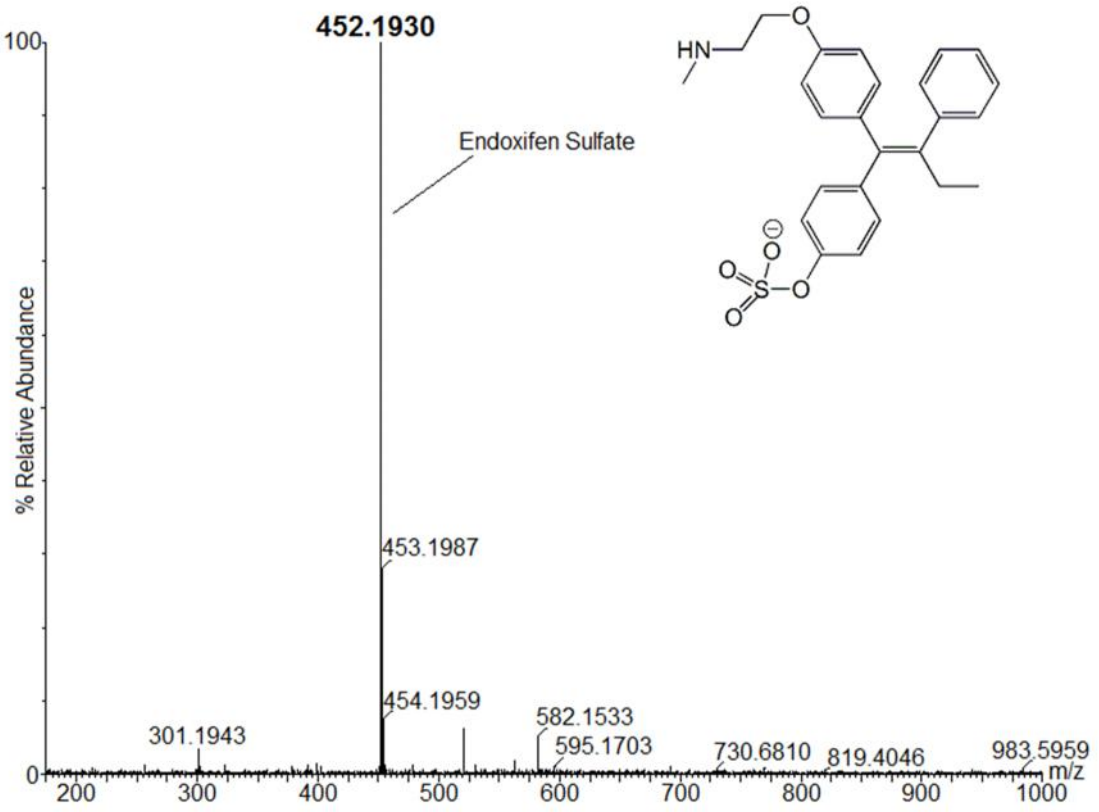

Figure 24. LC-MS analysis of endoxifen-sulfate as a product of sulfation catalyzed by hSULT2A1. The theoretical calculated m/z of endoxifen-sulfate is 452.1532 $[M - H]^-$.

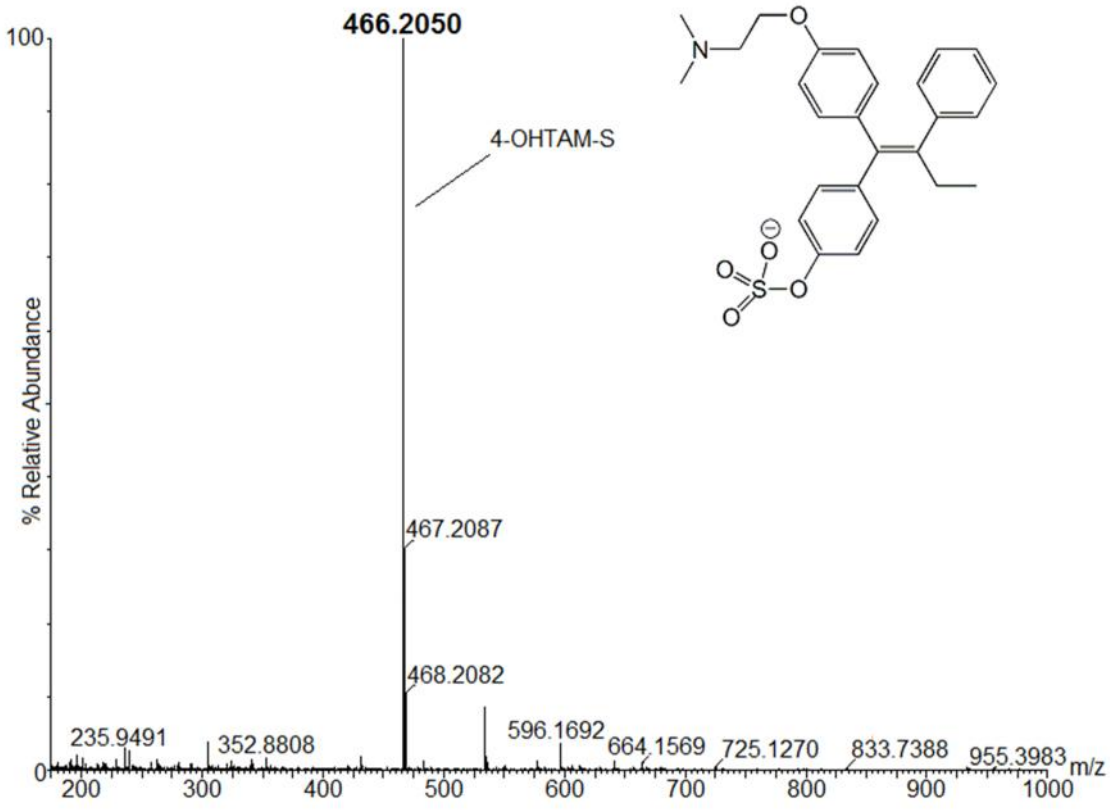

Figure 25. LC-MS analysis of 4-OHTAM-S as a product of sulfation catalyzed by hSULT2A1. The theoretical calculated m/z of 4-OHTAM-S is 466.1852 $[M - H]^-$.

N-desTAM-S and 4-OHTAM-S Inhibit the hSULT2A1-Catalyzed Sulfation of DHEA.

N-desTAM-S and 4-OHTAM-S were investigated as inhibitors of hSULT2A1. N-desTAM-S was a potent inhibitor of DHEA sulfation with calculated IC_{50} and Ki values of 7.7 µM and 4.8 µM, respectively, whereas 4-OHTAM-S was determined to be a very weak inhibitor of the enzyme with an IC_{50} value greater than 70 µM when examined with 1.0 µM DHEA as substrate (Figure 26A). The kinetic parameters for the inhibition of the DHEA sulfation by N-desTAM-S are shown in Table 6, with the kinetic mechanism of inhibition and initial velocity data in Figure 26B.

Metabolite	**IC_{50}**	**Ki**	**Km (DHEA)**	**Vmax (DHEA)**	**kcat/Km (DHEA)**
	µM	*µM*	*µM*	*nmol/min/mg*	*min^{-1} $µM^{-1}$*
N-desTAM-S	7.7 ± 1.2	4.8 ± 0.3	1.2 ± 0.2	159 ± 15	9.0
4-OHTAM-S	> 70				

Note: Data are the means ± standard deviation from triplicate determinations. Calculation of kcat values was based on 67,356 as the dimeric molecular mass of hSULT2A1

Table 6. The inhibition of DHEA sulfation was determined using either 1.0 µM DHEA (for IC_{50} values) or 0.2 µM – 1.0 µM DHEA for determination the mechanism of inhibition and related inhibition constants.

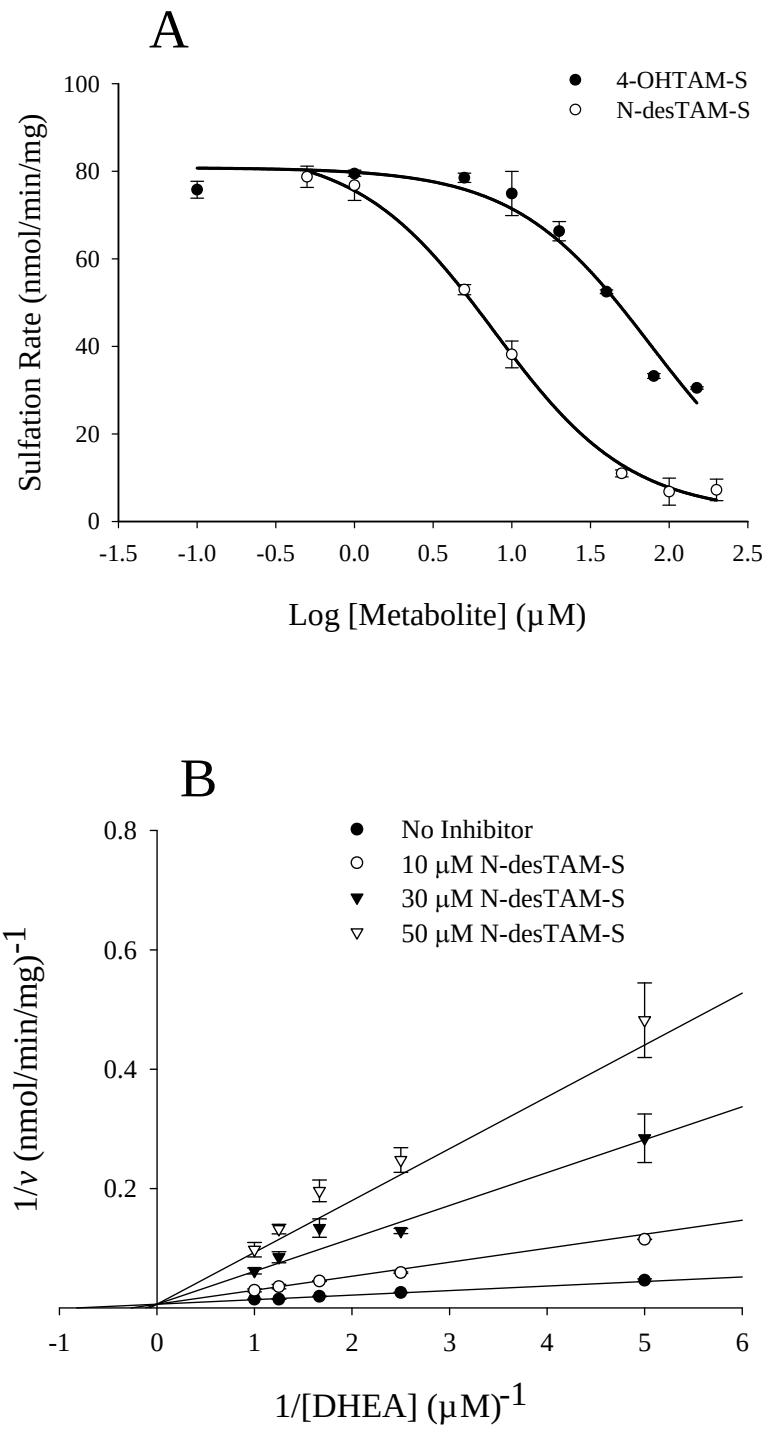

Figure 26. Inhibition of the hSULT2A1-catalyzed sulfation of 1.0 µM DHEA by (A), N-desTAM-S and 4-OHTAM-S, and competitive inhibition of DHEA sulfation by (B), N-desTAM-S. Data are the means ± standard error from triplicate determinations. Refer to Table 18 (Chapter 7) for rate equations.

Discussion

Of the metabolites tested, endoxifen was the most potent inhibitor of the sulfation of 1.0 μM DHEA and 0.4 μM PREG with IC50 values of 1.7 μM and 2.7 μM, respectively (Tables 2 and 4). This was an interesting finding because the inhibition constants for interactions between hSULT2A1 and endoxifen were of similar magnitude to the apparent Km values observed for the sulfation of DHEA and PREG, which are two of the best known substrates for the enzyme. The range of serum concentrations reported for DHEA and PREG are between 5 – 24 nM and 1 – 6 nM, respectively (176) whereas the mean plasma concentrations of tamoxifen metabolites have been reported to be in the general range of 14 – 130 nM for endoxifen, 3 – 17 nM for 4-OHTAM, 15 – 24 nM for TAM-NO, and 280 – 800 nM for N-desTAM (74). If the serum concentrations of DHEA, PREG, and the tamoxifen metabolites are an indication of their concentrations in peripheral tissues, then the metabolites have a potential to alter the homeostasis of steroid hormones by inhibiting the inactivation mechanism catalyzed by hSULT2A1. These effects would be amplified assuming the intracellular concentrations of the metabolites were to exceed those of the hydroxysteroids, and some studies report that the concentrations of tamoxifen metabolites in tissues are 6 – 60 fold higher than those in serum (66, 91, 92).

The inhibition studies with DHEA and PREG are also an indication of the possibility that several of these metabolites will inhibit the sulfation of α-OHTAM. Since endoxifen, 4-OHTAM, N-desTAM, and TAM-NO were shown to effectively inhibit hSULT2A1, it is predicted that in some cellular environments where these metabolites are produced, sufficient concentrations may be present to inhibit the hSULT2A1-catalyzed sulfation of α-OHTAM. Human SULT2A1 has a much lower catalytic efficiency with α-OHTAM than with DHEA (244), and α-OHTAM is reported to have a mean plasma concentration of only 1 nM (74). In the present study endoxifen was an inhibitor of hSULT2A1 with Ki values of 2.8 μM and 3.5 μM, respectively, with DHEA and pregnenolone as substrate. Apak and Duffel previously determined a Km value of 136 ± 7

μM for the sulfation of E-(±)-α-OHTAM catalyzed by hSULT2A1 with a kcat/Km value of 5.1 ± 0.3 min^{-1} mM^{-1} (244). Thus, it would be expected that endoxifen would inhibit the sulfation of α-OHTAM under the most likely *in vivo* conditions. Furthermore, N-desTAM-S was identified as a potent inhibitor of DHEA sulfation with a Ki value of 4.8 μM (Figure 25B), which was a significantly lower Ki value that seen for the parent metabolite in Table 2. The combination of N-desTAM serving as a substrate (i.e. binding in a catalytically productive conformation at the active site) and the affinity of the enzyme for the product sulfamate suggest that N-desTAM may also contribute to inhibition of hSULT2A1 *in vivo*.

The benefits of tamoxifen therapy are dependent on the *in vivo* formation of its active metabolites 4-OHTAM and endoxifen, which are derived from the CYP2D6-mediated oxidation of tamoxifen (245) and N-desTAM (74), respectively. CYP2D6 is polymorphic (74, 105), and such polymorphisms have been shown to lower the plasma levels of endoxifen and increase the risk of breast cancer mortality in tamoxifen-treated women (99). In order to overcome the pharmacogenetic variability between tamoxifen users, endoxifen has been proposed as an independent therapeutic agent for the treatment of patients with estrogen receptor-positive breast tumors and hormone receptor-positive solid tumors (NCT01327781 and NCT01273168; ClinicalTrials.gov). An additional advantage of direct use of endoxifen might be the lack of conversion to reactive intermediates analogous to α-sulfooxy-tamoxifen. Nevertheless, it is important to realize that the role of endoxifen as a clinically effective SERM might be affected by its potential to interfere in steroid hormone homeostasis, as is suggested by the inhibition studies with steroid substrates for hSULT2A1.

Summary

In summary, 4-OHTAM, TAM-NO, N-desTAM and endoxifen were inhibitors of the sulfation of DHEA and PREG catalyzed by hSULT2A1. Endoxifen was the most

potent inhibitor of the enzyme, which suggests that this metabolite may inhibit the role of hSULT2A1 in the metabolic pathway for genotoxicity that is seen with tamoxifen. N-desTAM was a substrate for the enzyme, and the product of this reaction, N-desTAM-S, displayed greater inhibition of the enzyme than its unconjugated precursor. Thus, endoxifen, N-desTAM, and N-desTAM-S might serve protective roles in some tissues as they may inhibit the sulfation of α-OHTAM. Furthermore, the formation of these metabolites in the human liver may regulate the activity of hSULT2A1 when in the vicinity of α-OHTAM, and this might contribute to the tissue differences in the carcinogenic response of tamoxifen that is observed between rodents and humans. The inhibition of the hSULT2A1-catalyzed sulfation of DHEA and PREG by the tamoxifen metabolites suggests a possible role of the metabolites in inhibiting the inactivation of other steroid hormones.

CHAPTER 4

INTERACTIONS OF TAMOXIFEN METABOLITES WITH HUMAN ESTROGEN SULFOTRANSFERASE SULT1E1

Introduction

Since estrogen metabolism plays an important role in therapeutic efficacy of tamoxifen, the second goal of the current study was to determine the interactions of tamoxifen and its major metabolites with the human estrogen sulfotransferase 1E1 (hSULT1E1). It was hypothesized that the tamoxifen metabolites could inhibit the inactivation of estrogens catalyzed by hSULT1E1. Such inhibition may increase the concentrations of biologically active estrogens in endocrine-responsive tissues such as the endometrium or breast. The proliferative action of estrogen in breast tissue would decrease the efficacy of tamoxifen as a SERM and may contribute to the mechanism of resistance in tamoxifen-treated women. Moreover, excessive estrogen receptor stimulation in endometrial tissue due to alterations in estrogen metabolism may contribute to the carcinogenic effects of tamoxifen. Due to the potential use of endoxifen as an independent SERM, it is particularly important to evaluate the interactions of this metabolite with hSULT1E1 to understand the role of the enzyme in the efficacy of endoxifen. To test this hypothesis, metabolites of tamoxifen were evaluated as inhibitors of the hSULT1E1-catalyzed sulfation of [^{3}H]-estradiol.

Expression and Purification of Recombinant hSULT1E1

Affinity chromatography has become a commonly employed purification procedure following the bacterial expression of hSULT1E1 (202, 204, 246, 247). While this method can expedite the purification process, it involves multiple modifications of the protein by the addition and removal of an affinity tag (i.e. 6x His or maltose binding protein), and these processes may increase the possibility of permanently altering the

structure or functional integrity of the protein. In efforts to minimize manipulations of the enzyme, hSULT1E1 was expressed and purified from bacteria in its native form without the use of affinity tags.

An expression clone (pReceiver-B02) harboring the gene encoding hSULT1E1 was transformed and expressed in *E. coli*. Cell cultures (1.0 L) were grown to an optical density of 1.0 at 600 nm (OD_{600}) and then induced with 300 µM Isopropyl β-D-1-thiogalactopyranoside (IPTG). The cultures were grown overnight at 30ºC and harvested for hSULT1E1 as described in Chapter 7. Following the bacterial expression of hSULT1E1, 44 ml of cell extract containing 437 mg of total protein in Buffer A (10 mM Tris-HCl, pH 7.5, containing 0.25 M sucrose, 1 mM dithiothreitol (DTT), 10 % (v/v) glycerol, 1 mM phenylmethyl sulfonyl fluoride (PMSF), 1 µM pepstatin A, 3.3 µM antipain, 10 µM trans-epoxysuccinyl-*L*-leucylamido-(4-guanidino)-butane (E-64), and 100 µM leupeptin) was subjected to DE-52 anion exchange column chromatography. After elution of those proteins that did not bind to the column, separation was achieved using a linear gradient formed between 200 ml Buffer B (50 mM Tris-HCl, pH 7.5, containing 0.25 M sucrose, 1 mM DTT, 10 % (v/v) glycerol, and 0.05 % (v/v) Tween 20) and 200 ml of Buffer B containing 100 mM KCl. Figure 27 illustrates the general elution profile obtained by monitoring the absorbance at 280 nm in relation to the profile of hSULT1E1 activity. Fractions that were active for hSULT1E1 were analyzed by SDS-PAGE in Figure 28. Fractions 34 – 40 were determined to be relatively pure, and these were pooled and concentrated by ultrafiltration. In order to prepare this mixture for the next step in purification, the buffer was changed to Buffer C (10 mM potassium phosphate, pH 6.8, 0.25 M sucrose, 1 mM DTT and 0.05 % (v/v) Tween 20) through successive dilution and concentration by ultrafiltration. The final volume of the mixture after concentration was 14 ml and the specific activity was calculated as 34 nmol/min/mg when examined with 25 µM estradiol as substrate at pH 7.4. As seen in Table 7, 24 % of the total enzyme units

were retained at the end of this step, while removing approximately 96 % of the total protein in the cell extract.

The hSULT1E1 obtained from DE-52 chromatography was then applied to a hydroxyapatite (HA) column that had been equilibrated with Buffer C. After elution of those proteins that did not bind to the hydroxyapatite, hSULT1E1 was eluted with a linear gradient formed between 100 ml Buffer C and 100 ml Buffer C containing 0.4 M potassium phosphate. The elution profile of total protein in relation to the activity of hSULT1E1 from hydroxyapatite is illustrated in Figure 29. Fractions 8 – 12 were concentrated into a final volume of 12 ml by ultrafiltration, and the specific activity was then determined. Approximately 13 % of enzyme units were retained at the end of this step, while removing approximately 98 % of total protein in the cell extract. As seen in Figure 30, hSULT1E1 displayed only minor low molecular weight impurities. The molecular mass of hSULT1E1 was found to be approximately 35 kDa, which is consistent with previously reported data for this enzyme (200). The purity of hSULT1E1 was greater than 94 % as determined by densitometry.

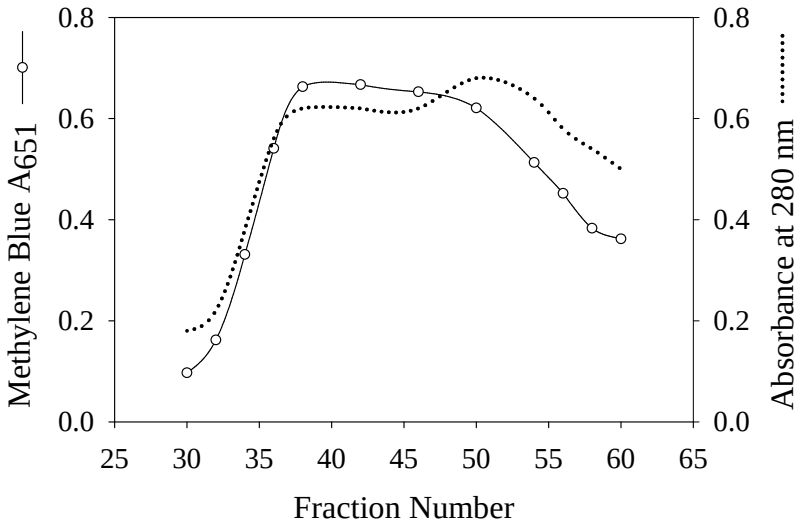

Note: The dashed line represents the general protein elution profile recorded at 280 nm, and the solid line indicates the distribution of hSULT1E1.

Figure 27. Elution profile of the DE-52 anion exchange cellulose column following the initial removal of non-binding proteins.

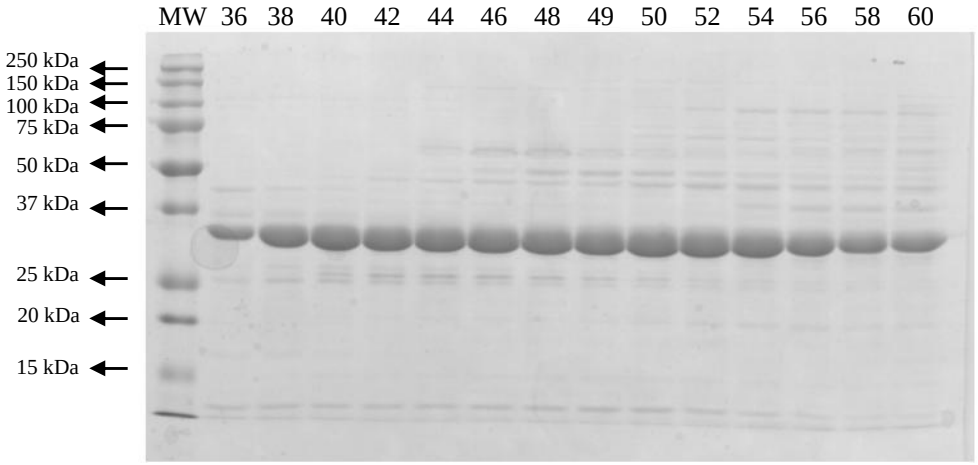

Note: The first lane (MW) contains the protein standards. The contents of the remaining lanes are identified by the fraction number collected from DE-52.

Figure 28. SDS-PAGE results obtained after the DE-52 anion exchange column.

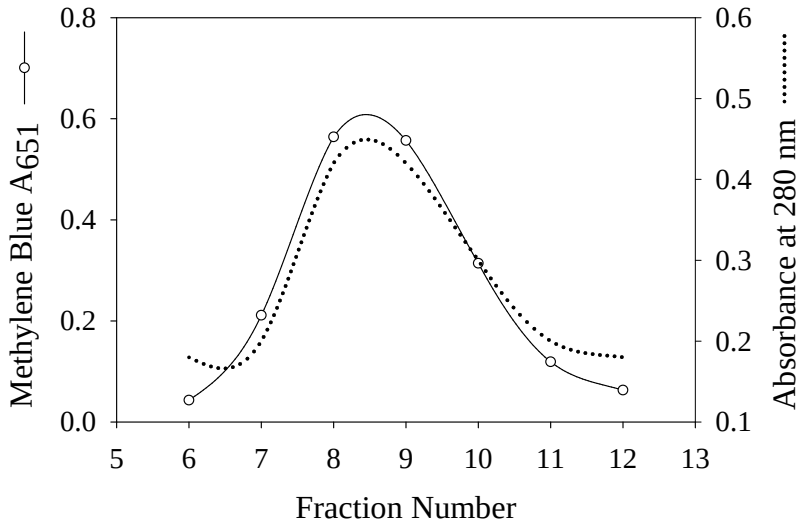

Note: The dashed line represents the general protein elution profile recorded at 280 nm, and the solid line indicates the distribution of hSULT1E1.

Figure 29. Elution profile of the hydroxyapatite column following the initial removal of non-binding proteins.

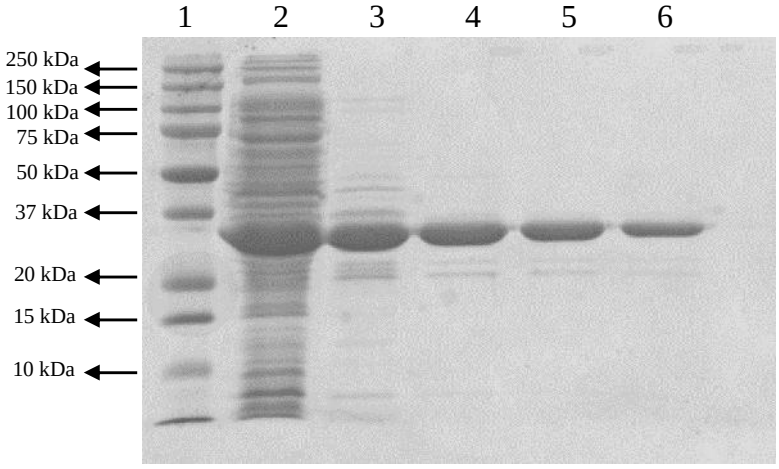

Note: Lane 1, protein standards; lane 2, cell extract (100 µg); lane 3, purified hSULT1E1 from DE-52 (20 µg); lane 4, purified hSULT1E1 from HA (15 µg); lane 5, purified hSULT1E1 from HA (10 µg); lane 6, purified hSULT1E1 from HA (5 µg).

Figure 30. SDS-PAGE results for the purification of hSULT1E1.

Step	Total Protein	Total Volume	Specific Activity	Total Units
	mg	*ml*	*nmol/min/mg*	*nmol/min*
Cell Lysate	437	44	8.6	3800
DE-52	26	14	34	900
HA	10	12	49	500

Note: Specific activity refers to the sulfation of estradiol at pH 7.4. Assay mixtures containing 25 µM estradiol, 200 µM PAPS, 8 mM 2-mercaptoethanol, 10 µl of protein obtained after each step, and 0.25 M potassium phosphate were incubated at 37ºC for 20 min.

Table 7. Summary of the purification of hSULT1E1 from *E coli.*

In summary, the native form of hSULT1E1 was purified from *E. coli* using DE-52 anion exchange and hydroxyapatite column chromatography to relative homogeneity as determined by SDS-PAGE. As seen in Table 7, ten mg of purified hSULT1E1 was recovered from 437 mg of total protein in the cell lysate. The specific activity of this single preparation of hSULT1E1 was calculated as 48 nmol/min/mg when examined with 25 µM estradiol at pH 7.4. The activity from this single preparation of hSULT1E1 is significantly higher than the activity of this enzyme reported in literature. Moreover, this method provided large amounts of active enzyme for subsequent kinetic studies without the need for affinity ligands that can sometimes alter the structure and functional integrity of the protein.

Inhibition of hSULT1E1 by Major Tamoxifen Metabolites

Endoxifen, 4-OHTAM, TAM-NO, and N-desTAM were investigated as inhibitors of hSULT1E1 using estradiol as substrate. The sulfation of estradiol was initially examined with 200 µM PAPS and a substrate concentration range between 5.0 – 200 nM to determine the concentrations of estradiol where minimal substrate inhibition occurred (Figure 31). The data for estradiol sulfation could not be described using a simple substrate inhibition model, nor could the data be described using an equation that assumes partial

substrate inhibition as noted in previous studies with hSULT1E1 (143). Due to variations in the methodology and reaction conditions used to monitor sulfation of estradiol in the current study, it is possible that changes in the enzyme environment (i.e. pH 7.4 in the current study vs pH 6.3 in previous work) could contribute to changes in the kinetic mechanism of the enzyme. Thus, an equation that accurately represents substrate inhibition during the hSULT1E1-catalyzed sulfation of estradiol may be more complex than previously assumed. In efforts to determine the kinetic constants for estradiol sulfation and to verify the kinetic mechanism of hSULT1E1, estradiol (50 µM) was examined with varied PAPS concentrations (50 nM – 100 µM) in order to determine those concentrations of PAPS where minimal substrate inhibition occurred. As seen in Figure 32, substrate inhibition was not observed with PAPS under the reaction conditions (i.e. pH 7.4), and this has been previously shown by Falany *et al*. (202). Sulfation rates were then examined with varied concentrations of estradiol (4 nM – 40 nM) and varied concentrations of PAPS (0.2 µM – 10.0 µM) (Figure 33). The results from this study were best described with a sequential rate equation as previously shown by Zhang *et al.* (143). Kinetic constants derived from the hSULT1E1-catalyzed sulfation of estradiol are summarized in Table 8.

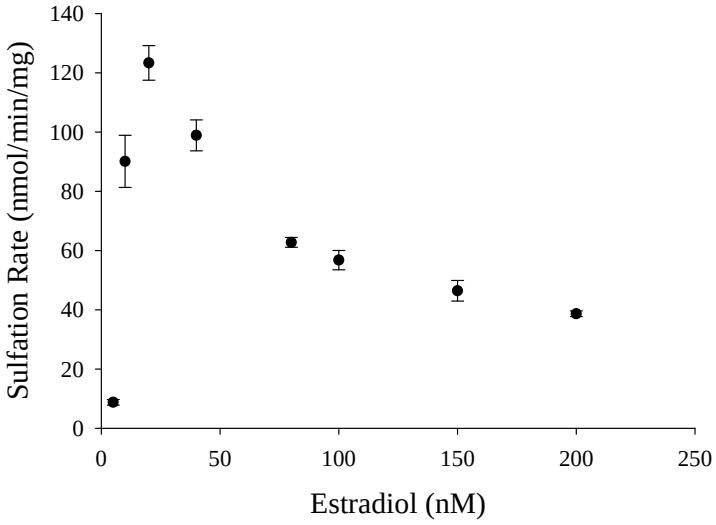

Figure 31. Initial velocities of the hSULT1E1-catalyzed sulfation of estradiol with 50 µM PAPS. Data are the means ± standard error from triplicate determinations and could not be described with a standard uncompetitive substrate inhibition model nor an equation that assumes partial substrate inhibition.

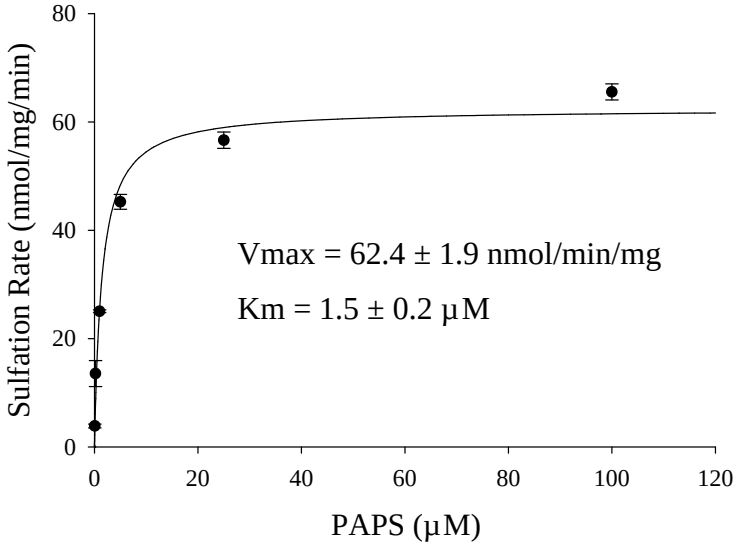

Figure 32. Initial velocities of the hSULT1E1-catalyzed sulfation of 50 µM estradiol with varied PAPS concentrations. Data were fit to a standard Michaelis-Menten equation are the means ± standard error from triplicate determinations. Refer to Table 18 (Chapter 7) for rate equations.

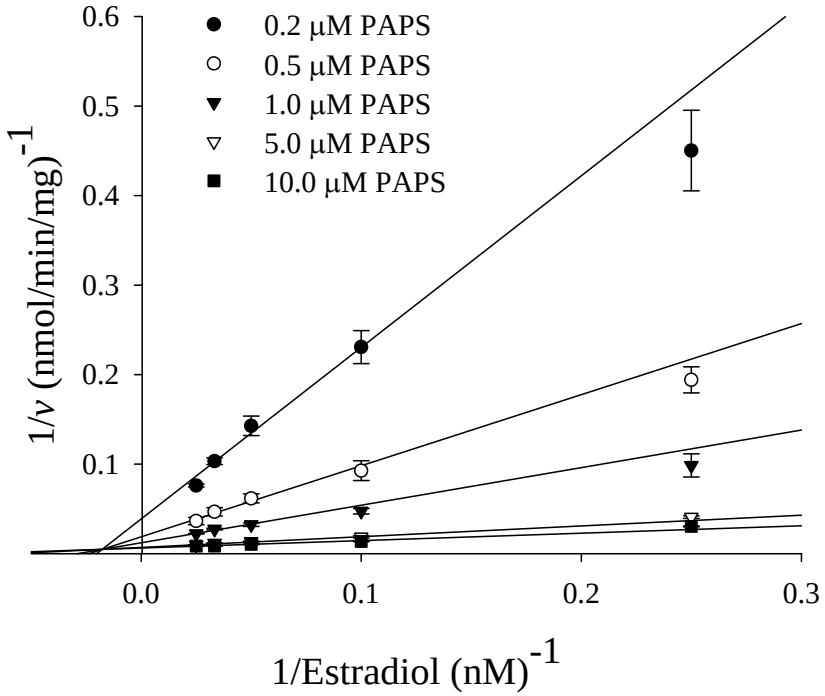

Figure 33. Kinetic mechanism of the hSULT1E1-catalyzed sulfation of estradiol. Data were fit to a random Bi Bi sequential rate equation are the means ± standard error from triplicate determinations. Refer to Table 18 (Chapter 7) for rate equations.

Substrate	Vmax	Ki	Km	kcat
Estradiol	179 ± 9 nmol/min/mg	56 ± 4 nM	8.1 ± 1.6 nM	12.6 min^{-1}
PAPS			1.2 ± 0.3 µM	

Note: Data are the means ± standard error from triplicate determinations. Calculation of kcat values was based on 70,252 as the dimeric molecular mass of hSULT1E1.

Table 8: Kinetic constants derived from the hSULT1E1-catalyzed sulfation of estradiol when analyzed by a random Bi Bi sequential rate equation.

Endoxifen, 4-OHTAM, N-desTAM, and TAM-NO were all weak inhibitors of estradiol sulfation catalyzed by hSULT1E1 (Figure 34). Tamoxifen did not exhibit significant inhibition of hSULT1E1 up to the limits of its solubility in the assay (data not shown). Endoxifen, 4-OHTAM, TAM-NO, and N-desTAM displayed greater than 95% inhibition of the enzyme within their solubility limits. The calculated IC_{50} values ranged from 7.0 μM to 21.0 μM for the inhibition of the sulfation of 7.0 nM estradiol, with 4-OHTAM being the most potent inhibitor. The apparent (app) Vmax and Km, as well as the Ki and kcat/Km for inhibitors of the hSULT1E1-catalyzed sulfation of estradiol are reported in Table 9, with the kinetic mechanism of inhibition and initial velocity data in Figures 35 and 36**.** Endoxifen, 4-OHTAM, and TAM-NO were noncompetitive inhibitors with Ki values of 30.0 μM, 37.8 μM, and 19.7 μM, respectively, whereas N-desTAM was a mixed inhibitor of hSULT1E1 with a Ki value of 10.3 μM.

Metabolite	**IC_{50}**	**Ki**	**Km(app) (Estradiol)**	**Vmax(app) (Estradiol)**	**kcat/Km (Estradiol)**
	μM	*μM*	*nM*	*nmol/min/mg*	*$min^{-1}nM^{-1}$*
Endoxifen	21 ± 1	30 ± 1	63 ± 25	680 ± 237	0.76
N-desTAM	8.2 ± 0.9	10 ± 1	38 ± 7	435 ± 66	0.81
4-OHTAM	7.0 ± 1.1	38 ± 1	57 ± 17	553 ± 149	0.68
TAM-NO	18 ± 1	20 ± 1	22 ± 7	265 ± 65	0.83

Note: Data are the mean ± standard error from triplicate determinations. Calculation of kcat values was based on 70,252 as the dimeric molecular mass of hSULT1E1.

Table 9. Estradiol sulfation was determined using varied concentrations of inhibitor and either 7.0 nM estradiol (for IC_{50} values) for 4.0 nM – 10.0 nM estradiol for determination of the mechanism of inhibition and related kinetic constants.

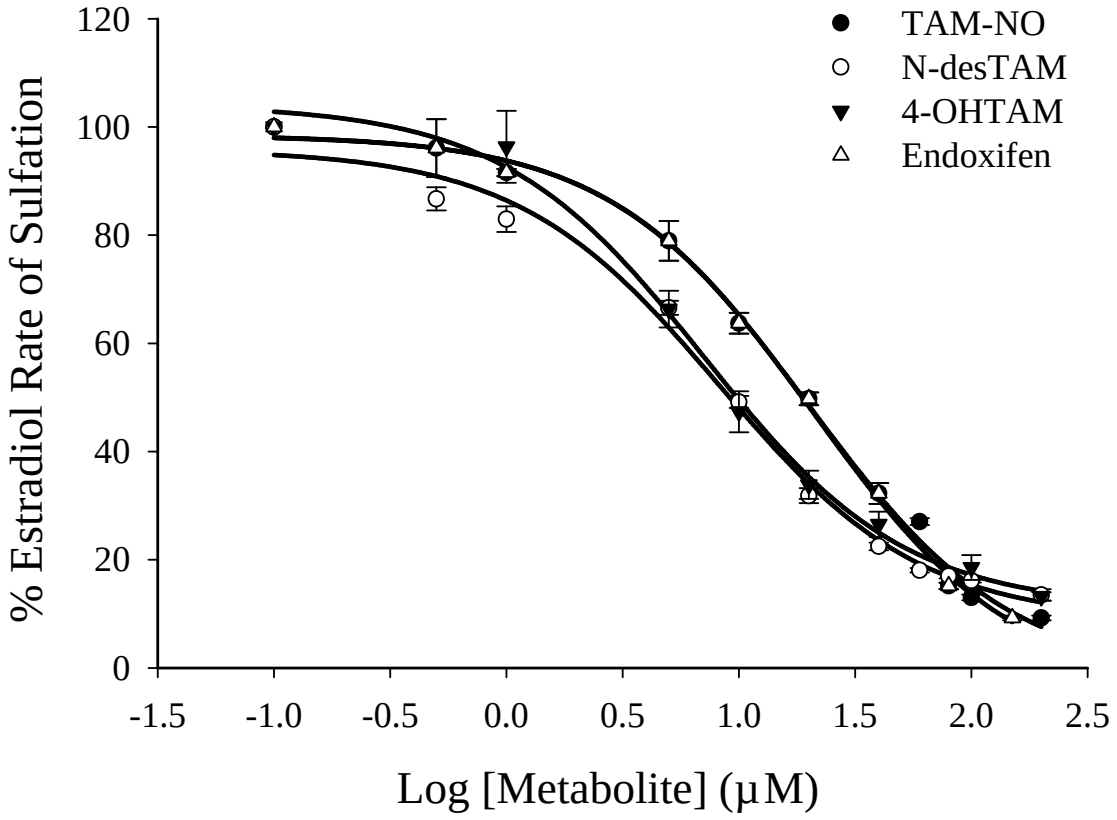

Figure 34. Inhibition of the hSULT1E1-catalyzed sulfation of 7.0 nM estradiol by major metabolites of tamoxifen. Sulfation rates of uninhibited controls for endoxifen, N-desTAM, 4-OHTAM, and TAM-NO were approximately 62, 67, 58, and 69 nmol/min/mg, respectively. Data are the mean ± standard error from triplicate determinations and were fit to a sigmoidal dose-response equation (Table 18, Chapter 7).

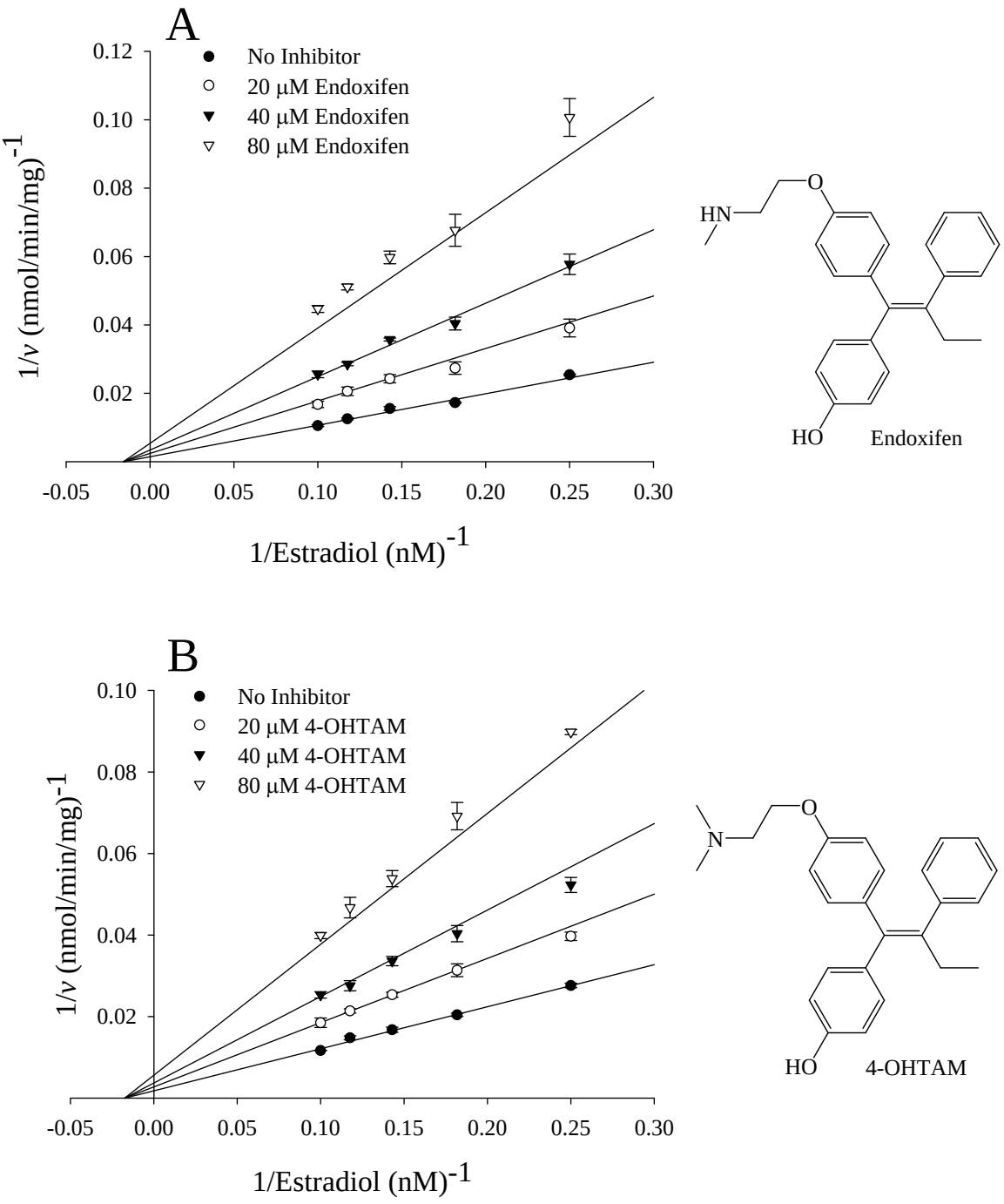

Figure 35. Noncompetitive inhibition of the hSULT1E1-catalyzed sulfation of estradiol by endoxifen (A) and 4-OHTAM (B). Data are the means ± standard error from triplicate determinations. Refer to Table 18 (Chapter 7) for rate equations.

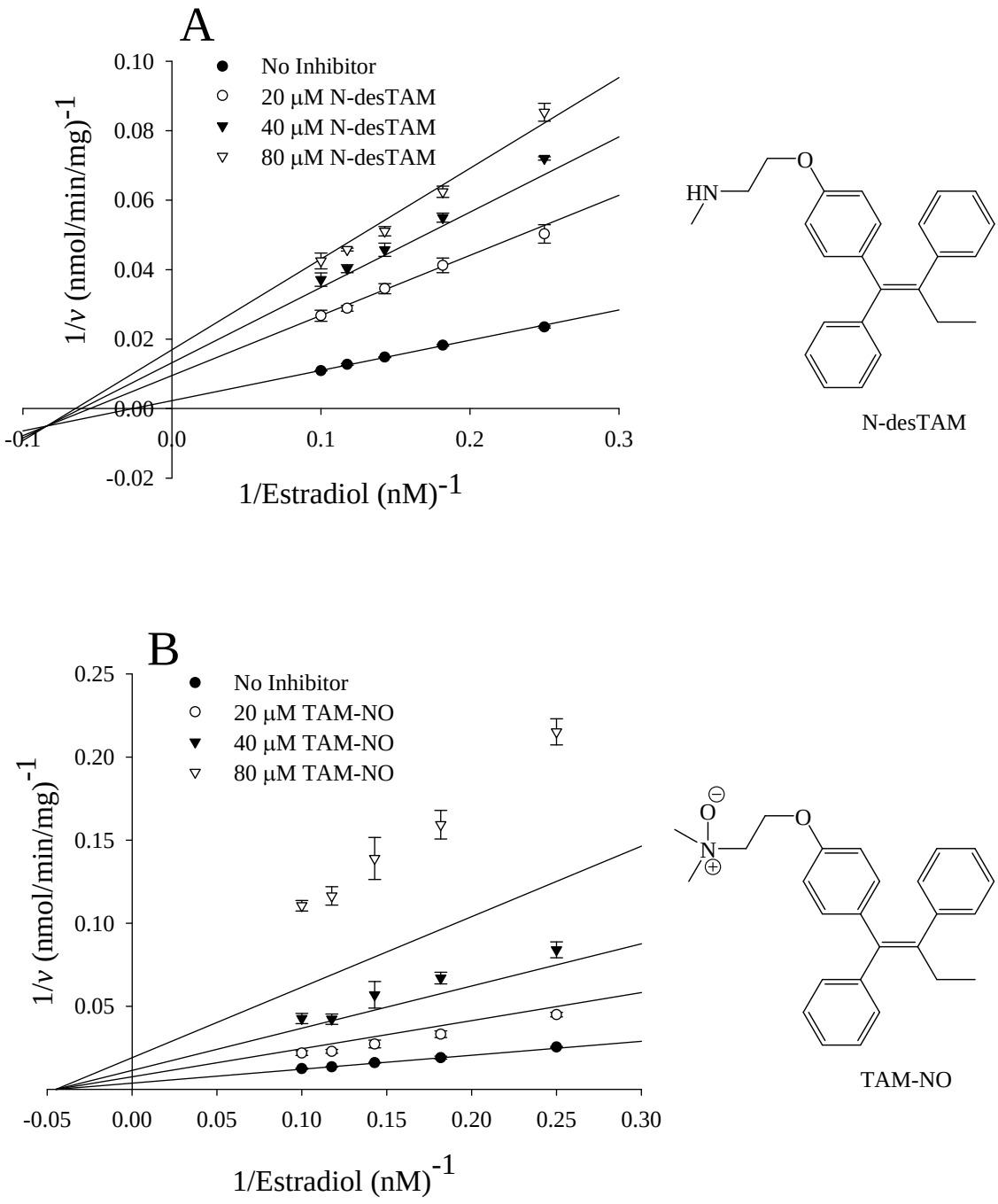

Figure 36. Mixed inhibition of the hSULT1E1-catalyzed sulfation of estradiol by N-desTAM (A), and noncompetitive inhibition of estradiol sulfation by TAM-NO (B). Data are the means ± standard error from triplicate determinations. Refer to Table 18 (Chapter 7) for rate equations.

Characterization of 4-OHTAM, N-desTAM, and Endoxifen as Substrates for hSULT1E1

Previous studies have shown that hSULT1E1 is capable of catalyzing the sulfation of 4-OHTAM (174), however, the kinetics of endoxifen sulfation catalyzed by this enzyme have not been characterized. Furthermore, kinetics for the hSULT1E1-catalyzed sulfation of N-desTAM have also not been documented. In efforts to ascertain the metabolic fate of these metabolites, 4-OHTAM, N-desTAM, and endoxifen were examined as substrates for hSULT1E1. As seen in Figure 37, 4-OHTAM, N-desTAM, and endoxifen were determined to be substrates for the enzyme. The kinetics of sulfation for 4-OHTAM, N-desTAM, and endoxifen were best described using a substrate inhibition model, and the kinetic constants obtained for the hSULT1E1-catalyzed sulfation of these metabolites are summarized in Table 10. The relative sulfation rates for the metabolites were endoxifen > 4-OHTAM > N-desTAM. The enzymatic reactions were analyzed by LC-MS, and the negative ion ESI-MS of the product formed by the hSULT1E1-catalyzed sulfation of N-desTAM is seen in Figure 38. Endoxifen-sulfate was also identified as a product of sulfation catalyzed by hSULT1E1. Analysis of the enzyme-catalyzed reaction revealed a product with m/z of 452.2 by negative ion ESI-MS (Figure 39), which confirms that sulfation had occurred at the phenolic group of endoxifen. The product of 4-OHTAM sulfation is shown in Figure 40 with a m/z of 466.2, as determined by negative ion ESI-MS. The retention times of 4-OHTAM-S, N-desTAM-S, and endoxifen-sulfate from LC chromatographs (See Appendix, Figures A-4, A-5, and A-6) were 16.30, 21.91, and 16.06 min, respectively.

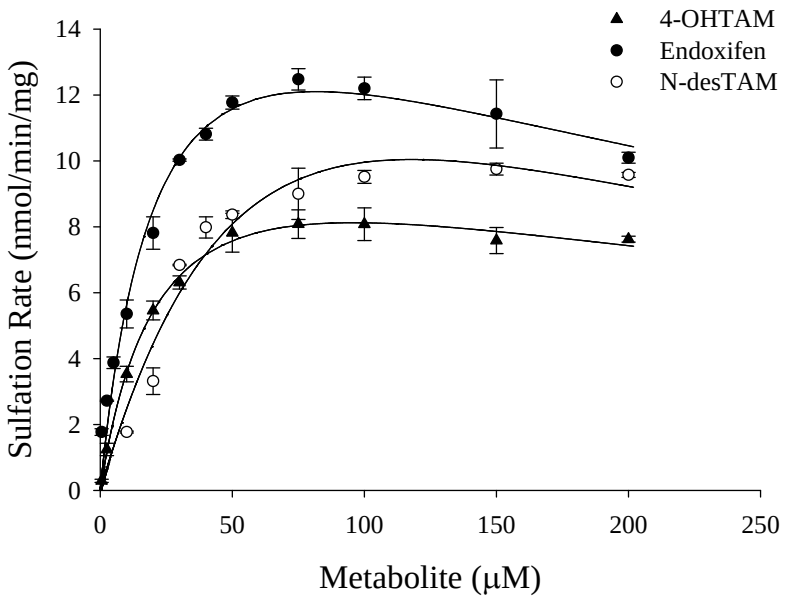

Figure 37. Initial velocities of the hSULT1E1-catalyzed sulfation of 4-OHTAM, endoxifen, and N-desTAM. Data are the means ± standard error from triplicate determinations and were fit to a standard uncompetitive substrate inhibition equation. Refer to Table 18 (Chapter 7) for rate equations.

Metabolite	**Km**	**Vmax**	**kcat/Km**	**Ki**
	μM	*nmol/min/mg*	$min^{-1}\mu M^{-1}$	*μM*
4-OHTAM	24 ± 5	12 ± 1	0.036	387 ± 133
Endoxifen	24 ± 5	19 ± 2	0.057	283 ± 86
N-desTAM	96 ± 52	26 ± 11	0.019	144 ± 105

Note: Data were fit to a standard uncompetitive substrate inhibition equation and are the means ± standard error from triplicate determinations. Calculation of kcat values was based on 70,252 as the dimeric molecular mass of hSULT1E1.

Table 10. Kinetic constants for the hSULT1E1-catalyzed sulfation of 4-OHTAM, N-desTAM, and endoxifen.

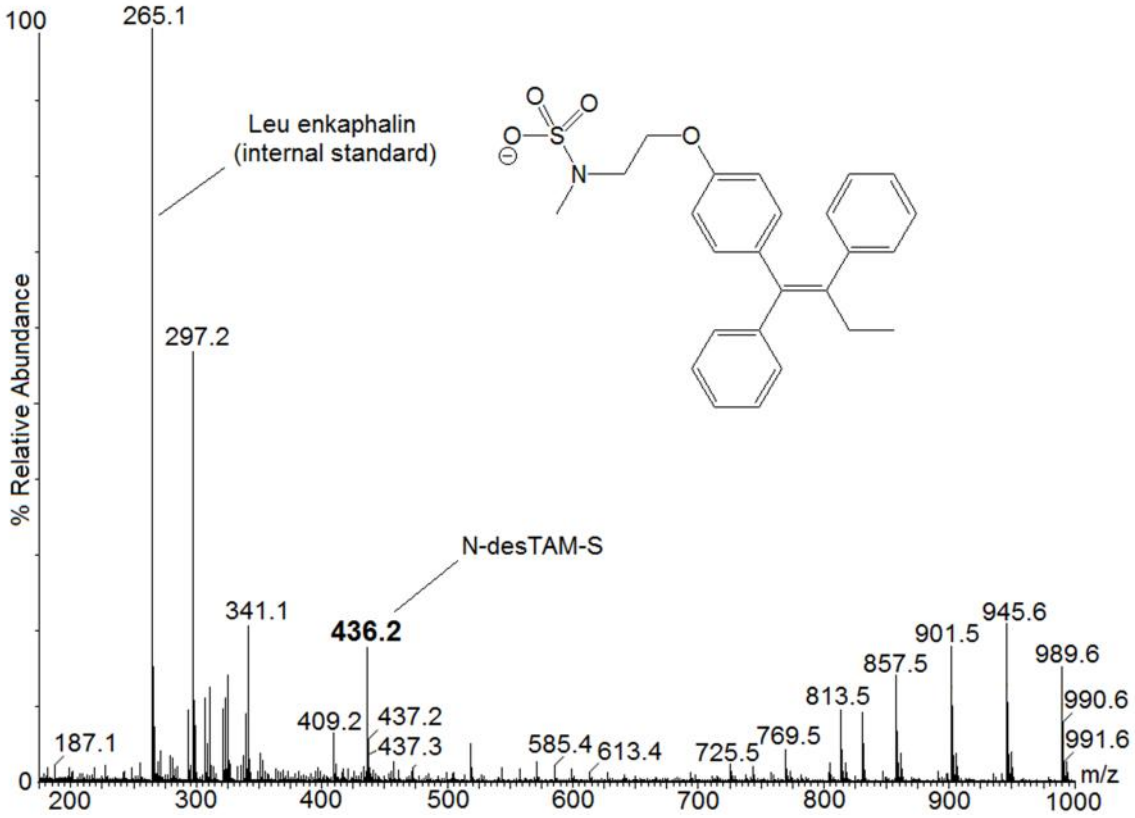

Figure 38. LC-MS analysis of N-desTAM-S as a product of sulfation catalyzed by hSULT1E1. The theoretical calculated m/z of N-desTAM-S is 436.1588 $[M - H]^-$.

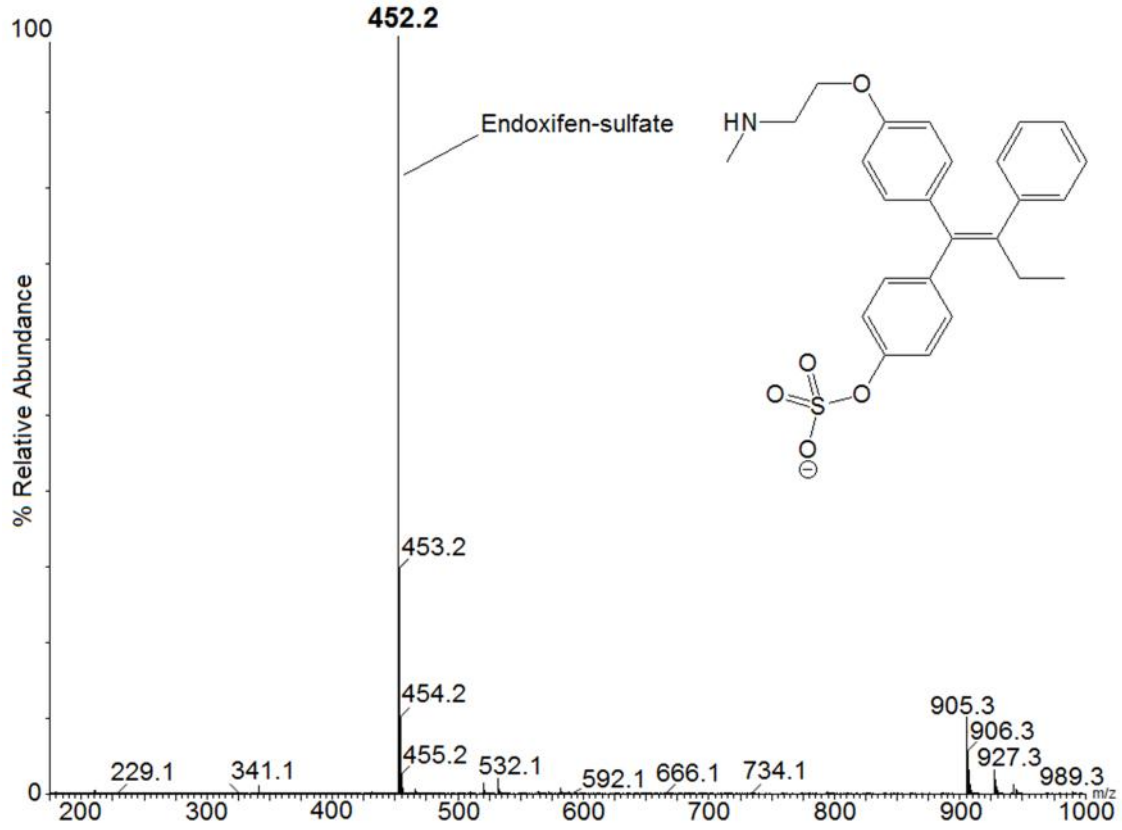

Figure 39. LC-MS analysis of endoxifen-sulfate as a product of sulfation catalyzed by hSULT1E1. The theoretical calculated m/z of endoxifen-sulfate is 452.1532 $[M - H]^-$.

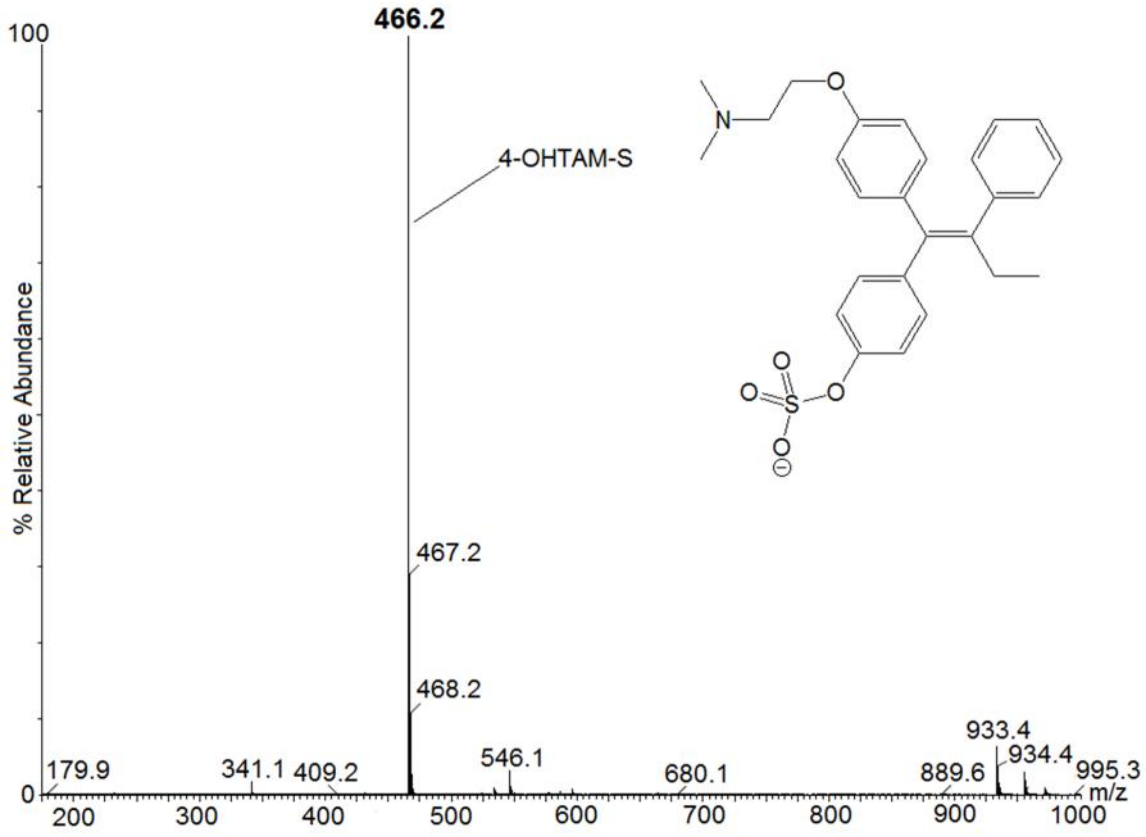

Figure 40. LC-MS analysis of 4-OHTAM-S as a product of sulfation catalyzed by hSULT1E1. The theoretical calculated m/z of 4-OHTAM-S is 466.1852 $[M - H]^-$.

4-OHTAM-S and N-desTAM-S are Weak Inhibitors of hSULT1E1

N-desTAM-S and 4-OHTAM-S were investigated as inhibitors of hSULT1E1. N-desTAM-S was a weak inhibitor of estradiol sulfation with calculated IC_{50} and Ki values of 5.6 µM and 3.3 µM, respectively, whereas 4-OHTAM-S was determined to be a very weak inhibitor of the enzyme with an IC_{50} value greater than 100 µM when examined with 7.0 nM estradiol as substrate (Figure 41A). The kinetic parameters for the inhibition of the estradiol sulfation by N-desTAM-S are shown in Table 11, with the kinetic mechanism of inhibition and initial velocity data in Figure 41B. As seen in Table 11, the Km and Vmax values for estradiol sulfation were very large when N-desTAM-S was examined as an inhibitor of hSULT1E1. While the reason for these exceptionally high kinetic parameters is unknown, the data were reproducible under the reaction conditions used for determining the inhibition of hSULT1E1.

Metabolite	**IC_{50}**	**Ki**	**Km (Estradiol)**	**Vmax (Estradiol)**	**kcat/Km (Estradiol)**
	µM	*µM*	*nM*	*nmol/min/mg*	$min^{-1}nM^{-1}$
N-desTAM-S	5.6 ± 0.9	3.3 ± 0.3	170 ± 330	1,500 ± 2,800	0.62
4-OHTAM-S	> 100				

Note: Data are the means ± standard deviation from triplicate determinations. Calculation of kcat values was based on 70,252 as the dimeric molecular mass of hSULT1E1.

Table 11. The inhibition of estradiol sulfation was determined using either 7.0 nM estradiol (for IC_{50} values) or 4.0 – 10.0 nM estradiol for determining the mechanism of inhibition and related inhibition constants.

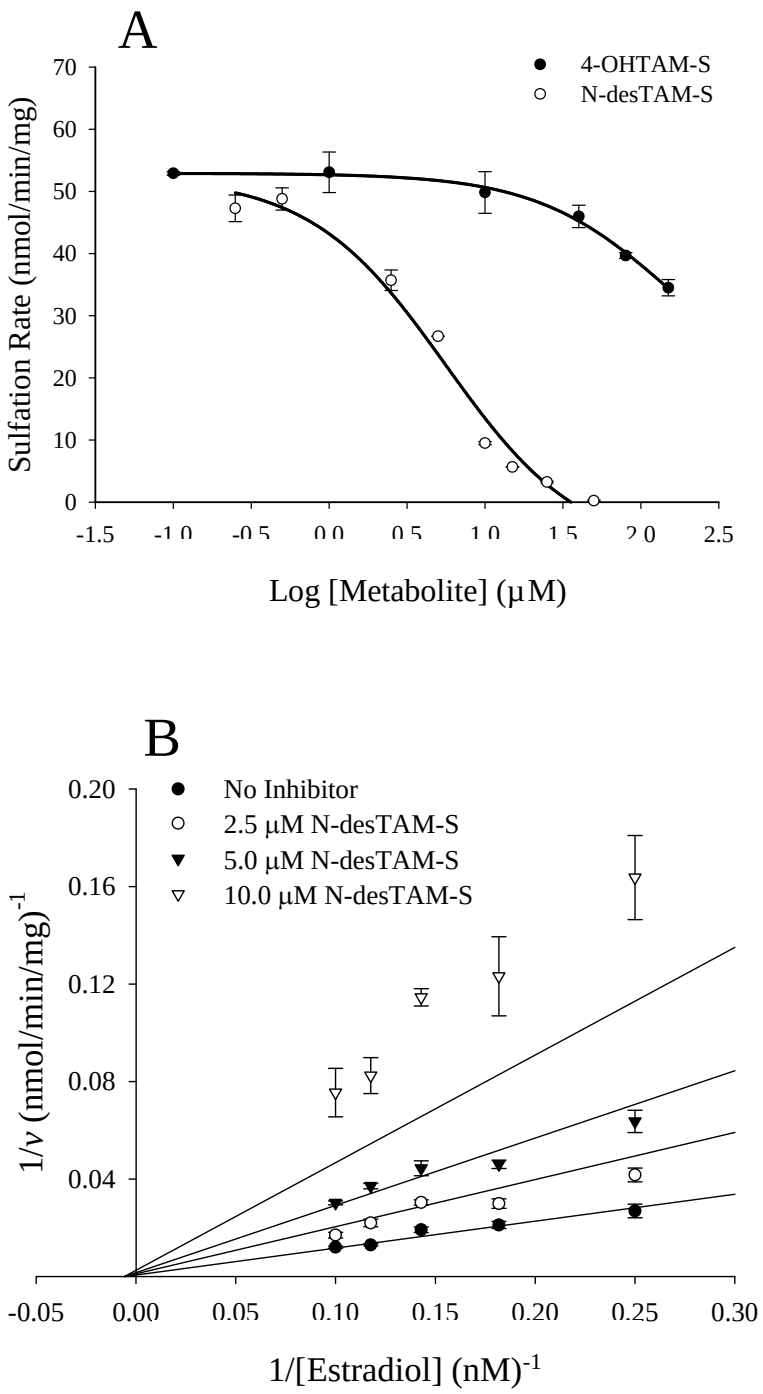

Figure 41. Inhibition of the hSULT1E1-catalyzed sulfation of (A) 7.0 nM Estradiol by N-desTAM-S and 4-OHTAM-S, and (B), non-competitive inhibition of estradiol sulfation by N-desTAM-S. Data are the means ± standard error from triplicate determinations. Refer to Table 18 (Chapter 7) for rate equations.

Discussion

4-OHTAM, N-desTAM, TAM-NO, and endoxifen were all weak inhibitors of the hSULT1E1-catalyzed sulfation of estradiol. The calculated IC_{50} values for 4-OHTAM, N-desTAM, TAM-NO, and endoxifen ranged from 7.0 µM – 21.0 µM, and these values were at least 1000-fold greater than the concentration of estradiol (7.0 nM) utilized for each IC_{50} determination (Table 9). Moreover, the Ki values for inhibitors of estradiol sulfation ranged from 10 µM – 30 µM, and these values were at least 1000-fold greater than the Km value determined for the sulfation of estradiol (Tables 8 and 9). Estradiol is one of the best known substrates for hSULT1E1, and its sulfation in tissues is tightly regulated by this enzyme. The mean plasma concentration of estradiol in postmenopausal women is 30 pM (191), whereas the mean plasma concentrations of tamoxifen metabolites have been reported to be in the general range of 14 – 130 nM for endoxifen, 3 – 17 nM for 4-OHTAM, 15 – 24 nM for TAM-NO, and 280 – 800 nM for N-desTAM (74). Given the abundance of the tamoxifen metabolites in relation to the physiological concentrations of estradiol, there is a possibility for 4-OHTAM, N-desTAM, TAM-NO, and endoxifen to inhibit the inactivation of estradiol in those tissues where the hSULT1E1 is highly expressed. However, hSULT1E1 is poorly expressed in breast cancer cells (187, 199). Thus, metabolites of tamoxifen are less likely to interfere with the hSULT1E1-catalyzed sulfation of estradiol in breast tumor tissue due to the lack of enzyme expression and the weak interactions of the metabolites with hSULT1E1. As a result, endoxifen is not likely to promote increased estrogen signaling in breast cancer tissue, which suggests that the inhibition of hSULT1E1 will not compromise the efficacy of endoxifen as a SERM in clinical trials.

4-OHTAM, N-desTAM, and endoxifen were all substrates for hSULT1E1. As seen in Table 5, hSULT1E1 displayed much lower catalytic activity with N-desTAM than with 4-OHTAM or endoxifen, which may indicate a preference for the enzyme in catalyzing the sulfation of phenolic substrates. Endoxifen was the best substrate for hSULT1E1 with a

calculated kcat/Km of 0.056 $min^{-1}\mu M^{-1}$. Thus, hSUTL1E1 could be one of the major SULT isoforms responsible for catalyzing the sulfation of endoxifen *in vivo*, and this information will be useful when evaluating the pharmacokinetic properties of endoxifen in clinical trials. Interestingly, the kcat/Km values for the hSULT1E1-catalyzed sulfation of N-desTAM was 8-fold higher than the corresponding value for the sulfation of this metabolite catalyzed by hSULT2A1 (Tables 5 and 10). These findings suggest that hSULT1E1 could also contribute to the *in vivo* formation of N-desTAM-S. As discussed earlier in Chapter 3, N-desTAM-S is a potent inhibitor of hSULT2A1 and its formation in tissues may inhibit the potential role(s) of hSULT2A1 in the genotoxic effects of tamoxifen. Since N-desTAM was shown to be a better substrate for hSUL1E1 in the current study, it is predicted that sufficient concentrations of N-desTAM-S may be generated by hSULT1E1 to inhibit the hSULT2A1-catalyzed sulfation of α-OHTAM. This would constitute an important role of hSULT1E1 in regulating the bioactivation of tamoxifen, which has not been recognized in the field of tamoxifen research. The interactions between hSULT1E1 and hSULT2A1 are plausible since both enzymes are expressed in tissues such as the liver (162, 195) and endometrium (77, 167, 197, 198).

Summary

As summarized in the discussion above, 4-OHTAM, TAM-NO, N-desTAM and endoxifen are weak inhibitors of the hSULT1E1-catalyzed sulfation of estradiol. These studies suggest that metabolites of tamoxifen are not likely to interfere in the inactivation of estrogen catalyzed by hSULT1E1 in breast tumor tissue. Moreover, these studies suggest that endoxifen is not likely to promote increased estrogen signaling in breast tissue when administered as an independent SERM in clinical trials. However, metabolites of tamoxifen may alter estrogen levels in tissues that highly express hSULT1E1, and this is plausible given the abundance of the metabolites in relation to the physiological concentrations of estrogens. N-desTAM was determined to a better substrate for

hSULT1E1 with a relatively higher kcat/Km than the catalytic efficiency constant previously determined with hSULT2A1. Thus, the hSULT1E1-catalyzed sulfation of N-desTAM may generate sufficient amounts of N-desTAM-S to inhibit the role of hSULT2A1 in the bioactivation of tamoxifen. The next chapter will be devoted to determining the interaction of metabolites of tamoxifen with hSULT1A1*1 due to the role of this enzyme in estrogen metabolism.

CHAPTER 5

INTERACTIONS OF TAMOXIFEN METABOLITES WITH HUMAN PHENOL SULFOTRANSFERASE SULT1A1*1

Introduction

Due to the role of estrogen metabolism in the therapeutic efficacy of tamoxifen, the third goal of the current study was to determine the interactions of tamoxifen and its major metabolites with the human phenol sulfotransferase 1A1 variant *1 (hSULT1A1*1). Human SULT1A1*1 is the dominant allelic form of phenol sulfotransferase in humans, and this enzyme catalyzes the inactivation of estrogen in those tissues where the principal estrogen sulfotransferase, hSULT1E1, is poorly expressed. Thus, it was hypothesized that the tamoxifen metabolites could inhibit catalytic activity of hSULT1A1*1. Such inhibition might increase the concentrations of biologically active estrogens and decrease the efficacy of tamoxifen as a SERM. This inhibition would contribute to the mechanism of resistance observed in tamoxifen-treated women and may increase estrogen receptor-related hormonal effects in endocrine-responsive tissues such as the endometrium. Furthermore, alterations in the catalytic activity of hSULT1A1*1 may reduce the therapeutic efficacy of tamoxifen by inhibiting the formation of 4-OHTAM-S, which has been shown to have therapeutic benefits (i.e. enhanced apoptotic properties) in breast cancer cells (216). On the other hand, inhibiting the activity of this enzyme may enhance bioavailability of tamoxifen metabolites (i.e. 4-OHTAM and endoxifen) in healthy tissues that would otherwise promote elimination of the product sulfates. To test this hypothesis, metabolites of tamoxifen were examined as inhibitors of the hSULT1A1*1-catalyzed sulfation of [^{3}H]-estradiol.

Expression and Purification of Recombinant hSULT1A1*1

Human SULT1A1*1 was expressed and purified from E. coli in its native form without the use of affinity tags in order to preserve the structure and functional integrity of the enzyme. An expression clone (pReceiver-B02) harboring the gene encoding hSULT1A1*1 was purchased and transformed into E. coli. Cell cultures (1.0) were grown to an OD_{600} of 1.0 and then induced with 300 µM IPTG. The cultures were grown overnight at 30ºC and harvested for hSULT1A1*1 as described in Chapter 7. The purification of hSULT1A1*1 was performed essentially as described for the purification of hSULT1E1 in Chapter 4, with the exception of a second hydroxyapatite column that was required to remove minor impurities following the rapid elution of hSULT1A1*1 from the first hydroxyapatite column. Buffers A, B, and C were utilized in the purification of hSULT1A1*1, and the recipe for each buffer is given in Chapter 4 under the section for the expression and purification of hSULT1E1.

Following the bacterial expression of hSULT1A1*1, 30 ml of cell extract containing 300 mg of total protein in Buffer A was subjected to DE-52 anion exchange column chromatography. After elution of those proteins that did not bind to the column, separation was achieved using a linear gradient formed between 200 ml Buffer B and 200 ml Buffer B containing 100 mM KCl. Following the completion of the linear gradient, the column was washed with 100 ml Buffer B containing 100 mM KCl to elute hSULT1A1*1. Figure 42 illustrates the general elution profile obtained by monitoring the absorbance at 280 nm in relation to the profile of hSULT1A1*1 activity. Fractions that contained catalytically active hSULT1A1*1 were analyzed by SDS-PAGE (Figure 43). Fractions 61 – 66 were determined to be of highest purity, and these were pooled and concentrated by ultrafiltration. In order to prepare this mixture for the next step in purification, the buffer was changed to Buffer C through successive dilution and concentration by ultrafiltration. The final volume of the mixture after concentration was 14 ml and the specific activity was calculated as 12 nmol/min/mg when examined with 25 µM 2-naphthol as substrate at pH

7.4. As seen in Table 12, 44 % of the total enzyme units were retained at the end of this step, while removing approximately 87 % of the total protein in the cell extract.

The hSULT1A1*1 obtained from DE-52 chromatography was then applied to a hydroxyapatite column that had been equilibrated with Buffer C. After the elution of the proteins that did not bind to the hydroxyapatite, hSULT1A1*1 was eluted with a linear gradient formed between 100 ml Buffer C and 100 ml Buffer C containing 0.4 M potassium phosphate. The elution profile of total protein in relation to the activity of hSULT1E1 from hydroxyapatite is illustrated in Figure 44. As seen in Figure 44, hSULT1A1*1 was distributed primarily to one peak during the gradient elution. Thus, fractions 33 – 36 were concentrated into a final volume of 12 ml by ultrafiltration and the specific activity was determined. Approximately 20 % of enzyme units were retained at the end of the first hydroxyapatite column, while removing approximately 95 % of total protein in the cell extract

Analysis by SDS-PAGE revealed minor impurities at the end of the hydroxyapatite chromatography (Figure 45), which was likely due to the rapid elution of hSULT1A1*1 from the hydroxyapatite under steep gradient conditions (i.e. 0.4 M potassium phosphate). Thus, a second hydroxyapatite column was employed as an additional step in the purification of the enzyme. This column utilized a shallow elution gradient to slowly remove hSULT1A1*1 from the hydroxyapatite. In order to prepare the mixture for the next step in purification, the buffer was changed back into Buffer C using ultrafiltration. The mixture was loaded onto a second hydroxyapatite column previously equilibrated with the same buffer. After the initial removal of the proteins that did not bind to the column, hSULT1A1*1 was eluted with linear gradient formed between 100 ml Buffer C and 100 ml Buffer C containing 80 mM potassium phosphate. The elution profiles for protein and hSULT1A1*1 activity for this step are shown in Figure 46. The activity for hSULT1A1*1 was distributed to a single peak, and these fractions were analyzed by SDS-PAGE (Figure

47). The fractions with the highest activities were pooled and concentrated into a final volume of 11 ml.

The final SDS-PAGE for the purification of hSULT1A1*1 is shown in Figure 48. Human SULT1A1*1 is clearly seen in lanes 2 – 9 as a thick protein band relative to the 37 kDa protein standard in lane 1 (Figure 48). The purity of hSULT1A1*1 was greater than 96% as determined by densitometry, and the final specific activity of the enzyme was determined to be 17 nmol/min/mg when examined with 25 µM 2-naphthol at pH 7.4. The subunit molecular mass of the homogenous hSULT1A1*1 was found to be approximately 34 kDa, which is consistent with previously reported data for this enzyme (218).

In summary, the native form of hSULT1A1*1 was successfully expressed and purified from *E. coli* using DE-52 anion exchange and hydroxyapatite column chromatography. As seen in Table 12, eight mg of purified hSULT1A1*1 was recovered from 300 mg of total protein in the cell lysate. This method provided large amounts of active enzyme for subsequent kinetic studies without the use of affinity tags. Moreover, this method was easily modified from the purification of hSULT1E1 in Chapter 4 and may be useful in the future purification of other recombinant and native human cytosolic SULTs.

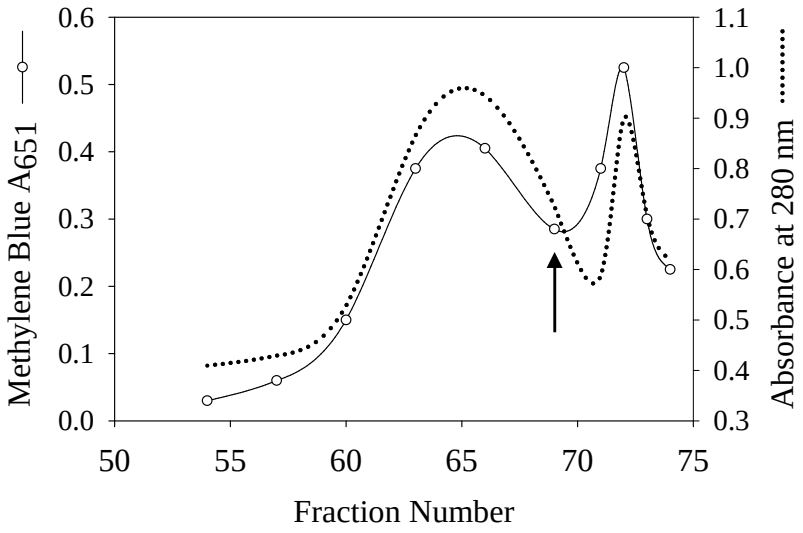

Note: The dashed line represents the general protein elution profile recorded at 280 nm, and the solid line indicates the distribution of hSULT1A1*1. The arrow indicates the end of the linear gradient and additional elution with 100 ml Buffer B containing 100 mM KCl.

Figure 42. Elution profile of the DE-52 anion exchange cellulose column following the initial removal of non-binding proteins.

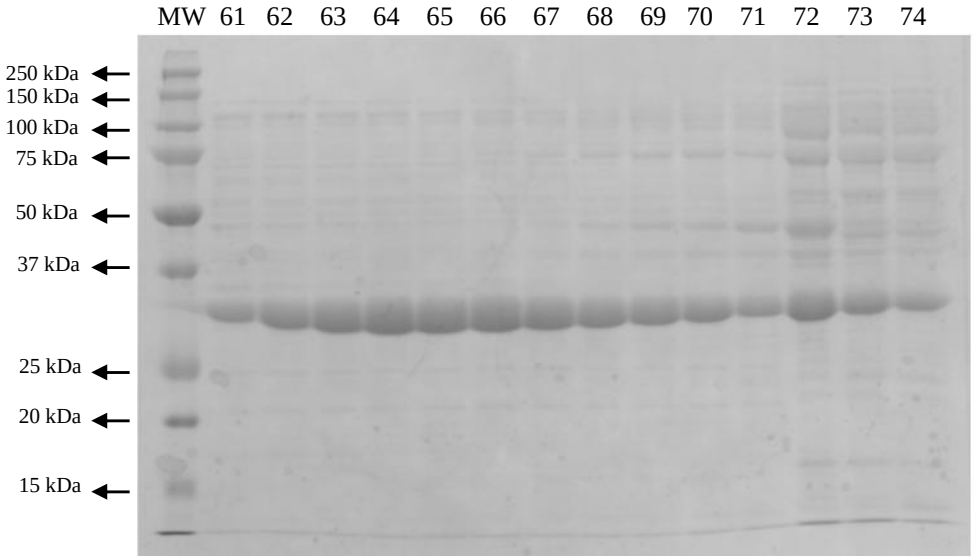

Note: The first lane (MW) contains the protein standards. The contents of the remaining lanes are indicated by the fraction number collected from the DE-52 column.

Figure 43. SDS-PAGE results obtained after the DE-52 anion exchange column.

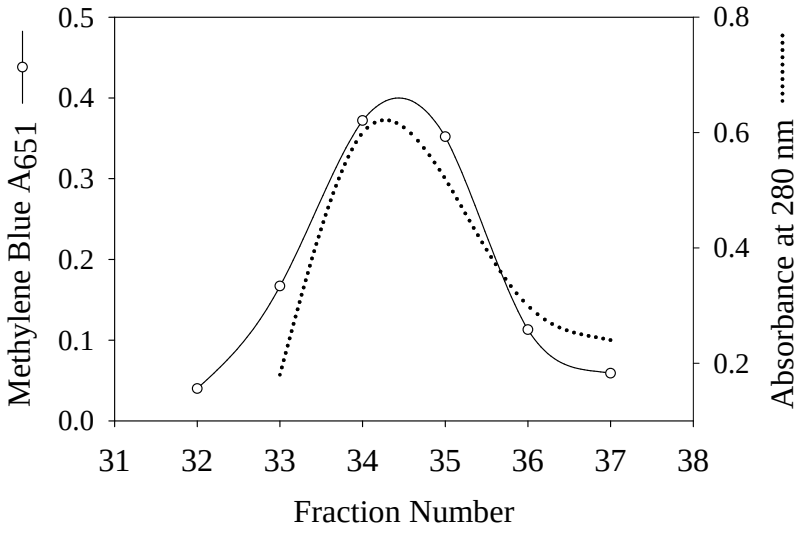

Note: The dashed line represents the general elution profile recorded at 280 nm, and the solid line indicates the distribution of hSULT1A1*1.

Figure 44. Elution profile of the 1st hydroxyapatite column following the initial removal of non-binding proteins.

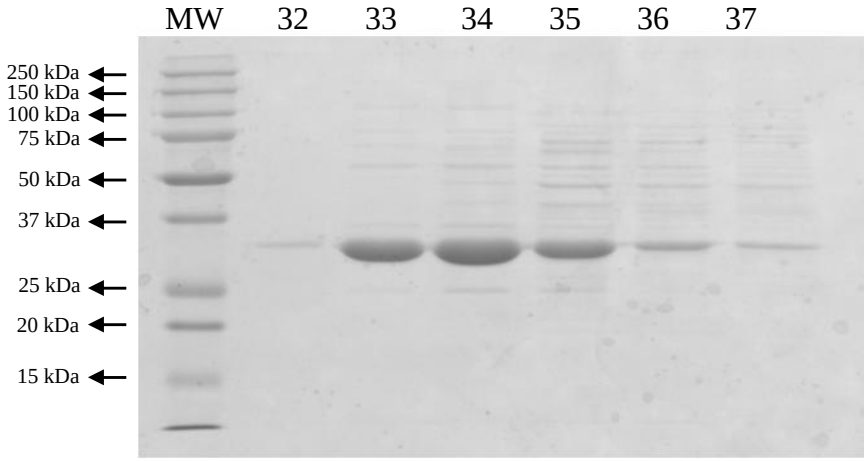

Note: The first lane (MW) contains the protein standards. The contents of the remaining lanes are indicated by the fraction number collected from the 1st HA column.

Figure 45. SDS-PAGE results obtained after the 1st HA column.

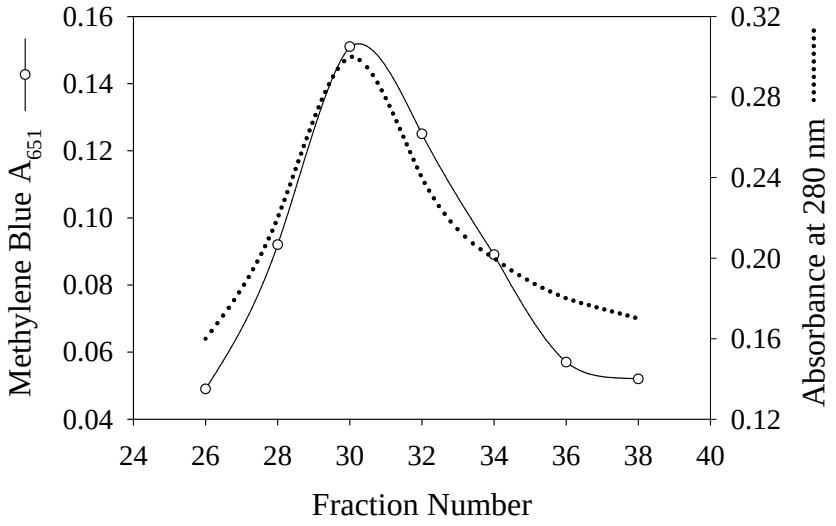

Note: The dashed line represents the general elution profile recorded at 280 nm, and the solid line indicates the distribution of hSULT1A1*1.

Figure 46. Elution profile of the 2nd HA column following the initial removal of non-binding proteins.

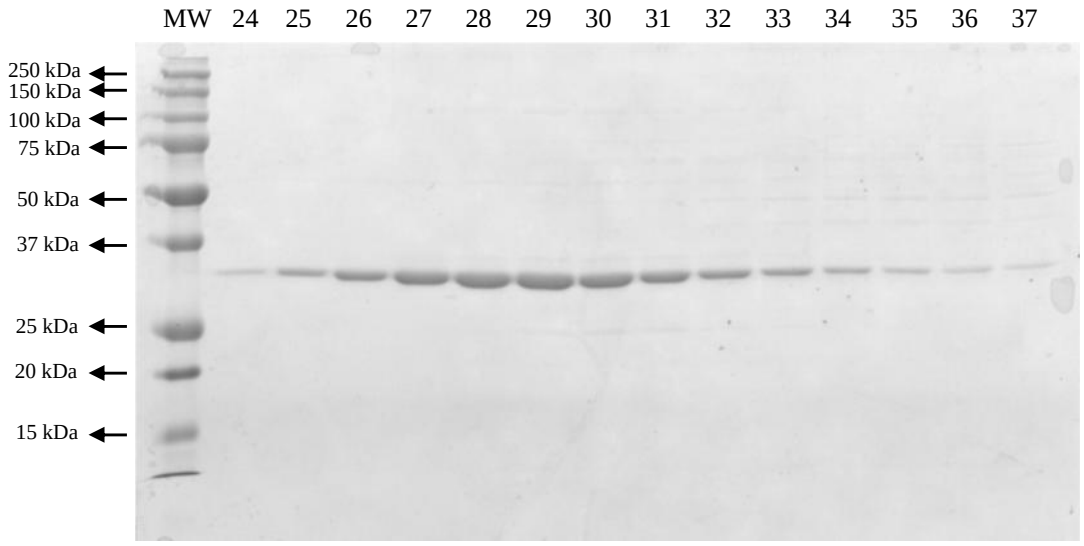

Note: The first lane (MW) contains the protein standards. The contents of the remaining lanes are indicated by the fraction number collected from the 2nd HA column.

Figure 47. SDS-PAGE results obtained after the 2nd HA column.

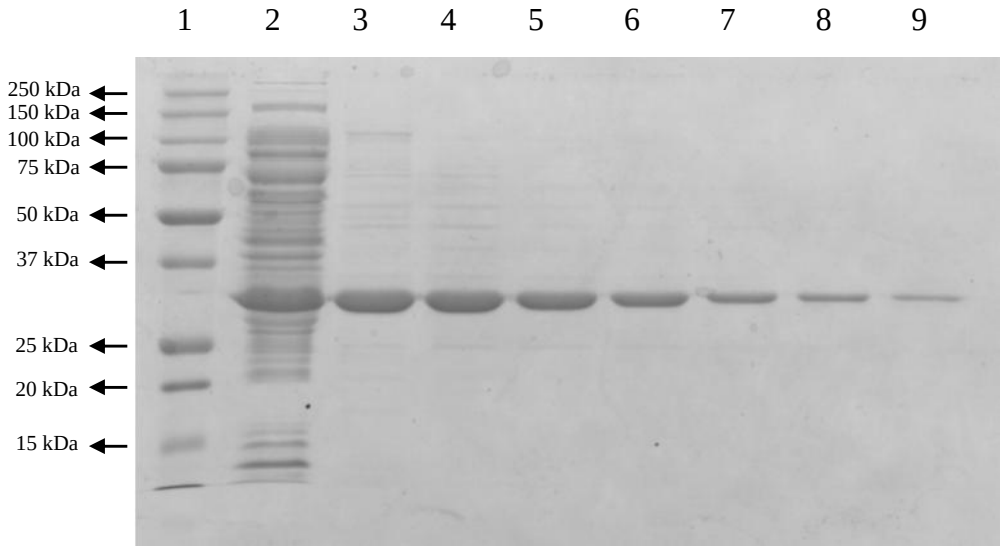

Note: Lane 1, protein standards; lane 2, cell extract (80 µg); lane 3, purified hSULT1A1*1 from DE-52 (20 µg); lane 4, purified hSULT1A1*1 from 1st HA (20 µg); lane 5, purified hSULT1A1*1 from 2nd HA (15 µg); lane 6, purified hSULT1A1*1 from 2nd HA (10 µg); lane 7, purified hSULT1A1*1 from 2nd HA (5 µg); lane 8, purified hSULT1A1*1 from 2nd HA (3 µg); lane 9, purified hSULT1A1*1 from 2nd HA (1 µg).

Figure 48. SDS-PAGE results of the purification of hSULT1A1*1.

Step	**Total Protein**	**Total Volume**	**Specific Activity**	**Total Units**
	mg	*ml*	*nmol/min/mg*	*nmol/min*
Cell Lysate	300	30	4.7	1100
DE-52	40	14	12	500
1st HA	16	12	14	220
2nd HA	8	11	17	130

Note: Specific activity refers to the sulfation of 2-naphthol at pH 7.4. Assay mixtures containing 25 µM 2-naphthol, 200 µM PAPS, 8 mM 2-mercaptoethanol, 40 µl of protein obtained after each step, and 0.25 M potassium phosphate were incubated at 37ºC for 20 min.

Table 12. Summary of the purification of hSULT1A1*1 from *E. coli*.

The Inhibition of hSULT1A1*1 by Major Tamoxifen Metabolites

Endoxifen, 4-OHTAM, TAM-NO, and N-desTAM were investigated as inhibitors of hSULT1A1*1 using estradiol as substrate at pH 7.4. The sulfation of estradiol was initially examined with PAPS (50 µM) using a concentration range between 0.1 – 25.0 µM in order to determine the concentrations of estradiol where minimal substrate inhibition occurred (Figure 49). Kinetic constants derived from the hSULT1A1*1-catalyzed sulfation of estradiol are summarized in Table 13. Estradiol sulfation was later examined using a single concentration of estradiol (5 µM) with varied concentrations of PAPS (1.0 – 100 µM) in order to determine the PAPS concentrations that were saturating for the enzyme. As seen in Figure 50, substrate inhibition was not observed with PAPS at high concentrations. Subsequent inhibition studies utilized 50 µM PAPS as co-substrate. Of the metabolites tested, only endoxifen and 4-OHTAM were significant inhibitors of estradiol sulfation catalyzed by hSULT1A1*1 (Figure 51). These metabolites displayed greater than 95% inhibition of the enzyme within their solubility limits. TAM-NO was also an inhibitor of the enzyme, however, the calculated IC_{50} value for this metabolite was greater than 100 µM when examined with 2 µM estradiol as substrate. N-desTAM and tamoxifen (not shown) were not significant inhibitors of estradiol sulfation within their solubility limits. The Ki, Km, Vmax, and kcat/Km for inhibitors of the hSULT1A1*1-catalyzed sulfation of estradiol are summarized in Table 14, with the mechanism of inhibition and initial velocity data in Figure 52. Endoxifen and 4-OHTAM were determined to be competitive inhibitors of the enzyme with Ki values of 1.6 µM and 5.6 µM, respectively.

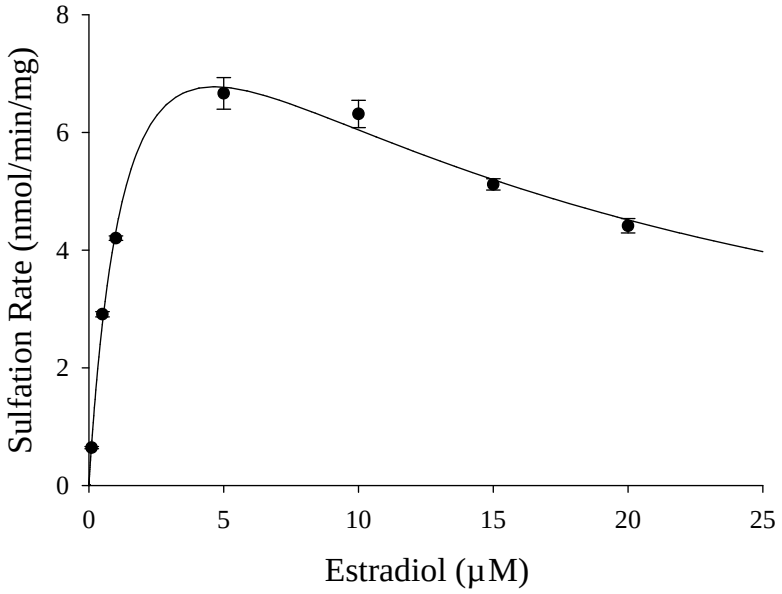

Figure 49. Initial velocities of the sulfation of estradiol catalyzed by hSULT1A1*1 with 50 µM PAPS. Data are the means ± standard error from triplicate determinations and were fit to a standard uncompetitive substrate inhibition equation. Refer to Table 18 (Chapter 7) for rate equations.

Substrate	**Km**	**Vmax**	**kcat/Km**	**Ki**
	µM	*nmol/min/mg*	$min^{-1}\mu M^{-1}$	*µM*
Estradiol	1.5 ± 0.2	11.2 ± 0.8	0.5	14.2 ± 2.1

Note: Data are the means ± standard error from triplicate determinations. Calculation of kcat values was based on 68,312 as the dimeric molecular mass of hSULT1A1*1.

Table 13. Kinetic constants obtained from the hSULT1A1*1-catalyzed sulfation of estradiol.

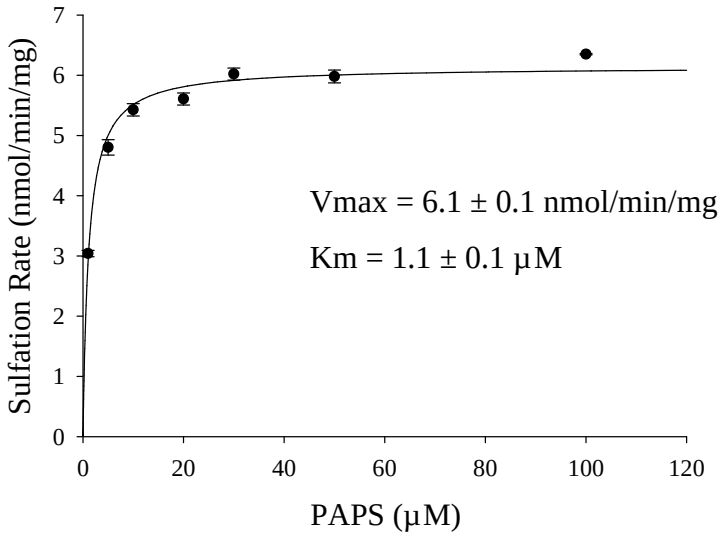

Figure 50. Initial velocities of the hSULT1A1*1-catalyzed sulfation of estradiol (5 µM) with varied concentrations of PAPS. Data are the means ± standard error from triplicate determinations and were fit to a standard Michaelis-Menten equation. Refer to Table 18 (Chapter 7) for rate equations.

Metabolite	**IC_{50}**	**Ki**	**Km (Estradiol)**	**Vmax (Estradiol)**	**kcat/Km (Estradiol)**
	µM	*µM*	*µM*	*nmol/min/mg*	$min^{-1}\mu M^{-1}$
4-OHTAM	1.6 ± 0.9	1.6 ± 0.1	3.9 ± 0.6	18 ± 2	0.3
Endoxifen	9.9 ± 0.9	5.6 ± 0.5	5.3 ± 1.4	23 ± 4	0.3
TAM-NO	> 100				

Note: Data are the mean ± standard error from triplicate determinations. Calculation of kcat values was based on 68,312 as the dimeric molecular mass of hSULT1A1*1.

Table 14. The sulfation of estradiol was determined using varied concentrations of inhibitor and either 2.0 µM estradiol (for IC_{50} values) for 0.5 – 2.5 µM estradiol for determination of the mechanism of inhibition and related kinetic constants.

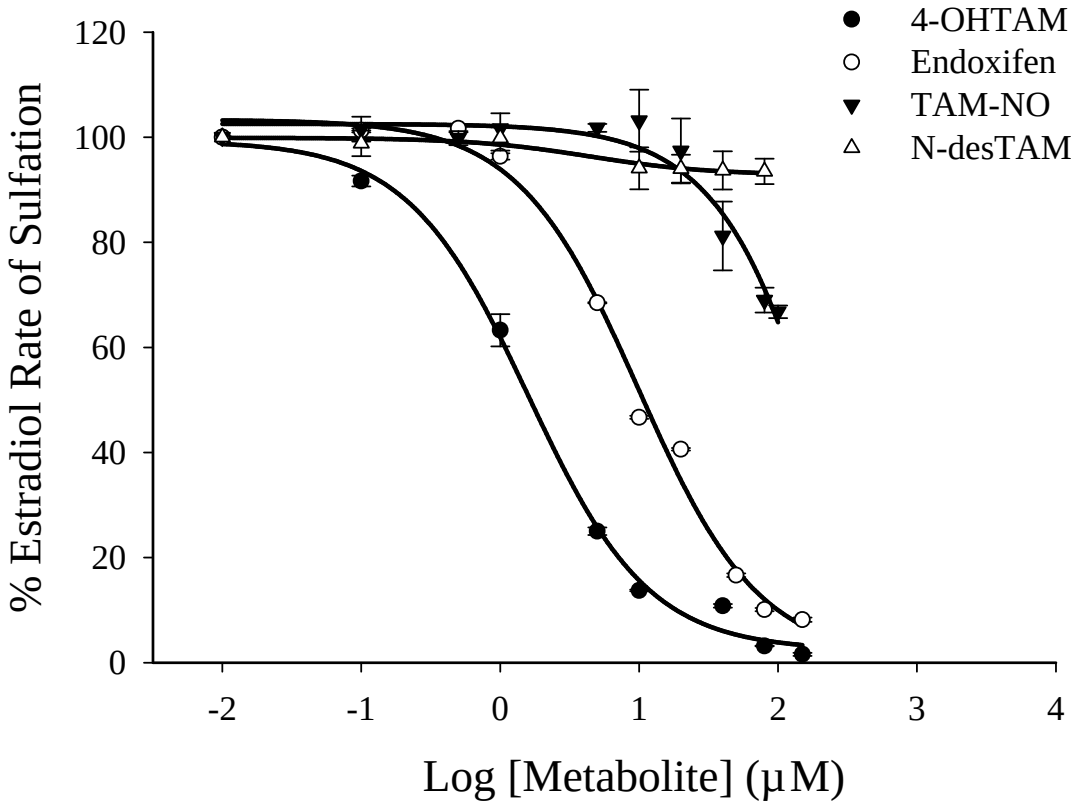

Figure 51. Inhibition of the hSULT1A1*1-catalyzed sulfation of 2.0 µM estradiol by major metabolites of tamoxifen. Sulfation rates of uninhibited controls for endoxifen, N-desTAM, 4-OHTAM, and TAM-NO were approximately 5.1, 5.8, 5.7, and 5.7 nmol/min/mg, respectively. Data are the mean ± standard error from triplicate determinations and were fit to a sigmoidal dose-response equation (Table 18, Chapter 7).

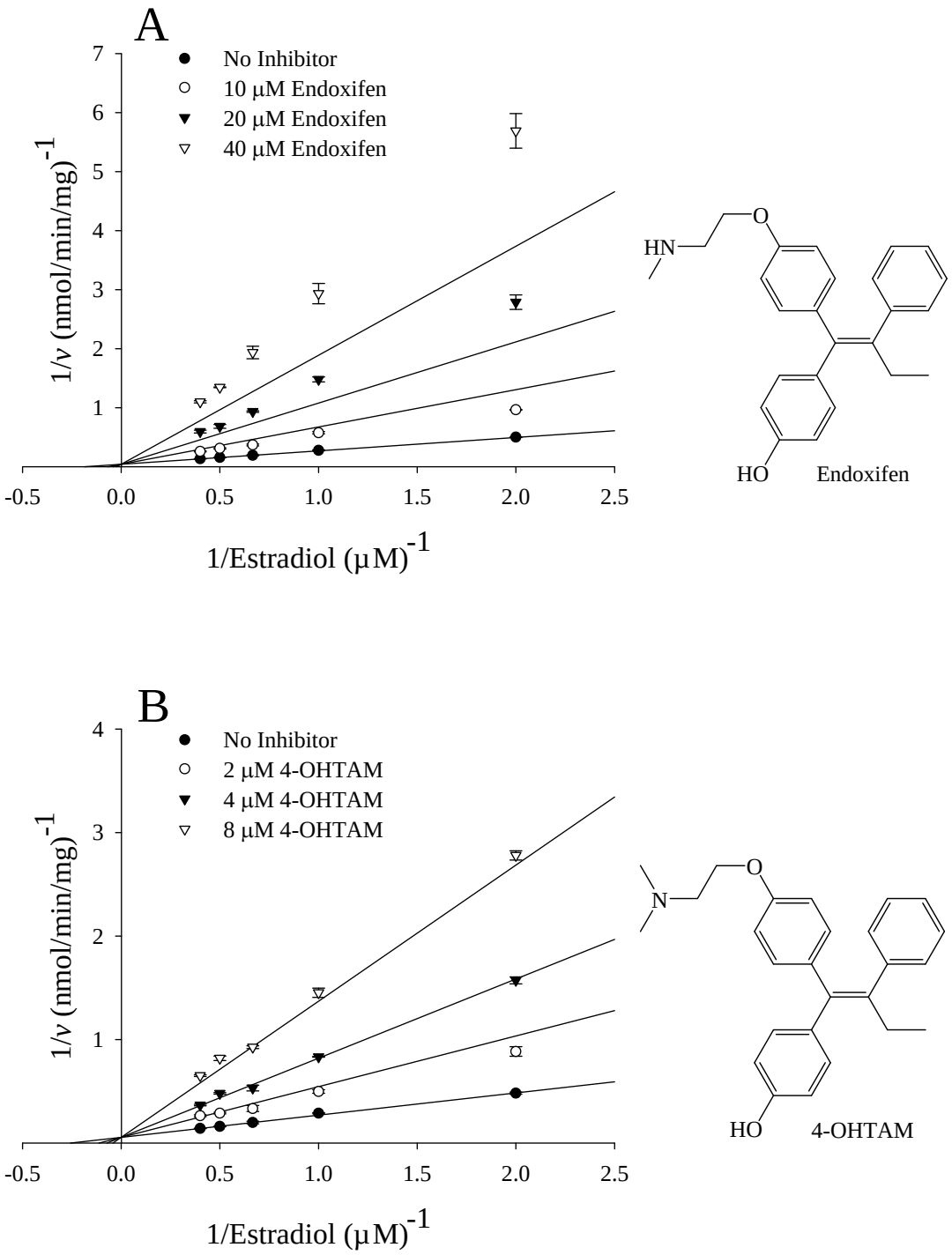

Figure 52. Competitive inhibition model for the hSULT1A1*1-catalyzed sulfation of estradiol by endoxifen (A) and 4-OHTAM (B). Data are the means ± standard error from triplicate determinations. Refer to Table 18 (Chapter 7) for rate equations.

Characterization of 4-OHTAM, N-desTAM, and Endoxifen as Substrates for hSULT1A1*1

4-OHTAM is a known substrate for hSULT1A1*1 (118), however, endoxifen and N-desTAM have never been formally examined as substrates for this enzyme. The results from the current study indicated that 4-OHTAM, N-desTAM, and endoxifen were all substrates for hSULT1A1*1. The kinetics of N-desTAM sulfation was best described using a Michaelis-Menten equation whereas the data for the sulfation of 4-OHTAM and endoxifen were best described using a substrate inhibition model (Figure 53). The kinetic constants for the sulfation of 4-OHTAM, N-desTAM, and endoxifen catalyzed by hSULT1A1*1 are summarized in Table 15. The enzyme displayed higher catalytic activity with endoxifen than with N-desTAM as seen by the 9-fold higher kcat/Km. Additionally, hSULT1A1*1 displayed a much higher catalytic activity with 4-OHTAM than N-desTAM with a 22-fold higher kcat/Km. The sulfation rates for the metabolites were 4-OHTAM > endoxifen >> N-desTAM. The enzymatic reactions were analyzed by LC-MS, and the negative ion ESI-MS of the product formed by the hSULT1A1*1-catalyzed sulfation of N-desTAM is seen in Figure 54. Endoxifen-sulfate was identified as a product of sulfation catalyzed by hSULT1A1*1 with a m/z of 452.2, indicating that sulfation had occurred at the phenolic hydroxyl group of endoxifen (Figure 55). The product of 4-OHTAM sulfation is shown in Figure 56 with a m/z of 466.2, as determined by negative ion ESI. The retention times of 4-OHTAM-S, N-desTAM-S, and endoxifen-sulfate from LC chromatographs (See Appendix, Figures A-7, A-8 and A-9) were 16.30, 21.81, and 16.07 min, respectively.

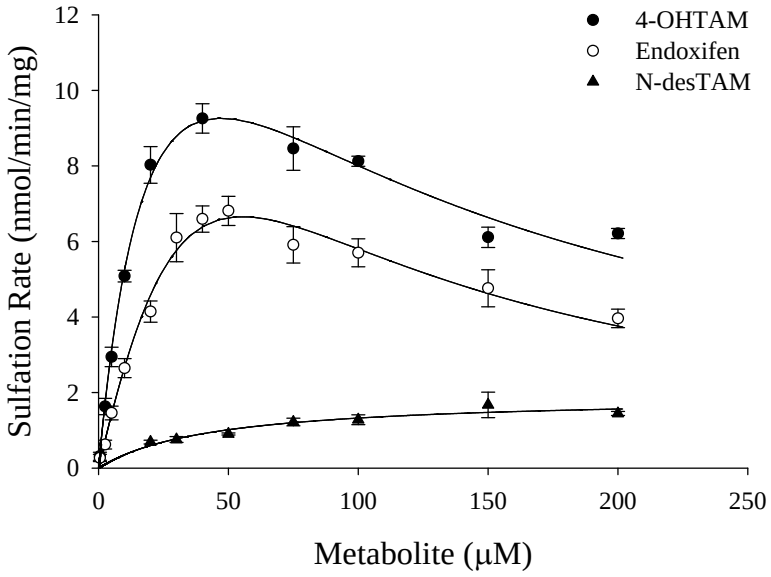

Figure 53. Initial velocities of the hSULT1A1*1-catalyzed sulfation of 4-OHTAM, N-desTAM, and endoxifen. Data are the means ± standard error from triplicate determinations and were fit to either an uncompetitive substrate inhibition equation (for 4-OHTAM and endoxifen) or a Michaelis Menten equation (for N-desTAM). Refer to Table 18 (Chapter 7) for rate equations.

Metabolite	**Km**	**Vmax**	**kcat/Km**	**Ki**
	μM	*nmol/min/mg*	$min^{-1}\mu M^{-1}$	*μM*
4-OHTAM	26 ± 5	20 ± 3	0.050	84 ± 19
Endoxifen	118 ± 82	35 ± 20	0.020	26 ± 18
N-desTAM	44 ± 14	1.9 ± 0.2	0.0022	

Note: Data are the means ± standard error from triplicate determinations. Calculation of kcat values was based on 68,312 as the dimeric molecular mass of hSULT1A1*1.

Table 15. Kinetic constants for the hSULT1A1*1-catalyzed sulfation of 4-OHTAM, N-desTAM, and endoxifen.

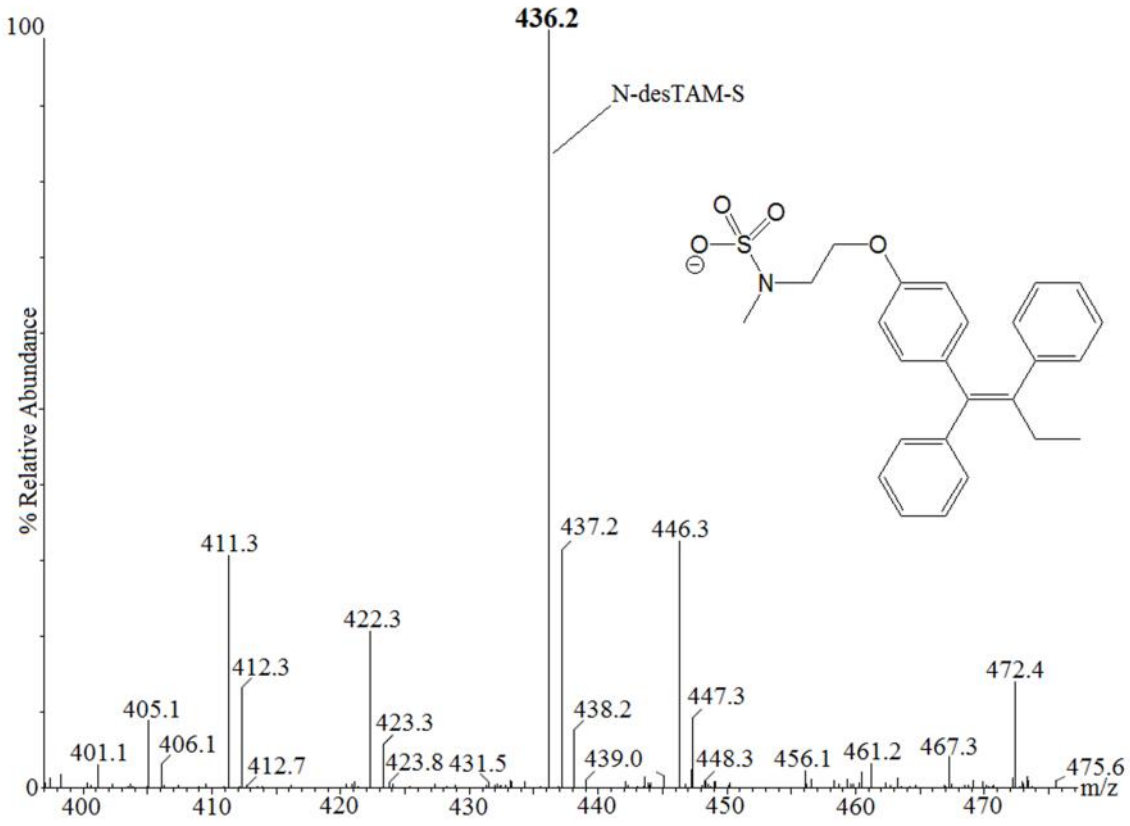

Figure 54. LC-MS analysis of N-desTAM-S as a product of sulfation catalyzed by hSULT1A1*1. The theoretical calculated m/z of N-desTAM-S is 436.1588 $[M - H]^-$.

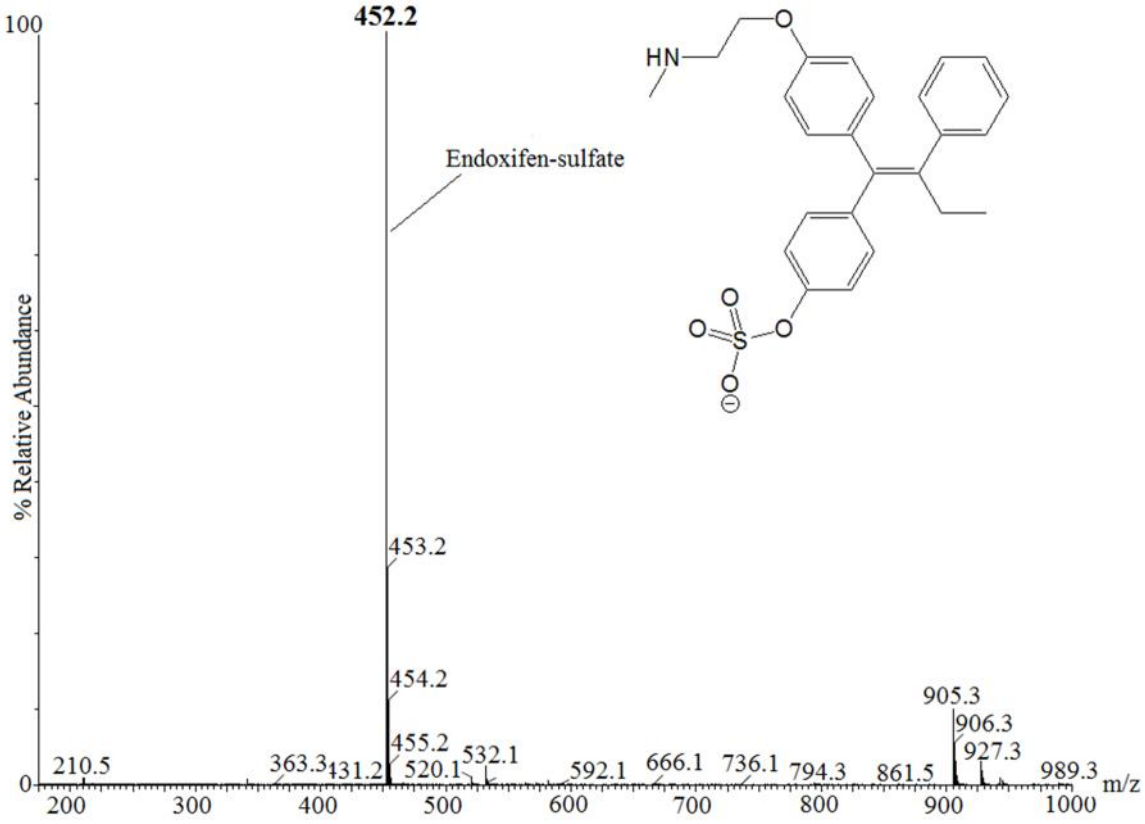

Figure 55. LC-MS analysis of endoxifen-sulfate as a product of sulfation catalyzed by hSULT1A1*1. The theoretical calculated m/z of endoxifen-sulfate is 452.1532 $[M - H]^-$.

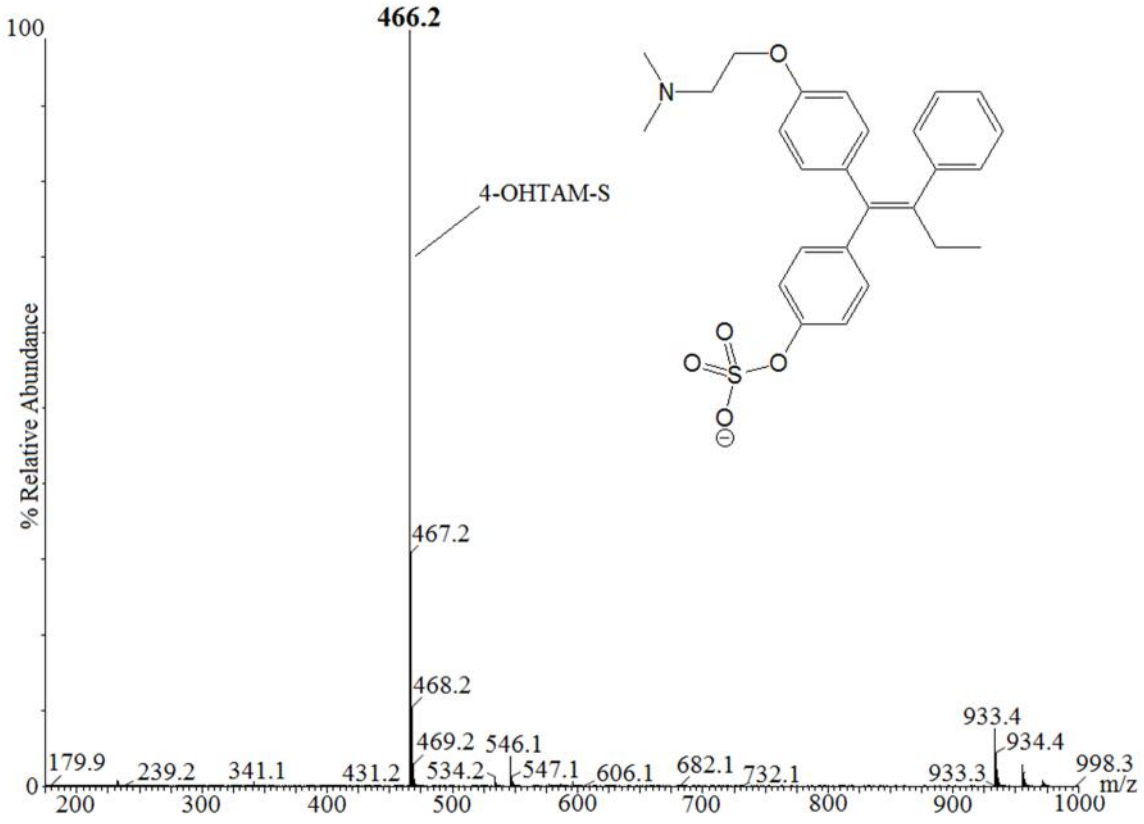

Figure 56. LC-MS analysis of 4-OHTAM-S as a product of sulfation catalyzed by hSULT1A1*1. The theoretical calculated m/z of 4-OHTAM-S is 466.1852 $[M - H]^-$.

4-OHTAM-S and N-desTAM-S are Weak Inhibitors of hSULT1A1*1

N-desTAM-S and 4-OHTAM-S were investigated as inhibitors of the hSULT1A1*1-catalyzed sulfation of estradiol. N-desTAM-S was a weak inhibitor of the enzyme with a calculated IC_{50} value of 14 ± 1 µM, whereas 4-OHTAM-S was determined to be a very weak inhibitor of the enzyme with an IC_{50} value greater than 70 µM when examined with 2.0 µM estradiol as substrate (Figure 57). The mechanism of inhibition and related inhibition constants for N-desTAM-S were not determined due to its poor interactions with the enzyme.

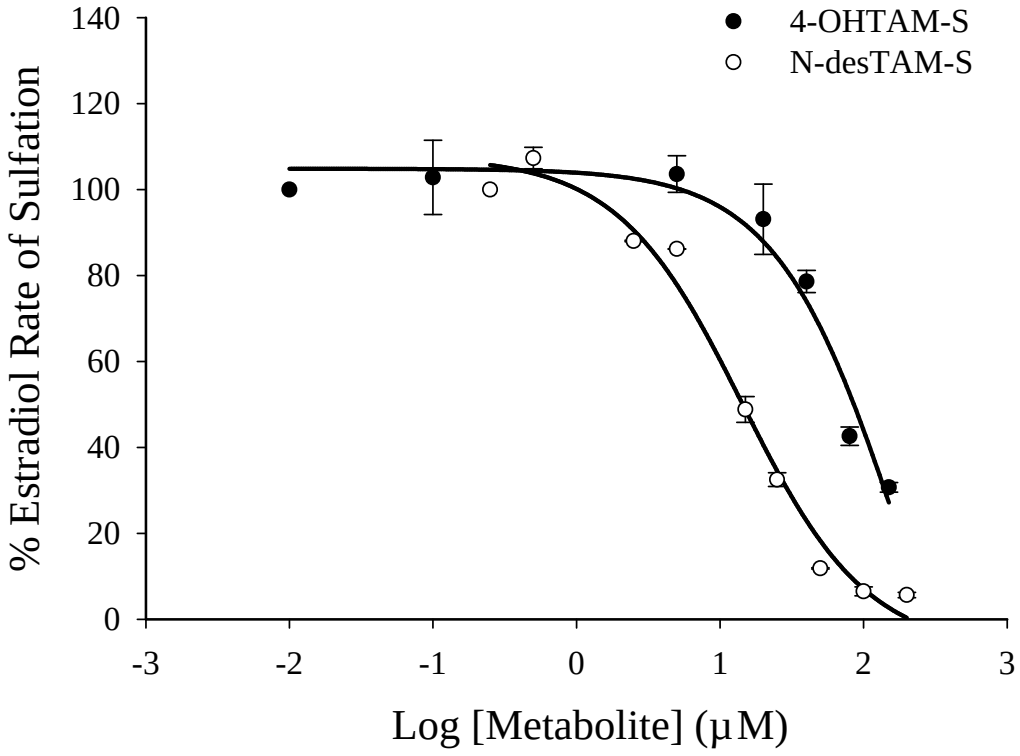

Figure 57. Inhibition of the hSULT1A1*1-catalyzed sulfation of 2.0 µM estradiol by N-desTAM-S and 4-OHTAM-S. Sulfation rates of uninhibited controls for N-desTAM-S and 4-OHTAM-S were 5.0 and 6.2 nmol/min/mg, respectively. Data are the means ± standard error from triplicate determinations and were fit to a sigmoidal does-response equation (Table 18, Chapter 7).

Discussion and Summary

Of the metabolites tested, 4-OHTAM was the most potent inhibitor of the hSULT1A1*1-catalyzed sulfation of estradiol with an IC_{50} and Ki value of 1.6 μM (Table 14). This was an interesting finding because the inhibition constant for interactions between hSULT1A1*1 and 4-OHTAM was of similar magnitude to the kinetic constant observed for the sulfation of estradiol (Table 13). The physiological concentrations of estrone and estradiol are 70 pM and 30 pM, respectively (191), whereas the serum concentration of 4-OHTAM is in a general range of 15 – 24 nM (74). Given the relative abundance of 4-OHTAM in relation to the physiological concentrations of estrogen, it is possible that 4-OHTAM could significantly alter estrogen homeostasis is those tissues that express hSULT1A1*1 instead of hSULT1E1. As a result, 4-OHTAM could promote excessive estrogenic effects in breast tumor tissue and decrease the therapeutic efficacy of tamoxifen as a potential mechanism of resistance.

4-OHTAM was determined to be one of the better substrates for hSULT1A1*1 as indicated by its relatively high catalytic efficiency constant (Table 15). Moreover, the rate of sulfation for 4-OHTAM was higher for hSULT1A1*1 than the sulfation rates previously determined with hSULT1E1 or hSULT2A1 (Tables 10 and 5). These studies suggest that hSULT1A1*1 could be the major SULT responsible for the *in vivo* formation of 4-OHTAM-S. Thus, changes in the catalytic activity or expression hSULT1A1*1 could significantly alter the formation of 4-OHTAM-S in tissues. This might be a concern for the population of patients who are homozygous for the thermally labile and low activity hSULT1A1*2 allele, as the formation of 4-OHTAM-S may be limited by this genetic polymorphism. It is important to realize sufficient levels of 4-OHTAM-S could be formed by other means since 4-OHTAM also serves as a substrate for hSULT2A1 and hSULT1E1, however, these enzymes are not expressed in breast cancer cells.

Since 4-OHTAM and endoxifen were relatively potent inhibitors of estradiol sulfation, there is a potential for these metabolites to inhibit the hSULT1A1*1-catalyzed

sulfation of 4-OHTAM, which displayed a much lower affinity for the enzyme with a Km value of 26.2 µM. The inhibition of 4-OHTAM sulfation would be favorable in healthy tissues since the sulfuric acid ester of 4-OHTAM would likely be excreted. Thus, endoxifen and 4-OHTAM may contribute to the bioavailability of 4-OHTAM and prolong the anti-estrogenic effects of tamoxifen. However, the inhibition of hSULT1A1*1 in breast tumor tissue may decrease the local concentrations 4-OHTAM-S, and this may reduce the efficacy of tamoxifen. The latter example seems unlikely given the strong association between the high activity hSULT1A1*1 allele and patient survival in tamoxifen-treated women (100, 214). Nevertheless, 4-OHTAM functions better as an inhibitor of hSULT1A1*1 than a substrate for the enzyme, and this suggests a possibility for 4-OHTAM to interfere in estrogen metabolism.

CHAPTER 6

CONCLUSIONS

Although tamoxifen has been successfully utilized for decades in the treatment and prevention of estrogen-dependent breast cancer, its use is limited by its low incidence of endometrial cancer in some patient populations (27-29, 38, 39). Moreover, nearly half of patients diagnosed with estrogen-dependent breast cancer fail to initially respond to tamoxifen, and those that do respond ultimately develop resistance to the therapy (93). Given the complexity of the carcinogenic and therapeutic response to tamoxifen, the goal of the current study was to investigate the interactions of 4-OHTAM, TAM-NO, N-desTAM, and endoxifen with enzymes that are important for the metabolic activation and therapeutic efficacy of tamoxifen. Thus, metabolites of tamoxifen were examined as substrates and inhibitors of hSULT2A1, hSULT1E1, and hSULT1A1*1.

Prior to kinetic studies with the tamoxifen metabolites, new procedures were developed for the expression and purification of recombinant hSULT1E1 and hSULT1A1*1 from *E. coli*. These methods utilized either two (hSULT1E1) or three (hSULT1A1*1) chromatographic steps following the bacterial expression of the enzymes. These protocols are now available for the large-scale purification of hSULT1E1 and hSULT1A1*1 for future studies. Metabolites of tamoxifen were investigated as inhibitors of hSULTs 2A1, 1E1, and 1A1*1 using radiolabeled steroid substrates for the enzymes. Metabolites that were determined to be inhibitors were then examined as alternate substrates for the enzymes. In order to confirm the identity of the products formed form the SULT-catalyzed reactions, non-radioactive enzymatic reaction mixtures were analyzed by LC-MS using synthetic standards for the sulfoconjugates of 4-OHTAM and N-desTAM. Table 16 summarizes the inhibition constants obtained for the tamoxifen metabolites. Table 17 summarizes kcat/Km for the sulfation of 4-OHTAM, N-desTAM, and endoxifen by each enzyme.

Inhibitor	hSULT2A1		hSULT1E1	hSULT1A1*1
	Ki^{DHEA} (μM)	Ki^{PREG} (μM)	Ki^{E2} (μM)	Ki^{E2} (μM)
Endoxifen	2.8 ± 0.2	3.5 ± 0.7	30 ± 1	5.6 ± 0.5
4-OHTAM	19 ± 2	13 ± 2	38 ± 1	1.6 ± 0.1
N-desTAM	17 ± 2	10 ± 1	10 ± 1	N.D.
TAM-NO	9.6 ± 0.2	17 ± 1	20 ± 1	N.D.
N-desTAM-S	7.7 ± 1.2	N.D.	5.6 ± 0.9	N.D.

Note: The substrate utilized for each Ki determination is shown in superscript. N.D., not determined.

Table 16. Summary of the inhibition constants determined for each inhibitor in the study.

Substrate	hSULT2A1	hSULT1E1	hSULT1A1*1
	kcat/Km ($min^{-1}\mu M^{-1}$)	kcat/Km ($min^{-1}\mu M^{-1}$)	kcat/Km ($min^{-1}\mu M^{-1}$)
Endoxifen	N.D.	0.057	0.020
4-OHTAM	0.015	0.036	0.050
N-desTAM	0.0024	0.019	0.0022

Note: N.D., not determined due to low sulfation rates.

Table 17. Catalytic efficiency constants determined for the sulfation of 4-OHTAM, N-desTAM, and endoxifen catalyzed by hSULTs 2A1, 1E1, and 1A1*1.

As seen in Table 16, endoxifen was the most potent inhibitor of hSULT2A1, which suggests that this metabolite may inhibit the role of hSULT2A1 in the metabolic pathway for genotoxicity that is seen with tamoxifen. N-desTAM was a substrate for hSULT2A1, and the product of this reaction, N-desTAM-S, displayed greater inhibition of the enzyme than its parent metabolite. Thus, endoxifen, N-desTAM, and N-desTAM-S might serve protective roles in some tissues as they may inhibit the sulfation of α-OHTAM. Furthermore, the distribution of these metabolites in the human liver may regulate the activity of hSULT2A1 when they are formed in the vicinity of α-OHTAM, and this might contribute to the tissue differences in the carcinogenic response of tamoxifen that is observed between rodents and humans. Of the enzymes tested, hSULT1E1 displayed the highest catalytic activity towards the sulfation of N-desTAM (Table 17). This suggests that hSUTL1E1 may generate sufficient amounts of N-desTAM-S to inhibit the hSULT2A1-catalyzed sulfation of α-OHTAM. Therefore, hSULT1E1 may modulate the toxicity of tamoxifen by catalyzing the formation of N-desTAM-S in the vicinity of hSULT2A1. The interactions of hSULT1E1 and hSULT2A1 are likely *in vivo* since these enzymes have similar tissue distributions.

Endoxifen is an estrogen receptor antagonist as well as a potent inhibitor of hSULT2A1. The *in vivo* formation of endoxifen is dependent upon the CYP2D6-catalyzed oxidation of N-desTAM (74). However, genetic polymophisms in CYP2D6 have been shown to lower the plasma levels of endoxifen and increase the risk of breast cancer mortality in tamoxifen-treated women (99, 248). Decreasing the plasma levels of endoxifen may also increase the risks for the genotoxic effects of tamoxifen, as there may not be sufficient concentrations of endoxifen in circulation to inhibit the hSULT2A1-catalyzed sulfation of α-OHTAM. Thus, poor metabolizers of tamoxifen may be at an additional disadvantage for the adverse events of tamoxifen therapy. Nevertheless, the direct use of endoxifen in clinical trials may eliminate the large interpatient variability in endoxifen plasma levels that is observed in tamoxifen-treated women.

Metabolites of tamoxifen were determined to be poor inhibitors of hSULT1E1 in the current investigation. Thus, it is predicted that the efficacy of endoxifen will not be compromised in clinical trials due to the inhibition of hSULT1E1. However, 4-OHTAM and endoxifen were determined to be potent inhibitors of hSULT1A1*1 when estradiol was utilized as a substrate, which suggests that the efficacy of endoxifen may be affected in breast tumor tissue by inhibiting the hormonal inactivation mechanism catalyzed by this enzyme; although the direct use of endoxifen in clinical trials might achieve higher steady state concentrations of endoxifen in the target tissues and counteract the excessive estrogenic effects due to the inhibition of hSULT1A1*1. Nevertheless, it is important to realize that endoxifen is a potent inhibitor of hSULT2A1 and hSULT1A1*1, which suggests that endoxifen has a potential to interfere in steroid hormone metabolism.

There may be variations in the therapeutic efficacy of endoxifen since this metabolite contains a phenolic group and the aliphatic secondary amine, which suggests that endoxifen could undergo extensive metabolism or inactivation before it can reach the target tissue(s). As shown in Table 17, endoxifen was a substrate for hSULT2A1, hSULT1E1, and hSULT1A1*1, and the LC-MS studies confirm that these enzymes catalyzed the sulfation of the phenolic group of endoxifen. However, other conjugation reactions (e.g. glucoronidation) could occur at the aliphatic amine of endoxifen or its phenolic moiety, and this may affect the disposition and tissue distribution of endoxifen *in vivo*. Due to recent findings of the potential therapeutic benefits of 4-OHTAM-S in breast cancer cells (216), there is a possibility that conjugation reactions may enhance the biological activity of some molecules. Thus, it would be interesting to determine if N-desTAM-S, endoxifen-sulfate, or endoxifen sulfamate possess any biological activities in breast cancer cells. This research could become the focus of future investigations.

TAM-NO is a metabolite that is of recent interest due to its potential role(s) in the activity of tamoxifen (69). TAM-NO is reduced back to tamoxifen in liver microsomes (249) and breast cancer cells (69), which suggests that TAM-NO may act as a reservoir for

tamoxifen in tissues (250), much like DHEA-S serves as a tissue reservoir for DHEA. Thus, if TAM-NO were converted to tamoxifen in the endometrium, this would increase the endometrial concentrations of tamoxifen. The accumulation of tamoxifen in the endometrium may increase the CYP3A4-catalyzed oxidation of tamoxifen to form α-OHTAM, which is metabolized by hSULT2A1 to form the genotoxic species responsible for DNA alkylation. Given the expression of CYP3A4 and hSULT2A1 in endometrial tissue (77, 167), it is possible that TAM-NO could contribute to the carcinogenetic endometrial effects of tamoxifen. Moreover, tamoxifen is an estrogen agonist in the uterine endometrium (251, 252), and the accumulation of tamoxifen in this tissue due to the action of TAM-NO might promote excessive estrogenic effects that augment the risk for endometrial toxicity when combined with the reactive α-sulfooxy derivative catalyzed by hSULT2A1. The effects of TAM-NO on the carcinogenic and therapeutic response to tamoxifen have not been examined in the field of tamoxifen research, and this could become the subject of future investigations.

In summary, the research presented in the current study has opened new avenues for future work on the roles of tamoxifen metabolites in the therapeutic action and toxicity of tamoxifen. At the same time it has also provided new insights into the use of endoxifen in clinical trials, as well as mechanisms that may contribute to variations in the carcinogenic response and efficacy of tamoxifen.

CHAPTER 7

MATERIALS AND METHODS

Chemicals and Instruments.

Expression plasmids (pReceiver-B02) for hSULT1E1 and hSULT1A1*1 were obtained from GeneCopoeia (Rockville, MD). The Pure Yield Plasmid Mini-Prep System was obtained from Promega (Madison, WI). Antisense (5'-CAG CCT AGG AAC GCC CAA CTT-3') and Sense (5'-GCG TAG AGG ATC GAG ATC GAT-3') primers for sequencing were obtained from Integrated DNA Technologies (Coralville, IA). BL21 (DE3) *E. coli* cells were obtained from Life Technologies (Grand Island, NY). DNA grade Hydroxyapatite was purchased from Bio-Rad (Hercules, CA). Bacto tryptone and yeast extract were purchased from Becton Dickinson, Co. (Sparks, MD). Ampicillin, dithiothreitol (DTT), Luria Broth (LB) Agar, and granulated LB Broth (Miller's LB Broth) were obtained from Research Products International (Mt. Pleasant, IL). Thin layer chromatography (TLC) sheets (60 angstrom, Silica Gel F_{254}, and 60 angstrom Silica Gel w/o indicator) were obtained from EMD Millipore (Billerica, MA). PAPS (Adenosine 3′-phosphate 5′-phosphosulfate lithium salt hydrate) was obtained from Sigma-Aldrich (St. Louis, MO) and purified upon arrival using a previously described protocol to a purity greater than 99% as determined by HPLC (253). Methylene blue, potassium phosphate, phenylmethylsulfonyl fluoride, pepstatin A, antipain, 2-mercaptothanol, DHEA, PREG, (*Z*)-Tamoxifen, (*Z*)-N-desmethyltamoxifen hydrochloride, (*Z*)-4-hydroxytamoxifen, (*E/Z*)-4-hydroxy-N-desmethyl-tamoxifen hydrochloride hydrate (endoxifen), and DE-52 cellulose were purchased from Sigma-Aldrich at the highest available purity (> 98%). [^{3}H]-DHEA (70.5 Ci/mmol), [^{3}H]-DHEA-Sulfate (63.0 Ci/mmol), [^{3}H]-Pregnenolone (22.9 Ci/mmol), and [^{3}H]-Estradiol (81.0 Ci/mmol) were obtained from Perkin Elmer (Waltham, MA). [^{3}H]-Pregnenolone Sulfate (0.20 Ci/mmol) was obtained from American Radiolabeled Chemicals (St. Louis, MO). All radioactive samples were analyzed using a

Tri-Carb 2900TR Liquid Scintillation Counter using Econo-Safe liquid scintillation cocktail (Research Products International; Mount Prospect, IL). Data were analyzed using the Enzyme Kinetics Module (version 1.3) of Sigma Plot 11.0 (Systat Software; San Jose, CA).

Expression and Purification of Recombinant hSULT2A1

Human SULT2A1 was expressed in, and extracted from BL21 (DE3) E. coli as previously described (89, 175). The enzyme was purified using DE-52 anion exchange chromatography followed by two hydroxyapatite columns to homogeneity as determined by SDS-PAGE. Protein concentration was determined at each step of the purification process with a modified Lowry method using bovine serum albumin (BSA) as a standard (240). Chromatography fractions were analyzed for enzyme activity at pH 5.45 using a previously reported methylene blue assay (241, 242) and 10 µM DHEA as substrate.

Expression and Purification of Recombinant hSULT1E1

The expression of recombinant hSULT1E1 in *E. coli* required the preparation of sterile Luria Broth (LB) and sterile Terrific Broth (TB). LB was prepared in a 500 ml Erlenmeyer culture flask by dissolving 3.0 g of granulated LB (Miller's LB Broth) into 120 ml of double distilled water. The resulting mixture was autoclaved and then cooled to room temperature. TB was prepared in a 2.0 L Erlenmeyer culture flask by dissolving 24.0 g yeast extract, 12.0 g tryptone, and 4.0 ml glycerol in 900 ml of double distilled water. In addition, a 100 ml solution of potassium phosphate (0.89 M, pH 7.6) was prepared in a separate bottle. The 900 ml solution of TB and the 100 ml solution of potassium phosphate were autoclaved and then cooled to room temperature. Afterwards, the 100 ml solution of potassium phosphate was added into the 2.0 L culture flask containing 900 ml TB. The resulting mixture was then supplemented with 30 µl of Anti-foam prior to culture inoculation.

BL21 (DE3) *E. coli* cells (50 µl) were transformed with 2 µl (108 ng) of pReceiver-B02 expression vector for hSULT1E1. The bacterial cells were incubated on ice for 20 min and then heat-shocked at 42ºC for exactly 32 sec. The cells were immediately cooled on ice for 2 min, after which was added 180 µl of sterile pre-warmed SOC (Super Optimal broth with Catabolite repressioin) media. The bacterial cells were grown for 1 hr on a reciprocating shaker (250 rpm) at 37ºC. Afterwards, a 35 µl aliquot of the cell suspension was added to an LB-ampicillin agar plate and incubated at 37ºC for 18 hours. A single colony from the LB-ampicillin agar plate was added to 8.0 ml of sterile LB media containing 100 µg/ml ampicillin and incubated overnight at 37ºC on a reciprocating shaker (250 rpm). The bacterial culture was later inoculated into 120 ml of sterile LB media containing 100 µg/ml ampicillin and incubated overnight at 37ºC on a reciprocating shaker (250 rpm). Afterwards, a 20 ml aliquot from the 120 ml bacterial culture was inoculated into 1.0 L of TB containing 100 µg/ml ampicillin and incubated at 37ºC on a reciprocating shaker (250 rpm). The bacterial culture was grown to an OD_{600} of 1.0 (which takes approximately 4 hours) and then induced with 300 µM IPTG. The culture was then incubated on a reciprocating shaker (250 rpm) overnight at 30ºC. Cells were subjected to centrifugation at 10,000 x g for 1 hr at 4ºC, re-suspended in 10 ml bacterial lysis Buffer A (10 mM Tris-HCl, pH 7.5, containing 0.25 M sucrose, 1 mM DTT, 10 % (v/v) glycerol, 1 mM PMSF, 1 µM pepstatin A, 3.3 µM antipain, 10 µM E-64, and 100 µM leupeptin), and snap-frozen in liquid nitrogen. The cells were thawed and supplemented with chicken lysozyme such that the final concentration of lysozyme was 0.5 mg/ml. Cells were gently shaken for 15 min at 4ºC and then snap-frozen in liquid nitrogen to complete the cell lysis. The thawed cells were supplemented with DNase (0.5 mg) and gently shaken for 15 min at 4ºC. The cytosolic fraction containing hSULT1E1 activity was recovered following centrifugation at 100,000 x g for 1 hr.

The cell extract was applied to a DE-52 anion exchange column (2.5 x 20 cm) equilibrated with Buffer B (50 mM Tris-HCl, pH 7.5, containing 0.25 M sucrose, 1 mM

DTT, 10 % (v/v) glycerol, and 0.05 % (v/v) Tween 20) and washed with approximately 1.0 L of Buffer B. Once the absorbance of the eluate at 280 nm had reached the original baseline value, the protein was eluted with a linear gradient formed between 200 ml of Buffer B and 200 ml of Buffer B containing 0.1 M KCl. The fractions containing hSULT1E1 were then combined and concentrated by ultrafiltration (Amicon stirred cell with a YM10 membrane, Millipore Corporation, Bedford MA). Three successive dilutions with Buffer C (10 mM potassium phosphate, pH 6.8, 0.25 M sucrose, 1 mM DTT and 0.05 % (v/v) Tween 20) and subsequent ultrafiltration were used to prepare the enzyme for the next step in purification.

The protein obtained from the DE-52 anion exchange column was applied to a hydroxyapatite column (2.5 x 3.0 cm) that had been equilibrated with Buffer C, and washed with Buffer C to elute those proteins that did not bind to the column. Once the absorbance of the eluate at 280 nm returned to baseline, separation was achieved by applying a linear gradient formed between 80 ml of Buffer C and 80 ml of Buffer C containing 0.4 M potassium phosphate. The fractions containing hSULT1E1 activity were pooled and concentrated by ultrafiltration using an Amicon membrane. Protein concentration was determined at each step of the purification process with a standard Bradford assay (254) using BSA as a standard. Chromatography fractions were analyzed for hSULT1E1 activity at pH 7.4 using the methylene blue assay and 25 µM estradiol as substrate. The complete DNA coding sequence of hSULT1E1 was verified using antisense (5'-CAG CCT AGG AAC GCC CAA CTT-3') and sense (5'-GCG TAG AGG ATC GAG ATC GAT-3') sequencing primers.

Expression and Purification of Recombinant hSULT1A1*1

BL21 (DE3) *E. coli* cells (50 µl) were transformed with 0.6 µl (114 ng) of pReceiver-B02 expression vector for hSULT1A1*1. The expression of hSULT1A1*1 in

bacterial culture and preparation of cell extract was performed essentially as described above for hSULT1E1.

The cell extract was applied to a DE-52 anion exchange column (2.5 x 15 cm) equilibrated with Buffer B and washed with approximately 1.0 L of Buffer B to elute non-binding proteins. Once the absorbance of the eluate at 280 nm had reached the original baseline value, the protein was eluted with a linear gradient formed between 200 ml of Buffer B and 200 ml of Buffer B containing 0.1 M KCl. The fractions containing hSULT1A1*1 were then combined and concentrated by ultrafiltration as described above. Three successive dilutions with Buffer C and subsequent ultrafiltration were used to prepare the enzyme for the next step in purification.

The protein obtained from the DE-52 anion exchange column was applied to a hydroxyapatite column (2.5 x 5.0 cm) that had been equilibrated with Buffer C, and washed with Buffer C to elute those proteins that did not bind to the column. Once the absorbance of the eluate at 280 nm returned to baseline, separation was achieved with a linear gradient formed between 100 ml of Buffer C and 100 ml of Buffer C containing 0.4 M potassium phosphate. The fractions containing hSULT1A1*1 activity were pooled and concentrated in Buffer C by ultrafiltration using an Amicon membrane.

The hSULT1A1*1 obtained from the hydroxyapaptite was loaded onto a second hydroxyapatite column (2.5 x 5.0 cm) equilibrated with Buffer C. Proteins that did not bind to the column were removed by washing with approximately 100 ml Buffer C. Separation was achieved with a linear gradient formed between 100 ml of Buffer C and 100 ml of Buffer C containing 80 mM potassium phosphate. The fractions containing hSULT1A1*1 with the highest activity were combined and concentrated. Protein concentration was determined at each step of the purification process with a standard Bradford assay using BSA as a standard. Chromatography fractions were analyzed for hSULT1A1*1 activity at pH 7.4 using the methylene blue assay and 25 µM 2-naphthol as substrate. The complete DNA coding sequence of hSULT1A1*1 was verified using

antisense (5'-CAG CCT AGG AAC GCC CAA CTT-3') and sense (5'-GCG TAG AGG ATC GAG ATC GAT-3') sequencing primers.

Inhibition of hSULT2A1-catalyzed Sulfation of DHEA.

Assays for the sulfation of DHEA were performed as previously described (129). Each 200 µl reaction was performed at pH 7.4 and contained 0.25 M potassium phosphate, 200 µM PAPS, and 8.3 mM 2-mercaptoethanol. [^{3}H]-DHEA and tamoxifen metabolites were dissolved in absolute ethanol and they were added to the reaction mixture in volumes such that the final concentration of ethanol in each assay was 2% (v/v). The reactions were initiated by the addition of purified hSULT2A1 (0.03 µg) for 4 min at 37°C. The reactions were then terminated by the addition of 800 µl of 50 mM potassium hydroxide and 500 µl of chloroform. Samples were vortexed vigorously for 20 sec and subjected to centrifugation at 3500 rpm for 5 min to separate the phases. A 100 µl aliquot of the upper aqueous phase containing [^{3}H]-DHEA-S was added to 10 ml Econo-Safe liquid scintillation cocktail and the radioactivity was determined using a Perkin Elmer Tri-Carb 2900TR liquid scintillation analyzer. Control experiments (A and B) with [^{3}H]-DHEA were carried out without PAPS and enzyme. Chloroform was not added to control A. The sulfation rates were expressed as nmol [^{3}H]-DHEA-S produced per minute per milligram hSULT2A1 using equation 1. Since only 100 µl of the 1.0 ml aqueous phase is analyzed, the cpm (counts per minute) measured from the radioactive samples are multiplied by 10 to account to for the dilution. Moreover, the measured cpm is divided by 0.85 to correct for the extraction efficiency of [^{3}H]-DHEA-S into the aqueous phase.

$$\text{Equation 1: Rate of Sulfation} = \frac{[^3\text{H}]\text{-DHEA-S formed (nmol)}}{\text{reaction time (min)} \times \text{protein (mg)}}$$

where:

$$[^3\text{H}]\text{-DHEA-S (nmol)} = \frac{(\text{nmol DHEA in assay}) \times (\text{measured cpm} - \text{control B cpm}) \times 10}{(\text{control A cpm} \times 10) \times 0.85}$$

Inhibition of hSULT2A1-catalyzed Sulfation of PREG

Assays for the sulfation of pregnenolone were performed using the following general procedure. Each 100 µl assay was performed at pH 7.4 and contained 0.25 M potassium phosphate, 200 µM PAPS, and 8.3 mM 2-mercaptoethanol. [^{3}H]-Pregnenolone and tamoxifen metabolites were dissolved in absolute ethanol and they were added to the reaction mixture in volumes such that the final concentration of ethanol in each assay was 2% (v/v). The reactions were initiated by the addition of 1.0 µl of purified hSULT2A1 (0.03 µg) at 37°C for 4 min and terminated with an equal reaction volume of methanol. A 10 µl aliquot of the resulting mixture was applied to Silica Gel 60 TLC sheets (w/o indicator) and developed in chloroform / methanol / acetone / acetic acid / water (80:20:40:20:10) (255) until the solvent moved approximately 8 cm from the origin. The area of the TLC encompassing 2 - 5 cm from the origin contained [^{3}H]-pregnenolone sulfate, and this section was excised and placed in 10 ml scintillation cocktail supplemented with 500 µl methanol and the radioactivity determined as described above. The location of [^{3}H]-pregnenolone sulfate on TLC sheets was previously determined with unlabeled pregnenolone sulfate. Methanol was added directly into the scintillation cocktail to increase the recovery of pregnenolone sulfate from the TLC sheets. Maximum recovery of pregnenolone sulfate under these conditions was 75%, and assay results were corrected for this extraction efficiency. Refer to equation 1 for determination of the rate of sulfation.

Inhibition of hSULT1E1-catalyzed Sulfation of Estradiol.

Assays for the sulfation of estradiol were performed utilizing the following procedure. Each 200 µl reaction was performed at pH 7.4 and contained 0.25 M potassium phosphate, 50 µM PAPS, and 8.3 mM 2-mercaptoethanol. [^{3}H]-estradiol and tamoxifen metabolites were dissolved in absolute ethanol and they were added to the reaction mixture in volumes such that the final concentration of ethanol in each assay was 2% (v/v). The reactions were initiated by the addition of 1.0 µl purified hSULT1E1 (3.0 ng) for 4 min at

37°C. The reactions were then terminated by the addition of 800 µl of 0.25 M Tris-HCl (pH 8.7) and 4.0 ml of chloroform. Samples were vortexed vigorously for 20 sec and subjected to centrifugation at 1500 rpm for 5 min to separate the phases. A 500 µl aliquot of the upper aqueous phase containing [^{3}H]-estradiol-sulfate was added to 10 ml Econo-Safe liquid scintillation cocktail and the radioactivity was determined as described above. Control experiments (A and B) with [^{3}H]-estradiol were carried out without PAPS and hSULT1E1. Chloroform was not added to control A. The sulfation rate was expressed as nmol estradiol-sulfate produced per minute per milligram protein. Refer to equation 1 for the determination of the rate of sulfation.

Inhibition of hSULT1A1*1-catalyzed Sulfation of Estradiol.

Assays for the sulfation of estradiol were performed as described below. Each 200 µl reaction was performed at pH 7.4 and contained 0.25 M potassium phosphate, 50 µM PAPS, and 8.3 mM 2-mercaptoethanol. [^{3}H]-estradiol and tamoxifen metabolites were dissolved in absolute ethanol and they were added to the reaction mixture in volumes such that the final concentration of ethanol in each assay was 2% (v/v). The reactions were initiated by the addition of purified 1.0 µl hSULT1A1*1 (0.74 µg) for 10 min at 37°C. The reactions were then terminated by the addition of 800 µl of 0.25 M Tris-HCl (pH 8.7) and 4.0 ml of chloroform. Samples were vortexed vigorously for 20 sec and subjected to centrifugation at 1500 rpm for 5 min to separate the phases. A 500 µl aliquot of the upper aqueous phase containing [^{3}H]-estradiol-sulfate was added to 10 ml Econo-Safe liquid scintillation cocktail and the radioactivity was determined as described above. Control experiments (A and B) with [^{3}H]-estradiol were carried out without PAPS and hSULT1E1. Chloroform was not added to control A. The sulfate rate was expressed as nmol estradiol-sulfate produced per minute per milligram protein. Refer to equation 1 for the determination of the rate of sulfation

Substrate Determinations for Tamoxifen Metabolites.

Tamoxifen metabolites were investigated as substrates for the enzymes using a previously described protocol that monitors the incorporation of a radiolabeled sulfuryl moiety from [^{35}S]-PAPS into products of the reaction (130). Each 50 µl reaction was performed at pH 7.4 and contained either 200 µM [^{35}S]-PAPS (for hSULT2A1) or 50 µM [^{35}S]-PAPS (for hSULTs 1E1 and 1A1*1), with 0.25 M potassium phosphate, 8.3 mM 2-mercaptoethanol, and 2 % DMSO (v/v) as solvent for tamoxifen metabolites. The reactions were initiated by the addition of either purified hSULT2A1 (0.52 µg), hSULT1E1 (0.86 µg) or hSULT1A1*1 (0.74 µg) at 37°C, incubated for 20 min, and terminated with 50 µl methanol. A 10 µl aliquot of the resulting mixture was applied to Silica Gel 60 TLC sheets (w/o indicator) and developed in chloroform / methanol (3:7) until the solvent migrated approximately 8 cm from the origin. An area of the TLC sheet 5.5 cm below and including the solvent front (i.e. that contained the section of the radiolabeled sulfated products) was excised and placed in 10 ml scintillation cocktail for determination of radioactivity. The location of the sulfated products on TLC was determined prior to the radiolabeled assay using synthesized standards for 4-OHTAM-S and N-desTAM-S. Negative control experiments were carried out without the tamoxifen metabolites. Controls for [^{35}S]-PAPS on the TLC plates were performed without enzyme.

Determination of the Kinetic Mechanism of Inhibition

Endoxifen, 4-OHTAM, N-desTAM, TAM-NO, N-desTAM-S, 4-OHTAM-S, and tamoxifen were used as inhibitors of the enzymes. Data were fit to rate equations for competitive, noncompetitive, uncompetitive, or mixed inhibition using a nonlinear least-squares algorithm in the Enzyme Kinetics Module (version 1.3) of Sigma Plot 11.0 and the model with the highest value for the coefficient of determination, r^2, was selected. In cases where r^2 was not significantly different, the model with the lowest corrected Akaike Information Criterion (AICc) was selected. Table 18 summarizes the rate equations used

to determine the kinetic mechanism of inhibition for each inhibitor as well as the equations used to describe the kinetics of sulfation for substrates for the enzymes.

$v = V_{max}/(1+(K_m/S)*(1+I/K_i))$	1
$v = V_{max}/(1+(K_m/S)*(1+I/K_i)/(1+I/(\alpha K_i)))$	2
$v = V_{max}/((1+I/K_i)*(1+K_m/S))$	3
$v = V_{max}/((1+K_m/S)*(1+I/K_i)/(1+I*\beta/K_i))$	4
$v = V_{max}/((K_m/S)*(1+I/K_i)+(1+I/\alpha K_i)))$	5
$v = V_{max}*((1+\beta*I/(\alpha K_i))/(1+I/(\alpha K_i)))/(1+(K_m/S))*(1+I/K_i)/(1+I/(\alpha K_i)))$	6
$v = V_{max}/(1+I/Ki+K_m/S)$	7
$v = V_{max}*(1+\beta*(I/K_i))/(1+I/K_i+K_m/S)$	8
$v = V_{max}*S/(K_m+S)$	9
$v = V_{max}/(1+(K_m/S)+(S/K_i)$	10
$v = V_1*(1+(V_2*S/V_1*K_i))/(1+(K_m/S)+(S/K_i))$	11
$v = (V_{max}*A*B)/((\alpha*K_a*K_b)+(K_b*A)+(K_a*B)+(A*B))$	12
$y = min+((max-min)/(1+(10^{(logEC50-x)}$)))	13

Note: (K_i), dissociation constant for binding of the inhibitor (I) to the free enzyme; (αK_i), dissociation constant for binding of the inhibitor to the enzyme-substrate complex; (α), the degree to which the binding of inhibitor changes the affinity of the enzyme for substrate; (β), the degree of partiality; (K_m), Michaelis-Menten constant; (V_{max}), maximum velocity; (S), substrate; (v), velocity; (V_1), initial velocity; (V_2), velocity at infinite substrate concentrations; (K_a), Michaelis-Menten constant for substrate "A"; (K_b), Michaelis-Menten constant for substrate "B"; (A), substrate "A"; (B), substrate "B"; (max), maximum concentration; (min), minimal concentration; (EC50), half-maximal effective concentration.

Table 18. Rate equations used to describe the kinetic mechanism of inhibition and the kinetics of sulfation: Full Competitive Inhibition (1), Partial Competitive Inhibition (2), Full Noncompetitive Inhibition (3), Partial Noncompetitive Inhibition (4), Full Mixed Inhibition (5), Partial Mixed Inhibition (6), Full Uncompetitive Inhibition (7), Partial Uncompetitive Inhibition (8), Michaelis-Menten Kinetics (9), Uncompetitive Substrate Inhibition (10), Partial Substrate Inhibition (11), Random Bi Bi Sequential (12), Sigmoidal Dose-Response (13).

Identification of Enzyme Reaction Products by Liquid Chromatography and Mass Spectrometry

Products of sulfation catalyzed by hSULTs 2A1, 1E1, and 1A1*1 were identified using liquid chromatography-mass spectrometry analysis performed on a Waters Q-TOF Premiere mass spectrometer. Each 50 µl reaction was performed at pH 7.4 and utilized 50 µM substrate with either 200 µM PAPS (for hSULT2A1) or 50 µM PAPS (for hSULTs 1E1 and 1A1*1) in the presence of 0.25 M potassium phosphate, 8.3 mM 2-mercaptoethanol, and 2 % ethanol (v/v). The reactions were initiated with the addition of either hSULT2A1 (2.6 µg), hSULT1E1 (4.6 µg), or hSULT1A1*1 (3.7 µg) at 37°C for 60 min and terminated with 50 µl methanol. A 10 µl aliquot of each sample was analyzed using an auto-sampler interfaced with an electrospray ionization source operated in negative ion mode and an absorbance wavelength of 213 nm. Sample separation was achieved on a Waters Aquity (UPLC) BEH C18 column (2.1 mm x 100 mm; 1.7 µm) using a flow rate of 0.25 ml/min. A linear gradient system was programmed to 40% acetonitrile with 0.1% (v/v) formic acid for 15 min, 40% - 70% (v/v) acetonitrile with 0.1% (v/v) formic acid for 5 min, and then sustained at 70% acetonitrile with 0.1% formic acid for 10 minutes.

Synthesis of TAM-NO

The *N*-oxide of tamoxifen was synthesized using a previously described procedure (256, 257). Aqueous hydrogen peroxide (1 ml, 30% w/w) was added to a solution of (*Z*)-tamoxifen (15 mg, 40 µmole) dissolved in methanol (3.0 ml). The reaction was stirred at room temperature for 10 hours in the dark. The resulting product was examined for homogeneity on Silica Gel 60 F_{254} analytical thin layer chromatography sheets developed in chloroform / methanol / ammonium hydroxide (8: 2: 0.05), which gave tamoxifen (R_f = 0.69) and its corresponding *N*-oxide (R_f = 0.40). The sample was concentrated under nitrogen and treated with absolute ethanol (3 ml) and dry benzene (3 ml) to remove excess

hydrogen peroxide and water, respectively. Afterwards, the sample was dried under nitrogen and stored overnight in a vacuum desiccator over phosphorus pentoxide to afford a white solid (15.3 mg, 97% yield). Positive ion ESI-MS m/z = 388.20 $[M + H]^+$ Theoretical calculated mass = 388.2277 $[M + H]^+$; [^{1}H NMR: (300 MHz, chloroform-*d*) ppm (δ) 0.94 (t, 3H, $CH_2C\underline{H}_3$); 2.48 (q, 2H, $C\underline{H}_2CH_3$); 3.29 [s, 6H, $N(C\underline{H}_3)_2$]; 3.65 (t, 2H, $OCH_2C\underline{H}_2N$); 4.69 (t, 2H, $OC\underline{H}_2CH_2N$); 6.57 (d, 2H, Ph); 6.79 (d, 2H, Ph); 7.11 – 7.39 (m, Ph).] Melting point: 136-138°C. The ^{1}H NMR spectrum of TAM-NO is shown in the Appendix, Figure A-10.

Synthesis of N-desTAM-S Ammonium Salt

The sulfamate of N-desTAM was prepared using sulfuryl imidazolium triflate (2,2,2-trichloroethoxysulfuryl-(2-methyl)-*N*-methylimidazolium trifate) as the sulfating reagent, and the synthesis of this reagent has been previously reported (258, 259). 1,2-Dimethylimidazole (14 µl, 157 µmole) was added to a solution of (*Z*)-N-desTAM (28 mg, 69 µmole) and sulfuryl imidazolium triflate (94 mg, 207 µmole) dissolved in dichloromethane (5 ml). The mixture was stirred at 0°C for 1 hour and gradually warmed to room temperature for a 12 hour reaction, then purified on a Silica Gel 60 flash column (1 cm x 10 cm) using ethyl acetate / hexanes (33: 67) as mobile phase. The eluent was concentrated, dissolved in DMSO (2 ml), and then added to a solution of ammonium formate (52 mg, 830 µmole) and zinc dust (27 mg, 410 µmole) (260) dissolved in methanol (1 ml). The reaction was stirred at room temperature for 2 hours and filtered through celite under vacuum. Methanol was removed by rotary evaporation and DMSO was removed by freeze-drying. The resulting mixture was purified on a Silica Gel 60 flash column (1 cm x 10 cm) using dichloromethane / methanol / ammonium hydroxide (20: 4: 1) as mobile phase. The sample was concentrated and the solvents removed to afford a yellow, flaky solid (28 mg, 90% yield). Negative ion ESI-MS m/z = 436.1586 $[M - H]^-$. Theoretical calculated mass = 436.1588 $[M - H]^-$; [^{1}H NMR: (600 MHz, methanol-d*4*) ppm (δ) 0.92

(t, 3H, $CH_2C\underline{H}_3$); 2.47 (q, 2H, $C\underline{H}_2CH_3$); 2.75 [s, 6H, $N(C\underline{H}_3)_2$]; 3.29 (t, 2H, $OCH_2C\underline{H}_2N$); 4.04 (t, 2H, $OC\underline{H}_2CH_2N$); 6.57 (d, 2H, Ph); 6.76 (d, 2H, Ph); 7.10 – 7.26 (m, Ph).] Melting point: 132-138°C. The ^{1}H NMR spectrum of N-desTAM-S is shown in the Appendix, Figure A-11.

Synthesis of 4-OHTAM-S Ammonium Salt

The sulfuric acid ester of 4-OHTAM was prepared similarly to the synthesis of N-desTAM-S with slight modifications. 1,2-Dimethylimidazole (2 µl, 23 µmole) was added to a solution of (*Z*)-4-OHTAM (4 mg, 10 µmole) and sulfuryl imidazolium triflate (14 mg, 30 µmole) dissolved in dichloromethane (5 ml). The mixture was stirred at 0°C for 1 hour and gradually warmed to room temperature for a 24 hour reaction. The product was then purified on a Silica Gel 60 flash column (1 cm x 10 cm) using chloroform / methanol (80: 20) as the mobile phase. The resulting reaction product was concentrated and then added to a solution of ammonium formate (8 mg, 120 µmole) and zinc (4 mg, 60 µmole) dissolved in methanol (3 ml). The reaction was stirred at room temperature for 30 minutes and vacuum filtered through celite. Afterwards, the mixture was purified on a Silica Gel 60 flash column (1 cm x 10 cm) using dichloromethane / methanol / ammonium hydroxide (20: 4: 1) as the mobile phase, and the eluent was concentrated and then lyophilized to a white powder (5 mg, 36% yield). Positive ion ESI-MS m/z = 468.1838 $[M + H]^+$. Theoretical calculated mass = 468.1852 $[M + H]^+$. ^{1}H NMR (600 MHz, dimethylsulfoxide-d*6*) isomeric mixture of 4-OHTAM-S is shown in the Appendix, Figure A-12. [**Major isomer of 4-OHTAM-S** – ppm (δ) 0.86 (t, 3H, $CH_2C\underline{H}_3$); 2.40 (q, 2H, $C\underline{H}_2CH_3$); 2.69 [s, 6H, $N(C\underline{H}_3)_2$]; 3.26 (t, 2H, $OCH_2C\underline{H}_2N$); 4.11 (t, 2H, $OC\underline{H}_2CH_2N$); 6.66 (d, 2H, Ph); 6.78 (d, 2H, Ph); 7.08 – 7.26 (m, Ph).] [**Minor isomer of 4-OHTAM-S** – ppm (δ) 0.86 (t, 3H, $CH_2C\underline{H}_3$); 2.40 (q, 2H, $C\underline{H}_2CH_3$); 2.75 [s, 6H, $N(C\underline{H}_3)_2$]; 3.36 (t, 2H, $OCH_2C\underline{H}_2N$); 4.28 (t, 2H, $OC\underline{H}_2CH_2N$); 6.71 (d, 2H, Ph); 6.82 (d, 2H, Ph); 7.00 (d, 2H, Ph); 7.08 – 7.26 (m, Ph).] Melting point: 270-275°C.

REFERENCES

1. Nandi, S., Guzman, R. C., and Yang, J. (1995) Hormones and mammary carcinogenesis in mice, rats, and humans: a unifying hypothesis. *Proceedings of the National Academy of Sciences* **92**, 3650-3657

2. (2013) Cancer Facts & Figures 2013. Vol. 2014, American Cancer Society, Atlanta, GA

3. (2013) U.S. Breast Cancer Statistics. Vol. 2014, Breastcancer.org

4. Schildhaus, H.-U., Schroeder, L., Merkelbach-Bruse, S., Binot, E., Büttner, R., Kuhn, W., and Rudlowski, C. Therapeutic strategies in male breast cancer: Clinical implications of chromosome 17 gene alterations and molecular subtypes. *The Breast* **22**, 1066-1071

5. Anderson, W., Althuis, M., Brinton, L., and Devesa, S. (2004) Is Male Breast Cancer Similar or Different than Female Breast Cancer? *Breast Cancer Res Treat* **83**, 77-86

6. (2012) What You Need to Know About Breast Cancer. Vol. 2014, National Cancer Institute

7. Breast Cancer. Vol. 2014, American Cancer Society

8. Kumler, I., Tuxen, M. K., and Nielsen, D. L. A systematic review of dual targeting in HER2-positive breast cancer. *Cancer Treatment Reviews* **40**, 259-270

9. Cleator, S. J., Ahamed, E., Coombes, R. C., and Palmieri, C. (2009) A 2009 Update on the Treatment of Patients with Hormone Receptor-Positive Breast Cancer. *Clinical Breast Cancer* **9, Supplement 1**, S6-S17

10. Johnston, S. R. D., and Dowsett, M. (2003) Aromatase inhibitors for breast cancer: lessons from the laboratory. *Nat Rev Cancer* **3**, 821-831

11. Goss, P. E., and Strasser, K. (2001) Aromatase Inhibitors in the Treatment and Prevention of Breast Cancer. *Journal of Clinical Oncology* **19**, 881-894

12. Campos, S. M. (2004) Aromatase Inhibitors for Breast Cancer in Postmenopausal Women. *Oncologist* **9**, 126-136

13. Howell, A., Cuzick, J., Baum, M., Buzdar, A., Dowsett, M., Forbes, J. F., Hoctin-Boes, G., Houghton, I., Locker, G. Y., and Tobias, J. S. (2005) Results of the ATAC (Arimidex, Tamoxifen, Alone or in Combination) trial after completion of 5 years' adjuvant treatment for breast cancer. *Lancet* **365**, 60-62

14. Williams, N. (2008) Effect of anastrozole and tamoxifen as adjuvant treatment for early-stage breast cancer: 100-month analysis of the ATAC trial. *Lancet Oncology* **9**, 45-53

15. Buzdar, A., Howell, A., Cuzick, J., Wale, C., Distler, W., Hoctin-Boes, G., Houghton, J., Locker, G. Y., and Nabholtz, J. M. (2006) Comprehensive side-effect profile of anastrozole and tamoxifen as adjuvant treatment for early-stage breast cancer: long-term safety analysis of the ATAC trial. *Lancet Oncology* **7**, 633-643

16. Chlebowski, R. T. (2009) Aromatase Inhibitor–Associated Arthralgias. *Journal of Clinical Oncology* **27**, 4932-4934

17. Gaillard, S., and Stearns, V. (2011) Aromatase inhibitor-associated bone and musculoskeletal effects: new evidence defining etiology and strategies for management. *Breast Cancer Research* **13**, 205

18. Hershman, D. L., Kushi, L. H., Shao, T., Buono, D., Kershenbaum, A., Tsai, W.-Y., Fehrenbacher, L., Lin Gomez, S., Miles, S., and Neugut, A. I. Early Discontinuation and Nonadherence to Adjuvant Hormonal Therapy in a Cohort of 8,769 Early-Stage Breast Cancer Patients. *Journal of Clinical Oncology* **28**, 4120-4128

19. Brzozowski, A. M., Pike, A. C. W., Dauter, Z., Hubbard, R. E., Bonn, T., Engstrom, O., Ohman, L., Greene, G. L., Gustafsson, J. A., and Carlquist, M. (1997) Molecular basis of agonism and antagonism in the oestrogen receptor. *Nature* **389**, 753-758

20. Lahti, E. I., Knip, M., and Laatikainen, T. J. (1994) Plasma insulin-like growth-factor-i and its binding protein-1 and protein-3 in postmenopausal patients with breast-cancer receiving long-term tamoxifen. *Cancer* **74**, 618-624

21. Warri, A. M., Huovinen, R. L., Laine, A. M., Martikainen, P. M., and Harkonen, P. L. (1993) Apoptosis in toremifene-induced growth-inhibition of human breast-cancer cells in-vivo and in-vitro. *Journal of the National Cancer Institute* **85**, 1412-1418

22. Clarke, R., van den Berg, H. W., and Murphy, R. F. (1990) Reduction of the Membrane Fluidity of Human Breast Cancer Cells by Tamoxifen and 17Î²-Estradiol. *Journal of the National Cancer Institute* **82**, 1702-1705

23. Wiseman, H. (1994) Tamoxifen - new membrane-mediated mechanisms of action and therapeutic advances. *Trends in Pharmacological Sciences* **15**, 83-89

24. Bolanz, K. A., Kovacs, G. G., Landowski, C. P., and Hediger, M. A. (2009) Tamoxifen Inhibits TRPV6 Activity via Estrogen Receptor-Independent Pathways in TRPV6-Expressing MCF-7 Breast Cancer Cells. *Molecular Cancer Research* **7**, 2000-2010

25. Song, J., Standley, P. R., Zhang, F., Joshi, D., Gappy, S., Sowers, J. R., and Ram, J. L. (1996) Tamoxifen (estrogen antagonist) inhibits voltage-gated calcium current and contractility in vascular smooth muscle from rats. *Journal of Pharmacology and Experimental Therapeutics* **277**, 1444-1453

26. Callaghan, R., and Higgins, C. F. (1995) Interaction of tamoxifen with the multidrug-resistance p-glycoprotein. *Br J Cancer* **71**, 294-299

27. Jordan, V. C. (2003) Antiestrogens and selective estrogen receptor modulators as multifunctional medicines.1. Receptor interactions. *J. Med. Chem.* **46**, 883-908

28. Fisher, B., Costantino, J. P., Wickerham, D. L., Redmond, C. K., Kavanah, M., Cronin, W. M., Vogel, V., Robidoux, A., Dimitrov, N., Atkins, J., Daly, M., Wieand, S., Tan-Chiu, E., Ford, L., and Wolmark, N. (1998) Tamoxifen for prevention of breast cancer: report of the National Surgical Adjuvant Breast and Bowel Project P-1 Study. *J. Nat. Cancer Inst.* **90**, 1371-1388

29. Jordan, V. C. (2007) New insights into the metabolism of tamoxifen and its role in the treatment and prevention of breast cancer. *Steroids* **72**, 829-842

30. Fisher, B., Costantino, J. P., Wickerham, D. L., Cecchini, R. S., Cronin, W. M., Robidoux, A., Bevers, T. B., Kavanah, M. T., Atkins, J. N., Margolese, R. G., Runowicz, C. D., James, J. M., Ford, L. G., and Wolmark, N. (2005) Tamoxifen for the Prevention of Breast Cancer: Current Status of the National Surgical Adjuvant Breast and Bowel Project P-1 Study. *Journal of the National Cancer Institute* **97**, 1652-1662

31. Osborne, C. K. (1998) Tamoxifen in the treatment of breast cancer. *New England J. Med.* **339**, 1609-1618

32. Jordan, V. C. (1997) Tamoxifen: the Herald of a New Era of Preventive Therapeutics. *Journal of the National Cancer Institute* **89**, 747-749

33. Macgregor, J. I., and Jordan, V. C. (1998) Basic Guide to the Mechanisms of Antiestrogen Action. *Pharmacological Reviews* **50**, 151-196

34. Hernandez, R. K., Sørensen, H. T., Pedersen, L., Jacobsen, J., and Lash, T. L. (2009) Tamoxifen treatment and risk of deep venous thrombosis and pulmonary embolism. *Cancer* **115**, 4442-4449

35. Decensi, A., Maisonneuve, P., Rotmensz, N., Bettega, D., Costa, A., Sacchini, V., Salvioni, A., Travaglini, R., Oliviero, P., D'Aiuto, G., Gulisano, M., Gucciardo, G., del Turco, M. R., Pizzichetta, M. A., Conforti, S., Bonanni, B., Boyle, P., Veronesi, U., and for the Italian Tamoxifen Study, G. (2005) Effect of Tamoxifen on Venous Thromboembolic Events in a Breast Cancer Prevention Trial. *Circulation* **111**, 650-656

36. Saphner, T., Tormey, D. C., and Gray, R. (1991) Venous and arterial thrombosis in patients who received adjuvant therapy for breast cancer. *Journal of Clinical Oncology* **9**, 286-294

37. Jin, Y., Desta, Z., Stearns, V., Ward, B., Ho, H., Lee, K. H., Skaar, T., Storniolo, A. M., Li, L., Araba, A., Blanchard, R., Nguyen, A., Ullmer, L., Hayden, J., Lemler, S., Weinshilboum, R. M., Rae, J. M., Hayes, D. F., and Flockhart, D. A. (2005) CYP2D6 genotype, antidepressant use, and tamoxifen metabolism during adjuvant breast cancer treatment. *J Natl Cancer Inst* **97**, 30-39

38. van Leeuwen, F. E., Benraadt, J., Coebergh, J. W. W., Kiemeney, L. A. L. M., Diepenhorst, F. W., van den Belt-Dusebout, A. W., and van Tinteren, H. (1994) Risk of endometrial cancer after tamoxifen treatment of breast cancer. *Lancet* **343**, 448-452

39. Bernstein, L., Deapen, D., Cerhan, J. R., Schwartz, S. M., Liff, J., McGann-Maloney, E., Perlman, J. A., and Ford, L. (1999) Tamoxifen therapy for breast cancer and endometrial cancer risk. *Journal of the National Cancer Institute.* **91**, 1654-1662

40. Kim, S. Y., Suzuki, H., Santosh Laxmi, Y. R., and Shibutani, S. (2004) Genotoxic mechanism of Tamoxifen in developing endometrial cancer. *Drug Metabolism Reviews* **36**, 199-218

41. Phillips, D. H., Hewer, A., Osborne, M. R., Cole, K. J., Churchill, C., and Arlt, V. M. (2005) Organ specificity of DNA adduct formation by tamoxifen and alpha-hydroxytamoxifen in the rat: implications for understanding the mechanism(s) of tamoxifen carcinogenicity and for human risk assessment. *Mutagenesis* **20**, 297-303

42. Dowers, T. S., Qin, Z.-H., Thatcher, G. R. J., and Bolton, J. L. (2006) Bioactivation of selective estrogen receptor modulators (SERMs). *Chem Res Toxicol* **19**, 1125-1137

43. Hayes, D. F., Van Zyl, J. A., Hacking, A., Goedhals, L., Bezwoda, W. R., Mailliard, J. A., Jones, S. E., Vogel, C. L., Berris, R. F., and Shemano, I. (1995) Randomized comparison of tamoxifen and two separate doses of toremifene in postmenopausal patients with metastatic breast cancer. *Journal of Clinical Oncology* **13**, 2556-2566

44. Gu, R., Jia, W., Zeng, Y., Rao, N., Hu, Y., Li, S., Wu, J., Jin, L., Chen, L., Long, M., Chen, K., Chen, L., Xiao, Q., Wu, M., Song, E., and Su, F. A comparison of survival outcomes and side effects of toremifene or tamoxifen therapy in premenopausal estrogen and progesterone receptor positive breast cancer patients: a retrospective cohort study. *BMC Cancer* **12**, 161

45. International Breast Cancer Study, G. (2004) Toremifene and tamoxifen are equally effective for early-stage breast cancer: first results of International Breast Cancer Study Group Trials 12-93 and 14-93. *Annals of Oncology* **15**, 1749-1759

46. Zhou, W.-B., Ding, Q., Chen, L., Liu, X.-A., and Wang, S. Toremifene is an effective and safe alternative to tamoxifen in adjuvant endocrine therapy for breast cancer: results of four randomized trials. *Breast Cancer Res Treat* **128**, 625-631

47. Shibutani, S., Ravindernath, A., Terashima, I., Suzuki, N., Laxmi, Y. R., Kanno, Y., Suzuki, M., Apak, T. I., Sheng, J. J., and Duffel, M. W. (2001) Mechanism of lower genotoxicity of toremifene compared with tamoxifen. *Cancer Research.* **61**, 3925-3931

48. Williams, G. M., Ross, P.M., Jeffrey, A.M., Karlsson, S. (1998) Genotoxicity studies with the antiestrogen toremifene. *Drug and Chemical Toxicology* **21**, 449-476

49. Cauley, J. A., Norton, L., Lippman, M.E., Eckert, S., Krueger, K.A., Purdie, D.W., Farrerons, J., Karasik, A., Mellstrom, D., Ng, K.W., Stepan, J.J., Powles, T.J., Morrow, M., Costa, A., Silfen, S.L., Walls, E.L., Schmitt, H., Muchmore, D.B., Jordan, V.C. (2001) Continued breast cancer risk reduction in postmenopausal women treated with raloxifene: 4-year results from the MORE trial. *Breast Cancer Res. Treat.* **65**, 125-134

50. Cummings, S. R., Eckert, S., Krueger, K.A., Grady, D., Powles, T.J., Cauley, J.A., Norton, L., Nickelsen, T., Bjarnason, N.H., Morrow, M., Lippman, M.E., Black, D., Glusman, J.E., Costa, A., Jordan, V.C. (1999) The effect of raloxifene on risk of breast cancer in postmenopausal women: results from the MORE randomized trial-Multiple Outcomes of Raloxifene Evaluation. *JAMA* **281**, 2189-2197

51. Vogel, V. G. (2009) The NSABP Study of Tamoxifen and Raloxifene (STAR) trial. *Expert Review of Anticancer Therapy* **9**, 51-60

52. Otto, A., Paddenberg, R., Schubert, S., and Mannherz, H. (1996) Cell-cycle arrest, micronucleus formation, and cell death in growth inhibition of MCF-7 breast cancer cells by tamoxifen and cisplatin. *J Cancer Res Clin Oncol* **122**, 603-612

53. Zhang, G.-J., Kimijima, I., Onda, M., Kanno, M., Sato, H., Watanabe, T., Tsuchiya, A., Abe, R., and Takenoshita, S. (1999) Tamoxifen-induced Apoptosis in Breast Cancer Cells Relates to Down-Regulation of bcl-2, but not bax and bcl-XL, without Alteration of p53 Protein Levels. *Clinical Cancer Research* **5**, 2971-2977

54. Osborne, C. K., Boldt, D. H., Clark, G. M., and Trent, J. M. (1983) Effects of Tamoxifen on Human Breast Cancer Cell Cycle Kinetics: Accumulation of Cells in Early G1 Phase. *Cancer Res* **43**, 3583-3585

55. Jamil, A., Croxtall, J. D., and White, J. O. (1991) The effect of anti-oestrogens on cell growth and progesterone receptor concentration in human endometrial cancer cells (Ishikawa). *Journal of molecular endocrinology* **6**, 215-221

56. Thompson, E. W., Katz, D., Shima, T. B., Wakeling, A. E., Lippman, M. E., and Dickson, R. B. (1989) ICI 164,384, a Pure Antagonist of Estrogen-stimulated MCF-7 Cell Proliferation and Invasiveness. *Cancer Res* **49**, 6929-6934

57. Watanabe, T., Inoue, S., Ogawa, S., Ishii, Y., Hiroi, H., Ikeda, K., Orimo, A., and Muramatsu, M. (1997) Agonistic Effect of Tamoxifen Is Dependent on Cell Type, ERE-Promoter Context, and Estrogen Receptor Subtype: Functional Difference between Estrogen Receptors α and β. *Biochem Biophys Res Commun* **236**, 140-145

58. Guetta, V., Lush, R. M., Figg, W. D., Waclawiw, M. A., and Cannon, R. O. (1995) Effects of the antiestrogen tamoxiten on low-density lipoprotein concentrations and oxidation in postmenopausal women. *The American journal of cardiology* **76**, 1072-1073

59. Love, R. R., Wiebe, D.A., Newcomb, P.A., Camero, L., Leventhal, H., Jordan, V.C., Feyzi, J., DeMets, D.L. (1991) Effects of tamoxifen on cardiovascular risk factors in postmenopausal women. *Ann. Intern. Med.* **115**, 860-864

60. Love, R. R., Mazess, R.B., Barden, H.S., Epstein, S., Newcomb, P.A., Jordan, V.C., Carbone, P.P., DeMets, D.L. (1992) Effects of tamoxifen on bone mineral density in postmenopausal women with breast cancer. *N. Engl. J. Med.* **326**, 852-856

61. Paganinihill, A., Ross, R. K., and Henderson, B. E. (1989) Endometrial cancer and patterns of use of estrogen replacement therapy - a cohort study. *Br J Cancer* **59**, 445-447

62. Taylor, H. S. (2009) Designing the ideal selective estrogen receptor modulator-an achievable goal? *Menopause* **16**, 609-615

63. Pinkerton, J. V., and Thomas, S. Use of SERMs for treatment in postmenopausal women. *J Steroid Biochem Mol Biol*

64. Crewe, H. K., Notley, L. M., Wunsch, R. M., Lennard, M. S., and Gillam, E. M. J. (2002) Metabolism of tamoxifen by recombinant human cytochrome P450 enzymes: formation of the 4-hydroxy, 4'-hydroxy and N-desmethyl metabolites and isomerization of trans-4-hydroxytamoxifen. *Drug. Metab. Dispos.* **30**, 869-874

65. Desta, Z., Ward, B. A., Soukhova, N. V., and Flockhart, D. A. (2004) Comprehensive evaluation of tamoxifen sequential biotransformation by the human cytochrome P450 system in vitro: prominent roles for CYP3A and CYP2D6. *J Pharmacol Exp Ther* **310**, 1062-1075

66. Lim, Y. C., Desta, Z., Flockhart, D. A., and Skaar, T. C. (2005) Endoxifen (4-hydroxy-N-desmethyl-tamoxifen) has anti-estrogenic effects in breast cancer cells with potency similar to 4-hydroxy-tamoxifen. *Cancer Chemother Pharmacol* **55**, 471-478

67. Lim, Y. C., Li, L., Desta, Z., Zhao, Q., Rae, J. M., Flockhart, D. A., and Skaar, T. C. (2006) Endoxifen, a secondary metabolite of tamoxifen, and 4-OH-tamoxifen induce similar changes in global gene expression patterns in MCF-7 breast cancer cells. *J Pharmacol Exp Ther* **318**, 503-512

68. Jordan, V. C., Collins, M. M., Rowsby, L., and Prestwich, G. (1977) A monohydroxylated metabolite of tamoxifen with potent antioestrogenic activity. *J Endocrinol* **75**, 305-316

69. Gjerde, J., Gandini, S., Guerrieri-Gonzaga, A., Haugan Moi, L. L., Aristarco, V., Mellgren, G., Decensi, A., and Lien, E. A. (2012) Tissue distribution of 4-hydroxy-N-desmethyltamoxifen and tamoxifen-N-oxide. *Breast Cancer Res Treat* **134**, 693-700

70. Lien, E. A., Anker, G., Lonning, P. E., Solheim, E., and Ueland, P. M. (1990) Decreased serum concentrations of tamoxifen and its metabolites induced by aminoglutethimide. *Cancer Res* **50**, 5851-5857

71. Wu, X., Hawse, J. R., Subramaniam, M., Goetz, M. P., Ingle, J. N., and Spelsberg, T. C. (2009) The Tamoxifen Metabolite, Endoxifen, Is a Potent Antiestrogen that Targets Estrogen Receptor alpha for Degradation in Breast Cancer Cells. *Cancer Res* **69**, 1722-1727

72. Mani, C., Hodgson, E., and Kupfer, D. (1993) Metabolism of the antimammary cancer antiestrogenic agent tamoxifen. II. Flavin-containing monooxygenase-mediated N-oxidation. *Drug. Metab. Dispos.* **21**, 657-661

73. Boocock, D. J., Brown, K., Gibbs, A. H., Sanchez, E., Turteltaub, K. W., and White, I. N. (2002) Identification of human CYP forms involved in the activation of tamoxifen and irreversible binding to DNA. *Carcinogenesis.* **23**, 1897-1901

74. Brauch, H., Murdter, T. E., Eichelbaum, M., and Schwab, M. (2009) Pharmacogenomics of tamoxifen therapy. *Clin Chem* **55**, 1770-1782

75. (1996) IARC Monograph conclusion on tamoxifen. *The Lancet* **347**, 605

76. Shibutani, S., Dasaradhi, L., Terashima, I., Banoglu, E., and Duffel, M. W. (1998) Alpha-hydroxytamoxifen is a substrate of hydroxysteroid (alcohol) sulfotransferase, resulting in tamoxifen DNA adducts. *Cancer Res.* **58**, 647-653

77. Singh, M. N., Stringfellow, H. F., Walsh, M. J., Ashton, K. M., Phillips, D. H., Martin-Hirsch, P. L., and Martin, F. L. (2007) Potential for phase I/II metabolism of tamoxifen in human endometrium: expression of CYP3A4 and SULT2A1. *Mutagenesis* **22**, 450-450

78. Sridar, C., D'Agostino, J., and Hollenberg, P. F. Bioactivation of the Cancer Chemopreventive Agent Tamoxifen to Quinone Methides by Cytochrome P4502B6 and Identification of the Modified Residue on the Apoprotein. *Drug Metabolism and Disposition* **40**, 2280-2288

79. Marques, M. M., Beland, F.A. (1997) Identification of tamoxifen-DNA adducts formed by 4-hydroxytamoxifen quinone methide. *Carcinogenesis* **18**, 1949-1954

80. Fan, P. W., and Bolton, J. L. (2001) Bioactivation of Tamoxifen to Metabolite E Quinone Methide: Reaction with Glutathione and DNA. *Drug Metabolism and Disposition* **29**, 891-896

81. Dehal, S. S., Kupfer, D. (1995) Evidence that the catechol 3,4-dihydroxytamoxifen is a proximate intermediate to the reactive species binding covalently to proteins. *Cancer Research.* **56**, 1283-1290

82. Zhang, F., Fan, P.W., Liu, X., Shen, L., van Bremen, R.B., Bolton, J.L. (2000) Synthesis and reactivity of a potential carcinogenic metabolite of tamoxifen: 3,4-dihydroxytamoxifen-*o*-quinone. *Chem. Res. Toxicol.* **13**, 53-62

83. White, I. N. H., de Matteis, F., Davies, A., Smith, L. L., Crofton-Sleigh, C., Venitt, S., Hewer, A., and Phillips, D. H. (1992) Genotoxic potential of tamoxifen and analogues in female Fischer F344/n rats, DBA/2 and C57BL/6 mice and in human MCL-5 cells. *Carcinogenesis* **13**, 2197-2203

84. Moorthy, B., Sriram, P., Pathak, D. N., Bodell, W. J., and Randerath, K. (1996) Tamoxifen metabolic activation: comparison of DNA adducts formed by microsomal and chemical activation of tamoxifen and 4-hydroxytamoxifen with DNA adducts formed in vivo. *Cancer Research.* **56**, 53-57

85. Phillips, D. H., Carmichael, P. L., Hewer, A., Cole, K. J., and Poon, G. K. (1994) alpha–Hydroxytamoxifen, a metabolite of tamoxifen with exceptionally high DNA-binding activity in rat hepatocytes. *Cancer Res* **54**, 5518-5522

86. Glatt, H., Davis, W., Meinl, W., Hermersdorfer, H., Venitt, S., and Phillips, D. H. (1998) Rat, but not human, sulfotransferase activates a tamoxifen metabolite to produce DNA adducts and gene mutations in bacteria and mammalian cells in culture. *Carcinogenesis.* **19**, 1709-1713

87. Randerath, K., Moorthy, B., Mabon, N., and Sriram, P. (1994) Tamoxifen: evidence by ^{32}P-postlabeling and use of metabolic inhibitors for two distinct pathways leading to mouse hepatic DNA adduct formation and identification of 4-hydroxytamoxifen as a proximate metabolite. *Carcinogenesis* **15**, 2087-2094

88. Kim, S. Y., Laxmi, Y. R., Suzuki, N., Ogura, K., Watabe, T., Duffel, M. W., and Shibutani, S. (2005) Formation of tamoxifen-DNA adducts via O-sulfonation, not O-acetylation, of alpha-hydroxytamoxifen in rat and human livers. *Drug Metab Dispos* **33**, 1673-1678

89. Gulcan, H. O., Liu, Y., and Duffel, M. W. (2008) Pentachlorophenol and other chlorinated phenols are substrates for human hydroxysteroid sulfotransferase hSULT2A1. *Chem. Res. Toxicol.* **21**, 1503-1508

90. Phillips, D. H., Carmichael, P. L., Hewer, A., Cole, K. J., Hardcastle, I. R., Poon, G. K., Keogh, A., and Strain, A. J. (1996) Activation of tamoxifen and its metabolite alpha-hydroxytamoxifen to DNA-binding products: comparisons between human, rat and mouse hepatocytes. *Carcinogenesis.* **17**, 89-94

91. Lien, E. A., Solheim, E., and Ueland, U. E. (1991) Distribution of Tamoxifen and its metabolites in rat and human tissues during steady-state treatment. *Cancer Res* **51**, 4837-4844

92. Decensi, A., Robertson, C., Viale, G., Pigatto, F., Johansson, H., Kisanga, E. R., Veronesi, P., Torrisi, R., Cazzaniga, M., Mora, S., Sandri, M. T., Pelosi, G., Luini, A., Goldhirsch, A., Lien, E. A., and Veronesi, U. (2003) A Randomized Trial of Low-Dose Tamoxifen on Breast Cancer Proliferation and Blood Estrogenic Biomarkers. *Journal of the National Cancer Institute* **95**, 779-790

93. Dorssers, L. C. J., van der Flier, S., Brinkman, A., van Agthoven, T., Veldscholte, J., Berns, E., Klijn, J. G. M., Beex, L., and Foekens, J. A. (2001) Tamoxifen resistance in breast cancer - Elucidating mechanisms. *Drugs* **61**, 1721-1733

94. Lammers, L. A., Mathijssen, R. H., van Gelder, T., Bijl, M. J., de Graan, A. J., Seynaeve, C., van Fessem, M. A., Berns, E. M., Vulto, A. G., and van Schaik, R. H. (2010) The impact of CYP2D6-predicted phenotype on tamoxifen treatment outcome in patients with metastatic breast cancer. *Br J Cancer* **103**, 765-771

95. Ruddy, K. J., Desantis, S. D., Gelman, R. S., Wu, A. H., Punglia, R. S., Mayer, E. L., Tolaney, S. M., Winer, E. P., Partridge, A. H., and Burstein, H. J. (2013) Personalized medicine in breast cancer: tamoxifen, endoxifen, and CYP2D6 in clinical practice. *Breast Cancer Res Treat*

96. Weinshilboum, R. (2008) Pharmacogenomics of endocrine therapy in breast cancer. *Adv Exp Med Biol* **630**, 220-231

97. Brauch, H., Schroth, W., Goetz, M. P., Mürdter, T. E., Winter, S., Ingle, J. N., Schwab, M., and Eichelbaum, M. Tamoxifen Use in Postmenopausal Breast Cancer: CYP2D6 Matters. *Journal of Clinical Oncology* **31**, 176-180

98. Beverage, J. N., Sissung, T. M., Sion, A. M., Danesi, R., and Figg, W. D. (2007) CYP2D6 polymorphisms and the impact on tamoxifen therapy. *J Pharm Sci* **96**, 2224-2231

99. Bijl, M. J., van Schaik, R. H., Lammers, L. A., Hofman, A., Vulto, A. G., van Gelder, T., Stricker, B. H., and Visser, L. E. (2009) The CYP2D6*4 polymorphism affects breast cancer survival in tamoxifen users. *Breast Cancer Res Treat* **118**, 125-130

100. Wegman, P., Vainikka, L., Stal, O., Nordenskjold, B., Skoog, L., Rutqvist, L. E., and Wingren, S. (2005) Genotype of metabolic enzymes and the benefit of tamoxifen in postmenopausal breast cancer patients. *Breast Cancer Res* **7**, R284-290

101. Goetz, M. P., Rae, J. M., Suman, V. J., Safgren, S. L., Ames, M. M., Visscher, D. W., Reynolds, C., Couch, F. J., Lingle, W. L., Flockhart, D. A., Desta, Z., Perez, E. A., and Ingle, J. N. (2005) Pharmacogenetics of tamoxifen biotransformation is associated with clinical outcomes of efficacy and hot flashes. *J Clin Oncol* **23**, 9312-9318

102. Serrano, D., Lazzeroni, M., Zambon, C. F., Macis, D., Maisonneuve, P., Johansson, H., Guerrieri-Gonzaga, A., Plebani, M., Basso, D., Gjerde, J., Mellgren, G., Rotmensz, N., Decensi, A., and Bonanni, B. Efficacy of tamoxifen based on cytochrome P450 2D6, CYP2C19 and SULT1A1 genotype in the Italian Tamoxifen Prevention Trial. *Pharmacogenomics Journal* **11**, 100-107

103. Schroth, W., Goetz, M. P., Hamann, U., Fasching, P. A., Schmidt, M., Winter, S., Fritz, P., Simon, W., Suman, V. J., Ames, M. M., Safgren, S. L., Kuffel, M. J., Ulmer, H. U., Bolander, J., Strick, R., Beckmann, M. W., Koelbl, H., Weinshilboum, R. M., Ingle, J. N., Eichelbaum, M., Schwab, M., and Brauch, H. (2009) Association between CYP2D6 polymorphisms and outcomes among women with early stage breast cancer treated with tamoxifen. *JAMA* **302**, 1429-1436

104. Trojan, A., Vergopoulos, A., Breitenstein, U., Tausch, C., Seifert, B., and Joechle, W. (2013) CYP2D6 phenotype indicative for optimized antiestrogen efficacy associates with outcome in early breast cancer patients. *Cancer Chemother Pharmacol* **71**, 301-306

105. Zanger, U., Raimundo, S., and Eichelbaum, M. (2004) Cytochrome P450 2D6: overview and update on pharmacology, genetics, biochemistry. *Naunyn-Schmiedeberg's Archives of Pharmacology* **369**, 23-37

106. Baumann, E. (1876) Ueber sulfosauren im harn. In *Ber. Dtsch. Chem. Ges.* p. 54

107. Hell, R., Dahl, C., Knaff, D., Leustek, T., Hernàndez-Sebastiá, C., Varin, L., and Marsolais, F. (2008) Sulfotransferases from Plants, Algae and Phototrophic Bacteria. In *Sulfur Metabolism in Phototrophic Organisms* Vol. 27 pp. 111-130, Springer Netherlands

108. Blanchard, R. L., Freimuth, R. R., Buck, J., Weinshilboum, R. M., and Coughtrie, M. W. (2004) A proposed nomenclature system for the cytosolic sulfotransferase (SULT) superfamily. *Pharmacogenetics* **14**, 199-211

109. Nagata, K., and Yamazoe, Y. (2000) Pharmacogenetics of sulfotransferase. *Ann Rev Pharmacol Toxicol.* **40**, 159-176

110. Falany, C. N. (1997) Enzymology of human cytosolic sulfotransferases. *FASEB J.* **11**, 206-216

111. Negishi, M., Pedersen, L. G., Petrotchenko, E., Shevtsov, S., Gorokhov, A., Kakuta, Y., and Pedersen, L. C. (2001) Structure and function of sulfotransferases. *Arch. Biochem. Biophys.* **390**, 149-157

112. Gamage, N., Barnett, A., Hempel, N., Duggleby, R. G., Windmill, K. F., Martin, J. L., and McManus, M. E. (2006) Human sulfotransferases and their role in chemical metabolism. *Toxicol. Sci.* **90**, 5-22

113. Buhl, A. E., Waldon, D.J., Baker, C.A., Johnson, G.A. (1990) Minoxidil sulfate is the active metabolite that stimulates hair follicles. *AACN Clin. Issues* **95**, 553-557

114. Glatt, H. (2000) Sulfotransferases in the bioactivation of xenobiotics. *Chem Biol Interact.* **129**, 141-170

115. Glatt, H. (1997) Sulfation and sulfotransferases 4: bioactivation of mutagens via sulfation. *FASEB Journal.* **11**, 314-321

116. Ozawa, S., Chou, H. C., Kadlubar, F. F., Nagata, K., Yamazoe, Y., and Kato, R. (1994) Activation of 2-hydroxyamino-1-methyl-6-phenylimidazo[4,5-*b*]pyridine by cDNA-expressed human and rat aryl sulfotransferases. *Jpn J Canc Res.* **85**, 1220-1228

117. Gamage, N. U., Tsvetanov, S., Duggleby, R. G., McManus, M. E., and Martin, J. L. (2005) The structure of human SULT1A1 crystallized with estradiol. An insight into active site plasticity and substrate inhibition with multi-ring substrates. *J Biol Chem.* **280**, 41482-41486

118. Nagar, S., Walther, S., and Blanchard, R. L. (2006) Sulfotransferase (SULT) 1A1 polymorphic variants *1, *2, and *3 are associated with altered enzymatic activity, cellular phenotype, and protein degradation. *Mol Pharmacol* **69**, 2084-2092

119. Glatt, H. (1997) Bioactivation of mutagens via sulfation. *FASEB J.* **11**, 314-321

120. Taskinen, J., Ethell, B. T., Pihlavisto, P., Hood, A. M., Burchell, B., and Coughtrie, M. W. (2003) Conjugation of catechols by recombinant human sulfotransferases, UDP-glucuronosyltransferases, and soluble catechol O-methyltransferase: structure-conjugation relationships and predictive models. *Drug Metabolism & Disposition.* **31**, 1187-1197

121. Kreis, P., Brandner, S., Coughtrie, M. W., Pabel, U., Meinl, W., Glatt, H., and Andrae, U. (2000) Human phenol sulfotransferases hP-PST and hM-PST activate propane 2-nitronate to a genotoxicant. *Carcinogenesis.* **21**, 295-299

122. Kester, M. H., Kaptein, E., Roest, T. J., van Dijk, C. H., Tibboel, D., Meinl, W., Glatt, H., Coughtrie, M. W., and Visser, T. J. (1999) Characterization of human iodothyronine sulfotransferases. *Journal of Clinical Endocrinology & Metabolism* **84**, 1357-1364

123. Hempel, N., Negishi, M., and McManus, M. E. (2005) Human SULT1A genes: cloning and activity assays of the SULT1A promoters. *Methods Enzymol* **400**, 147-165

124. Xu, Y., Liu, X., Guo, F., Ning, Y., Zhi, X., Wang, X., Chen, S., Yin, L., and Li, X. Effect of estrogen sulfation by SULT1E1 and PAPSS on the development of estrogen-dependent cancers. *Cancer Science* **103**, 1000-1009

125. Falany, J., Macrina, N., and Falany, C. (2002) Regulation of MCF-7 Breast Cancer Cell Growth by β-estradiol Sulfation. *Breast Cancer Res Treat* **74**, 167-176

126. Qian, Y., Deng, C., and Song, W. C. (1998) Expression of estrogen sulfotransferase in MCF-7 cells by cDNA transfection suppresses the estrogen response: potential role of the enzyme in regulating estrogen-dependent growth of breast epithelial cells. *Journal of Pharmacology & Experimental Therapeutics* **286**, 555-560

127. Poisson Pare, D., Song, D., Luu-The, V., Han, B., Li, S., Liu, G., Labrie, F., and Pelletier, G. (2009) Expression of Estrogen Sulfotransferase 1E1 and Steroid Sulfatase in Breast Cancer: A Immunohistochemical Study. *Breast cancer : basic and clinical research* **3**, 9-21

128. Huang, J., Bathena, S. P., Tong, J., Roth, M., Hagenbuch, B., and Alnouti, Y. (2010) Kinetic analysis of bile acid sulfation by stably expressed human sulfotransferase 2A1 (SULT2A1). *Xenobiotica* **40**, 184-194

129. Gulcan, H. O., and Duffel, M. W. (2011) Substrate inhibition in human hydroxysteroid sulfotransferase SULT2A1: studies on the formation of catalytically non-productive enzyme complexes. *Arch. Biochem. Biophys.* **507**, 232-240

130. Lyon, E. S., Marcus, C. J., Wang, J. L., and Jakoby, W. B. (1981) Hydroxysteroid Sulfotransferases. *Methods Enzymol* **77**, 206-213

131. Lyon, E. S., and Jakoby, W. B. (1980) The identity of alcohol sulfotransferases with hydroxysteroid sulfotransferases. *Arch. Biochem. Biophys.* **202**, 474-481

132. Senggunprai, L., Yoshinari, K., and Yamazoe, Y. (2009) Selective role of SULT2A1 in the N-sulfoconjugation of quinolone drugs in human. *Drug Metab Dispos* **37**, 1711-1717

133. Falany, C. N., Xie, X., Wang, J., Ferrer, J., and Falany, J. L. (2000) Molecular cloning and expression of novel sulphotransferase-like cDNAs from human and rat brain. *Biochem J.* **346**, 857-864

134. Liyou, N. E., Buller, K. M., Tresillian, M. J., Elvin, C. M., Scott, H. L., Dodd, P. R., Tannenberg, A. E., and McManus, M. E. (2003) Localization of a brain sulfotransferase, SULT4A1, in the human and rat brain: an immunohistochemical study. *Journal of Histochemistry & Cytochemistry.* **51**, 1655-1664

135. Freimuth, R. R., Wiepert, M., Chute, C. G., Wieben, E. D., and Weinshilboum, R. M. (2004) Human cytosolic sulfotransferase database mining: identification of seven novel genes and pseudogenes. *Pharmacogenomics J* **4**, 54-65

136. Nimmagadda, D., Cherala, G., and Ghatta, S. (2006) Cytosolic sulfotransferases. *Indian journal of experimental biology* **44**, 171-182

137. Cole, G. B., Keum, G., Liu, J., Small, G. W., Satyamurthy, N., Kepe, V., and Barrio, J. R. (2010) Specific estrogen sulfotransferase (SULT1E1) substrates and molecular imaging probe candidates. *Proc Natl Acad Sci U S A* **107**, 6222-6227

138. Berger, I., Guttman, C., Amar, D., Zarivach, R., and Aharoni, A. The Molecular Basis for the Broad Substrate Specificity of Human Sulfotransferase 1A1. *PLoS One* **6**

139. Banoglu, E., and Duffel, M. W. (1997) Studies on the interactions of chiral secondary alcohols with rat hydroxysteroid sulfotransferase STa. *Drug Metab Dispos.* **25**, 1304-1310

140. Petrotchenko, E. V., Pedersen, L. C., Borchers, C. H., Tomer, K. B., and Negishi, M. (2001) The dimerization motif of cytosolic sulfotransferases. *FEBS Lett.* **490**, 39-43

141. Cook, I. T., Leyh, T. S., Kadlubar, S. A., and Falany, C. N. (2010) Lack of substrate inhibition in a monomeric form of human cytosolic SULT2A1. *Horm Mol Biol Clin Investig* **3**, 357-366

142. Lu, L. Y., Chiang, H. P., Chen, W. T., and Yang, Y. S. (2009) Dimerization is responsible for the structural stability of human sulfotransferase 1A1. *Drug Metab Dispos* **37**, 1083-1088

143. Zhang, H., Varlamova, O., Vargas, F. M., Falany, C. N., and Leyh, T. S. (1998) Sulfuryl transfer: the catalytic mechanism of human estrogen sulfotransferase. *J. Biol. Chem.* **273**, 10888-10892

144. Rehse, P. H., Zhou, M., and Lin, S. X. (2002) Crystal structure of human dehydroepiandrosterone sulphotransferase in complex with substrate. . *Biochem. J.* **364**, 165-171

145. Duffel, M. W. (2010) Sulfotransferases. In *Comprehensive Toxicology, Vol. 4 Biotransformation (F.P. Guengerich, Vol. Ed.)* (McQueen, C. A., ed) Vol. 4 pp. 367-384, Elsevier, Oxford

146. Falany, C. N., Wheeler, J., Oh, T. S., and Falany, J. L. (1994) Steroid Sulfation by Expressed Human Cytosolic Sulfotransferases. *J Steroid Biochem Molec Biol.* **48**, 369-375

147. Strott, C. A. (2005) Hydroxysteroid sulfotransferases SULT2A1, SULT2B1a, and SULT2B1b. In *Human cytosolic sulfotransferases* (Pacifici, G. M., and Coughtrie, M. W. H., ed) pp. 231-253, CRC Press, Boca Raton, FL

148. Falany, C. N., Vazquez, M. E., and Kalb, J. M. (1989) Purification and characterization of human liver dehydroepiandrosterone sulphotransferase. *Biochem. J.* **260**, 641-646

149. Barker, E. V., Hume, R., Hallas, A., and Coughtrie, W. H. (1994) Dehydroepiandrosterone sulfotransferase in the developing human fetus: quantitative biochemical and immunological characterization of the hepatic, renal, and adrenal enzymes. *Endocrinology* **134**, 982-989

150. Majewska, M. D. (1995) Neuronal actions of dehydroepiandrosterone. Possible roles in brain development, aging, memory, and affect. *Ann N Y Acad Sci.* **774**, 111-120

151. Vallee, M., Mayo, W., and Le Moal, M. (2001) Role of pregnenolone, dehydroepiandrosterone and their sulfate esters on learning and memory in cognitive aging. *Brain Research Reviews* **37**, 301-312

152. Arlt, W. (2004) Dehydroepiandrosterone and ageing. *Best Pract Res Clin Endocrinol Metab.* **18**, 363-380

153. Naylor, J., Li, J., Milligan, C. J., Zeng, F., Sukumar, P., Hou, B., Sedo, A., Yuldasheva, N., Majeed, Y., Beri, D., Jiang, S., Seymour, V. A. L., McKeown, L., Kumar, B., Harteneck, C., O'Regan, D., Wheatcroft, S. B., Kearney, M. T., Jones, C., Porter, K. E., and Beech, D. J. Pregnenolone Sulphate- and Cholesterol-Regulated TRPM3 Channels Coupled to Vascular Smooth Muscle Secretion and Contraction. *Circulation Research* **106**, 1507-U1138

154. Kroboth, P. D., Salek, F. S., Pittenger, A. L., Fabian, T. J., and Frye, R. F. (1999) DHEA and DHEA-S: a review. *J Clin Pharmacol.* **39**, 327-348

155. Otterness, D. M., Wieben, E. D., Wood, T. C., Watson, R. W. G., Madden, B. J., McCormick, D. J., and Weinshilboum, R. M. (1992) Human liver dehydroepiandrosterone sulfotransferase: molecular cloning and expression of cDNA. *Mol Pharmacol.* **41**, 865-872

156. Chang, H. J., Zhou, M., and Lin, S. X. (2001) Human dehydroepiandrosterone sulfotransferase: purification and characterization of a recombinant protein. *J Steroid Biochem Mol Biol* **77**, 159-165

157. Lu, L. Y., Hsieh, Y. C., Liu, M. Y., Lin, Y. H., Chen, C. J., and Yang, Y. S. (2008) Identification and characterization of two amino acids critical for the substrate inhibition of human dehydroepiandrosterone sulfotransferase (SULT2A1). *Mol Pharmacol* **73**, 660-668

158. Kudlacek, P. E., Clemens, D. L., Halgard, C. M., and Anderson, R. J. (1997) Characterization of recombinant human liver dehydroepiandrosterone sulfotransferase with minoxidil as the substrate. *Biochem Pharmacol.* **53**, 215-221

159. Comer, K. A., and Falany, C. N. (1992) Immunological characterization of dehydroepiandrosterone sulfotransferase from human liver and adrenal. *Mol Pharmacol.* **41**, 645-651

160. Falany, C. N., Comer, K. A., Dooley, T. P., and Glatt, H. (1995) Human Dehydroepiandrosterone Sulfotransferase. *Ann N Y Acad Sci* **774**, 59-72

161. Parker, C. R., Falany, C. N., Stockard, C. R., Stankovic, A. K., and Grizzle, W. E. (1994) Immunohistochemical localization of dehydroepiandrosterone sulfotransferase in human fetal tissues. *The Journal of Clinical Endocrinology & Metabolism* **78**, 234-236

162. Radominska, A., Comer, K. A., Zimniak, P., Falany, J., Iscan, M., and Falany, C. N. (1990) Human liver steroid sulphotransferase sulphates bile acids. *Biochem J.* **272**, 597-604

163. Her, C., Szumlanski, C., Aksoy, I. A., and Weinshilboum, R. M. (1996) Human jejunal estrogen sulfotransferase and dehydroepiandrosterone sulfotransferase - Immunochemical characterization of individual variation. *Drug Metabolism and Disposition* **24**, 1328-1335

164. Tashiro, A., Sasano, H., Nishikawa, T., Yabuki, N., Muramatsu, Y., Coughtrie, M. W., Nagura, H., and Hongo, M. (2000) Expression and activity of dehydroepiandrosterone sulfotransferase in human gastric mucosa. *J Steroid Biochem Mol Biol* **72**, 149-154

165. Falany, C. N. (2004) Human Cytosolic Sulfotransferases. pp. 341-378

166. Javitt, N. B., Lee, Y. C., Shimizu, C., Fuda, H., and Strott, C. A. (2001) Cholesterol and hydroxycholesterol sulfotransferases: identification, distinction from dehydroepiandrosterone sulfotransferase, and differential tissue expression. *Endocrinology.* **142**, 2978-2984

167. Andersson, H., Helmestam, M., Zebrowska, A., Olovsson, M., and Brittebo, E. (2010) Tamoxifen-induced adduct formation and cell stress in human endometrial glands. *Drug Metab Dispos* **38**, 200-207

168. Neale, G., Lewis, B., Weaver, V., and Panveliw.D. (1971) Serum bile acids in liver disease. *Gut* **12**, 145-&

169. Back, P. (1982) Phenobarbital-induced alterations of bile acid metabolism in cases of intrahepatic cholestasis. *Klinische Wochenschrift* **60**, 541-549

170. Degirolamo, C., Modica, S., Palasciano, G., and Moschetta, A. Bile acids and colon cancer: Solving the puzzle with nuclear receptors. *Trends in Molecular Medicine* **17**, 564-572

171. Nagengast, F. M., Grubben, M. J. A. L., and van Munster, I. P. (1995) Role of bile acids in colorectal carcinogenesis. *European Journal of Cancer* **31**, 1067-1070

172. Adjei, A. A., Gaedigk, A., Simon, S. D., Weinshilboum, R. M., and Leeder, J. S. (2008) Interindividual variability in acetaminophen sulfation by human fetal liver: Implications for pharmacogenetic investigations of drug-induced birth defects. *Birth Defects Research Part A: Clinical and Molecular Teratology* **82**, 155-165

173. Wang, M., Ebmeier, C. C., Olin, J. R., and Anderson, R. J. (2006) Sulfation of tibolone metabolites by human postmenopausal liver and small intestinal sulfotransferases (SULTs). *Steroids* **71**, 343-351

174. Falany, J. L., Pilloff, D. E., Leyh, T. S., and Falany, C. N. (2006) Sulfation of raloxifene and 4-hydroxytamoxifen by human cytosolic sulfotransferases. *Drug Metab Dispos.* **34**, 361-368

175. Liu, Y., Apak, T. I., Lehmler, H. J., Robertson, L. W., and Duffel, M. W. (2006) Hydroxylated polychlorinated biphenyls are substrates and inhibitors of human hydroxysteroid sulfotransferase SULT2A1. *Chem. Res. Toxicol.* **19**, 1420-1425

176. Labrie, F., Belanger, A., Cusan, L., Gomez, J.-L., and Candas, B. (1997) Marked decline in serum concentrations of adrenal C19 sex steroid precursors and conjugated androgen metabolites during aging. *J Clin Endocrinol Metab.* **82**, 2396-2402

177. Salvadori, B., and Lauritzen, C. (1975) Experiences with Administration of Dehydroepiandrosterone-Sulfate and Pregnenolone in Cases of Feto-Placental Insufficiency. In *Therapy of Feto-Placental Insufficiency* pp. 318-329, Springer Berlin Heidelberg

178. Glatt, H., Christoph, S., Czich, A., Pauly, K., Vierzok, A., Seidel, A., Coughtrie, M. W. H., Doehmer, J., Falany, C. N., Philips, D. H., Yamazoe, Y., and Bartsch, I. (1997) Rat and Human Sulfotransferases Expressed in Ames's Salmonella typhimurium strains and Chinese hamster V79 cells for the Activation of Mutagens. In *Control Mechanisms of Carcinogenesis* (Hengstler, J. G., and Oesch, F., eds) pp. 98-115, Druckerei Thieme, Meissen

179. Shibutani, S., Shaw, P. M., Suzuki, N., Dasaradhi, L., Duffel, M. W., and Terashima, I. (1998) Sulfation of alpha-hydroxytamoxifen catalyzed by human hydroxysteroid sulfotransferase results in tamoxifen-DNA adducts. *Carcinogenesis.* **19**, 2007-2011

180. Surh, Y.-J., and Miller, J. A. (1994) Roles of electrophilic sulfuric acid ester metabolites in mutagenesis and carcinogenesis by some polynuclear aromatic hydrocarbons. *Chem. Biol. Interact.* **92**, 351-362

181. Watabe, T., Ishizuka, T., Isobe, M., and Ozawa, N. (1982) A 7-hydroxymethyl sulfate ester as an active metabolite of 7,12-dimethylbenz[a]anthracene. *Science* **215**, 403-405

182. Surh, Y. J. (1998) Bioactivation of benzylic and allylic alcohols via sulfo-conjugation. *Chemico-Biol. Interact.* **109**, 221-235

183. Miller, E. C., and Miller, J. A. (1966) Mechanisms of chemical carcinogenesis - nature of proximate carcinogens and interactions with macromolecules. *Pharmacological Reviews* **18**, 805-838

184. Miller, E. C., and Miller, J. A. (1981) Mechanisms of chemical carcinogenesis. *Cancer* **47**, 1055-1064

185. Miller, J. A. (1973) Mechanisms of chemical carcinogenesis. *Radiation Research* **55**, 507-508

186. Clemons, M., and Goss, P. (2001) Estrogen and the Risk of Breast Cancer. *New England Journal of Medicine* **344**, 276-285

187. Suzuki, T., Nakata, T., Miki, Y., Kaneko, C., Moriya, T., Ishida, T., Akinaga, S., Hirakawa, H., Kimura, M., and Sasano, H. (2003) Estrogen sulfotransferase and steroid sulfatase in human breast carcinoma. *Cancer Research.* **63**, 2762-2770

188. Pasqualini, J. R. (2009) Estrogen Sulfotransferases in Breast and Endometrial Cancers. *Ann N Y Acad Sci* **1155**, 88-98

189. Saal, F. S. V., Grant, W. M., McMullen, C. W., and Laves, K. S. (1983) High fetal estrogen concentrations - correlation with increased adult sexual-activity and decreased aggression in male-mice. *Science* **220**, 1306-1309

190. Hilakivi-Clarke, L., Cho, E., Raygada, M., and Kenney, N. (1997) Alterations in mammary gland development following neonatal exposure to estradiol, transforming growth factor α, and estrogen receptor antagonist ICI 182,780. *Journal of Cellular Physiology* **170**, 279-289

191. Rizner, T. L. Estrogen biosynthesis, phase I and phase II metabolism, and action in endometrial cancer. *Mol Cell Endocrinol* **381**, 124-139

192. Huhtinen, K., Ståhle, M., Perheentupa, A., and Poutanen, M. Estrogen biosynthesis and signaling in endometriosis. *Mol Cell Endocrinol* **358**, 146-154

193. Raju, U. M. A., Bradlow, H. L., and Levitz, M. (1990) Estriol-3-Sulfate in Human Breast Cyst Fluida. *Ann N Y Acad Sci* **586**, 83-87

194. Otake, Y., Nolan, A. L., Walle, U. K., and Walle, T. (2000) Quercetin and resveratrol potently reduce estrogen sulfotransferase activity in normal human mammary epithelial cells. *J Steroid Biochem Mol Biol* **73**, 265-270

195. Miki, Y., Nakata, T., Suzuki, T., Darnel, A. D., Moriya, T., Kaneko, C., Hidaka, K., Shiotsu, Y., Kusaka, H., and Sasano, H. (2002) Systemic distribution of steroid sulfatase and estrogen sulfotransferase in human adult and fetal tissues. *Journal of Clinical Endocrinology & Metabolism.* **87**, 5760-5768

196. Dooley, T. P., Haldeman-Cahill, R., Joiner, J., and Wilborn, T. W. (2000) Expression profiling of human sulfotransferase and sulfatase gene superfamilies in epithelial tissues and cultures cells. *Biochem Biophys Res Commun.* **277**, 236-245

197. Falany, J. L., Azziz, R., and Falany, C. N. (1998) Identification and characterization of cytosolic sulfotransferases in normal human endometrium. *Chem Biol Interact* **109**, 329-339

198. Rubin, G. L., Harrold, A. J., Mills, J. A., Falany, C. N., and Coughtrie, M. W. (1999) Regulation of sulphotransferase expression in the endometrium during the menstrual cycle, by oral contraceptives and during early pregnancy. *Molecular Human Reproduction* **5**, 995-1002

199. Falany, J. L., and Falany, C. N. (1996) Expression of Cytosolic Sulfotransferases in Normal Mammary Epithelial Cells and Breast Cancer Cell Lines. *Cancer Res* **56**, 1551-1555

200. Aksoy, I. A., Wood, T. C., and Weinshilboum, R. (1994) Human liver estrogen sulfotransferase: identification by cDNA cloning and expression. *Biochem Biophys Res Commun.* **200**, 1621-1629

201. Her, C., Aksoy, I. A., Kimura, S., Brandriff, B. F., Wasmuth, J. J., and Weinshilboum, R. M. (1995) Human estrogen sulfotransferase gene (STE): cloning, structure, and chromosomal localization. *Genomics* **29**, 16-23

202. Falany, C. N., Krasnykh, V., and Falany, J. L. (1995) Bacterial expression and characterization of a cDNA for human liver estrogen sulfotransferase. *J Steroid Biochem Molec Biol.* **52**, 529-539

203. Schrag, M. L., Cui, D., Rushmore, T. H., Shou, M., Ma, B., and Rodrigues, A. D. (2004) Sulfotransferase 1E1 is a low km isoform mediating the 3-O-sulfation of ethinyl estradiol. *Drug Metab Dispos* **32**, 1299-1303

204. Nishiyama, T., Ogura, K., Nakano, H., Kaku, T., Takahashi, E., Ohkubo, Y., Sekine, K., Hiratsuka, A., Kadota, S., and Watabe, T. (2002) Sulfation of environmental estrogens by cytosolic human sulfotransferases. *Drug Metab Pharmacokinet* **17**, 221-228

205. Miksits, M., Maier-Salamon, A., Aust, S., Thalhammer, T., Reznicek, G., Kunert, O., Haslinger, E., Szekeres, T., and Jaeger, W. (2005) Sulfation of resveratrol in human liver: Evidence of a major role for the sulfotransferases SULT1A1 and SULT1E1. *Xenobiotica* **35**, 1101-1119

206. Chen, X.-W., Serag, E. S., Sneed, K. B., and Zhou, S.-F. Herbal bioactivation, molecular targets and the toxicity relevance. *Chem Biol Interact* **192**, 161-176

207. Furimsky, A. M., Green, C. E., Sharp, L. E., Catz, P., Adjei, A. A., Parman, T., Kapetanovic, I. M., Weinshilboum, R. M., and Iyer, L. V. (2008) Effect of Resveratrol on 17 -Estradiol Sulfation by Human Hepatic and Jejunal S9 and Recombinant Sulfotransferase 1E1. *Drug Metab Dispos* **36**, 129-136

208. Adjei, A. A., and Weinshilboum, R. M. (2002) Catecholestrogen sulfation: possible role in carcinogenesis. *Biochem Biophys Res Commun.* **292**, 402-408

209. Nakano, H., Ogura, K., Takahashi, E., Harada, T., Nishiyama, T., Muro, K., Hiratsuka, A., Kadota, S., and Watabe, T. (2004) Regioselective monosulfation and disulfation of the phytoestrogens daidzein and genistein by human liver sulfotransferases. *Drug Metab Pharmacokinet* **19**, 216-226

210. Falany, C. N., Strom, P., and Swedmark, S. (2005) Sulphation of o-desmethylnaproxen and related compounds by human cytosolic sulfotransferases. *Br J Clin Pharmacol* **60**, 632-640

211. Raftogianis, R. B., Wood, T. C., Otterness, D. M., Van Loon, J. A., and Weinshilboum, R. M. (1997) Phenol sulfotransferase pharmacogenetics in humans: Association of common SULT1A1 alleles with TS PST phenotype. *Biochem Biophys Res Commun.* **239**, 298-304

212. Raftogianis, R. B., Wood, T. C., and Weinshilboum, R. M. (1999) Human phenol sulfotransferases SULT1A2 and SULT1A1: genetic polymorphisms, allozyme properties, and human liver genotype-phenotype correlations. *Biochem. Pharmacol.* **58**, 605-616

213. Coughtrie, M. W., Gilissen, R. A., Shek, B., Strange, R. C., Fryer, A. A., Jones, P. W., and Bamber, D. E. (1999) Phenol sulphotransferase SULT1A1 polymorphism: molecular diagnosis and allele frequencies in Caucasian and African populations. *Biochemical Journal* **337**, 45-49

214. Nowell, S., Sweeney, C., Winters, M., Stone, A., Lang, N. P., Hutchins, L. F., Kadlubar, F. F., and Ambrosone, C. B. (2002) Association between sulfotransferase 1A1 genotype and survival of breast cancer patients receiving tamoxifen therapy. *Journal of the National Cancer Institute.* **94**, 1635-1640

215. Grabinski, J. L., Smith, L. S., Chisholm, G. B., Drengler, R., Rodriguez, G. I., Lang, A. S., Kalter, S. P., Garner, A. M., Fichtel, L. M., Hollsten, J., Pollock, B. H., and Kuhn, J. G. (2006) Genotypic and allelic frequencies of SULT1A1 polymorphisms in women receiving adjuvant tamoxifen therapy. *Breast Cancer Res Treat* **95**, 13-16

216. Mercer, K. E., Apostolov, E. O., da Costa, G. G., Yu, X., Lang, P., Roberts, D. W., Davis, W., Basnakian, A. G., Kadlubar, F. F., and Kadlubar, S. A. Expression of sulfotransferase isoform 1A1 (SULT1A1) in breast cancer cells significantly increases 4-hydroxytamoxifen-induced apoptosis. *International journal of molecular epidemiology and genetics* **1**, 92-103

217. Falany, C. N., Vazquez, M. E., Heroux, J. A., and Roth, J. A. (1990) Purification and characterization of human liver phenol-sulfating phenol sulfotransferase. *Archives of Biochemistry and Biophysics* **278**, 312-318

218. Wilborn, T. W., Comer, K.A., Dooley, T.P., Reardon, I.M., Heinrikson, R.L., Falany, C.N. (1992) Sequence analysis and expression of the cDNA for the phenol-sulfating form of human liver phenol sulfotransfeases. *Mol. Pharmacol.* **43**, 70-77

219. Campbell, N. R. C., Loon, J. A. v., and Weinshilboum, R. M. (1987) Human liver phenol sulfotransferase: assay conditions, biochemical properties and partial purification of isozymes of the thermostable form. *Biochem. Pharmacol.* **36**, 1435-1446

220. Veronese, M. E., Burgess, W., Zhu, X., McManus, M.E. (1994) Functional characterization of two human sulphotransferase cDNAs that encode monoamine- and phenol-sulphating forms of phenol sulphotransferase: substrate kinetics, thermal-stability and inhibitor sensitivity studies. *Biochem. J.* **302**, 497-502

221. Rein, G., Glover, V., and Sandler, M. (1982) Multiple forms of phenol sulfotransferases in human tissues: selective inhibition by dichloronitrophenol. *Biochem. Pharmacol.* **31**, 1893-1897

222. Riches, Z., Stanley, E. L., Bloomer, J. C., and Coughtrie, M. W. (2009) Quantitative evaluation of the expression and activity of five major sulfotransferases (SULTs) in human tissues: the SULT "pie". *Drug Metab Dispos* **37**, 2255-2261

223. Falany, C. N., and Kerl, E. A. (1990) Sulfation of minoxidil by human liver phenol sulfotransferase. *Biochem. Pharmacol.* **40**, 1027-1032

224. Tabrett, C. A., and Coughtrie, M. W. (2003) Phenol sulfotransferase 1A1 activity in human liver: kinetic properties, interindividual variation and re-evaluation of the suitability of 4-nitrophenol as a probe substrate. *Biochemical Pharmacology.* **66**, 2089-2097

225. Frame, L. T., Ozawa, S., Nowell, S. A., Chou, H. C., DeLongchamp, R. R., Doerge, D. R., Lang, N. P., and Kadlubar, F. F. (2000) A simple colorimetric assay for phenotyping the major human thermostable phenol sulfotransferase (SULT1A1) using platelet cytosols. *Drug Metabolism & Disposition* **28**, 1063-1068

226. Rohn, K. J., Cook, I. T., Leyh, T. S., Kadlubar, S. A., and Falany, C. N. (2012) Potent inhibition of human sulfotransferase 1A1 by 17alpha-ethinylestradiol: role of 3'-phosphoadenosine 5'-phosphosulfate binding and structural rearrangements in regulating inhibition and activity. *Drug Metab Dispos* **40**, 1588-1595

227. Glatt, H., Pabel, U., Meinl, W., Frederiksen, H., Frandsen, H., and Muckel, E. (2004) Bioactivation of the heterocyclic aromatic amine 2-amino-3-methyl-9H-pyrido [2,3-b]indole (MeAalphaC) in recombinant test systems expressing human xenobiotic-metabolizing enzymes. *Carcinogenesis* **25**, 801-807

228. Spink, B. C., Katz, B. H., Hussain, M. M., Pang, S. K., Connor, S. P., Aldous, K. M., Gierthy, J. F., and Spink, D. C. (2000) SULT1A1 catalyzes 2-methoxyestradiol sulfonation in MCF-7 breast cancer cells. *Carcinogenesis* **21**, 1947-1957

229. Aust, S., Jaeger, W., Klimpfinger, M., Mayer, K., Baravalle, G., Ekmekcioglu, C., and Thalhammer, T. (2005) Biotransformation of melatonin in human breast cancer cell lines: role of sulfotransferase 1A1. *J Pineal Res* **39**, 276-282

230. Vietri, M., Pietrabissa, A., Mosca, F., Rane, A., and Pacific, G. M. (2001) Human adult and foetal liver sulphotransferases: inhibition by mefenamic acid and salicylic acid. *Xenobiotica* **31**, 153-161

231. Richard, K., Hume, R., Kaptein, E., Stanley, E. L., Visser, T. J., and Coughtrie, M. W. H. (2001) Sulfation of thyroid hormone and dopamine during human development: Ontogeny of phenol sulfotransferases and arylsulfatase in liver, lung, and brain. *Journal of Clinical Endocrinology & Metabolism* **86**, 2734-2742

232. Kwon, M. S., Kim, S. J., Lee, S. Y., Jeong, J. H., Lee, E. S., and Kang, H. S. (2006) Epigenetic silencing of the sulfotransferase 1A1 gene by hypermethylation in breast tissue. *Oncology reports* **15**, 27-32

233. Shatalova, E., Walther, S., Favorova, O., Rebbeck, T., and Blanchard, R. (2005) Genetic polymorphisms in human SULT1A1 and UGT1A1 genes associate with breast tumor characteristics: a case-series study. *Breast Cancer Research* **7**, R909 - R921

234. Seth, P., Lunetta, K. L., Bell, D. W., Gray, H., Nasser, S. M., Rhei, E., Kaelin, C. M., Iglehart, D. J., Marks, J. R., Garber, J. E., Haber, D. A., and Polyak, K. (2000) Phenol sulfotransferases: hormonal regulation, polymorphism, and age of onset of breast cancer. *Cancer Res* **60**, 6859-6863

235. Chen, G., Yin, S., Maiti, S., and Shao, X. (2002) 4-Hydroxytamoxifen sulfation metabolism. *J Biochem Mol Toxicol.* **16**, 279-285

236. Chou, H. C., Lang, N. P., and Kadlubar, F. F. (1995) Metabolic activation of *N*-hydroxy arylamines and *N*-hydroxy heterocyclic amines by human sulfotransferase(s). *Cancer Res.* **55**, 525-529

237. Chou, H.-C., Lang, N. P., and Kadlubar, F. F. (1995) Metabolic activation of the N-hydroxy derivative of the carcinogen 4-aminobiphenyl by human tissue sulfotransferases. *Carcinogenesis.* **16**, 413-417

238. Williams, J. A., Stone, E. M., Fakis, G., Johnson, N., Cordell, J. A., Meinl, W., Glatt, H., Sim, E., and Phillips, D. H. (2001) N-Acetyltransferases, sulfotransferases and heterocyclic amine activation in the breast. *Pharmacogenetics* **11**, 373-388

239. Moore, C. J., Tricomi, W. A., and Gould, M. N. (1986) Interspecies comparison of polycyclic aromatic hydrocarbon metabolism in human and rat mammary epithelial-cells. *Cancer Res* **46**, 4946-4952

240. Bensadoun, A., and Weinstein, D. (1976) Assay of proteins in the presence of interfering materials. *Anal. Biochem.* **70**, 241-250

241. Nose, Y., and Lipmann, F. (1958) Separation of steroid sulfokinases. *J Biol Chem* **233**, 1348-1351

242. Duffel, M. W., Binder, T. P., and Rao, S. I. (1989) Assay of purified aryl sulfotransferase suitable for reactions yielding unstable sulfuric acid esters. *Anal. Biochem.* **183**, 320-324

243. Beland, F. A., Churchwell, M. I., Hewer, A., Phillips, D. H., da Costa, G. G., and Marques, M. M. (2004) Analysis of tamoxifen-DNA adducts in endometrial explants by MS and P-32-postlabeling. *Biochem Biophys Res Commun* **320**, 297-302

244. Apak, T. I., and Duffel, M. W. (2004) Interactions of the stereoisomers of alpha-hydroxytamoxifen with human hydroxysteroid sulfotransferase SULT2A1 and rat hydroxysteroid sulfotransferase STa. *Drug Metab Dispos.* **32**, 1501-1508

245. Dehal, S. S., and Kupfer, D. (1997) CYP2D6 Catalyzes Tamoxifen 4-Hydroxylation in Human Liver. *Cancer Res* **57**, 3402-3406

246. Vineetha Koroth Edavana, X. Y., Ishwori B Dhakal, Suzanne Williams, Baitang Ning, Ian T Cook, David Caldwell, Charles N Falany, Susan Kadlubar. (2011) Sulfation of fulvestrant by human liver cytosols and recombinant SULT1A1 and SULT1E1. *Pharmacogenomics and Personalized Medicine* **4**, 137-145

247. Ung, D., and Nagar, S. (2007) Variable sulfation of dietary polyphenols by recombinant human sulfotransferase (SULT)1A1 genetic variants and SULT1E1. *Drug Metab Dispos.* **35**, 740-746

248. Zafra-Ceres, M., de Haro, T., Farez-Vidal, E., Blancas, I., Bandres, F., de Duenas, E. M., Ochoa-Aranda, E., Gomez-Capilla, J. A., and Gomez-Llorente, C. (2013) Influence of CYP2D6 polymorphisms on serum levels of tamoxifen metabolites in Spanish women with breast cancer. *Int J Med Sci* **10**, 932-937

249. Parte, P., and Kupfer, D. (2005) Oxidation of tamoxifen by human flavin-containing monooxygenase (FMO) 1 and FMO3 to tamoxifen-N-oxide and its novel reduction back to tamoxifen by human cytochromes P450 and hemoglobin. *Drug Metabolism and Disposition* **33**, 1446-1452

250. Krueger, S. K., VanDyke, J. E., Williams, D. E., and Hines, R. N. (2006) The role of flavin-containing monooxygenase (FMO) in the metabolism of tamoxifen and other tertiary amines. *Drug Metabolism Reviews* **38**, 139-147

251. Gottardis, M. M., Robinson, S. P., Satyaswaroop, P. G., and Jordan, V. C. (1988) Contrasting Actions of Tamoxifen on Endometrial and Breast Tumor Growth in the Athymic Mouse. *Cancer Res* **48**, 812-815

252. Satyaswaroop, P. G., Zaino, R. J., and Mortel, R. (1984) Estrogen-like effects of tamoxifen on human endometrial carcinoma transplanted into nude-mice. *Cancer research* **44**, 4006-4010

253. Sheng, J. J., and Duffel, M. W. (2001) Bacterial expression, purification, and characterization of rat hydroxysteroid sulfotransferase STa. *Protein Expression & Purification* **21**, 235-242

254. Bradford, M. M. (1976) Rapid and sensitive method for quantitation of microgram quantities of protein utilizing principle of protein-dye binding. *Analytical Biochemistry* **72**, 248-254

255. Fuda, H., Lee, Y. C., Shimizu, C., Javitt, N. B., and Strott, C. A. (2002) Mutational analysis of human hydroxysteroid sulfotransferase SULT2B1 isoforms reveals that exon 1B of the SULT2B1 gene produces cholesterol sulfotransferase, whereas exon 1A yields pregnenolone sulfotransferase. *J Biol Chem.* **277**, 36161-36166

256. Foster, A. B., Griggs, L. J., Jarman, M., Vanmaanen, J. M. S., and Schulten, H. R. (1980) Metabolism of tamoxifen by rat-liver microsomes - formation of the n-oxide, a new metabolite. *Biochemical pharmacology* **29**, 1977-1979

257. Mani, C., Kupfer, D. (1991) Cytochrome P-450-mediated activation and irreversible binding of the antiestrogen tamoxifen to proteins in rat and human liver: possible involvement of flavin-containing monooxygenases in tamoxifen activation. *Cancer Research.* **51**, 6052-6058

258. Desoky, A. Y., Hendel, J., Ingram, L., and Taylor, S. D. Preparation of trifluoroethyl- and phenyl-protected sulfates using sulfuryl imidazolium salts. *Tetrahedron* **67**, 1281-1287

259. Ingram, L. J., and Taylor, S. D. (2006) Introduction of 2,2,2-Trichloroethyl-Protected Sulfates into Monosaccharides with a Sulfuryl Imidazolium Salt and Application to the Synthesis of Sulfated Carbohydrates. *Angewandte Chemie International Edition* **45**, 3503-3506

260. Liu, Y., Lien, I. F. F., Ruttgaizer, S., Dove, P., and Taylor, S. D. (2003) Synthesis and Protection of Aryl Sulfates Using the 2,2,2-Trichloroethyl Moiety. *Organic Letters* **6**, 209-212

APPENDIX

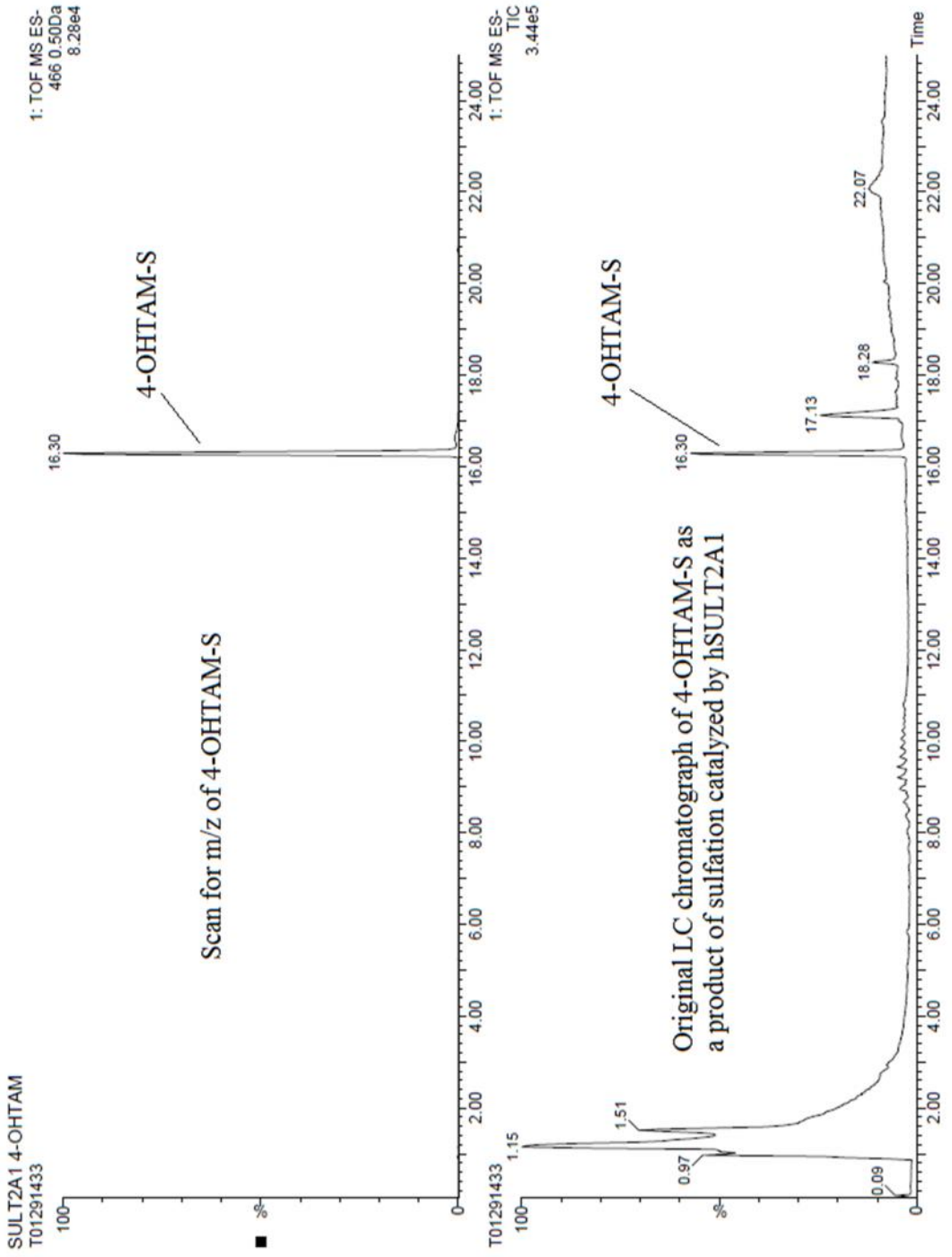

Figure A-1. LC chromatograph of the hSULT2A1-catalyzed sulfation 4-OHTAM.

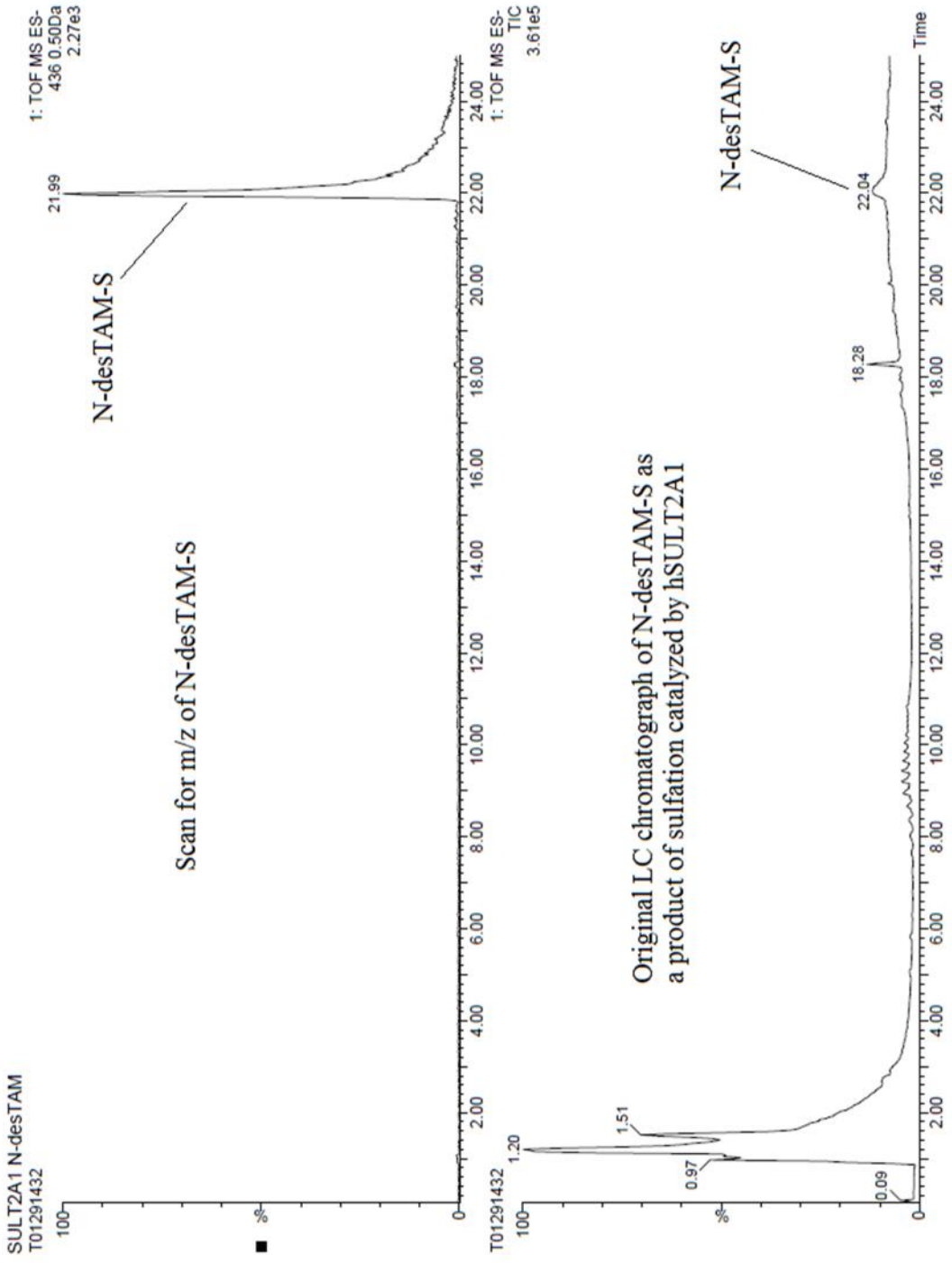

Figure A-2. LC chromatograph of the hSULT2A1-catalyzed sulfation of N-desTAM

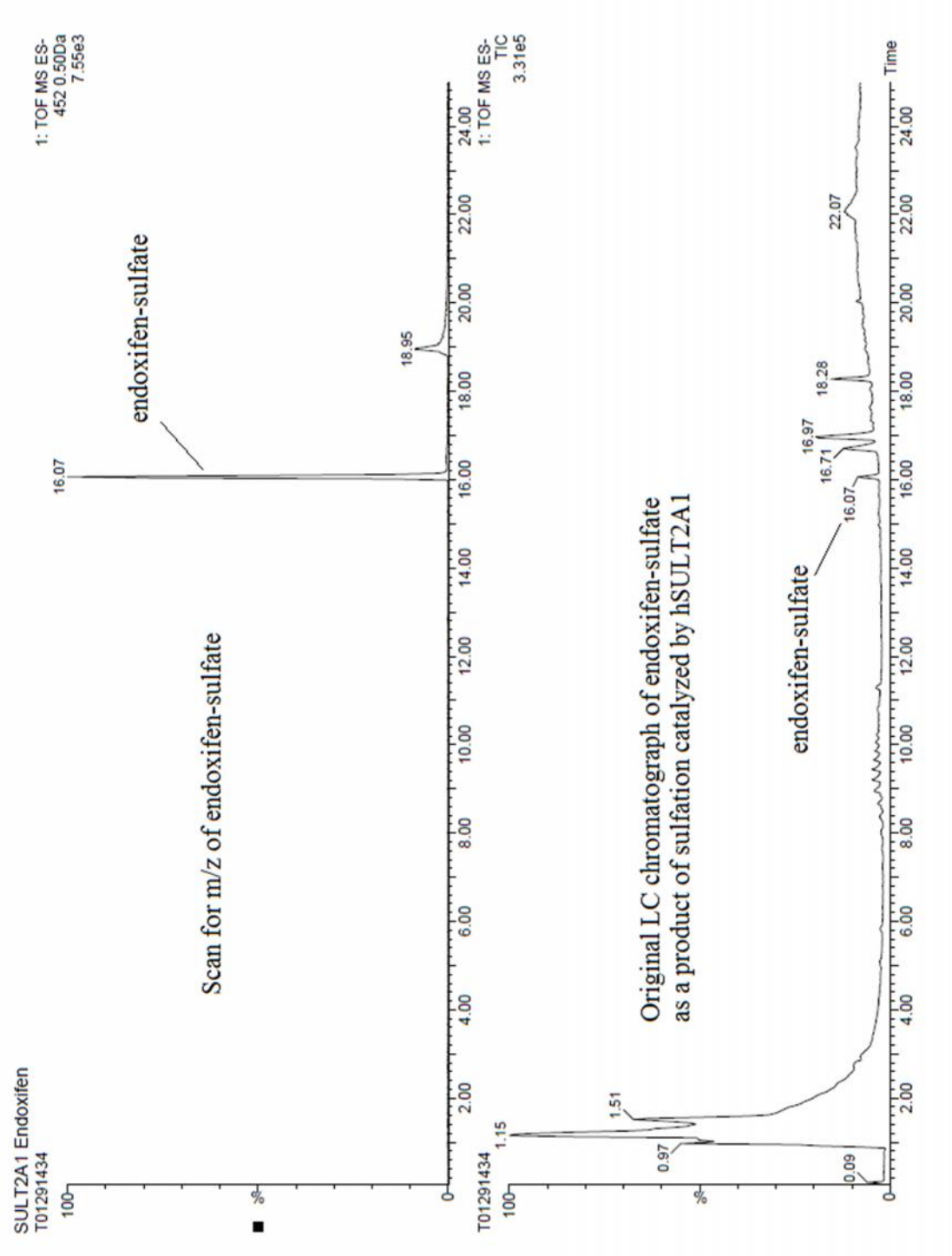

Figure A-3. LC chromatograph of the hSULT2A1-catalyzed sulfation of endoxifen.

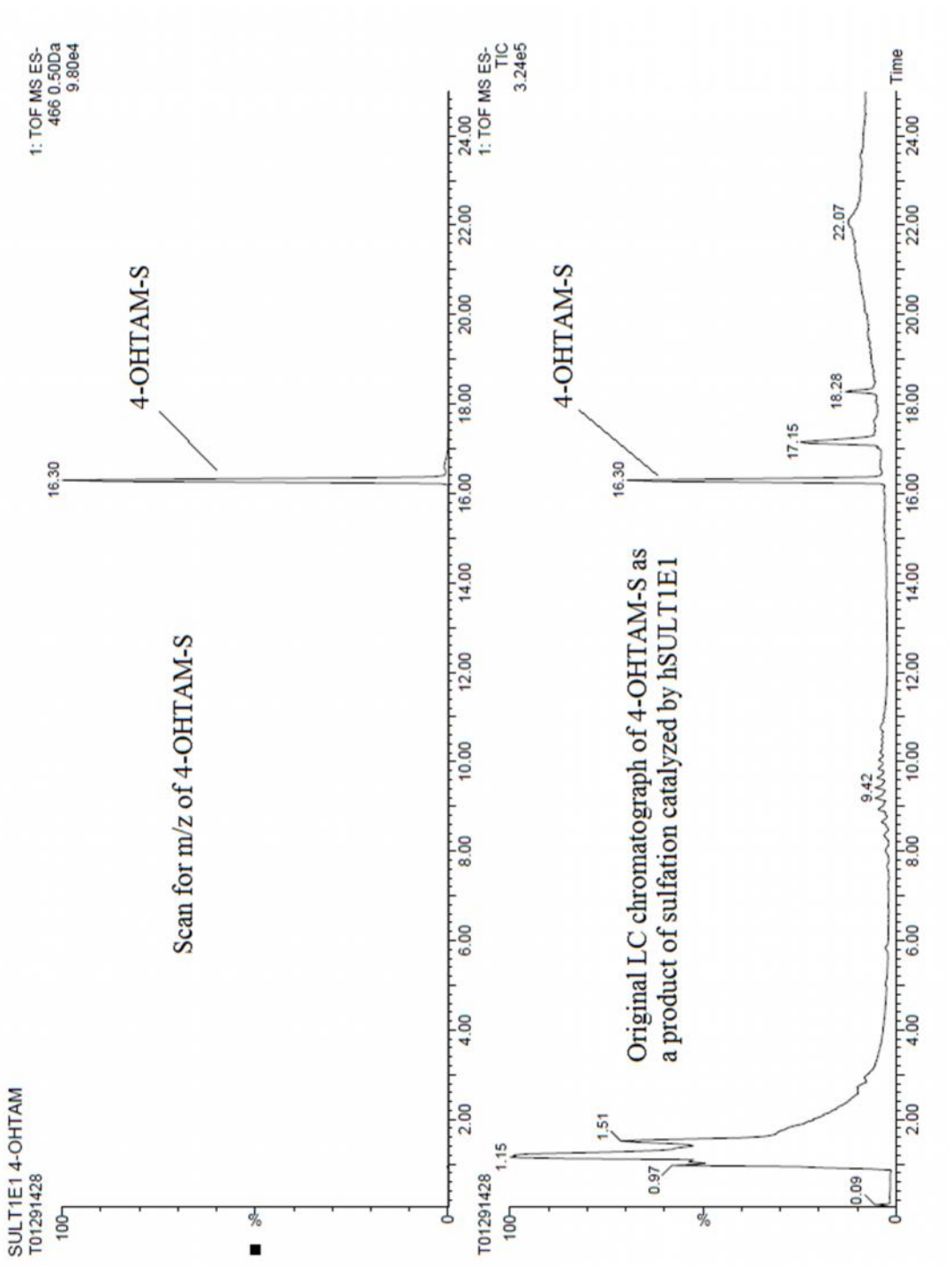

Figure A-4. LC chromatograph of the hSULT1E1-catalyzed sulfation of 4-OHTAM.

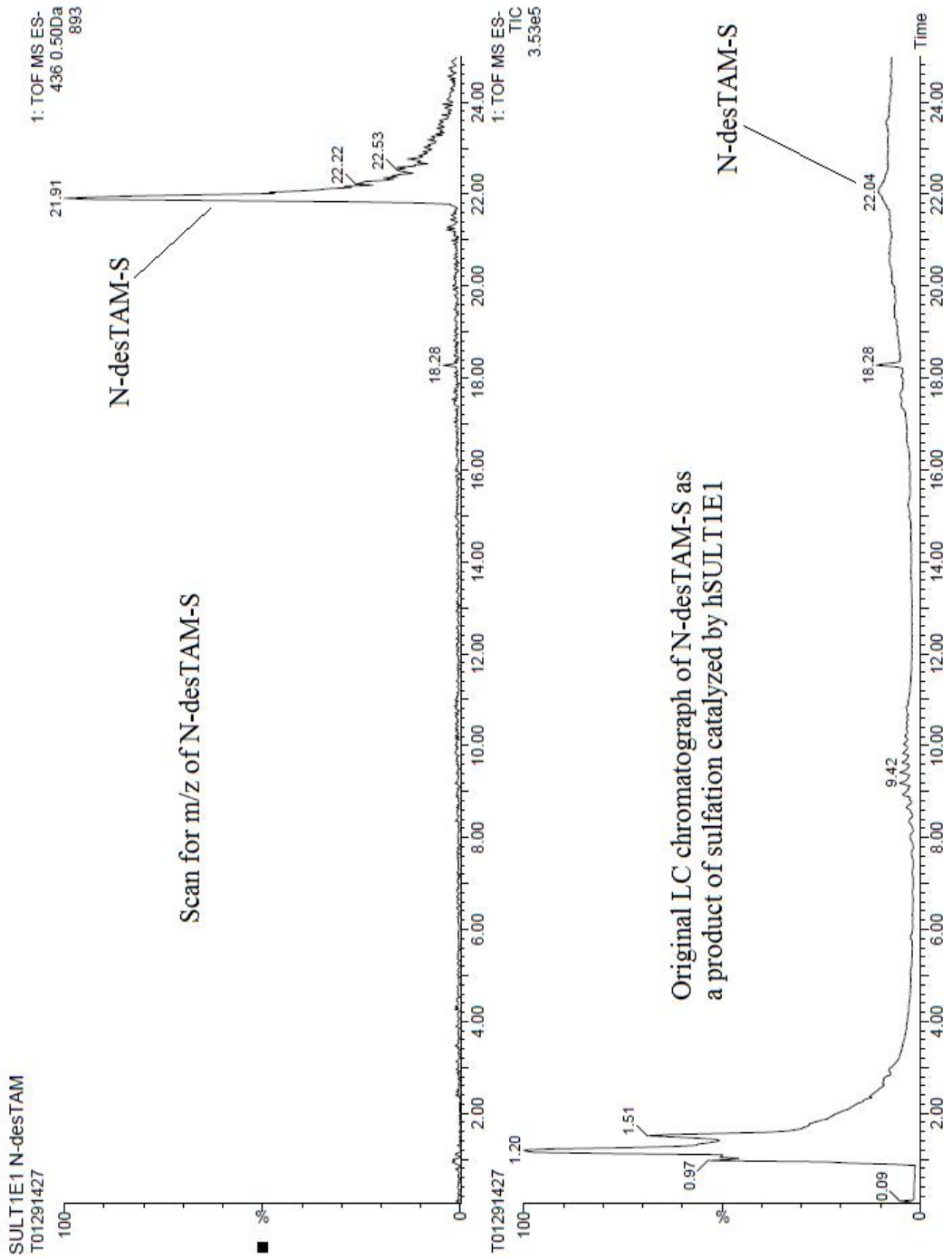

Figure A-5. LC chromatograph of the hSULT1E1-catalyzed sulfation of N-desTAM.

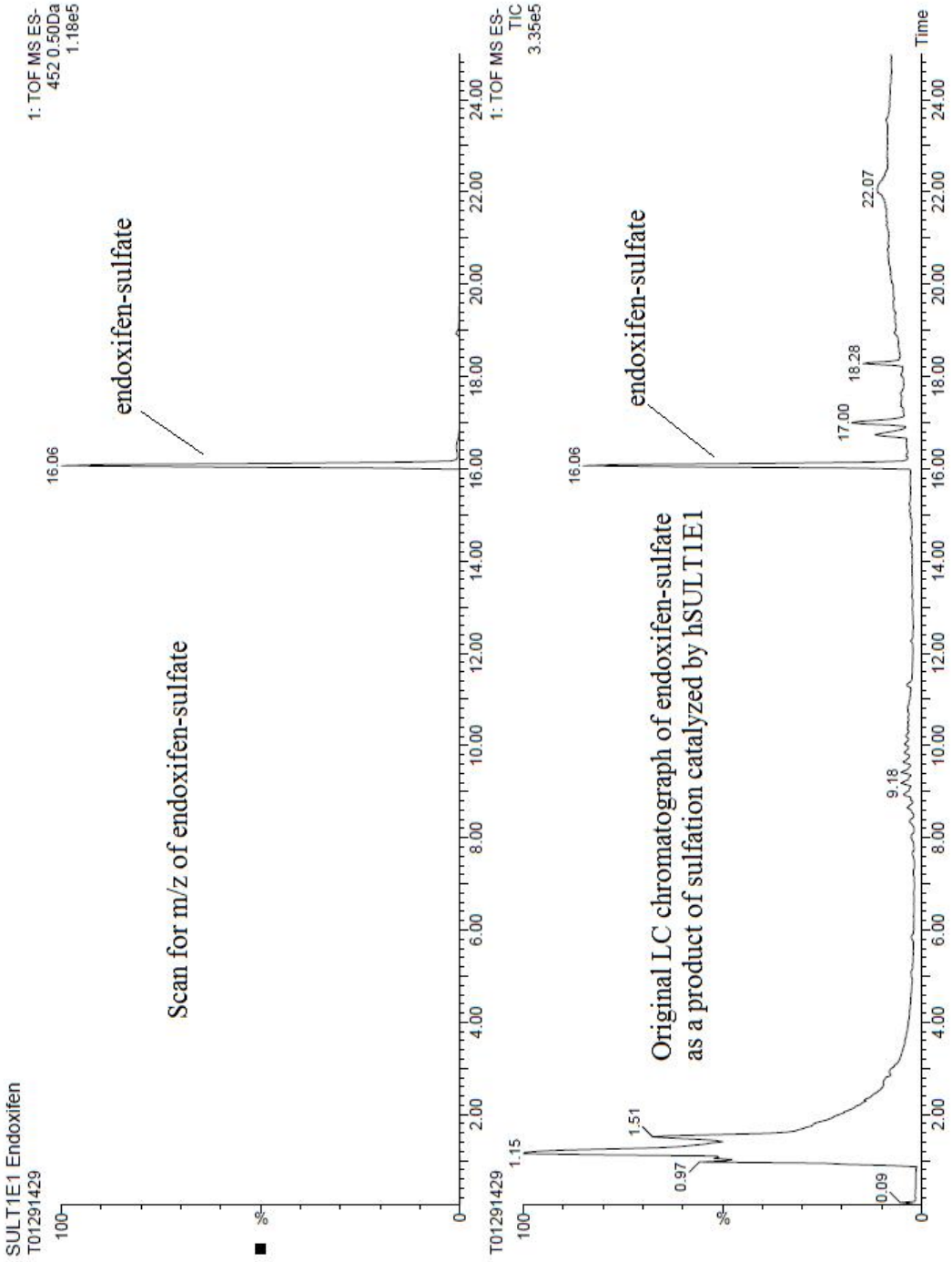

Figure A-6. LC chromatograph of the hSULT1E1-catalyzed sulfation of endoxifen

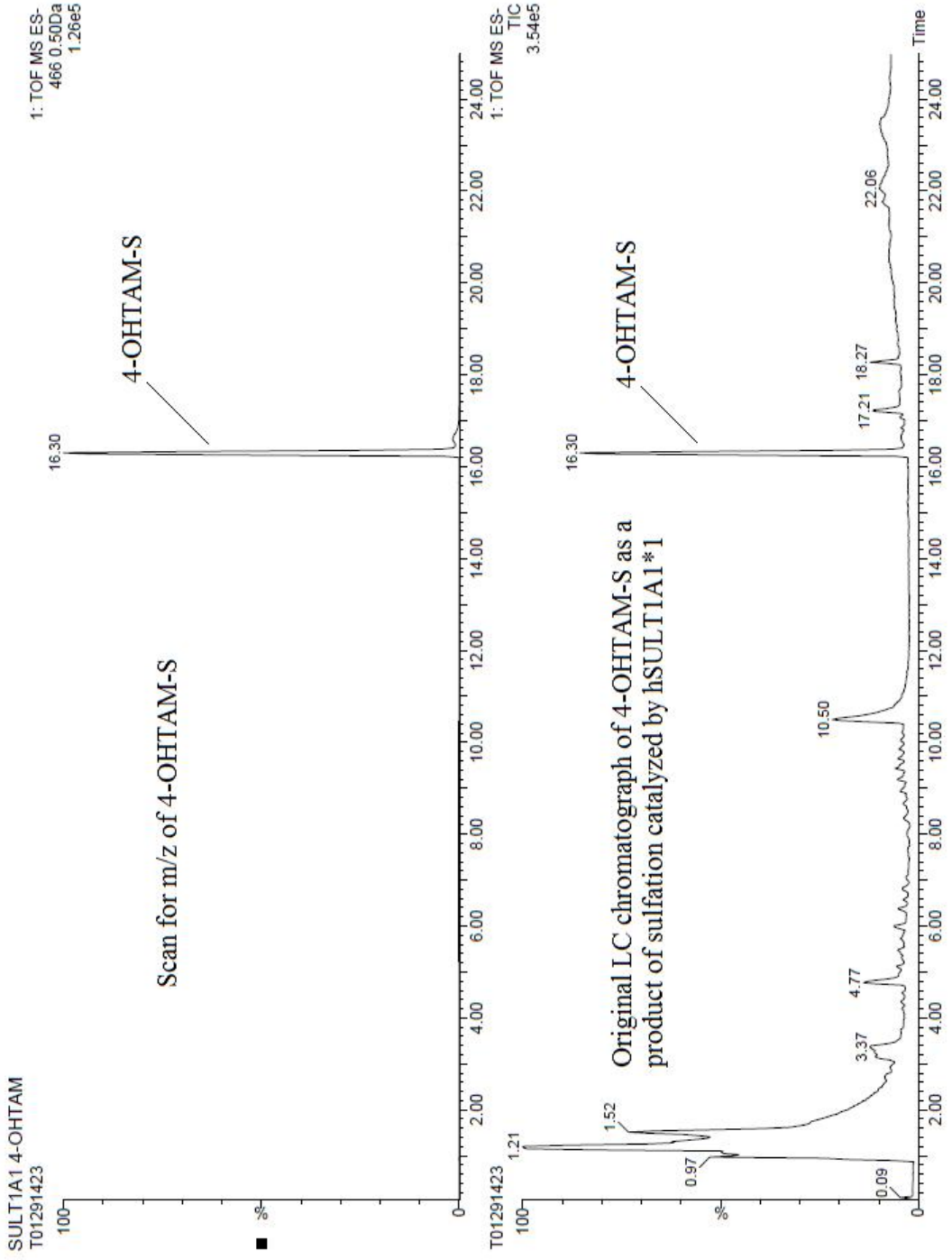

Figure A-7. LC chromatograph of the hSULT1A1*1-catalyzed sulfation of 4-OHTAM.

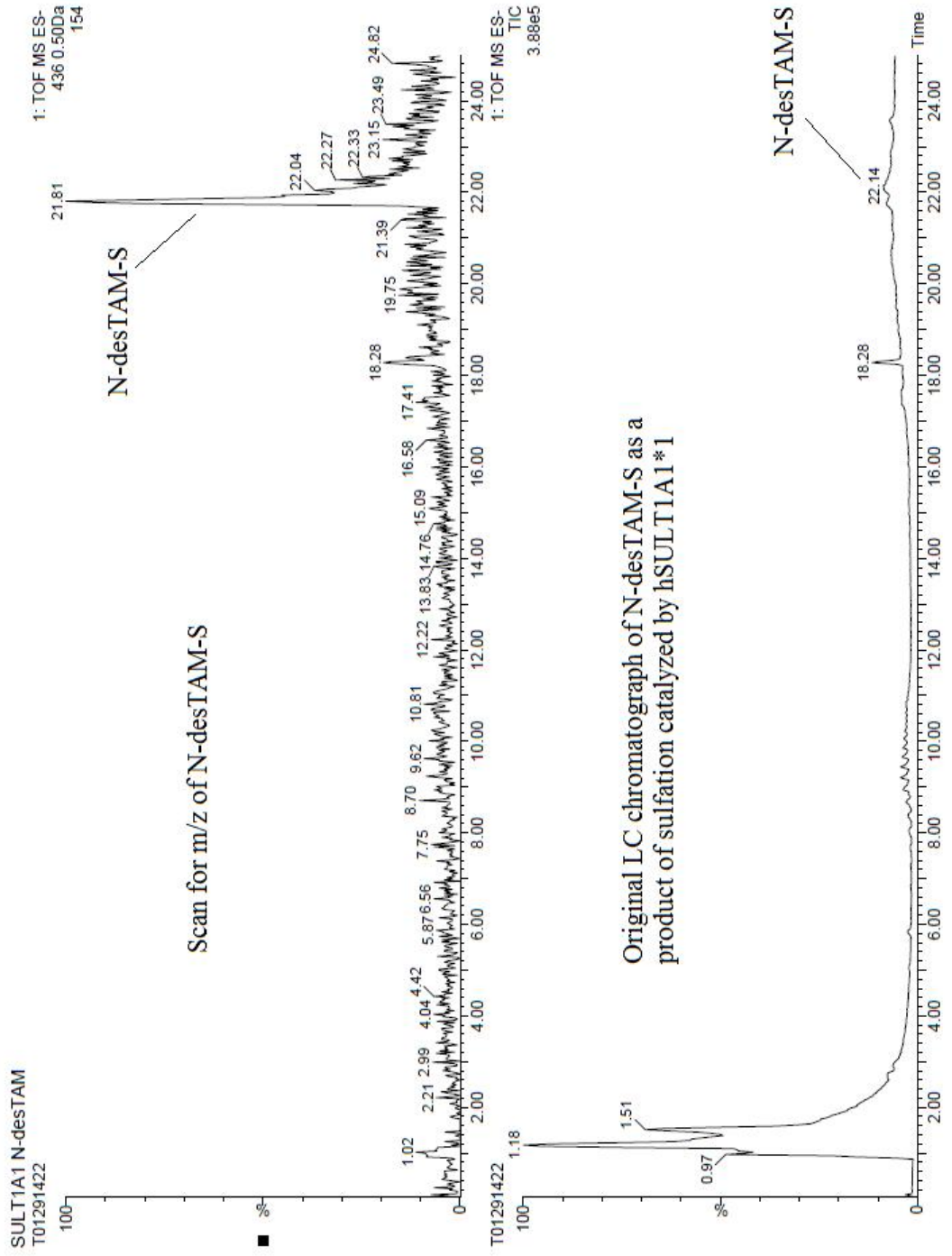

Figure A-8. LC chromatograph of the hSUTL1A1*1-catalyzed sulfation of N-desTAM.

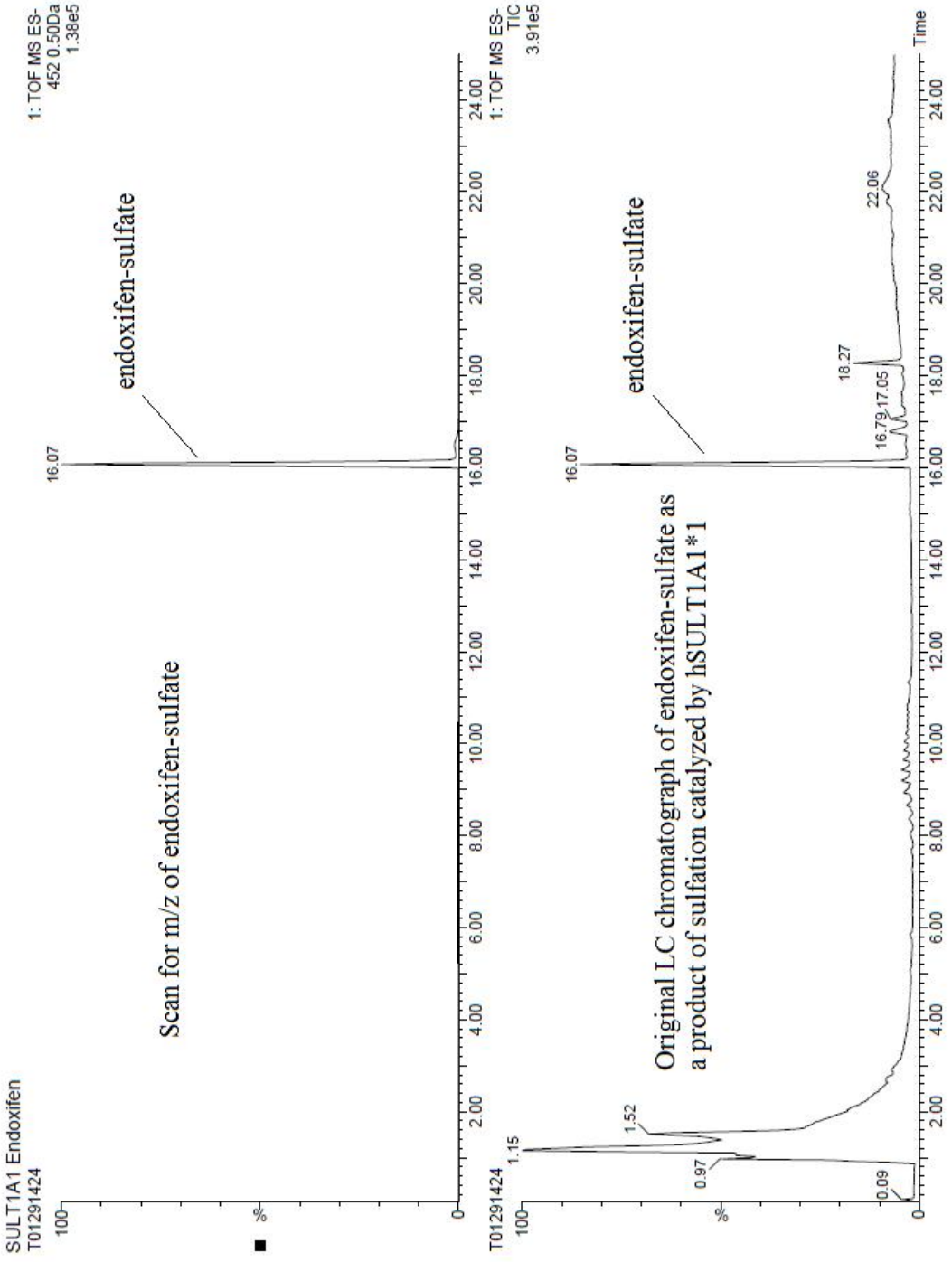

Figure A-9. LC chromatograph of the hSULT1A1*1-catalyzed sulfation of endoxifen.

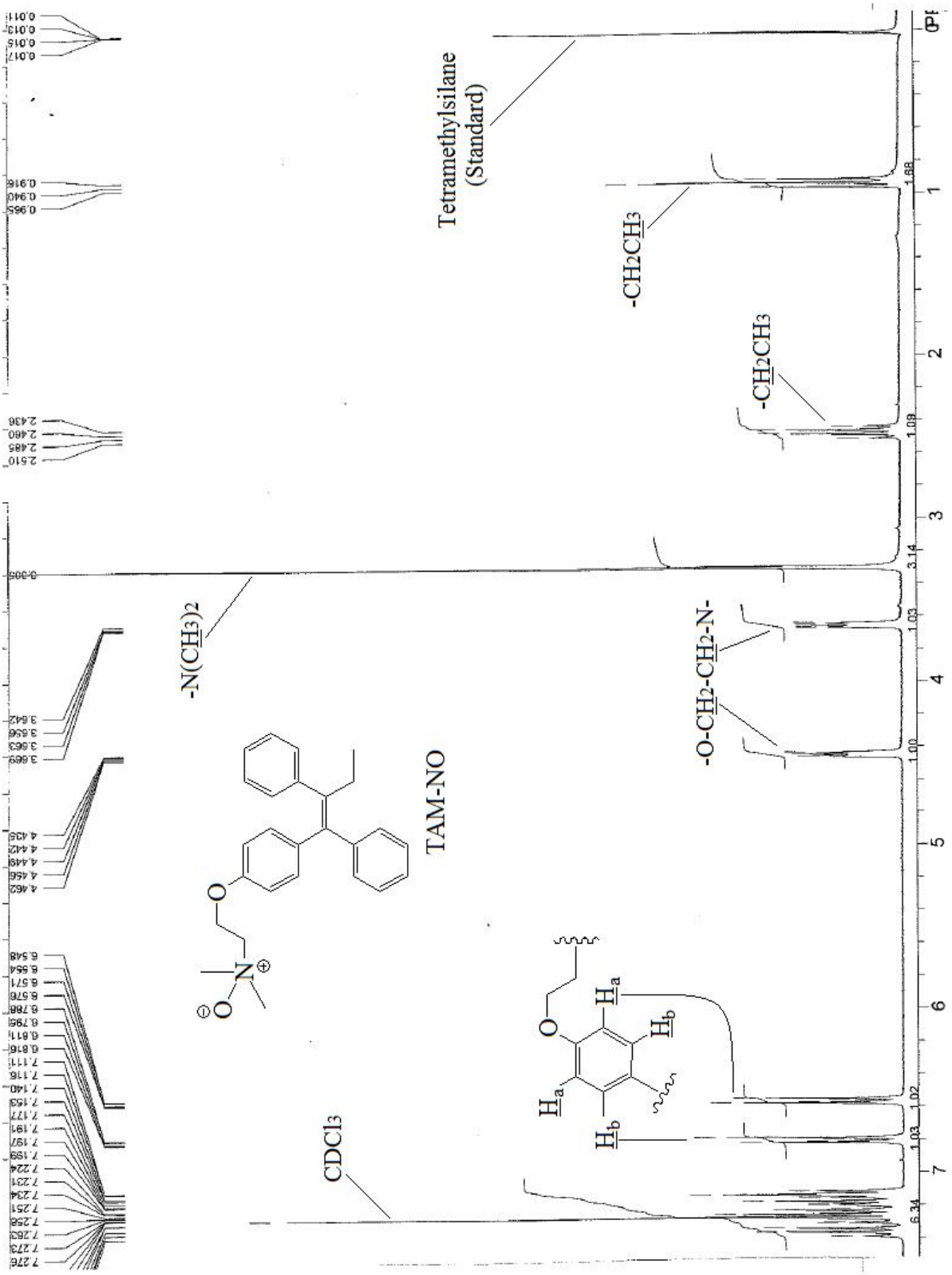

Figure A-10. ^{1}H NMR spectrum of TAM-NO in deuterated chloroform ($CDCl_3$).

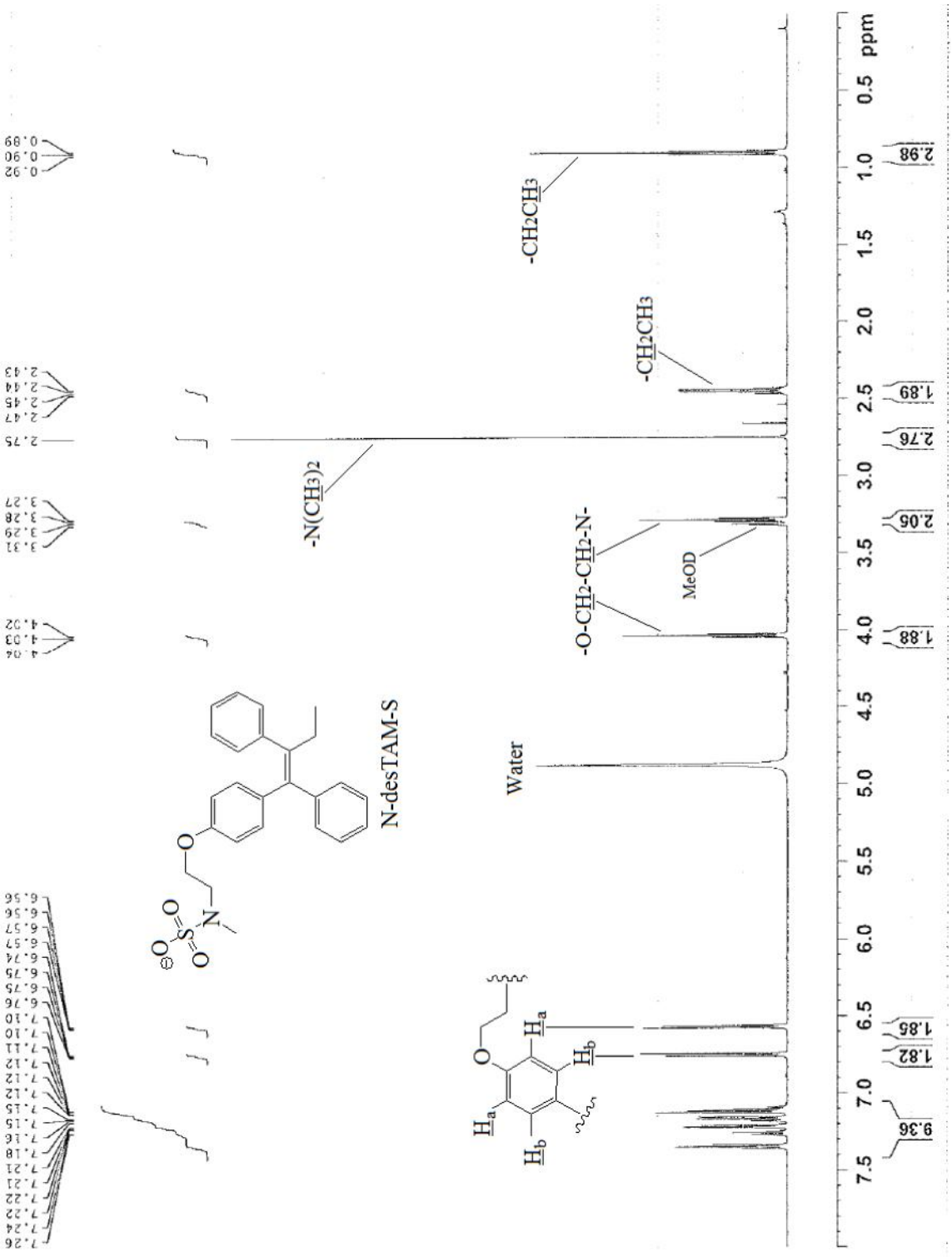

Figure A-11. ^{1}H NMR spectrum of N-desTAM-S in deuterated methanol (MeOD).

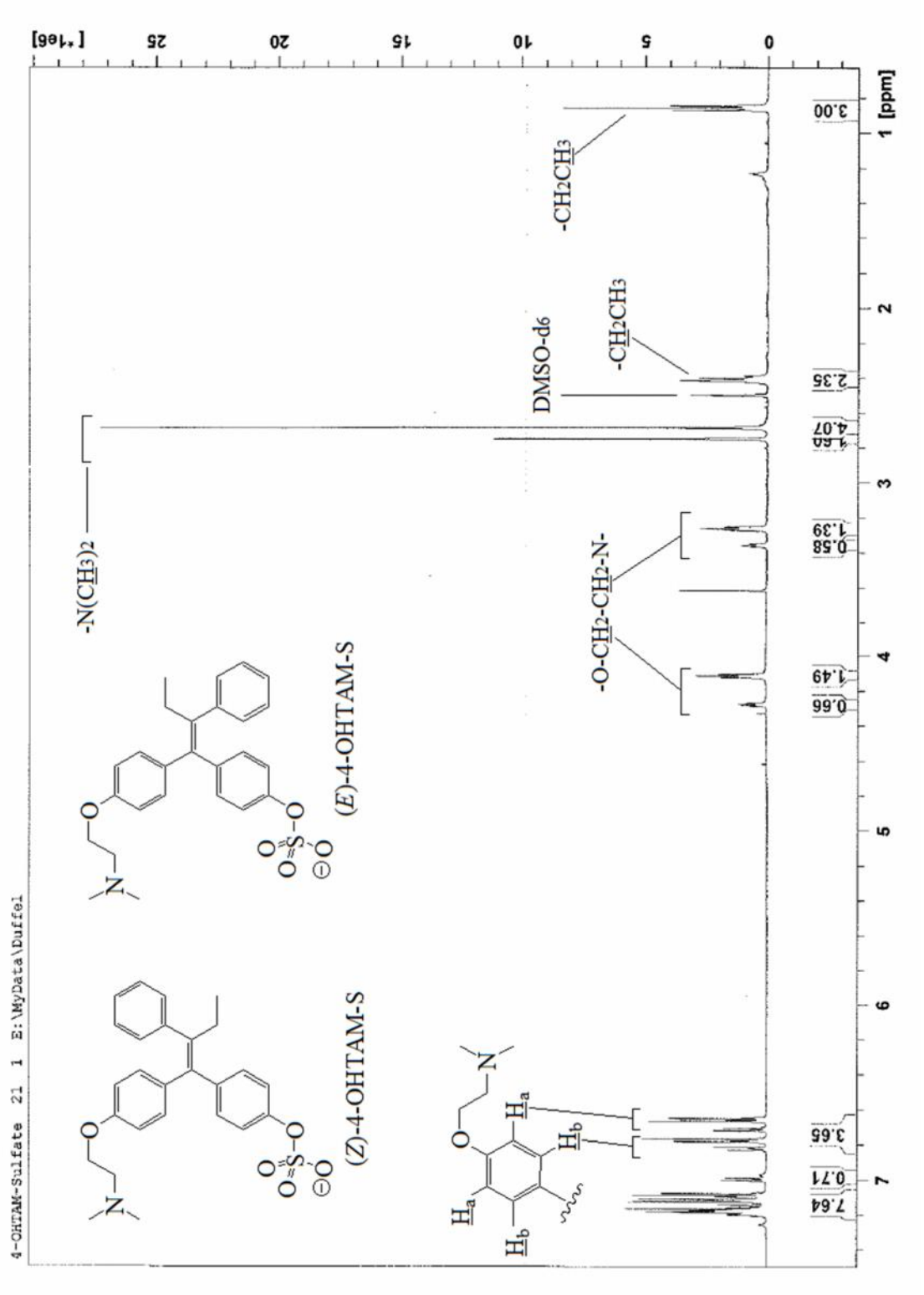

Figure A-12. ^{1}H NMR spectrum of 4-OHTAM-S in deuterated DMSO (DMSO-d*6*).

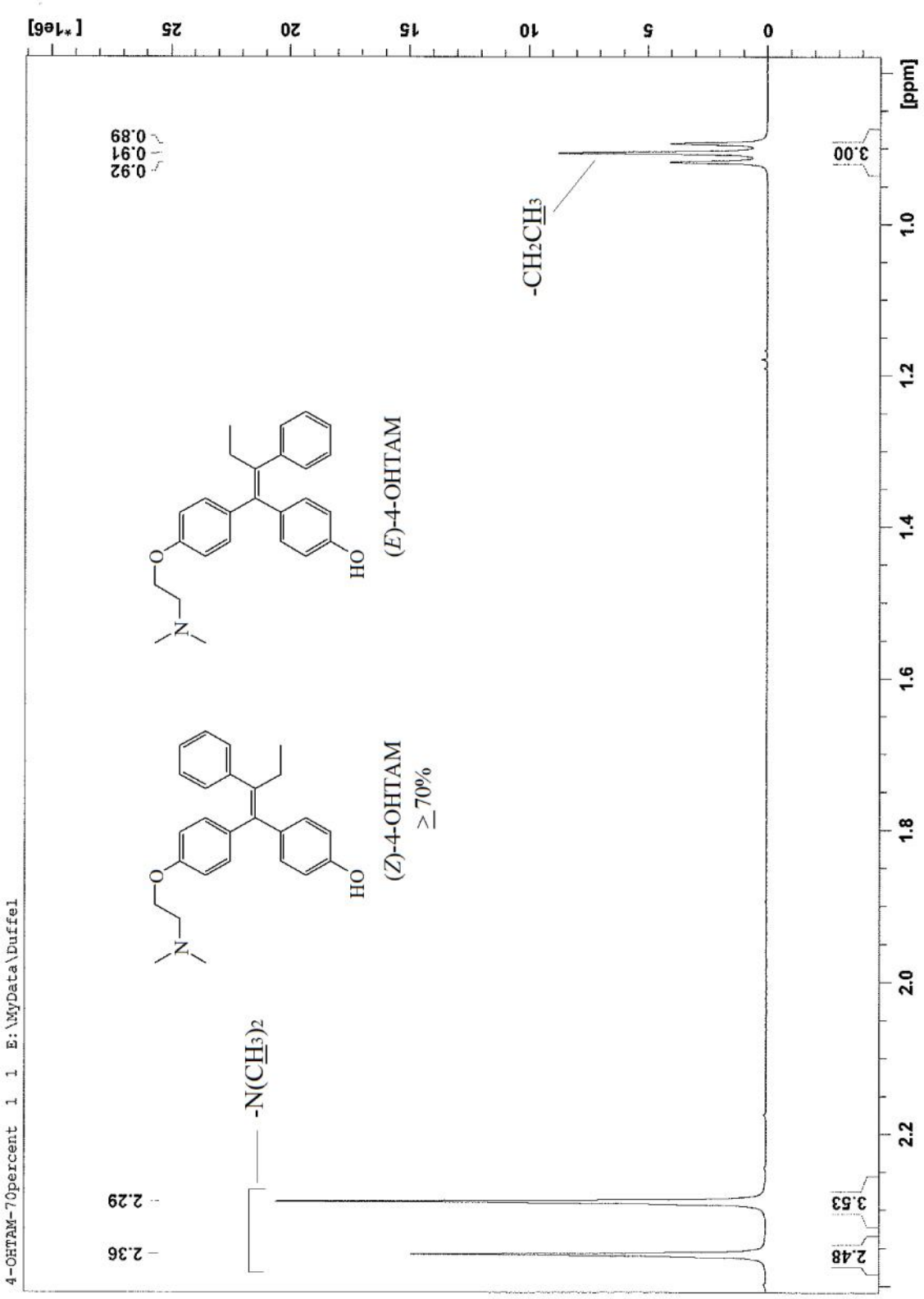

Figure A-13. ^{1}H NMR spectrum of ≥ 70% (*Z*)-4-OHTAM in deuterated methanol

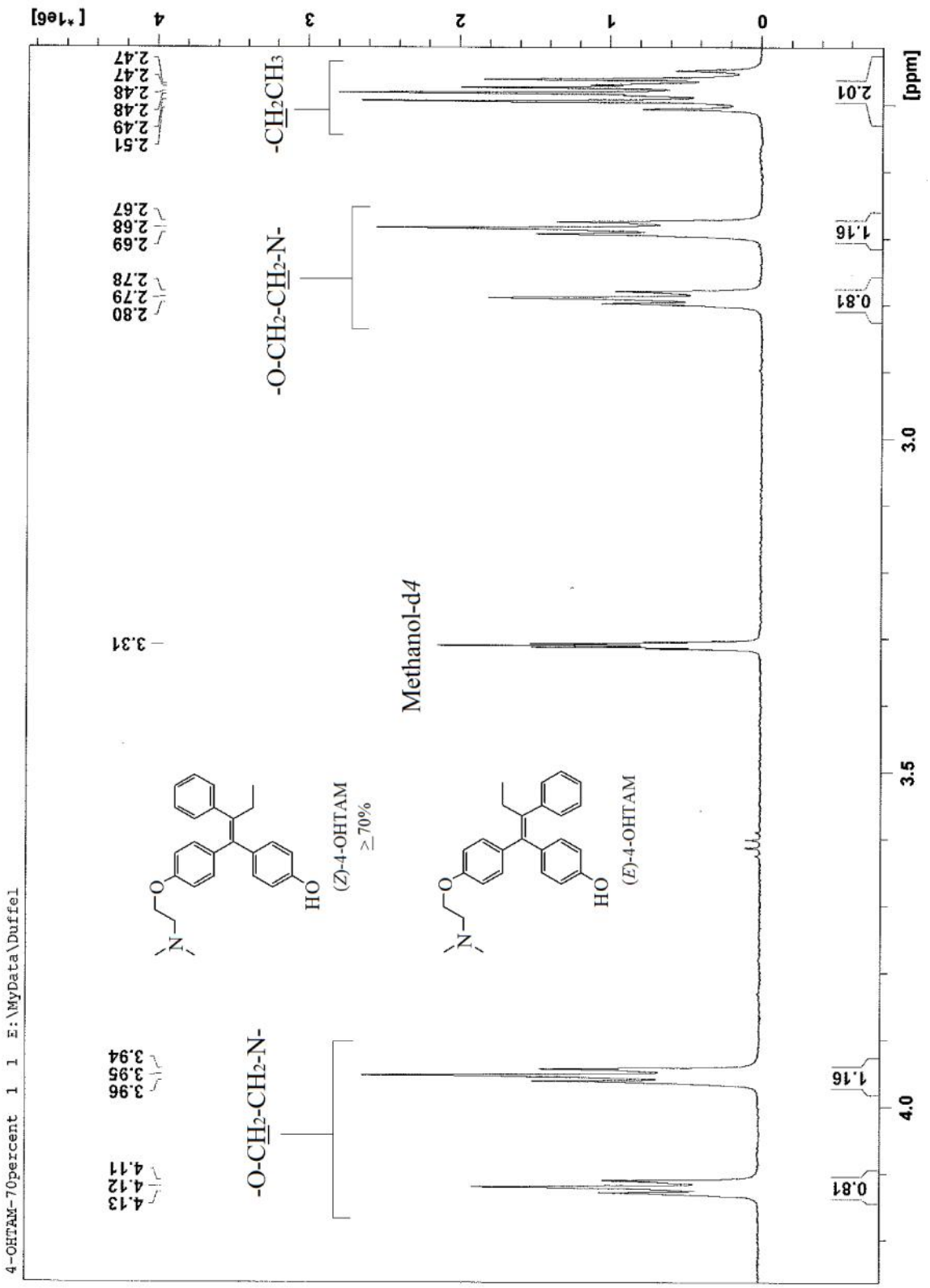

Figure A-14. ^{1}H NMR spectrum of ≥ 70% (*Z*)-4-OHTAM in deuterated methanol

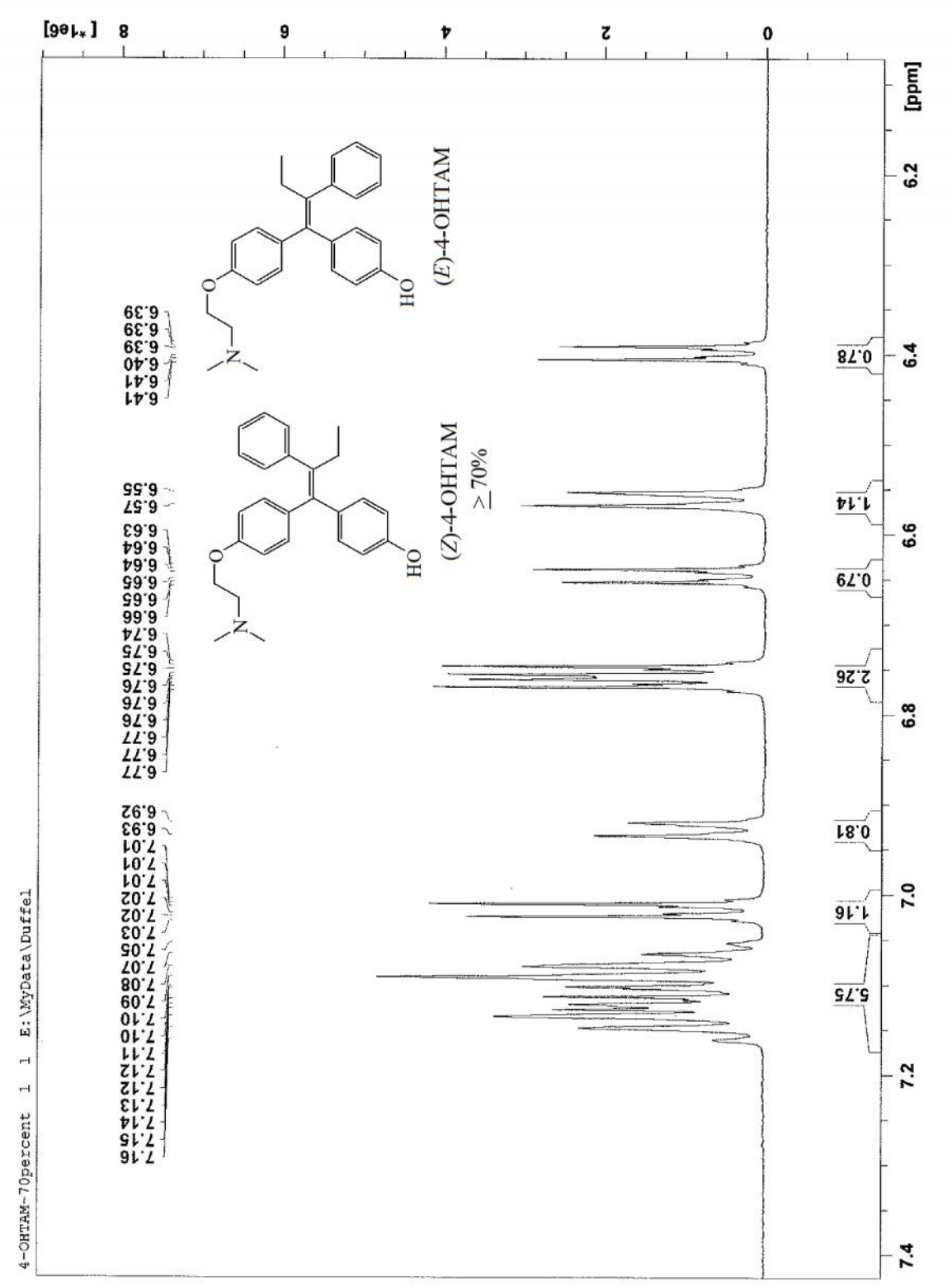

Figure A-15. ^{1}H NMR spectrum of ≥ 70% (*Z*)-4-OHTAM in deuterated methanol

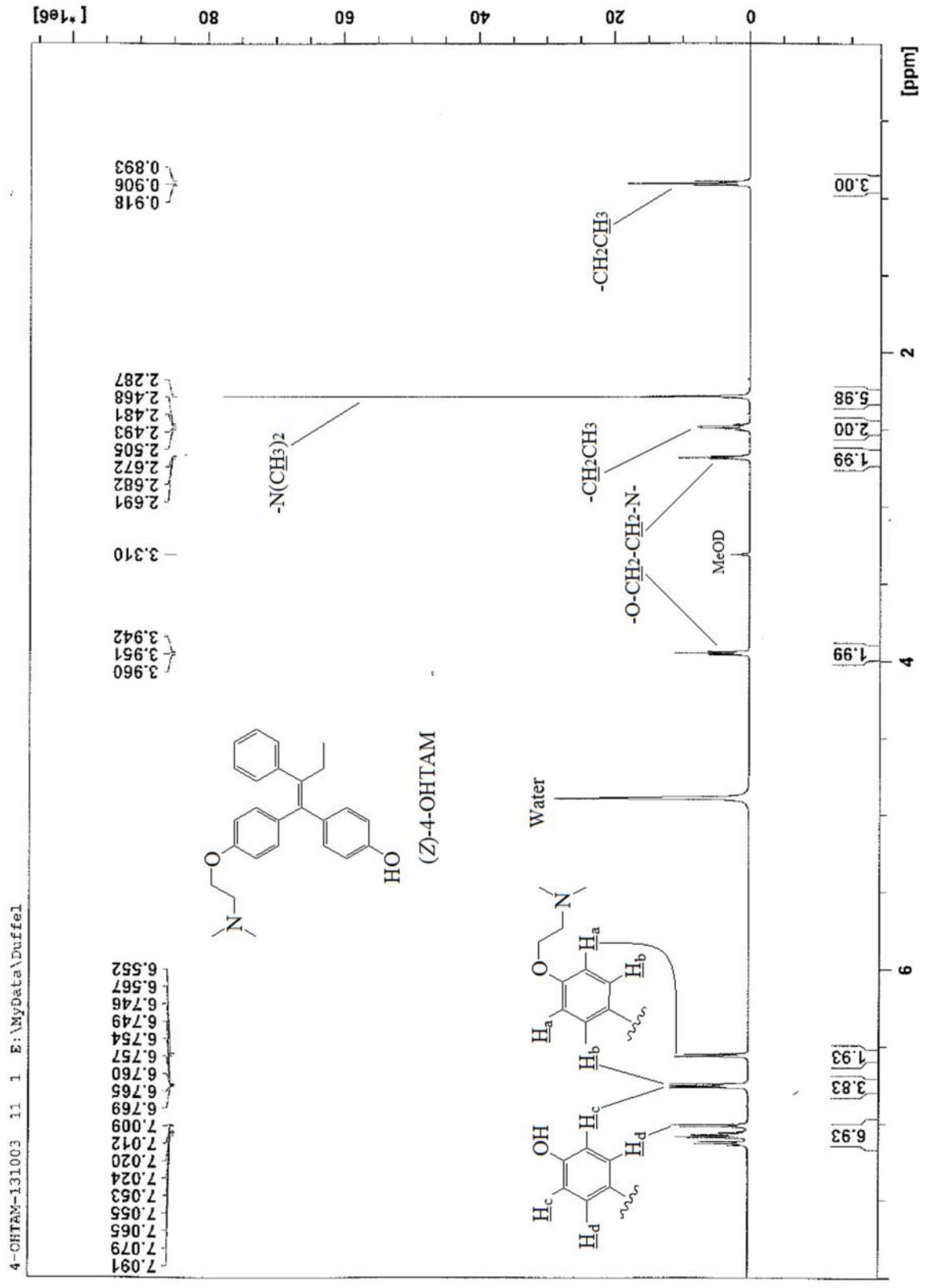

Figure A-16. ^{1}H NMR spectrum of (*Z*)-4-OHTAM in deuterated methanol